The expression and characteristics of ion channels in osteoblasts: putative roles for TRP and K^+ channels

Neil C. Henney

A thesis submitted to Cardiff University in accordance with the requirements
for the degree of Philosophiæ Doctor

November 2008
(submitted)

Cardiff University
Welsh School of Pharmacy
Redwood Building
King Edward VII Avenue
Cardiff CF10 3NB

UMI Number: U584601

UMI U584601

"The most exciting phrase to hear in science, the one that heralds new discoveries, is not 'Eureka!' but 'That's funny...'"

Isaac Asimov

SUMMARY

Bone turnover is regulated by a cocktail of hormones and signalling factors controlling key cell processes such as proliferation, differentiation, mineralisation and apoptosis. Disruption to the overall mineralisation-resorption balance leads to bone disorders, such as osteoporosis – a 'silent' disease affecting around 7 million people in England and Wales. Ion channels that are presumed targets for bone signalling factors include voltage-gated K^+ channels, ATP-dependent K^+ channels and transient receptor potential (TRP) channels, and several of these channel-types reportedly have roles in cell proliferation, apoptosis, and differentiation in various tissues. This Thesis shows that human osteoblasts express a number of channels in these families, including maxi-K, ATP-dependent K^+ channels, TRPV1 and TRPM7. The maxi-K channel, displaying characteristic electrophysiological hallmarks, is abundant in patch-clamp recordings of primary human osteoblasts implying a functional role, and the K_{ATP} agonist pinacidil is shown to promote osteoblast proliferation. Electrophysiological evidence for the TRPV1 channel is not found, although the mRNA signal for a TRPV1 splice variant (TRPV1b) may provide an answer, as it renders the channel less sensitive to capsaicin and protons. However, Ca^{2+} imaging indicates that osteoblastic TRPV1 channels allow Ca^{2+} influx, and are sensitive to 1 µM capsaicin and protons. In functional studies the TRPV1 ligands capsaicin and capsazepine do not influence mineralisation, but interestingly the TRPV1 agonists capsaicin, resiniferatoxin and anandamide appear to prevent differentiation of osteoblastic pre-cursor cells to adipocytes, and instead encourage maturation along the osteoblast pathway, whilst TRPV1 antagonists do not affect adipocyte differentiation. In conclusion, a number of K^+ channels and the TRPV1 channel are expressed in osteoblasts and may have important putative roles in osteoblast cell function. Further steps are required to confirm this before the channels can be considered targets for drug development to treat bone disorders.

TABLE OF CONTENTS

ACKNOWLEDGEMENTS

LIST OF FIGURES & TABLES

Figures

Tables

ABBREVIATIONS

A (pA)	Amperes (pico-Amperes)
AC	Alternating current
AD	Analogue-digital
AEBST	4-(2-aminoethyl) benzenesulfonyl fluoride HCl
ALP	Alkaline phosphatase
AMV	Avian myeloblastosis virus
APS	Ammonium persulfate
ATCC	American Type Culture Collection
ATP	Adenosine triphosphate
BK_{Ca}	Big (large) conductance, calcium-activated K channel
Blotto	5 % Blotto = 5 % w/v non-fat dried milk powder in distilled water, with 0.1 % v/v Tween-20
BMD	Bone mineral density
BMP	Bone morphogenetic protein
BNF	British National Formulary
BSA	Bovine serum albumin
CaR	Calcium receptor
CB	Cannabinoid
CCE	Capacitative calcium entry
cDNA	Complementary deoxyribonucleic acid
CDS	Coding sequence
ClC	Chloride channel
CNS	Central nervous system
CRACM	Calcium release-activated calcium modulator
CTX	Charybdotoxin
DAG	Diacyl glycerol
dB	Decibel
DC	Direct current
DEXA	Dual energy x-ray absorptiometry
DMEM	Dulbecco's modified Eagle medium
DMSO	Dimethyl sulfoxide

DNA	Deoxyribonucleic acid
dNTP	Deoxyribonucleotide triphosphate
D-PBS	Dulbecco's phosphate buffered saline
DRG	Dorsal root ganglia
EAG	Ether-a-go-go
EC_{50}	Effective concentration at 50% of the maximum response
ECL	Enhanced chemi-luminescence
ECACC	European Collection of Cell Cultures
EDTA	Ethylenediaminetetraacetic acid
EGF	Endothelin growth factor
EGTA	Ethyleneglycoltetraacetic acid
ELISA	Enzyme-linked immunosorbent assay
ER	Endoplasmic reticulum
E_{rev}	Reversal potential
FGF	Fibroblast growth factor
G	Gravity
GABA	γ-amino butyric acid
GPCR	G protein-coupled receptor
HEPES	4-(2-hydroxyethyl)-1-piperazineethanesulfonic acid
HRP	Horseradish peroxidase
HRT	Hormone replacement therapy
I	Current
IbTX	Iberiotoxin
I_{CRAC}	Calcium release-activated calcium current
IGF	Insulin-like growth factor
IK_{Ca}	Intermediate conductance K channel
IL	Interleukin
IP_3	Inositol 1,4,5-trisphosphate
IR	Infrared
K_{2P}	2-pore domain potassium channel
K_{ATP}	ATP-dependent potassium channel
K_{Ca}	Calcium-dependent potassium channel
KCB	Potassium channel blocker
KCO	Potassium channel opener
K_d	Dissociation constant
K_{IR}	Inward-rectifier potassium channel
KOH	Potassium hydroxide
K_v	Voltage-regulated potassium channel
MEM-α	Alpha-minimum essential medium

mRNA	messenger RNA
MTS	3-(4,5-dimethylthiazol-2-yl)-5-(3-carboxymethoxyphenyl)-2-(4-sulfophenyl)-2H-tetrazolium
NBD	Nucleotide binding domain
NK	Neurokinin
NMDA	N-methyl D-aspartic acid
NP_o	Open probability where > 1 channels exists per patch
OAP	Odd area profile
OAS	Odd area set
PCR	Polymerase chain reaction
PDF	Probability density function
PDGF	Platelet derived growth factor
PIP_2	Phosphatidylinositol 4,5-bisphosphate
PLC	Phospholipase-C
PLIK	Phospholipase C-interacting kinase
PM	Plasma membrane
PMS	Phenazine ethosulfate
PMSF	Phenylmethanesulfonyl fluoride
P_o	Open probability
P_{open}	Open probability
PPARγ	Peroxisome proliferator-activated receptor-γ
PTH	Parathyroid hormone
PTHrP	Parathyroid hormone-related peptide
PUFA	Polyunsaturated fatty acid
PVDF	Polyvinylidene difluoride
R	Resistance
RANKL	Receptor activator of nuclear factor kappa B ligand
RCF	Relative centrifugal force
RFI	Relative fluorescence intensity
RMP	Resting membrane potential
RMS	Root mean square
RNA	Ribonucleic acid
Rpm	Revolutions per minute
RPMI 1640	Roswell Park Memorial Institute 1640 medium
RT	Reverse transcription
RT-PCR	Reverse transcription polymerase chain reaction
RUNX2	Runt-related transcription factor 2
SDS-PAGE	Sodium dodecyl sulfate polyacrylamide gel electrophoresis
SE	Standard error

SEM	Standard error of the mean
SERCA	Sarcoplasmic/endoplasmic reticulum Ca^{2+}-ATPase
SK_{Ca}	Small conductance K channel
SOC	Store-operated channel
SOCE	Store-operated calcium entry
STIM	Stromal interaction molecule
SUR	Sulphonylurea receptor
τ_o	Open time constant
τ_c	Closed time constant
TAE Buffer	Tris-acetate EDTA
TBS	Tris-buffered saline
TBST	Tris-buffered saline with 0.1 % Tween®-20
TEMED	N,N,N',N'-tetramethylethylenediamine
TGF	Transforming growth factor
TK	Tyrosine kinase
Tris	Tris(hydroxymethyl)aminomethane
TRP	Transient receptor potential
TRPA	Transient receptor potential, ankyrin-type
TRPC	Transient receptor potential, canonical-type
TRPM	Transient receptor potential, melastatin-type
TRPML	Transient receptor potential, mucolipin-type
TRPN	Transient receptor potential, no mechanopotential-type
TRPP	Transient receptor potential, polycystin-type
TRPV	Transient receptor potential, vanilloid-type
TTX	Tetrodotoxin
UV	Ultraviolet
V	Voltage
VDCC	Voltage-dependent calcium channel
VR	Vanilloid receptor
WHO	World Health Organisation

CHAPTER 1:
INTRODUCTION

1   INTRODUCTION

1.1 Outline

Bone tissue is in a constant dynamic state, balanced between the removal of old bone by resorptive osteoclasts and the construction of new bone by mineralizing osteoblasts, to allow growth and repair of the tissue, and to maintain blood-plasma calcium homeostasis. The proliferation, differentiation, secretion and apoptosis of osteoblasts and osteoclasts are finely tuned to ensure that bone mineral density (BMD) is maintained during remodelling. Disruption of the mineralisation-resorption equilibrium results in bone disorders such as osteomalacia, Paget's disease and osteoporosis: the latter of these affects 1 in 2 women and 1 in 5 men over the age of 50 in England and Wales (van Staa *et al.*, 2001) which approximates 7 million people, and hip fractures in women due to osteoporosis cost the NHS £1.73 billion per annum in treatment and respite (National Osteoporosis Society, 2006). Osteoblast functions are regulated by hormones, signalling factors, growth factors and ion channels, and osteoblasts secrete signalling factors such as osteoprotegerin and receptor activator of nuclear factor kappa B ligand (RANKL), which regulate osteoclast differentiation. Therefore osteoblasts are important not only for the synthesis of bone, but also in controlling bone resorption (Mackie, 2003). A variety of ion

channels have been identified in osteoblasts, which are putative target receptors for hormones, signalling factors, cytokines, etc. It is emerging that this complement of ion channels includes voltage-gated K^+ channels, ATP-dependent K^+ channels and transient receptor potential (TRP) channels – a large and diverse superfamily of cation channels that are permeable to Ca^{2+}, Mg^{2+}, Na^+, K^+ and other monovalent cations. Interestingly, many TRP channels have recently been shown to have roles in cell proliferation, apoptosis, and differentiation in a variety of tissue and cell types and several specific TRP channels, such as TRPV1, TRPM7, TRPV5 and TRPV6, likely have roles in osteoblast cell function (Abed & Moreau, 2007; Arnett, 2008; Brandao-Burch et al., 2006; Elizondo et al., 2005; van der Eerden et al., 2005; Hoenderop et al., 2003a). The cellular influx of Ca^{2+} and Mg^{2+} ions is important for many cellular functions including proliferation, differentiation, secretion and apoptosis (Berridge et al., 2000) and Ca^{2+} signalling is known to be implicated in osteoblast cell functions (e.g. Labelle et al., 2007). Whilst the roles of TRP channels in osteoblast cell function are becoming more evident, only the tip of the iceberg has been uncovered and the full remit of TRP channels in these cells has yet to be defined. In the search for new therapeutic strategies for the treatment of bone diseases such as osteoporosis, TRP channels are potential targets for drug treatments which warrants further investigation in this field. The introduction to this Thesis describes the background to the problem of bone diseases, the current situation with regard to ion channel functionality in bone, gives an overview of the superfamily of TRP channels, and finally presents the aims and objectives of the Thesis.

1.2 Bone and bone disorders

1.2.1 Bone

Bone is a dynamic tissue that is constantly being remodelled, depending on a fine balance between the removal of old bone by resorption and the construction of new bone by mineralisation (Hadjidakis & Androulakis, 2006). Osteoclast cells dissolve the mineral matrix while osteoblast cells secrete collagenous and non-collagenous components of bone matrix to promote mineralisation (Eriksen, 1986). Cellular proliferation, differentiation, secretion and apoptosis are critical to ensuring that bone mineral density (BMD) is maintained (Abed & Moreau, 2007). A short description of bone composition and regulation follows.

1.2.1.1 Bone composition

The osseous (mineralised) tissue of bone is composed mostly of calcium phosphate, which in bone is deposited as calcium hydroxyapatite, $Ca_{10}(PO_4)_6(OH)_2$ (Weiner & Traub, 1992). Osteoblasts secrete bone matrix in the form of osteoid containing collagens and alkaline phosphatase, causing dephosphorylation and allowing Ca^{2+} and phosphate crystals to form (Ali *et al.*, 1970; Anderson, 2003). The non-osseous component of bone is collagen which provides some elasticity to an otherwise fragile structure (under tensile strength) (Viguet-Carrin *et al.*, 2006). Two basic 'types' of osseous bone are constructed by the processes carried out by osteoblasts and osteoclasts: cortical bone (also known as compact bone) is dense and forms the outermost layers of bone, and trabecular bone (also called cancellous bone) is sponge-like in

construction, forming lots of space for blood vessels and marrow and making

bone light whilst retaining strength (Hadjidakis & Androulakis, 2006).

1.2.1.2 Cellular complement

It has been stated above that bone formation and destruction are tasks carried

out by osteoblasts and osteoclasts respectively, but bone also contains other

cells as described here, and also in Figure 1.1.

Osteoblasts are osteoid-producing cells that are responsible for promoting

mineralisation and bone construction. These cells also secrete hormones and

signalling factors which act upon osteoblasts themselves, or on osteoclasts, and

therefore osteoblasts are able to partly regulate the entire cycle of bone

remodelling. Parathyroid hormone, oestrogens and androgens are examples of

osteoblast-regulating hormones (Pugsley & Selye, 1933; Endoh *et al.*, 1997;

Notini *et al.*, 2007). Osteoblasts are formed from osteoprogenitor cells found

mainly in the bone marrow and periosteum, which differentiate in response to

growth factors including fibroblast growth factor (FGF), platelet derived

growth factor (PDGF), transforming growth factor (TGF) and bone

morphogenetic proteins (BMPs) (Datta *et al.*, 2008; Karsenty & Wagner,

2002). Markers of osteoblastic formation and activity include alkaline

phosphatase (ALP), osteocalcin and the master regulatory factor RUNX2 (runt-

related transcription factor 2) (Ducy *et al.*, 1997).
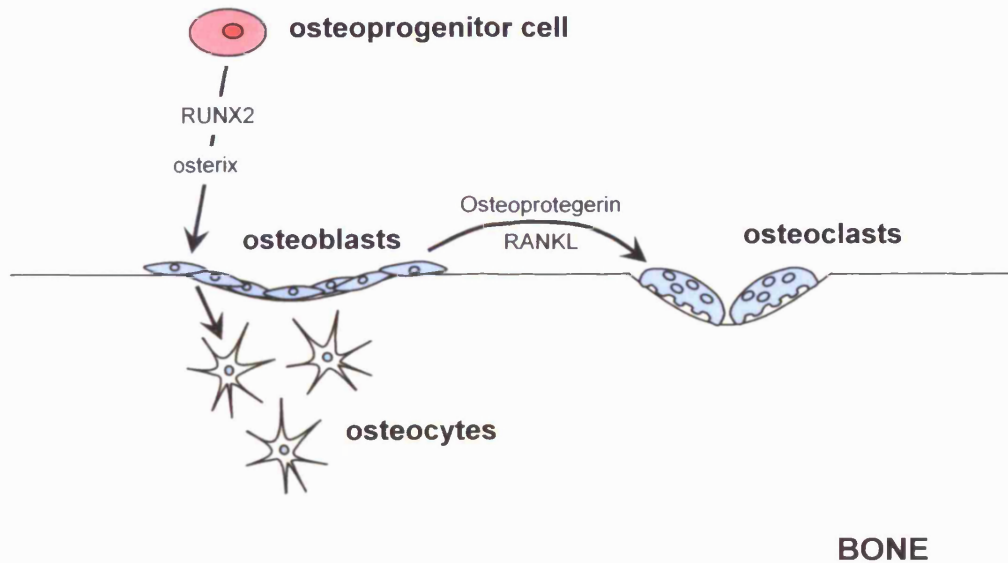
Figure 1.1 **Illustration of cells required for normal bone turnover**. Osteoprogenitor cells differentiate into osteoblasts under the influence of RUNX2 and osterix. Osteoblasts mineralise new bone matrix, and embedded osteoblasts become osteocytes which have a putative paracrine role. Osteoclasts resorb bone and are influenced by RANKL and osteoprotegerin signalling from osteoblasts.

As the mineral matrix is formed, osteoblasts become trapped within, stop producing osteoid and promoting mineralisation and become osteocytes, the roles of which are unclear but may be involved in mechanosensation and paracrine signalling (Han *et al.*, 2004; Marotti, 2000; Zhao *et al.*, 2000).

Osteoclasts are large, multinucleate bone-destroying cells that work in opposition to osteoblasts. Osteoclasts form resorption pits in the mineral matrix by secreting enzymes to disrupt the mineralised tissue and solubilise it for resorption. Like osteoblasts, osteoclasts are subject to hormonal, cytokine and

other forms of chemical stimuli, in particular receptor activator for nuclear factor kappa B ligand (RANKL) and osteoprotegerin which are secreted by osteoblasts, and are inhibitory to osteoclast activity (Takahashi *et al.*, 1988; Yasuda *et al.*, 1998).

1.2.2 Bone disorders

1.2.2.1 Osteoporosis

Osteoporosis is a disorder of the skeleton in which the bone mineral density is diminished and the trabecular bone microarchitecture is weakened, leading to fragility and increased risk of fracture (see Figure 1.2). The morbidity of osteoporosis is far higher in the elderly than the young and is therefore typically, though not exclusively, a disease of the aging: postmenopausal or ovariectomised women are at risk of osteoporosis due to lower levels of the bone-promoting female sex-hormone oestrogen, and to a lesser extent men are also at risk from middle-age onwards when levels of the male sex-hormone testosterone begin to decrease. In England and Wales alone, 1 in 2 women and 1 in 5 men over the age of 50 years can expect to sustain a fracture, probably due to osteoporosis (van Staa *et al.*, 2001) which is a staggeringly high cohort of this age-group, and approximates to 7 million people. To put this into context, the projected risk of fracture in women from 50 years old is greater than the risk of breast cancer or cardiovascular disease (WHO study group, 1994). The financial burden to the NHS of treating hip fractures in the elderly is approximately £1.73 billion per annum and is comparable to the cost of

treating coronary heart disease at £1.75 billion per annum (National Osteoporosis Society, 2006).

Risk factors that further increase the likelihood or severity of osteoporosis include genetics (Kanis *et al.*, 2004a), prolonged periods of low physical activity (Bonauiuti *et al.*, 2002; Wallace & Cumming, 2000), history of poor calcium and vitamin D intake (Tang *et al.*, 2007; Dept. of Health, 1998) (particularly important up to the age of 25), menopause or hysterectomy with ovariectomy (Aitken *et al.*, 1973), tobacco smoking (Kanis *et al.*, 2004b; Wong *et al.*, 2007), high alcohol consumption (Berg *et al.*, 2008; Khanis *et al.*, 2005), and medication – particularly chronic use of glucocorticoids (Bone and Tooth Society of Great Britain, National Osteoporosis Society, & Royal College of Physicians, 2003; McKenzie *et al.*, 2000), but also antiepileptics (Petty *et al.*, 2007), peroxisome proliferator-activated receptor-γ (PPARγ)-inhibitors (Murphy & Rodgers, 2007), and many others.

A   B
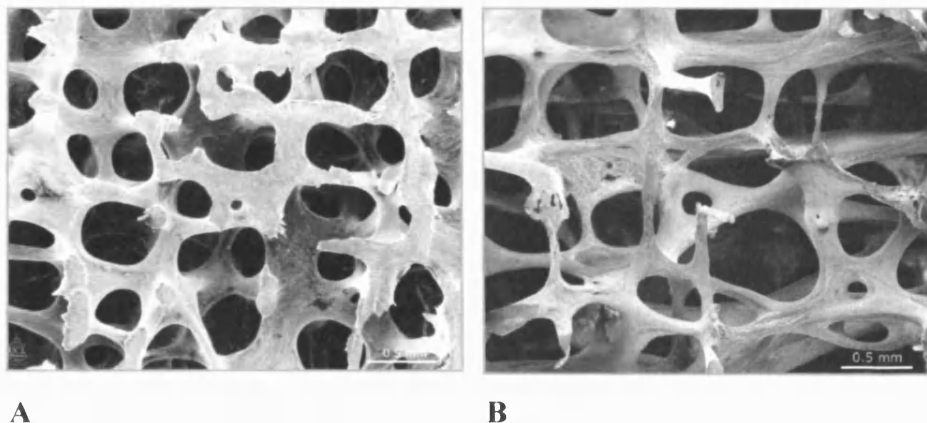
Figure 1.2 Low-power scanning electron microscope images of (A) normal bone in the 3rd lumbar vertebra of a 30 year old woman, and (B) osteoporotic bone in the 3rd lumbar vertebra of a 71 year old woman. Notice the eroded, thin rods of bone in (B) resulting in bone fragility, which is characteristic of this disease. (Images courtesy of T. Arnett, downloaded June 2008. http: //www.anat.ucl.ac.uk/research/arnett_lab/gallery.html).

1.2.2.2 Diagnosis, prognosis and current treatments for osteoporosis

Osteoporosis is a disease which is symptom-free or has no specific symptoms and is usually only identified after a fracture. Because of this, it has been called the 'silent epidemic' (Kanis, 1989). Diagnosis is made by measuring bone mineral density (BMD) by dual energy x-ray absorptiometry (DEXA) scanning, which calculates absorbance by bone of two x-ray beams of different energies – the principle is the higher the absorbance, the higher the BMD (Sartoris & Resnick, 1989). A T-score is given which is a comparison of the patient's BMD with that of a 30-year old of the same sex, and osteoporosis is diagnosed when the T-score is -2.5 or lower (i.e. 2.5 standard deviations below the mean of the compared 30-year old BMD) (WHO Scientific Group, 2003). The prognosis for patients with osteoporosis depends on the severity of the disease and whether they sustain serious fractures, such as hip or vertebral fractures. Complications from sustaining serious fractures lead to an increased mortality, but generally patients do not die of osteoporosis itself.

Current treatments include weight-bearing exercise, a nutritious diet often with calcium and vitamin D supplements, and medication (Bonaiuti et al., 2002; Tang et al., 2007). The mainstay of medical intervention is the group of drugs known as bisphosphonates (BNF 54, Sept. 2007), which inhibit osteoclast bone resorption by either disrupting ATP metabolism or preventing prenylation, and ultimately forcing osteoclasts to undergo apoptosis (Fleisch, 2002; Frith et al., 1997; van Beek et al., 1999). Other treatments include teriparatide which is a synthetic parathyroid hormone analogue which stimulates osteoblasts to

proliferate and mineralise, strontium ranelate which promotes osteoblast function and inhibits osteoclast activity (Meunier *et al.*, 2004), and hormone replacement therapy (HRT) which replaces lost oestrogens in post-menopausal women (Villareal *et al.*, 2001).

1.2.2.3 Other bone disorders

Osteoporosis is not, of course, the only bone disorder but it is certainly the most prevalent (e.g., Zmuda *et al.*, 2006). Other bone disorders include osteomalacia (rickets) which is characterised by 'soft' bones due to much reduced mineralised matrix (Lips, 2006), osteogenesis imperfecta (brittle bone disease) which is caused by a mutation in the collagen gene (Martin & Shapiro, 2008), Paget's disease which is characterised by localised remodelling abnormalities producing deformities (Ralston, 2008), and bone cancers which can be 'lytic' or 'blastic' (Lipton *et al.*, 2001), meaning respectively that the bone is dissolved or heavily overgrown.

1.3   Ion channels and receptors in bone

The evidence in the literature with regard to ion channels and receptors in bone will now be reviewed, beginning with what was known at the outset of this work in January 2005.

1.3.1   Functional ion channels in non-excitable cells

At the beginning of 2005, there was a growing body of evidence indicating that ion channels were involved in a variety of key cellular processes of non-

excitable cells, such as proliferation, apoptosis and secretion. For example, several ion channels were found to be implicated in tumour growth and metastasis suggesting important roles in proliferation, including various voltage- and ligand-gated K^+ channels (Farias *et al.*, 2004; Klimatcheva *et al.*, 1999; Pardo *et al.*, 1999; Parihar *et al.*, 2003; Wang, Z. 2004), chloride channels (Shuba *et al.*, 2000) and voltage-dependent Ca^{2+} channels (VDCCs) (Wang *et al.*, 2000).

In particular, voltage-gated K^+ channels, previously thought to be limited to excitable cells and which control firing patterns and repolarisation rate following an action potential in nerve cells (Hille, 2001), were found to have important physiological roles in cell proliferation of immune and cancer cells (Leonard *et al.*, 1992; Wonderlin & Strobl, 1996; Chandy *et al.*, 2004) and secretion in osteoblasts (Moreau *et al.*, 1997). Ligand-gated K^+ channels, such as ATP-dependent K^+ (K_{ATP}) channels, also have recognised roles in non-excitable cells; for example, K_{ATP} channels are involved in secretion of insulin from pancreatic β cells (Aguilar-Bryan & Bryan, 1999). Involvement of K_{ATP} channels in proliferation has also been shown in cancer cells (Wondergem *et al.*, 1998), nephrons (Braun *et al.*, 2002) and in hair growth (Goldberg *et al.*, 1988). Clearly, important physiological roles for K^+ channels were being unveiled in non-excitable cells, undoubtedly with more roles yet to be identified.

At the same time, an entirely new and exciting family of ion channels had recently been identified which became known as transient receptor potential (TRP) channels, owing to the transient Ca^{2+} response observed in a mutant *Drosophila* TRP channel (see section 1.4). This ion channel family, which is non-selective and is permeable to Ca^{2+}, Mg^{2+} and monovalent cations, was showing signs of a diverse range of functions and the family appeared to be expressed in a wide variety of excitable and non-excitable tissues. TRP channels were found to be involved in various sensory processes, including temperature sensation (Caterina *et al.*, 1997; McKemy *et al.*, 2002; Peier *et al.*, 2002a), mechanosensation (Corey, 2003; Nauli *et al.*, 2003), osmosensation (Liedtke *et al.*, 2000; Strotmann *et al.*, 2000) and pain (Caterina *et al.*, 1997; Caterina *et al.*, 2000; Story *et al.*, 2003). But as with the K^+ channels, TRP channels which were originally discovered in excitable tissues were beginning to emerge as putative key players in vital non-excitable cell processes: for example, the cold-sensitive channel TRPM8 was found to be upregulated in androgen-sensitive prostate cancer, implying a role for this channel in cell proliferation (Tsavaler *et al.*, 2001; Zhang *et al.*, 2004) and TRPM7 was shown to be vital for cellular Mg^{2+} uptake and progression through the cell cycle (Nadler *et al.*, 2001; Schmitz *et al.*, 2003). Although in the early stages of discovery, TRP channels were showing promise as functional channels in non-excitable cells.

1.3.2 The evidence for functional ion channels in bone

The proliferation, differentiation and secretory properties of osteoblast cells *in vivo* are intrinsically regulated by a cocktail of hormonal and signalling factors to maintain the correct balance between bone resorption and bone production. The plasma membranes of osteoblasts are found to be suitably decorated with a complement of ion channels and receptors which are putative targets for oestrogens (Endoh *et al.*, 1997; Lieberherr *et al.*, 1993), androgens (Vanderschueren *et al.*, 2004), prostaglandins and other inflammatory cytokines (Moreau *et al.*, 1996; Rezzonico *et al.*, 2002), neuro-excitatory amino acids such as glutamate (Gu *et al.*, 2000; Gu *et al.*, 2002), adenosine and other nucleosides and nucleotides (Hoebertz *et al.*, 2003), parathyroid hormone (Ryder & Duncan, 2001), and calcium (Dvorak *et al.*, 2004; Dvorak & Riccardi, 2004) to name but a few. All the above are known to influence bone turnover.

By early 2005, the complement of ion channels found in osteoblasts and osteoprogenitor cells with evidence of putative involvement in the regulation of bone function included an inward rectifier K^+ channel (Yellowley *et al.*, 1998), K_{ATP} channels (Moreau *et al.*, 1997; Gu *et al.*, 2001a), Ca^{2+}-activated K^+ channels including a small conductance Ca^{2+}-activated K^+ channel (Gu *et al.*, 2001a), an intermediate conductance Ca^{2+}-activated K^+ channel (Weskamp *et al.*, 2000) and a large conductance Ca^{2+}-activated K^+ channel (Moreau *et al.*, 1996; Moreau *et al.*, 1997; Rezzonico *et al.*, 2002; Rezzonico *et al.*, 2003; Weskamp *et al.*, 2000), TTX-insensitive Na^+ channels (Richter & Ferrier,

1991), voltage-dependent calcium channels (VDCCs) (Gu *et al.*, 2001b; Hattori *et al.*, 2001), a volume-sensitive Cl$^-$ channel (Steinert & Grissmer, 1997) and mechanosensitive cation channels (Davidson *et al.*, 1996; Duncan & Hruska, 1994). By implication, TRPV5 was thought to be expressed in mouse bone (Hoenderop *et al.*, 2003b) as TRPV5$^{-/-}$ mice were phenotypically underdeveloped skeletally.

It is worth noting that such a large complement of ion channels and receptors in cultured cells may well be an artefact of the culture conditions, rather than a true representation of the expression of these proteins *in vivo* (*e.g.* see Ma *et al.*, 2005). But given the role of osteoblasts in bone, it must be presumed that some of these ion channels and receptors are involved in the proliferation, differentiation, secretion or apoptosis of these cells.

1.3.2.1 K$^+$ channel functions in bone

In osteocytes, K$^+$ channels and VDCCs were shown to be involved in paracrine signalling and mechanotransduction (Gu *et al.*, 2001a; Gu *et al.*, 2001b). In osteoblasts, the Ca^{2+}-activated K$^+$ channels appear to contribute to cell volume (Weskamp *et al.*, 2000) and to resting membrane potential (RMP): K$_{Ca}$ channel activation would hyperpolarise the membrane, which may balance the depolarisation associated with [Ca^{2+}]$_i$ increases, thus regulating [Ca^{2+}]$_i$ by feedback (Moreau *et al.*, 1996; Ravesloot *et al.*, 1990; Yellowley *et al.*, 1998). The large conductance calcium-activated K$^+$ channel, maxi K$^+$, and K$_{ATP}$ channels have been shown to be involved in osteocalcin secretion by

osteoblasts (Moreau *et al.*, 1997) and presumably have roles in other vital cell processes (see above).

1.3.2.2 TRP channel functions in bone

By the end of 2004, there was very little evidence of TRP channel expression in bone, let alone any evidence for functional TRP channels. However, one encouraging publication reported that the phenotypes of TRPV5-knockout mice showed reduced bone thickness and hypercalciuria (Hoenderop *et al.*, 2003b). This implied a role for TRPV5 in osteoblast proliferation and secretion.

1.3.3   The thesis: which way forward?

The outline plan for the thesis was to research an ion channel or group of ion channels and investigate the electrophysiology and functional aspects of the channels in human osteoblasts. Given the literature at the end of 2004, there were two groups of ion channels which clearly showed potential as important regulators of osteoblast cell functions; namely the Ca^{2+}-activated K^+ channels (in particular maxi K^+) and the K_{ATP} channels. There was growing evidence for these as functional channels in a variety of non-excitable cells, including osteoblasts, with roles in proliferation, apoptosis and secretion (see above). In addition to this, evidence for functional TRP channels in non-excitable cells was beginning to build. These channels were relatively newly discovered and functions appeared to be extraordinarily diverse, but these channels potentially also had important roles in key cellular processes.

Whilst the K^+ channels could be considered a relatively safe bet for developing the understanding of their functions in osteoblasts, the TRP channels were more of a long-shot with only a modicum of evidence in comparison, but were attractive due to their novelty and potential for discovery.

With this in mind, the path chosen to follow was that of TRP research in human osteoblasts. The original thesis was that TRP channels would be found to be expressed and functional in human osteoblasts and osteoblast-like cells, with the aim to investigate a selection of promising TRP channels, and that at least one of these would have an important role in cell proliferation, secretion, differentiation or cell death. The choice of TRP channels to research was to include TRPM8 (given its putative role in proliferation), TRPV1 (due to relatively well defined pharmacology), TRPV5 and TRPV6 (as highly Ca^{2+} permeable channels, which may be of particular interest in bone), and TRPM7 (which had evidence for importance in cell progression). In addition, due to the obvious importance of K^+ channels in non-excitable cell functions, and rather than neglect this entirely, a short investigation into the expression and functions of maxi-K^+ and K_{ATP} channels would be pursued at the outset, and for purposes of comparison with TRP channels.

What now follows is a review of the evidence to date, which has been published during the work for this thesis.

1.3.4   Ion channels and receptors in bone: an update

Since the beginning of the research for this thesis, there have been a number of important publications in the fields of TRP channels and K^+ channels in bone cells and other non-excitable cells. Some of the ideas and opportunities created by the data published during this time were able to be incorporated into this Thesis.

Some particularly interesting findings have recently been reported in the field of ion channels and receptors in bone, including identification of functional adenosine receptors (Notini *et al.*, 2007; Vanderschueren, *et al.*, 2008) and androgen receptors (Evans *et al.*, 2006; Orriss *et al.*, 2006), which have clear implication for growth and proliferation. Extracellular calcium concentration is now known to regulate the expression of parathyroid hormone-related peptide (Ahlstrom *et al.*, 2008), thus in turn regulating bone turnover by switching osteoclasts and osteoblasts on or off. In addition, the complement of ion channels known to be expressed in bone cells has increased, and now includes a two-pore domain K^+ channel in osteoblasts which may have a role in mechanotransduction and promote bone remodelling (Hughes *et al.*, 2006), a TTX-sensitive Na^+ channel (Li *et al.*, 2005; Li *et al.*, 2006) (a TTX-insensitive Na^+ channel was reported previously – see above), chloride channels (ClC-3 and ClC-7) which promote osteoclastic bone resorption (Okamoto *et al.*, 2008), and further evidence of voltage-gated K^+ channel expression, including maxi K^+ (Li *et al.*, 2005; Li *et al.*, 2006).

The number of identified roles for K^+ channels in non-excitable cells has expanded to now include apoptosis (Burg *et al.*, 2006) and further evidence strengthens the arguments for the involvement of maxi K^+ channels, and various other K^+ channels, in cancer cell proliferation (e.g. Bloch *et al.*, 2005; Kunzelmann, 2005) and cell volume regulation (Lang *et al.*, 2007).

Similarly, the number of reports of TRP channels expressed in bone and other non-excitable cells has increased during this project from very little (Hoenderop *et al.*, 2003a), to an encouraging list of expressions and functions in a wide variety of tissues. Further evidence has been reported for the increased expression of the cold-sensitive channel TRPM8 in early stage androgen-sensitive prostate cancer compared with normal tissue, and that this channel down-regulates in line with androgen receptor expression, and therefore androgen-sensitivity, and metastasis (Bidaux *et al.*, 2005; Zhang & Barritt, 2006). TRPV6, a highly calcium-selective cation channel, may also be implicated in prostate cancer proliferation (Lehen'kyi *et al.*, 2007) and as TRPV6 expression is mediated by vitamin D (Taparia *et al.*, 2006), channel expression in bone could have implications for calcium regulation. Bianco *et al.*, (2007) show that TRPV6 appears to play a role in calcium homeostasis of the bone. TRPV1 has also been shown to have altered levels of expression in prostate and bladder cancers compared to normal tissues/cells (Lazzeri *et al.*, 2005; Sanchez *et al.*, 2005) and capsaicin appears to inhibit androgen-sensitive prostate cancer progression (Mori *et al.*, 2006).

Recent publications have shown that various TRP channels are expressed in osteoblasts, osteoclasts and osteoprogenitor cells, in which they appear to have roles in fundamental bone cell functions. The highly calcium-selective TRPV5 channel expressed in osteoclasts appears to be necessary for normal osteoclastic function including resorption (van der Eerden *et al.*, 2005). TRPM7 expression is reportedly important for osteoblast cell proliferation (Abed & Moreau, 2007) and TRPM7 mutations in dwarf zebrafish result in defective skeletogenesis phenotypes (Elizondo *et al.*, 2005). Ghilardi *et al.* (2005) have shown that TRPV1 block relieves bone cancer pain, implicating these channels in this particular pain pathway. TRPV1 is also expressed in human osteoclasts and has a putative role in resorption activity (Brandao-Burch *et al.*, 2006), and Arnett's group has extensively researched the effects of pH changes on osteoclast and osteoblast activity, and TRPV1 is emerging as a candidate for the sensor of extracellular pH changes in these cells (Arnett, 2008).

1.3.4.1 Osteoporosis: obesity of the bones?

Two disorders of tissue composition, obesity and osteoporosis, were previously thought to be unrelated, but studies now show similarities between these disorders, with common genetic and environmental factors (e.g. Zhao *et al.*, 2008). With age, bone marrow adipocyte content increases, osteoclast activity increases and osteoblast activity decreases leading to osteoporosis (Rosen & Bouxsein, 2006). Thompson *et al.* (1998) reported that adipocytes and osteoblasts have a common precursor cell, and that differentiation into

adipocytes occurs at the expense of osteoblast maturation. Further supporting the link, several factors and hormones secreted by adipocytes directly influence osteoblast and osteoclast functions and therefore fatty tissue may play a part in regulating bone turnover and composition. For example, leptin, the appetite-suppressant hormone derived from adipocytes, influences bone turnover (Zhao *et al.*, 2008) and may also promote differentiation of mesenchymal stem cell precursors into osteoblasts, rather than adipocytes (Thomas *et al.*, 1999). Also, the inflammatory cytokine interleukin-6 (IL-6), which is secreted by adipocytes, influences bone turnover either as a resorptive factor (Roodman, 1992) or by promoting proliferation or differentiation of osteoblasts (Taguchi *et al.*, 1998; Yoshitake *et al.*, 2008), although it appears not to be essential for normal bone turnover (Franchimont *et al.*, 2005).

Importantly, an interesting and very recent publication shows that TRPV1 is expressed in 3T3-L1 mouse pre-adipocyte cells, and implicates TRPV1 in the regulation of precursor cell differentiation into mature lipid-producing adipocytes (Zhang *et al.*, 2007). What remains unanswered by this article and by the findings of Thompson *et al.* (1998) discussed above, is whether TRPV1 has a role in regulating the differentiation of common precursor cells into either adipocytes or osteoblasts. Clearly, if this is the case, this would make TRPV1 an obvious target for novel drug treatments of diseases such as osteoporosis.

Given that the major focus of this thesis is on TRP channels in osteoblasts, an up-to-date overview of TRP channels now follows, which introduces the

structures, putative functions and electrophysiological characteristics of the

TRP channel superfamily, and the TRP channelopathies currently known. An

overview of the K^+ channels (Ca^{2+}-activated K^+ channels and K_{ATP} channels)

investigated in this thesis can be found in the introduction to chapter 3.

1.4 Transient receptor potential channels – an overview

Recent years have seen a spurt of growth in the scientific interest of the

transient receptor potential, or TRP, family of ion channels, which shows far

from any sign of plateau and is reflected by a proportionately proliferative

output of publications. A quick PubMed search clearly shows this: as of June

2008 at least 1,837 publications exist with "transient receptor potential" in the

title or abstract (Figure 1.3). So, the question is: what are TRP channels and

why the interest?
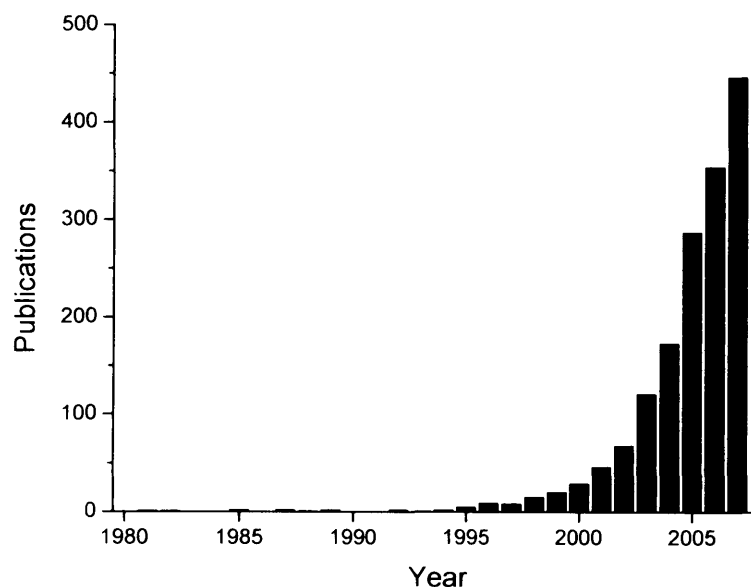
Figure 1.3 Number of publications found by a PubMed search with "transient receptor potential" as part of the title or abstract, by year.

1.4.1 TRP channels: Background

The importance of calcium for the survival and function of animal cells was first described by Sydney Ringer, FRS whose pioneering research showed that calcium was required for the normal contraction of the frog heart (Ringer, 1882). Since this major discovery over 125 years ago, research in living tissues and animal cells has revealed a variety of biological roles for calcium which can be subdivided into four categories: structural, electrical, as a cofactor for extracellular enzymes and proteins, and regulatory (Campbell, 1983). Calcium signalling regulates many essential cellular processes, including muscle contraction, secretion, gene expression and many others (Berridge *et al.*, 2000), which in turn regulate cellular proliferation and apoptosis. The intracellular calcium signal is, in part, controlled by plasma membrane calcium-permeable ion channels which permit an influx of Ca^{2+} ions (Campbell, 1983). Coupled with this, the depletion of intracellular Ca^{2+} stores by endoplasmic reticulum (ER) Ca^{2+} channels stimulates currently undefined Ca^{2+}-permeable channels in the plasma membrane to replenish the stores from extracellular fluid – this is termed store operated calcium entry (SOCE) (Parekh & Putney, 2005).

The relatively recent discovery of a novel superfamily of ion channels called transient receptor potential (TRP) channels has aided the advance in our knowledge of calcium signalling mechanisms. Almost all TRP channels are Ca^{2+} permeable and contribute to cytoplasmic changes in free Ca^{2+} concentration, either by permitting Ca^{2+} entry across the plasma membrane, or Ca^{2+} release from intracellular organelles. The contribution of TRP channels to

calcium signalling and therefore essential functions of the cell are becoming clearer as research into this interesting group of ion channels advances, and there is evidence to suggest that several TRP channels may be implicated in the pathogenesis of disease, either in part or as full channelopathies (Nilius *et al.*, 2007).

1.4.2 TRP channel discovery

The first TRP protein genes were discovered and defined in the fruitfly *Drosophila melanogaster* (Montell *et al.*, 1985; Montell *et al.*, 1989; Hardie & Minke, 1992). Flies with TRP mutant genes expressed photoreceptors that responded transiently to continuous light producing an abnormality in the electroretinogram recording (hence the name *transient receptor potential*), rendering the flies temporarily blind after the initial response to the light (Figure 1.4) due to a lack of sustained Ca^{2+} entry. Wild-type flies produced a sustained response throughout the exposure to light.

The origins of TRP channels are certainly very old as members are found in all *Animalia* in which the full genome has been sequenced, including worm (*Caenorhabditis elegans*), fly (*Drosophila*), mouse, and human (Clapham *et al.*, 2005; Harteneck *et al.*, 2000). The *Drosophila* genome is now known to encode for at least 13 TRPs, and 28 human TRP and TRP-related proteins have been identified to date plus splice variants (Montell, 2005a).
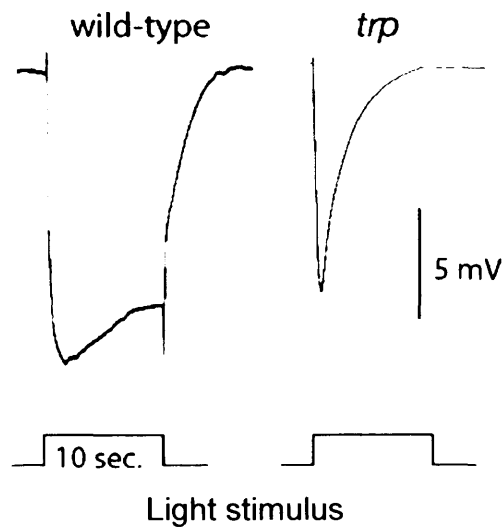
Figure 1.4 Electroretinogram recordings obtained from wild-type and TRP mutant *Drosophila*, showing different responses to 10 second pulses of light (figure adapted from Montell, 2005a).

1.4.3 TRP channel structural homology & nomenclature

All of the TRP channel subunits are putatively built of six-transmembrane domains S1-S6 analogous to so many voltage-gated ion channels, with the S5 and S6 subunits forming the pore of the tetramerically assembled channel and the S5-S6 loop of amino acids forming the channel selectivity filter (Hoenderop *et al.*, 2003c) (Figure 1.5). Both NH_2 and COOH termini are intracellular but vary in length and are poorly conserved throughout the superfamily, whereas the transmembrane subunits are relatively well conserved. Unlike the voltage-gated K^+ channels, the S4 transmembrane domain does not contain the regularly spaced positively charged lysine and arginine amino acids that are thought to be responsible for the voltage gating in the K^+ channels (Long *et al.*, 2005; Montell, 2005b), but several of the

mammalian TRP channels are weakly voltage sensitive although the voltage sensing structure remains to be identified (Nilius *et al.*, 2005). TRP channels are *generally* said to be non-selective (but see p. 27): Ca^{2+}, Mg^{2+}, Na^+, K^+ and other monovalent cations are all permeant to some extent, though in their physiological environment each TRP channel has its own preferential permeability and selectivity.

The most conserved regions within and between subfamilies of the TRPs are parts of the transmembrane domains, the N-terminal 33 amino acid ankyrin repeats, and the highly conserved 25 amino acid region C-terminal to S6 which contains a 6 amino acid chain (EWKFAR) known as the TRP domain because of its unvarying sequence (Ramsey *et al.*, 2006). It must be stressed that even these features are not universal, but other than these the TRP channels are structurally diverse, and TRP sequence length varies from 553 up to 2,022 amino acids in length.
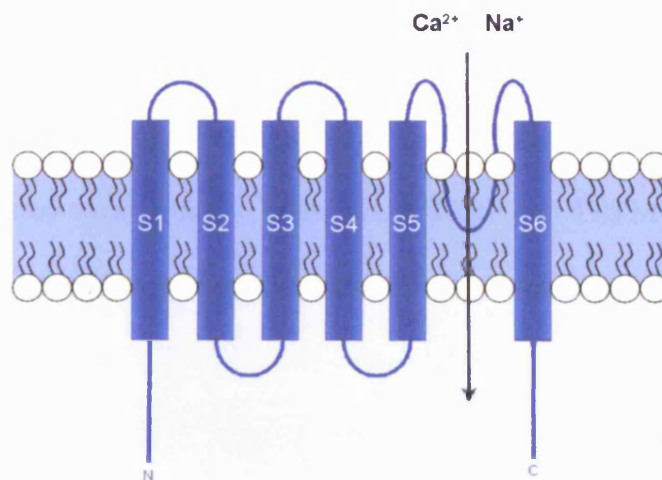
Figure 1.5 **General architecture of the TRP superfamily of ion channels.** This figure shows the S1 to S6 transmembrane domains, with the S5-S6 linking amino acid loop forming the putative pore. Both N and C termini are intracellular, and contain features such as ankyrin repeats (N terminus) and the TRP domain (C terminus).

The TRP superfamily is categorised into seven subfamilies according to amino acid sequence homology and structural similarities as the functions, gating mechanisms and ligand selectivity of the TRP channels are poorly understood (Clapham, 2003; Corey, 2003; Delmas, 2004; Montell *et al.*, 2002a; Montell *et al.*, 2002b; Moran *et al.*, 2004; Pederson *et al.*, 2005). These subfamilies are TRPC (canonical) consisting of 7 channels, TRPM (melastatin) with 8 channels, TRPV (vanilloid) with 6 channels, TRPA (ankyrin) with only 1 member, TRPP (polycystin) and TRPML (mucolipin) each have 3 channels, and TRPN (no mechanopotential) with 1 channel. TRPN has not yet been identified in mammals (Nilius *et al.*, 2007).

Until recently there was no standardisation of the nomenclature, often leading to complex and confusing names that bore no resemblance to channels in the same subfamily. Montell *et al.* (2002b) proposed the current unified nomenclature, which focussed on three of the subfamilies (TRPC, TRPV and TRPM) related to the founding *Drosophila* TRP. Figure 1.6 shows the phylogenetic basis for this nomenclature. These three subfamilies plus TRPA and TRPN have the strongest homology to the founding *Drosophila* TRP and are often referred to as group 1 TRPs, while TRPP and TRPML subfamilies, having more distantly related homologies, make up the group 2 TRPs (Montell, 2004).

TRPC3
TRPC7
TRPC6
TRPC4
TRPC5
TRPC1
TRPC2

TRPV1
TRPV2
TRPV4
TRPV3
TRPV6
TRPV5

TRPM2
TRPM8
TRPM5
TRPM4
TRPM3
TRPM1
TRPM6
TRPM7
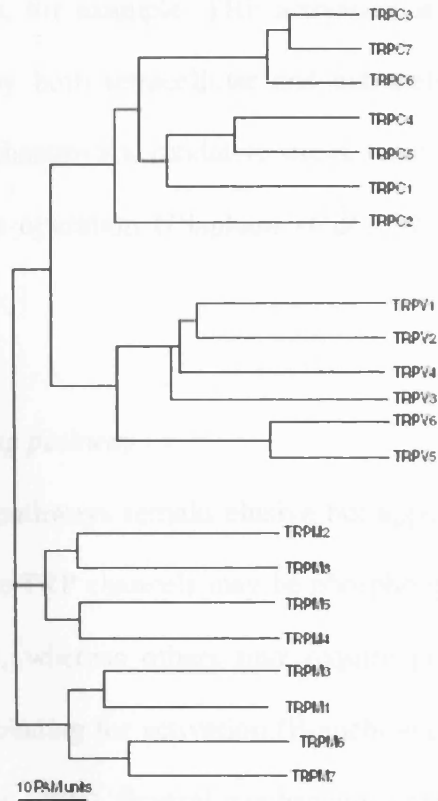
10 PAM units

Figure 1.6. **Phylogenetic relationship between TRPC, TRPV and TRPM subfamilies.** The evolutionary distance is shown by the total branch lengths in point accepted mutation (PAM) units, which is the mean number of substitutions per 100 residues. Here, the unifying nomenclature as recommended by Montell *et al.* (2002b) is used. Figure adapted from Clapham *et al.* (2001).

1.4.4 TRP functional features

Ca^{2+} permeability is one functional feature of almost all TRP channels, with the notable exceptions of TRPM4 and TRPM5 which select for monovalent cations only (Hofmann *et al.*, 2003; Launay *et al.*, 2002). TRPV5 and TRPV6 are highly selective for Ca^{2+}, each with a permeability ratio $P_{Ca}/P_{Na} > 100$ (Den Dekker *et al.*, 2003; Nijenhuis *et al.*, 2003a; Nijenhuis *et al.*, 2003b), but all other TRP channels are relatively non selective. As stated above, voltage sensitivities of TRP channels are heterogeneous and weaker than for voltage-

sensitive K^+ channels, for example. TRP activation is by diverse means and channels are gated by both intracellular and extracellular ligands, chemical stressors such as pH changes and oxidative stress, temperature changes, and the much-discussed store operation (Clapham *et al.*, 2005; Nilius *et al.*, 2003; Ramsey *et al.*, 2006).

1.4.4.1 TRP signalling pathway

The TRP signalling pathways remain elusive but appear to be diverse across the subfamilies. Some TRP channels may be phospholipase-C (PLC) activated (Nilius *et al.*, 2004), whereas others may require phosphatidylinositol 4,5-bisphosphate (PIP$_2$) binding for activation (Brauchi *et al.*, 2007; Lukacs *et al.*, 2007; Voets & Nilius, 2007). Several mechanisms have been proposed which in principle link PLC activation/inhibition and TRP channel opening. The three main and recurring theories are the receptor-operated theory of G-protein activation, the cellular-sensing theory, and the much discussed and contentious store-operated channel theory (Clapham, 2003; Minke *et al.*, 2002).

1.4.4.1.1   Receptor operated theory

The receptor operated theory involves G-protein activation of an unknown messenger which directly and specifically activates a TRP channel. Clapham *et al.* (2003) suggest that this is the most likely mechanism for gating of TRPC channels, as all TRPC channels in mammals can be activated by G protein-coupled receptors (GPCRs): TRPC1, TRPC4 and TRPC5 by muscarinic type 1 receptors, TRPC3 and TRPC6 by histaminergic type 1 receptors, and TRPC7

by purinergic receptors. Unfortunately, identification of this messenger is complicated by the fact that uncoupled G-proteins often activate phosopholipase C (PLC), hydrolysing PIP_2 and forming secondary messengers such as diacyl glycerol (DAG), polyunsaturated fatty acids (PUFAs) and inositol 1,4,5-trisphosphate (IP_3) (Clapham *et al.*, 2003). IP_3 then subsequently activates the IP_3 receptor on the endoplasmic reticulum (ER), releasing intracellular Ca^{2+} from ER stores. However, PIP_2 itself is a candidate as a direct second messenger, and is known to regulate the activity of several ion channels, including TRPV1 and TRPM4, for example (Hilgemann *et al.*, 2001; Voets & Nilius, 2007). The latter authors state that PIP_2 binding promotes TRP channel activation, but in some cases, PIP_2 binding prevents channel gating, and thus hydrolysis by PLC 'frees' the channel for gating. Rohacs *et al.* (2005) have shown that PIP_2 regulates the activation of TRPM8 via the TRP domain and suggest that PIP_2 could be a generic modulator of TRP channels. Unfortunately, this mechanism of PIP_2 activation does not unify all TRP channels. PUFAs or DAG are also candidates for direct activation of TRP channels, but there is no conclusive evidence for this to date.

1.4.4.1.2   Cellular sensing theory

As previously mentioned, all manner of sensations can produce TRP responses: temperature changes, mechanical force and intracellular messengers all activate TRP channels. The principle of the cellular sensing theory is that the total energy transduction to each channel must be large enough to result in gating, and that this energy can be directly imparted by the above forces (Clapham *et*

al., 2003; Minke *et al.*, 2002). The measure of the change in channel opening due to energy transfer can be quantified by the temperature coefficient value Q_{10}, a factor by which the rate of change increases for every 10 °C rise in temperature. Mechanical forces that induce membrane distortion transfer more than enough energy to mechano-sensitive TRP channels to overcome the required threshold energy for channel gating. Ciliated cells may aid this mechanical transduction from sound waves, osmolarity, taste, stretch, etc. The binding of intracellular signalling molecules may also provide enough energy to activate channels, dependent on the binding affinity of each molecule for its receptor. The signal transduction mechanism of temperature-sensitive TRP channels remains unsolved, but may involve protein unfolding and refolding at different temperatures (Brauchi *et al.*, 2004), or perhaps by messengers regulated by an unidentified temperature-sensitive intracellular enzyme (Clapham *et al.*, 2003). Alternatively, temperature-sensitivity of the channels may depend on membrane potential, and that temperature-activation of a channel, either by increased or decreased temperatures, shifts the voltage-dependence of the channel activation towards physiological potentials. In support of this, Voets *et al.* (2004) showed that for TRPM8 the Q_{10} value for channel opening was much smaller than the value for channel closing, and vice versa for TRPV1, indicating channel activation with cooling and heating respectively. This theory is perhaps not unifying for the TRP superfamily, but may hold in part for some TRP channels, such as the temperature-gated channels.

1.4.4.1.3 Store operated channel (SOC) theory

The release of free Ca^{2+} ions from intracellular stores is regulated, at least in part, by G-protein or tyrosine kinase activation of PLC, hydrolysing PIP_2 to form IP_3 which opens IP_3-sensitive ion channels on the endoplasmic reticulum (ER). Depletion of internal Ca^{2+} stores provokes the influx of Ca^{2+} through Ca^{2+}-permeable channels in the plasma membrane, but both the signal for this and the store-operated channels, as they are known, remain elusive. Store operated calcium entry (SOCE) presents as a transient Ca^{2+} influx followed by a high $[Ca^{2+}]_i$ plateau and is dependent on $[Ca^{2+}]_o$ (Clapham *et al.*, 2005; Parekh & Putney, 2005). Channel currents measured in the plasma membrane on store-depleted activation have revealed channels known as I_{CRAC} channels (Ca^{2+} release activated channel) which are highly Ca^{2+} selective. Early excitement that TRP channels may be SOCs has since waned as most TRP channels do not have the necessary electrophysiological characteristics displayed by SOCs (Parekh & Putney, 2005; Venkatachalam *et al.*, 2002). However, several of the canonical TRPs (1-5 and 7) and TRPV6 do show some promise as store operated channels. TRPV6 is particularly interesting as it has several features in common with I_{CRAC} channels, but problematically there are inequalities in voltage-dependent Mg^{2+} blockade and current rectification (Nilius, 2003). So, TRPV6 is perhaps not an I_{CRAC} channel but remains a candidate for a SOC. It would be wrong to call all TRP channels SOCs, but some SOCs could be TRPs.

1.4.5   TRP subfamilies

1.4.5.1 The canonical TRP subfamily (TRPC)

Sharing the closest similarity to the Drosophila TRP sequence, with between 32 % and 47 % overall sequence identity (Schilling *et al.*, 2004), members appear to exist in all cell types tested (Riccio *et al.*, 2002). The canonical subfamily has seven members, plus splice variants, which can be further subdivided into two groups: TRPC1, C4 and C5, and TRPC3, C6 and C7. TRPC2 is a pseudogene in humans (Wes *et al.*, 1995; Zhang *et al.*, 2003), but plays a vital role in pheromone sensing in the vomeronasal organ of rodents (Liman *et al.*, 1999). TRPC2-deficient mice are unable to distinguish between male and female mice (Stowers *et al.*, 2002). Channels of the TRPC subfamily appear to form heteromultimers within the above assigned subgroups, but not between these subgroups (Clapham *et al.*, 2001).
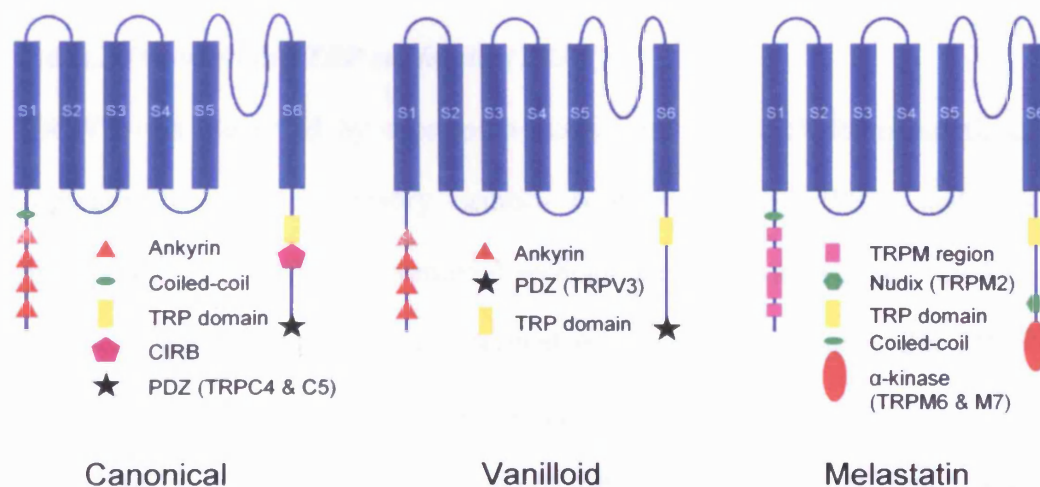
Figure 1.7   **Structural similarities and differences between TRPC, TRPV and TRPM subfamilies**. (CIRB: calmodulin and IP$_3$R binding).

TRPC members are activated by G protein-coupled receptors (GPCR) or receptor tyrosine kinases (TK) linked to PLC. TRPC3, C6 and C7 appear to be regulated by DAG (independent of protein kinase C), whereas TRPC1, C4 and C5 channels are not. TRPC2 may be gated in a similar fashion to TRPC3, C6 and C7 (Clapham *et al.*, 2003; Schilling *et al.*, 2004). Conserved regions of the TRPCs include 3 – 4 N-terminal ankyrin repeats, a proline-rich sequence in the C terminus, and the highly conserved TRP domain (Minke & Cook, 2002). TRPC channels do not exhibit voltage regulation.

Members are between 793 and 1,172 amino acids in length and are non-selective for cations with $P_{Ca}/P_{Na} \leq 10$. TRPC channels are widely expressed with the highest expression in brain, heart, testis and ovary (Wes *et al.*, 1995) but general functions are unknown, although possible roles exist in proliferation in the CNS and prostate cancer (Wissenbach *et al.*, 2004a).

1.4.5.2 The vanilloid TRP subfamily (TRPV)

TRPV1 was identified by expression cloning in the search for a functional capsaicin receptor in sensory neurons (Caterina *et al.*, 1997), and was originally termed VR1, for vanilloid receptor subtype 1 as it is activated by capsaicin, a vanilloid compound derived from hot chilli peppers. Six TRPV members in total are known to exist (Caterina *et al.*, 1999; Hoenderop *et al.*, 2003a; Peier *et al.*, 2002b; Peng *et al.*, 1999; Strotmann *et al.*, 2000) plus several splice variants (Lu *et al.*, 2005; Wang, C. *et al.*, 2004) which likely form channels as heteromeric or homomeric tetramers (Kedei *et al.*, 2001;

Kuzhikandathil *et al.*, 2001). TRPV channels are activated by chemical and mechanical stimuli, lipids, pH changes and hot and cold temperatures, and although their functions have not generally been determined, at least some of the TRPV members have a role to play in nociception and thermosensation. Mechanisms of signal transduction in the TRPV subfamily are largely unknown.

Conserved structural features within the TRPVs are 3 - 4 N-terminal ankyrin repeats, and a less conserved C-terminal TRP domain. Members of the TRPV subfamily are between 725 and 871 amino acids in length, and are relatively non-selective with the notable exceptions of TRPV5 and TRPV6, which both have high selectivity for Ca^{2+} ions ($P_{Ca}/P_{Na} > 100$).

TRPV1, V2, V3 and V4 are temperature sensitive channels, and several TRPVs are upregulated by translocation to the plasma membrane in response to cell swelling in hypotonic solutions (Liedtke *et al.*, 2000; Muraki *et al.*, 2003; Strotmann *et al.*, 2000) and in response to insulin-like growth factor 1 (IGF-1) (Kanzaki *et al.*, 1999). TRPV5 and TRPV6 are the two non-temperature sensitive members of the TRPV subfamily and share 66% identity (Clapham *et al.*, 2001). Both TRPV5 and V6 are the only TRPs that are highly Ca^{2+} selective ($P_{Ca}/P_{Na} > 100$) and strongly *inwardly*-rectifying, which suggests a role in Ca^{2+} uptake. They are expressed in prostate, kidney, ileum and placenta tissues, and are thought to be involved in epithelial transport of Ca^{2+} (Den Dekker *et al.*, 2003; Nijenhuis *et al.*, 2003a; Nijenhuis *et al.*, 2003b). As these

processes are regulated by 1,25-dihydroxyvitamin D3 and parathyroid

hormone, there may be a role for these two TRPV members in other tissues in

which Ca^{2+} transport is important, such as bone.

1.4.5.2.1 TRPV1

As mentioned above, TRPV1 was originally identified by Caterina *et al.* (1997)

by expression cloning with capsaicin in dorsal root ganglia, but is also

expressed in brain, heart, skeletal muscle, lung, liver, pancreas, kidney, colon,

bladder, spleen, thymus and neutrophils. It is a relatively nonselective cation

channel ($P_{Ca}/P_{Na} \sim 10$) with a single channel conductance of about 80 pS, a

reversal potential (E_{rev}) of ~ 0 mV and an outwardly rectifying I/V relationship.

Heat > 42 °C activates the channel, along with capsaicin and other more

recently identified ligands: the capsaicin analogue, resiniferatoxin (Raisinghani

et al., 2005), the cannabinoid anandamide (Smart *et al.*, 2000), the compound

responsible for the pungency of garlic, allicin (Macpherson *et al.*, 2005), and

olvanil (Appendino *et al.*, 2005), and also acidic cytoplasmic conditions (Ryu

et al., 2003). Channel blockers include ruthenium red, the synthetic vanilloid

receptor antagonist capsazepine (Bevan *et al.*, 1992), the more selective

compound SB366791 (Rami *et al.*, 2004), PIP_2 (Chuang *et al.*, 2001) and

adenosine (Puntembekar *et al.*, 2004). A splice variant has been identified and

termed TRPV1b, which has an N-terminal 60 amino acid deletion which

includes a deletion of one of the ankyrin repeats. This shortened variant is

activated by temperatures > 44 °C, but is not activated by capsaicin or any of

the other known ligands or pH 5.0 (Lu *et al.*, 2005). Additionally, capsazepine

does not inhibit the heat-induced currents of this splice variant, but ruthenium red was able to completely abolish them. TRPV1 is known to play a role in pain sensation pathways and has been linked with heat hyperalgesia following trauma (Pogatzki-Zahn et al., 2005). Anandamide may cause vasodilatation via TRPV1, and also the channel participates in bladder purinergic signalling (Birder et al., 2002) but the functions of TRPV1 in other tissues are less clear.

Interestingly, the activation of TRPV1 in sensory nerve fibres may be potentiated by or sensitized to temperature and protons by inflammatory mediators such as ATP (Tominaga et al., 2001), bradykinin and nerve growth factor (Chuang et al., 2001). TRPV1 activation and resultant cytosolic Ca^{2+} increase in primary afferent spinal cord nerve terminals results in enhanced adenosine release (Cahill et al., 1993a; Cahill et al., 1993b; Sweeney et al., 1989) which promotes analgesia through adenosine A_1 and A_{2A} receptor activation (Sawynok & Liu, 2003). Puntembekar et al. (2004) have shown that in TRPV1-transfected HEK-293 cells, adenosine does indeed act as an inhibitor of both capsaicin- and resiniferatoxin-induced TRPV1 channel activity and that adenosine analogues have similar effects, all by direct interaction with the TRPV1 receptor and competing with capsaicin and resiniferatoxin binding.

1.4.5.3 The melastatin TRP subfamily (TRPM)

Named after the founding member, melastatin (termed TRPM1) (Duncan et al., 1998), the TRPM subfamily has eight members which can be further

subgrouped into four pairs of homologous channels: TRPM1 and M3; M2 and

M8; M4 and M5; and M6 and M7 (Fleig *et al.*, 2004). Functional properties of

the TRPMs are diverse, as are the gating mechanisms, regulation, current-

voltage relationships and voltage-dependence, but the possibility of

heteromultimeric tetramers seems likely, particularly for each pair: M6 and M7

are already known to coassemble (Chubanov *et al.*, 2004). Splice variants have

been identified for the first five TRPM channels (Fleig *et al.*, 2004) and could

occur for all eight, leading to further diversity and complexity within this

subfamily. Unique within the TRP superfamily are TRPM2, M6 and M7,

which also have enzymatic properties (Cahalan, 2001; Runnels *et al.*, 2001).

The TRPM subfamily was originally termed TRP-L (long) due to the length of

the N-termini. The diverse characteristics of the members of the TRPM

subfamily may be due, at least in part, to the varied C-terminal lengths and

structures, with the protein lengths ranging from 1,104 to 2,022 amino acids.

Ankyrin repeats are not conserved in the N-termini, which instead contain four

regions of amino acids that share similarity within the subfamily known as the

TRPM homology region. N-terminal coiled-coil domains may play a role in the

formation of the tetrameric channels (Fleig *et al.*, 2004). On the C-termini the

TRP domain is conserved and TRPM2 has a Nudix enzymatic domain

(nucleoside diphosphate pyrophosphatase) that binds ADP-ribose which gates

the channel (Perraud *et al.*, 2001). TRPM6 and TRPM7 also have C-terminal

enzymatic activity in the form of α-kinase (phospholipase C-interacting kinase,

or PLIK) (Fleig *et al.*, 2004).

TRPM channels display variable Ca^{2+} and Mg^{2+} permeabilities: TRPM4 and

M5 are Ca^{2+}-impermeable, whereas TRPM6 and M7 are highly permeable to

Ca^{2+} and Mg^{2+}. Activation mechanisms of the TRPMs include oxidative stress

and heat (TRPM2), mechanical stimuli (TRPM3), $[Ca^{2+}]_i$ increases and heat

(TRPM4 and M5), $[Mg^{2+}]_i$ and $[MgATP]_i$ (TRPM6 and M7), and cooling

agents or cold (TRPM8) (McKemy *et al.*, 2002; Peier *et al.*, 2002a). Duncan *et*

al. (2001) have shown that downregulation of TRPM1 in primary melanomas

is a prognostic marker for metastasis, showing that TRPM1 is clearly involved

in cell proliferation and differentiation. TRPM7 is also thought to be

responsible for Mg^{2+} transduction and may also be important for cell

proliferation and viability (Nadler *et al.*, 2001) due to its role in cellular Mg^{2+}

homeostasis (Schmitz *et al.*, 2004). The sensitivity of TRPM2 to oxidative

stress suggests a role in apoptosis (Fleig *et al.*, 2004; Hara *et al.*, 2002). The

expression of TRPM8 in prostate cancer cells (Bidaux *et al.*, 2005; Tsavaler *et*

al., 2001) suggests perhaps a proliferative role. Bidaux *et al* (2005) report that

TRPM8 expression requires a functional androgen receptor, so TRPM8 is

androgen-dependent, and TRPM8 ligands could possibly be used to target

prostate cancer growth and treat this disease.

1.4.5.4 Other TRP subfamilies

TRPA

TRPA1 (ankyrin) is a cold-sensitive, Ca^{2+}-permeable nonselective channel

activated by temperatures < 15 °C and icilin but not menthol, and is found to

be co-expressed with TRPV1, but not TRPM8 (Story *et al.*, 2003). TRPA1 contains 14 N-terminal ankyrin repeats.

TRPML

The mucolipins (TRPML) are involved in Mucolipidosis Type IV (TRPML1) and Ashkenazi Jewish alleles (TRPML2 & TRPML3) (Wissenbach *et al.*, 2004b), a neurodegenerative lysosomal storage disorder, and affect the late endocytic pathway (Clapham *et al.*, 2001).

TRPP

The Ca^{2+}-permeant polycystic kidney disease proteins TRPP2, TRPP3 and TRPP5 may result in polycystic kidney disease when the channel is mutated and function is lost (Wissenbach *et al.*, 2004b).

TRPN

TRPN channels have not been identified in mammals, but are present in fish, insects and nematodes and appear to be involved in mechanosensory transduction (Wissenbach *et al.*, 2004b).

1.4.6 TRP-related diseases and channelopathies

Given the presumed roles of TRP channels in cellular proliferation, differentiation and apoptosis, it is likely that channel dysfunctions manifest as various diseases. Indeed, at least five TRP channelopathies have been identified to date due to defective genetic encoding of TRP channels, namely

focal segmental glomerulosclerosis (TRPC6 mutation), hypomagnesaemia and secondary hypocalcaemia (TRPM6 mutation), autosomal dominant polycystic kidney disease (TRPP1/2 mutations), mucolipidosis type IV (TRPML1 mutation), and Guamanian amyotrophic lateral sclerosis/Parkinsonism dementia (TRPM7) (Nilius *et al.*, 2007).

Other diseases relate to the functions of TRP channels (e.g. the temperature sensitive TRPs in pain sensation (Caterina *et al.*, 1997)), or the expressions (e.g. TRPM8 is upregulated in androgen-dependent prostate cancers (Tsavaler *et al.*, 2001)). Clearly in these cases, TRP channels are obvious targets for new drugs, and certainly a great deal of research is currently being pursued to target TRPV1, for example in the treatment of neuropathic and bladder pain (Dray, 2008; Tamayo *et al.*, 2008; Wang, 2008; Birder, 2007).

1.5 Hypothesis, aims, and experimental strategies

The principle hypothesis of this thesis is that ion channels belonging to the transient receptor potential channel superfamily and to the K^+ channel superfamily are expressed, active and functional in human osteoblasts, where they are involved in the regulation of key cellular processes such as proliferation, differentiation, secretion and apoptosis.

In light of the advances in TRP channel research and the recent evidence for the putative functions of TRP channels in non-excitable cells, especially osteoblasts and osteoclasts, and given that bone disorders such as osteoporosis

are so costly, in terms of reduced quality of life, increased risk of death due to a serious fracture, and financial burden on the health services, it seems pertinent to pursue research into the role of TRP channels in bone. Of course, idealistically the long term goal would be to develop drugs that target TRP channels to address the imbalance in bone remodelling that forms the basis of many bone disorders. However, as the roles of TRP channels in osteoblasts and osteoclasts are still emerging, research must for now concentrate on developing and mapping out these roles, discovering new roles, and understanding the machinery of the channels and signalling cascades, including that of the universal regulator, Ca^{2+}. It is emerging that TRPV1 has putative key roles in the fundamental cell functions of osteoblasts, and is likely to be an important target for new therapies.

The key aims of this thesis were:

1   to establish working *in vitro* cultures of human osteoblast-like cells in the laboratory, including the non-mineralising MG63 and mineralising SaOS-2 cell lines, the mouse 7F2 mineralising osteoblast cell-line which also has the ability to undergo complete adipocyte differentiation, and HOB-c human primary mineralising osteoblasts.

2   to show whether or not selected TRP channels, maxi K^+ channels and K_{ATP} channels are expressed at messenger (mRNA) level, and later at protein level in the membrane, in human osteoblasts and osteoblast-like cells and mouse 7F2 cells.

3   to identify and characterise any channels found electrophysiologically using the patch-clamp technique, with appropriate channel agonists and antagonists or blockers, with particular emphasis on the maxi K channel and the heat- and capsaicin-sensitive channel, TRPV1.

4   to test whether the above channels are involved in key functional processes in osteoblasts, including proliferation, mineralisation and differentiation, which have obvious consequences for bone mineral density.

5   to test whether TRPV1 is directly involved in calcium signalling in osteoblasts, using recognised TRPV1 ligands and fluorescent calcium-chelating dyes.

1.5.1 Experimental strategies

In order to fulfil the above aims, a host of experimental techniques were employed including reverse transcription polymerase chain reaction (RT-PCR) for messenger RNA detection, gene sequencing for validation of RT-PCR products, the patch-clamp technique (as described by Hamill *et al.*, (1981) for electrophysiological recording of ion channel activity, cell counting by means of haemocytometry and MTS-dye conversion measurements, osteoblast cell mineralisation and differentiation assays, and free-Ca^{2+} imaging with fluorescent dyes using confocal microscopy.

CHAPTER 2:

METHODS & MATERIALS

2 METHODS & MATERIALS

2.1 Cell Culture

2.1.1 Culture media

Specific culture media were selected for each cell-type according to instructions from the respective suppliers. Prepared culture media were kept refrigerated between 2 and 8 °C and warmed to room temperature or 37 °C prior to use. Generally, media were used within 14 days of preparation or discarded. All cell culture media ingredients, unless otherwise stated, were obtained from Gibco®, Invitrogen Ltd., Paisley, UK.

DMEM for MG63, SaOS-2 and HOB-c cell culture

Dulbecco's modified Eagle medium (DMEM) containing L-glutamine, pyruvate and 4.5g l^{-1} glucose was supplemented with 5% foetal bovine serum (FBS) and with 100 μg ml^{-1} streptomycin and 100 U ml^{-1} penicillin (Penicillin-Streptomycin 10,000: 10,000, Invitrogen).

DMEM for DU145 cell culture

As above but supplemented with 10% FBS.

RPMI 1640 for LNCaP and MCF-7 cell culture

Roswell Park Memorial Institute (RPMI) 1640 culture medium was supplemented with 10% FBS, 100 μg ml^{-1} streptomycin and 100 U ml^{-1} penicillin.

MEM-α for 7F2 cell culture

Alpha minimum essential medium, containing Earl's salts, 1 mM sodium pyruvate and 2 mM L-glutamine, but without ribonucleosides or dexoxyribonucleosides, was supplemented with 10% FBS, 100 μg ml^{-1} streptomycin and 100 U ml^{-1} penicillin.

7F2 cell adipocyte differentiation medium

This medium was based on the above MEM-α for 7F2 cell culture, but further supplemented with 50 μM indomethacin, 50 μg ml^{-1} ascorbic acid and 100 nM dexamethasone (all supplements from Sigma) to induce adipocyte differentiation (Thompson *et al.*, 1998).

2.1.2 Cell husbandry

MG63, SaOS-2 and HOB-c cells were kindly supplied by Dr B.A.J. Evans, Department of Child Health, School of Medicine, Cardiff University. MG63 human osteosarcoma cells are originally derived from a 14-year-old male

(Heremans *et al.*, 1978). SaOS-2 human primary osteogenic sarcoma cells are derived (Fogh & Trempe, 1975) from an 11-year-old female Caucasian (ATCC). HOB-c human primary osteoblast cells are derived from the normal hipbone of a 64 year old Caucasian female during routine operation. Passage numbers 3 and 4 were obtained from PromoCell GmbH, and maintained as proliferating cultures. PromoCell confirm that the cells are positive for osteocalcin by immunofluorescence, and maintain their osteoblast phenotype for at least 10 passages.

Rat osteoclasts (kindly supplied by Dr B.A.J. Evans) were derived from monocytes/macrophages (from rat bone marrow), by supplementation of α-MEM (containing 10% FBS) with macrophage colony-stimulating factor (M-CSF) and RANKL to encourage osteoclast differentiation.

LNCaP, DU145 and MCF-7 cells were kindly supplied by the Tenovus Centre for Cancer Research at Cardiff University. LNCaP human Caucasian prostate carcinoma cells are originally derived (Horoszewicz *et al.*, 1983) from 'a metastasis at the left supraclavicular lymph node of a 50 year old patient with a confirmed diagnosis of metastatic prostate carcinoma' (ECACC) and are androgen-sensitive. DU145 human metastatic prostate carcinoma cells are derived (Stone *et al.*, 1978) from 'a lesion in the brain of a patient with metastatic carcinoma of the prostate and a 3 year history of lymphocytic leukaemia' (ATCC) and are not sex-hormone sensitive. MCF-7 human

Caucasian breast adenocarcinoma cells are originally derived (Soule *et al.*, 1973) from the pleural effusion of a 69-year-old female Caucasian (ATCC).

All cells were cultured in 25 cm^2 or 75 cm^2 flasks and incubated at 37 °C in 5% CO_2 humidified air, with a working volume of 3 ml or 9 ml medium, respectively. Confluent cultures were divided weekly and cell medium was replaced every 3 - 4 days. To detach cells, cultures were washed with 1× D-PBS (calcium- and magnesium-free, Gibco®, Invitrogen Ltd.) and then 500 µl trypsin solution (trypsin 0.025 %, EDTA 0.2 %) (trypsin from bovine pancreas, Sigma; EDTA, Sigma) per 25 cm^2 was added for up to 10 minutes. When cells were detached, 2 - 3 ml of culture medium was added to stop the trypsinisation and cells were evenly suspended by gentle repeated pipetting. The suspension was centrifuged at 500 ×g for 3 minutes at room temperature to pellet the cells, the supernatant was aspirated and replaced with culture medium. The pellet was resuspended and aliquots were pipetted accordingly into flasks.

2.1.3 Cell-seeding onto coverslips

Cells were detached as above, resuspended in medium and centrifuged at 500×g for 3 minutes to form a pellet. The supernatant was removed by aspiration and the pellet of cells was resuspended in a known volume of the working culture medium. Cells were counted using a Neubauer haemocytometer (see below) and then a new suspension was created of density 3,000 or 5,000 cells per 100 µl. Heat-sterilised 16 mm diameter circular glass coverslips (Best - Gerhard Menzel) in 6-well plates were seeded with 3,000 or

5,000 cells and left to attach in the incubator for several hours before topping up the culture medium to 2 ml per well. All cell types were usually attached and considered ready for electrophysiological recording after approximately 24 hours.

2.2 Cell counting

2.2.1 Haemocytometry

Haemocytometry is the process of counting cells to determine the density of a cell suspension. The Neubauer haemocytometer is a slide with two flat chambers, each engraved with a microscopic grid of 1 mm squares, and when fixed with a coverslip the chambers have a depth of 0.1 mm. Thus, each 1 mm × 1mm square of depth 0.1 mm has a volume of 0.1 μl. The coverslip is properly attached to the slide when the interference patterns known as Newton's rings can be seen.

Cells were detached and pelleted as above (see section 2.1.2), and the pellet of cells was resuspended evenly in a known volume of culture medium. 8 μl of suspension was pipetted into each of the haemocytometer chambers and allowed to be drawn in by capillary action. At 10× magnification under a microscope, the central 1 mm^2 square of one chamber was found and all cells within the boundaries were counted including cells that lay on the top and left-hand boundary lines, but not those on the right or bottom to ensure only 1 mm^2 was counted. If the square contained less than 100 cells, one or more additional

squares in the same chamber were counted to improve accuracy. Counting was

also performed on the second chamber in the same way.

The average of the counts was calculated and the density of the cell suspension

was determined using the equation:

$$CD = n_{av}/v$$

where CD is cell density, n_{av} is average number of cells counted, and v is

volume in ml. Effectively, as the volume counted is 10^{-4} ml:

$$CD = n_{av}/10^{-4} \quad \text{or} \quad CD = n_{av} \times 10^{4}$$

2.2.2 Cell counting by dye-conversion assay

Cells were counted and then seeded into the central 60 wells of 96-well plates

(*i.e.* omitting the 36 wells around the perimeter)[*] at 3,000 cells per well in 100

µl and left to settle for 24 hours in culture medium under normal growth

conditions (see above). The medium was then aspirated and replaced with

medium containing various concentrations of test drugs and incubated for 2 to

7 days in the usual conditions unless otherwise stated. For the assay, the

CellTiter 96 AQ$_{ueous}$ Non-radioactive Cell Proliferation Assay (Promega)

protocol was followed using the tetrazolium compound MTS[†] and the electron

coupling reagent PES[‡] combined in the ratio 20:1, such that 20 µl of the

---

[*] Cultures in the perimeter wells have been observed in the laboratory to grow at a different
rate to the central wells. Culture media containing phenol red indicates a pH difference here.
[†] 3-(4,5-dimethylthiazol-2-yl)-5-(3-carboxymethoxyphenyl)-2-(4-sulfophenyl)-2H-tetrazolium
[‡] Phenazine ethosulfate

MTS/PMS mixture was added to each test well on top of the 100 µl test medium. Results were read with a Tecan® ELISA plate reader at 490 nm following 1 – 4 hours incubation in the dark at 37 °C. Figure 2.1 shows that there is a linear correlation between MG63 cell number and absorbance at 490 nm between 0 and 25,000 cells (typical culture density range).
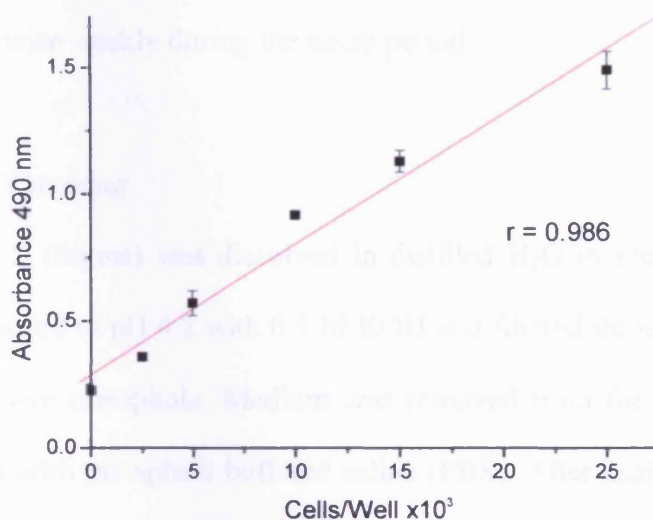
Figure 2.1. Correlation curve of absorbance/MG63 cell number for MTS assay. Cells in DMEM were added to wells and allowed to equilibrate for 1 hour, then MTS/PMS was added. After 1 hour at 37 °C, absorbance at 490 nm was measured using an ELISA plate reader. Each point represents mean ± SE of 4 replicates. Background absorbance at zero cells/well was not subtracted.

2.3   Cell function assays

2.3.1   Mineralisation assays

Assay cultures of SaOS-2 or 7F2 cells were incubated for up to 14 days in cell-specific growth medium (see above) with 50 µg ml^{-1} L-ascorbic acid 2-phosphate and 2 mM β-glycerol 2-phosphate (Sigma) at a density of 100,000 cells per well in 6-well plates for SaOS-2 cells, and 10,000 cells per well in 24-well plates for 7F2 cells. Test compounds and the β-glycerol 2-phosphate were not added until day 2 of the assay and then media and test compounds were replenished twice weekly during the assay period.

Alizarin red S staining

Alizarin red S (Sigma) was dissolved in distilled H$_2$O to prepare a 1% w/v solution, adjusted to pH 4.2 with 0.5 M KOH and filtered through coarse filter paper to remove precipitate. Medium was removed from the wells and cells were washed with phosphate buffered saline (PBS). After aspirating the PBS, cells were fixed with formal saline (10% formaldehyde in PBS) for 15 minutes, then washed with distilled H$_2$O and allowed to dry completely. Fixed and dried cells were stained with 1% alizarin red S stain for 5 minutes, then the stain was aspirated and cells were washed 5× with 50% ethanol to remove excess stain, leaving the last wash on the cells for 15 minutes. After removing the final wash, cells were left to dry completely. Stained mineral nodules in wells were photographed at 100× - 400× magnification.

2.3.2 Adipocyte differentiation assays (7F2 cells)

Mouse primary bone marrow stromal (7F2) cells, which have the ability to differentiate into adipocytes under certain conditions, were used for these assays. Cells were seeded into 24-well plates at a density of 10,000 cells/well and left overnight to attach in 7F2 culture medium. The next day, the medium was aspirated and replaced with adipocyte differentiation medium and test compounds. Cultures were incubated under the usual conditions for 7 days, and medium/test compounds were replenished every 2 - 3 days.

Oil red O staining for lipids

A 0.5% w/v stock solution of stain was prepared by dissolving Oil Red O (Sigma) in isopropanol. An Oil Red O working solution was prepared by mixing 6 parts Oil Red O stock solution with 4 parts distilled water (e.g. for 10 ml working solution, mix 6 ml Oil Red O stock solution with 4 ml distilled water). The staining procedure was as follows: the medium was aspirated from the cells, wells were washed with PBS and the cells were fixed with formal saline (10% formaldehyde in PBS) for 15 minutes. Cells were then washed 2× with distilled water and allowed to dry completely. Stain was applied to each well and incubated for 15 minutes on a plate rocker, and then wells were washed with 60% isopropanol to remove excess stain, followed by several washes with PBS until no further pink colour could be removed. Cells were stored in PBS and photographed under the microscope. Lipids droplets were stained pink/red.

2.4 Electrophysiology

2.4.1 Physiological recording solutions

Physiological solutions were routinely prepared as required and stored at 2 - 8 °C for up to one week when not in use. All chemical components were obtained from Sigma and were prepared in distilled H_2O. Table 2.1 lists the composition of each solution. 'Extracellular' physiological solutions high in Na^+ ion content were termed 'Locke' solutions (sodium chloride Locke or sodium gluconate Locke as appropriate) and will be referred to as such from here on. Following unsuccessful attempts to detect TRPV1 in Ca^{2+}-containing solutions, low- and zero-Ca^{2+} solutions were prepared to minimise possible TRPV1 channel desensitisation (see *e.g.* Koplas *et al.*, 1997), particularly within the interval between seal formation and the start of recording. Drug solutions were prepared in an appropriate physiological solution suitable for experimental requirements, from drug stock solutions as specifically stated. All electrophysiological solutions were filtered on application through a non-sterile 0.2 μm PVDF-membrane 4 mm syringe filter (Whatman).

2.4.2 Electrode fabrication

Recording electrodes were pulled from 1.5 mm outside-diameter, 0.86 mm inside-diameter borosilicate glass capillaries (GC150-F10, Harvard Apparatus Ltd.) by one of two available means:

    (i)   a Narashige PP-83 two-stage vertical electrode puller set to produce two equal length electrodes with an outside tip diameter of

approximately 1 μm. These were then heat-polished using a

Narashige MF-83 microforge to smooth the tip.

(ii)   a DMZ-Universal Puller (Zeitz-Instruments GmbH), set to pull and

heat-polish two equal-length electrodes, again with an outside tip

diameter of approximately 1 μm.

Reference electrodes were pulled in the same way but were not heat-polished

and the electrode tips were gently broken back slightly to reduce the resistance

of the electrode to < 1 MΩ to minimise contribution to the overall resistance of

the circuit. The reference electrodes were backfilled as standard with NaCl or

Na gluconate Locke using a Microfil 34G fused-silica syringe needle to create

a salt-solution reference. Recording electrodes were backfilled in the same way

with an appropriate recording solution.

Table 2.1 **Chemical composition of physiological solutions**

	NaCl Locke (mM)	Na gluconate Locke (mM)	High K$^+$ solution (mM)	TRP K gluconate solution (mM)	TRP Na gluconate solution (mM)
NaCl	150	-	5	-	10
NaGluc	-	150	5	-	140
KCl	3	3	140	2.5	-
KGluc	-	-	-	140	-
CaCl$_2$	2	2	1*	-	-
MgCl$_2$	2	2	1	1	1
HEPES	10	10	10	5	5
EGTA	-	-	11	1.5	1.5
D-glucose	10	10	-	-	-
pH	7.4	7.4	7.2	7.35	7.35

* free [Ca^{2+}] has been measured as 30 nM by ion sensing electrode.
NB: Sodium-based solutions were adjusted to desired to pH with NaOH or HCl, and potassium-based solutions were adjusted with KOH or HCl.

2.4.3 Electrophysiology apparatus

An Ag-AgCl recording wire was connected to an I-V converter amplifying headstage (CV4, Axon Instruments) mounted on a Narishige HW-3 three-dimensional hydraulic micromanipulator. Electrical activity was represented visually on a Gould 400 oscilloscope (Gould Instrument Systems). Signals were amplified by an Axopatch 1D amplifier (Axon Instruments) with filter cut-off at 5 kHz (unless otherwise stated) by a -3 dB, four pole Bessel filter, and then digitised at 20 kHz (unless otherwise stated) by a 12-bit AD converter (Digidata 1200A, Axon Instruments).

Due to the sensitivity of the patch-clamp technique, recordings were acquired within a Faraday cage surrounding an anti-vibration table (TMC 63-540) supplied by a Jun-Air Compressor Model 3, in order to minimise electrical and vibrational interference. As much as possible, all metallic apparatus and electronic instruments in use were electrically earthed, and mains circuitry supplying the apparatus was surge-protected.

2.4.4 Patch-clamp methodology

Cells were cultured on 16 mm circular glass coverslips at seeding densities of 3,000 or 5,000 cells (see 2.1.3). Cultures were inspected by microscope before use to check they were healthy-looking (clean membranes, agranular) and subconfluent. In a class 2 laminar-flow cabinet, a coverslip was rinsed with the bathing solution and transferred to a Perspex recording chamber, using a small amount of petroleum jelly to hold it in place. Approximately 50 μl of bathing

solution was gently dropped onto the coverslip to form a convex meniscus of solution. The Perspex recording chamber was then transferred to the stage of the inverted microscope set on the antivibration table, and the reference electrode tip was placed into solution. At 100× magnification, the coverslip was visually scanned for physically isolated cells, which offered a higher seal success rate than tight clusters of cells or confluent cultures. At 400× magnification, a cell was chosen to patch-clamp that was phase-bright, agranular and preferably not in contact with another cell. A recording electrode was backfilled with the appropriate solution and threaded over the Ag-AgCl wire and sealed into place. The electrode tip was advanced into solution and positive pressure was applied to prevent the build-up of debris on the tip. Any junction potential[*] that appeared was adjusted to zero with the DC offset on the amplifier (true junction potential corrections were made during data analysis as described in section 3.3.1.1.1). A 20 mV DC oscillating square-wave pulse (seal test) was applied across the electrode tip so that the electrode resistance could be determined from the current amplitude seen on the oscilloscope, using Ohm's Law ($R = V/I$). Ideal electrode resistances[†] were between 4 and 8 MΩ with High K^+ solution in the electrode and NaCl Locke as the bathing solution.

The recording electrode tip was advanced towards the cell using the micromanipulator and contact was seen both by the appearance of a halo around the electrode tip on the cell membrane and an increase in electrical resistance in the seal test. Positive pressure was removed and gentle suction

---

[*] A junction potential is created when two solutions with different compositions come into contact, and is created by different concentrations of ions with different ionic mobilities.

[†] The resistance gives a good indication of electrode reproducibility.

applied to form a seal, with application of depolarising voltage (typically around 60 mV) in some cases to encourage seal formation. Seals with electrical resistance in the giga-Ohm range (a giga-seal) were typically achieved quickly in a matter of seconds, but occasionally took up to 3 or 4 minutes with gentle encouragement by applying voltages, as above.

The patch-clamp techniques, as described by Hamill *et al.* (1981), were used to form desired patch configurations, and recordings were begun soon after at room temperature (20 – 26 °C) unless otherwise stated. Coverslips were discarded after approximately one or two hours because cells began to deteriorate significantly after this period.

2.4.5 Data acquisition and analysis

For cell-attached or excised patches, recordings of (usually) thirty seconds and between ±200 mV were made onto the hard-disk of a PC and saved as PAT files or EDR files, using Windows Electrophysiology Disk Recorder (WinEDR) software (Dr J. Dempster, University of Strathclyde). Data were regularly written to compact disk for analysis on a different PC, and for back-up/storage purposes. For cell-attached and inside-out patch-clamp configurations, voltages and currents were inverted during analysis; the terms 'depolarisation' (more positive) and 'hyperpolarisation' (more negative) used with regard to these configurations therefore refer to patch membrane potential rather than patch holding potential throughout this Thesis.

Cell-attached and excised patch data recordings were analysed using WinEDR v2.2.4 or v2.5.9. Origin 7 software (OriginLab®) was used to perform statistical tests and to plot graphs. In statistical tests, significance was set at the 0.05 level. Data are presented as mean ± SEM where n > 1.

2.4.6 Junction potential adjustments

To achieve true reversal potential values, liquid junction potentials were calculated and adjustments were made accordingly throughout the Thesis as described: the magnitudes of the junction potentials were calculated using the generalised Henderson Liquid Junction Potential Equation (quoted from Barry & Lynch, 1991), giving the potential E of bathing solution S with respect to pipette solution P, by:

$$E^S - E^P = (RT/F)S_F \ln \left\{ \sum_{i=1}^{N} z_i^2 u_i a_i^P \bigg/ \sum_{i=1}^{N} z_i^2 u_i a_i^S \right\} \qquad (Eqn. \ 2.1)$$

where

$$S_F = \sum_{i=1}^{N} [(z_i u_i)(a_i^S - a_i^P)] \bigg/ \sum_{i=1}^{N} [z_i^2 u_i (a_i^S - a_i^P)] \qquad (Eqn. \ 2.2)$$

and where N represents the number of polyvalent ions, and u, a and z respectively represent mobility, activity and valency of each ion. The above complex equations can be simplified according to Barry & Lynch (1991) into the following equation for a simple bi-ionic setup:

$$E^S - E^P = \frac{RT}{F} \frac{[a^S(u^S_+ - u^S_-) - a^P(u^P_+ - u^P_-)]}{[a^S(u^S_+ + u^S_-) - a^P(u^P_+ + u^P_-)]} \cdot ln \frac{[a^P(u^P_+ + u^P_-)]}{[a^S(u^S_+ + u^S_-)]}$$

<div align="right">(Eqn. 2.3)</div>

where u_+ and u_- represent the mobilities of cations and anions. For the purpose of this thesis, the simplified equation 3.3 will be used to calculate junction potentials as the presence of other ionic species are relatively minor in concentration and will make very little difference to the final figures. Ionic mobilities with respect to K^+ are quoted as $K^+ = 1.0$, $Na^+ = 0.68$, $Cl^- = 1.04$, gluconate $= 0.33$ (Barry & Lynch, 1991; Ng & Barry, 1995).

Therefore, with 140 mM KCl in the pipette and 150 mM NaCl as the bathing solution at 293 K room temperature, the junction potential created is given by:

$$E^S - E^P = 0.0252 \frac{[150(0.68 - 1.04) - 140(1 - 1.04)]}{[150(0.68 + 1.04) - 140(1 + 1.04)]} \cdot ln \frac{[140(1 + 1.04)]}{[150(0.68 + 1.04)]}$$

$$= +4.5 \, mV$$

<div align="right">(Eqn. 2.4)</div>

and, with 140 mM KCl in the pipette and 150 mM Na gluconate as the bathing solution, the junction potential created is:

$$E^S - E^P = 0.0252 \frac{[150(0.68 - 0.33) - 140(1 - 1.04)]}{[150(0.68 + 0.33) - 140(1 + 1.04)]} \cdot ln \frac{[140(1 + 1.04)]}{[150(0.68 + 0.33)]}$$

$$-6.92 \, mV$$

<div align="right">(Eqn. 2.5)</div>

One further essential consideration is whether the calculated junction potential value should be added to or subtracted from the membrane potential (given here as E_{rev}). For an intact cell-attached patch with a nullified patch-clamp amplifier, the membrane potential across the patch, V_m, is given by the equation:

$$V_m = (E_m - V_P) + E_L \qquad\qquad Eqn.\ 2.6$$

according to Kirchoff's Loop Rule, where E_m is the actual membrane potential, V_P is the patch potential, and E_L is the liquid junction potential between bath solution and pipette. This equation implies that the calculated junction potential value should be *added* to the membrane potential (or E_{rev}) value, which shifts the curve along the abscissa of the I/V graph.

For an excised inside-out configuration patch, where $E_m = 0$:

$$V_m = -V_P + E_L \qquad\qquad Eqn.\ 2.7$$

Therefore, the calculated junction potential values also require *addition* to the experimentally derived values.

2.5   Molecular Biology

2.5.1   RT-PCR

Some aspects of this work were carried out with the help of Dr. B.A.J. Evans at the Department of Child Health, School of Medicine, Cardiff University.

2.5.1.1   RNA Extraction

Method A: Total RNA was extracted from one 25 cm^2 culture flask of MG63 cells (passage number 70) using the Midas® PureRNA Isolation Kit (Biogene, UK).

Method B: Total RNA was extracted from one 25 cm^2 culture flask each of MG63 cells (passage number 34), LNCaP cells, DU145 cells, MCF-7 cells, SaOS-2 cells, and HOB-c cells using Trizol® (Invitrogen) following the manufacturer's protocols to give final volumes of between 30 and 150 μl of product each time.

Following an overnight freeze-thaw cycle to −80 °C, each RNA sample was DNase treated with DNA-*free* (Ambion Ltd.) to clean up the product, according to the product protocol provided.

RNA was then quantified by absorption at 260 nm and 280 nm (A260/280). An absorbance ratio close to 2 (and at least > 1.6) was taken to be indicative of high quality nucleic acid. For all samples reported in this Thesis, the A260/280 values were above 1.6. RNA samples were diluted

when necessary with nuclease-free H_2O to a maximum concentration of 1

$\mu g \, \mu l^{-1}$. RNA was aliquoted and stored at $-80 \, °C$.

2.5.1.2 *Reverse transcription*

Reverse transcription (RT) was carried out with the Promega Improm-II

Reverse Transcription System, using 1 μg RNA in a 20 μl reaction (see

Table 2.2 for composition) alongside a negative control, from which avian

myeloblastosis virus (AMV) reverse transcriptase was omitted. The RNA

template, primer and nuclease-free H_2O initial 5 μl reaction mixture was

run at 70 °C for 5 minutes then held on ice until needed. The RT was run at

25 °C for 5 minutes annealing time, 42 °C for 60 minutes extension time,

and 70 °C for 15 minutes to heat-inactivate the AMV-reverse transcriptase,

in a Perkin Elmer 480DNA Thermal Cycler (Applied Biosystems,

Cheshire). The cDNA product was stored at $-20 \, °C$.

Table 2.2 **Composition of reverse transcription reaction.**

Components	Final concentrations	Volumes
RNA template	1 μg	
Random Primers	0.5 μg	1 μl
Nuclease-free H_2O		to 5 μl
Improm-II™ 5× Reaction Buffer	1×	4 μl
$MgCl_2$ (25 mM)	3 mM	2.4 μl
dNTP mixture (10 mM each)	0.5 mM each dNTP	1 μl
Recombinant RNasin® Ribonuclease Inhibitor	1 u/μl	0.5 μl
Improm-II™ AMV Reverse Transcriptase*	15 u/μg	1 μl
Nuclease-free H_2O		to 20 μl total volume

* omitted from negative control reaction

2.5.1.3 Polymerase Chain Reaction (PCR)

Amplification of the cDNA took place in 12.5 µl or 25 µl reactions using oligonucleotide primers obtained from Invitrogen, Ltd. (see relevant chapter for primer details). PCR was conducted using the GoTaq® Flexi DNA Polymerase kit (Promega) and control reactions were carried out either with sterile nuclease-free water instead of cDNA, or using the no-AMV-RT reaction samples instead of cDNA. The standard composition of PCR reactions is shown in table 2.3, but it should be noted that in some cases MgCl₂ and oligonucleotide primer concentrations were adjusted for optimum performance and adjusted compositions are shown in the relevant chapters. The PCR amplification products were analysed by gel electrophoresis and stained with ethidium bromide, in 1× TAE buffer*, and visualised under UV light.

Table 2.3 **Composition of 12.5 µl PCR reactions**

Components	Final concentrations	Volumes
5× Green GoTaq® Flexi Buffer	1×	2.5 µl
MgCl₂, 25 mM	1.5 mM	0.75 µl
PCR nucleotide (dNTP) mixture	200 µM each dNTP	1.25 µl
Forward primer (sense)	0.4 µM	0.5 µl
Reverse primer (antisense)	0.4 µM	0.5 µl
GoTaq® DNA polymerase (5u µl⁻¹)	0.3125 u	0.0625 µl
cDNA (or H₂O, or No-AMV.RT)		0.5 µl
Nuclease-free H₂O		to 12.5 µl

2.5.1.4 Sequencing

Visualised bands cut from agarose gels were dissolved in water and sequenced to confirm identity, using the same primers as in RT-PCR reactions.

---

* 40 mM Tris-Acetate, 1 mM EDTA

CHAPTER 3:

FUNCTIONAL K$^+$ CHANNELS IN OSTEOBLAST CELL MEMBRANES

3 FUNCTIONAL K⁺ CHANNELS IN OSTEOBLAST CELL MEMBRANES

3.1 Introduction

3.1.1 Potassium channels

With more than 80 genes identified, potassium channels are a large family of ion channels heterogeneously expressed in the cell plasma membrane controlling membrane potential. The roles of K^+ channels in excitable cells (i.e. those cells that can conduct action potentials such as neurones and myocytes) are clear and have been extensively studied, showing that K^+ channels, for example, control the repolarisation rate following an action potential and firing patterns (Hille, 2001; Shao *et al.*, 1999). Now the K^+ channel family is emerging as a major player in non-excitable cells with important physiological roles in key cellular processes such as apoptosis (Burg *et al.*, 2006), volume regulation (Lang *et al.*, 2007), cell proliferation (Wonderlin & Strobl, 1996; Chandy *et al.*, 2004), differentiation (Roura-Ferrer *et al.*, 2008) and secretion (Moreau *et al.*, 1997). As a variety of potassium channel subtypes have been identified in bone (Gu *et al.*, 2001a; Hughes *et al.*, 2006; Moreau *et al.*, 1996;

Ravesloot *et al.*, 1990; Yellowley *et al.*, 1998; Weskamp *et al.*, 2000) their presumed role is to contribute to these processes.

3.1.2 K channel subtypes

K$^+$ channels can be divided into 5 subcategories by function and structure: voltage-gated K$^+$ channels (K$_v$), calcium-activated K$^+$ channels (K$_{Ca}$), inward-rectifier K$^+$ channels (K$_{IR}$), ATP-dependent K$^+$ channels (K$_{ATP}$) and 2-pore domain K$^+$ channels (K$_{2P}$). This chapter will concentrate on maxi-K (BK$_{Ca}$) and K$_{ATP}$ channels which are described in detail below.
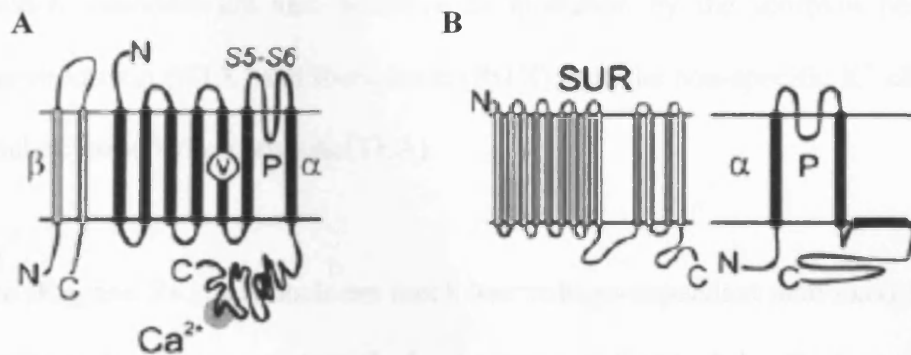
Figure 3.1 **Architecture of the maxi-K and K$_{ATP}$ channels. (A)** maxi-K α subunits are 7-transmembrane (TM) domain structures which associate with 2-TM domain regulatory β subunits. Maxi-K has a unique calcium bowl near the end of the α subunit C-terminus. **(B)** K$_{ATP}$ channels are built from pore-forming 2-TM domain structure homologous with K$_{IR}$ channels and multiple TM domain SUR regulatory subunits. (Figure adapted from Burg, *et al.*, 2006).

3.1.2.1 Calcium-activated K^+ channels (K_{Ca})

K_{Ca} channels have been subcategorized into large conductance (BK_{Ca}), intermediate conductance (IK_{Ca}) and small conductance (SK_{Ca}) channels and each subgroup also has slightly different pharmacological characteristics. BK_{Ca} (also known as maxi-K) channels have conductances in the range 150 – 300 pS and are typically >200 pS. They are voltage-dependent channels but an increased $[Ca^{2+}]_i$ into the micromolar range shifts the P_{open}/V curve to the left indicating that calcium enhances the voltage activation of the channel. Because of this calcium-dependence, maxi-K channels have been implicated in the negative feedback of voltage-dependent calcium channels (VDCC): increased $[Ca^{2+}]_i$ by VDCCs activates maxi-K which causes membrane hyperpolarisation and subsequent inactivation of VDCCs, ultimately limiting calcium entry. Maxi-K channels are also sensitive to inhibition by the scorpion peptides charybdotoxin (CTX) and iberiotoxin (IbTX), and the non-specific K^+ channel blocker tetraethylammonium (TEA).

The IK_{Ca} and SK_{Ca} channels are much less voltage-dependent than maxi-K and rectify at depolarising potentials due to intracellular block by divalent cations such as Mg^{2+} (Soh & Park, 2001; Xia et al., 1998). Conductance values range from 50 to 180 pS for IK_{Ca} and the much smaller 2 to 15 pS for SK_{Ca}. Both are sensitive to block by TEA, and are more selectively blocked by clotrimazole (Ouadid-Ahidouch et al., 2004) or apamin (Stocker, 2004) respectively.

The K_{Ca} channel α subunits which form the channel pore are structurally similar to those of the voltage-dependent K^+ channels. The α subunits comprise six transmembrane domains S1-S6 for IK_{Ca}/SK_{Ca}, with an extra S0 domain in the maxi-K α subunit. The S5-S6 pore-forming loop and K^+ selective-region are highly conserved, and S4 contains positively charged arginine and lysine residues which confer voltage-sensitivity to the channel. SK_{Ca} and IK_{Ca} have fewer of these residues than maxi-K which might explain the reduced voltage-dependence of these sub-types. The additional S0 domain of maxi-K is thought to link with regulatory β subunits which associate with the α subunits in a 1: 1 stoichiometric ratio in this sub-type. All three sub-types form α tetrameric structures, with associated β subunits for maxi-K. The C-termini of the α subunits are less conserved and maxi-K has a calcium-sensitive region (Toro et al., 1998) which is not found in IK_{Ca} or SK_{Ca} which instead rely on calmodulin binding near to the S6 transmembrane domain for their weaker calcium-sensitivity (Keen et al., 1999).

There are now four known maxi-K β subunit types, labelled $\beta 1 - \beta 4$. Each β double transmembrane-spanning subunit links with an S0 domain of the maxi-K α subunit and affects the channel's calcium- and voltage-dependence and determines its pharmacology (Wang et al., 2002). The β subunits appear to heteromultimerise (Joiner et al., 1998) to create maxi-K channels with differing electrophysiological and pharmacological profiles.

3.1.2.1.1   BK$_{Ca}$ or maxi-K

The existence and role of maxi-K channels in excitable cells have been described previously (above and Hille, 2001) but maxi-K is also known to be almost ubiquitously expressed in mammalian tissues, including skeletal tissues (Grandolfo *et al.*, 1992; Ravesloot *et al.*, 1990). Evidence is building that the remit of maxi-K includes roles in bone cell metabolism, secretion, mineralisation, bone resorption, and apoptosis (Guggino *et al.*, 1989; Moreau *et al.*, 1996; Ypey *et al.*, 1988). The channel composition with regard to β subunit arrangement and co-expression is currently unknown in bone cells and various conflicting reports of sensitivities to CTX and IbTX (Moreau *et al.*, 1997; Rezzonico *et al.*, 2002; Weskamp *et al.*, 2000), and voltage-dependence have been made for MG63 osteoblast-like cells. As the β subunits likely heteromultimerise but can also homomultimerise, the possibilities for different pharmacological and electrophysiological profiles are 35 different permutations. The profile of the maxi-K channel in primary human osteoblasts so far remains unexplored.

3.1.2.2 ATP-dependent K⁺ channels

K$_{ATP}$ channels are expressed in many tissues including pancreatic β cells (Schmid-Antomarchi *et al.*, 1987), skeletal muscle (Chutkow *et al.*, 1996), hippocampal cells (Mourre *et al.*, 1989), liver (Malhi *et al.*, 2000) and in some cancers (Kunzelmann, 2005), where they have roles in secretion, proliferation, and metabolism. Perhaps the best studied role of K$_{ATP}$ channels is in pancreatic β cells where they are involved in regulation of insulin secretion (Aguilar-

Bryan & Bryan, 1999). High intracellular glucose is thought to increase [ATP]$_i$

which closes the channels, resulting in membrane depolarisation and Ca^{2+} entry

via VDCCs, which in turn causes insulin secretion (Ashcroft & Gribble, 2000).

Amoroso *et al* (1990) have also identified a secretory role for K$_{ATP}$ channels in

Substantia Nigra GABA release.

As the name suggests, these K$^+$ channels are sensitive to changes in [ATP]$_i$

which inhibits the channel when at sufficient concentrations. Activation can

occur by binding of nucleotide diphosphates (e.g. ADP) which in the presence

of Mg$^{2+}_i$ antagonise inhibition by ATP$_i$, and channels are modulated by

phospholipids (PIP$_2$) which also decrease ATP-binding to the regulatory SUR

channel subunit. K$_{ATP}$ channels can be subcategorised into smaller conductance

K$_{IR}$6.1 channels (35 – 40 pS) or larger conductance K$_{IR}$6.2 channels (65 – 80

pS) according to their subunit composition, and also by their pharmacology.

Both types are relatively voltage-independent and display inward-rectification

at depolarising potentials due to time-dependent blockade by Mg^{2+} ions in the

pore (Lopatin *et al.*, 1994). Probably all K$_{ATP}$ subtypes are sensitive to some

degree to inhibition by sulphonylureas such as glibenclamide and tolbutamide,

but their pharmacological profiles differ with regard to K$_{ATP}$ channels openers

(KCOs). There is no clear pharmacophore link between the known KCOs, but

they can be broadly categorised into four groups: benzothiadiazines (such as

diazoxide), pyrimidines (such as minoxidil), cyanoguanidines (pinacidil), and

benzopyrans (such as cromakalim or the eutomer levcromakalim).

Diazoxide   Pinacidil

Levcromakalim   Minoxidil
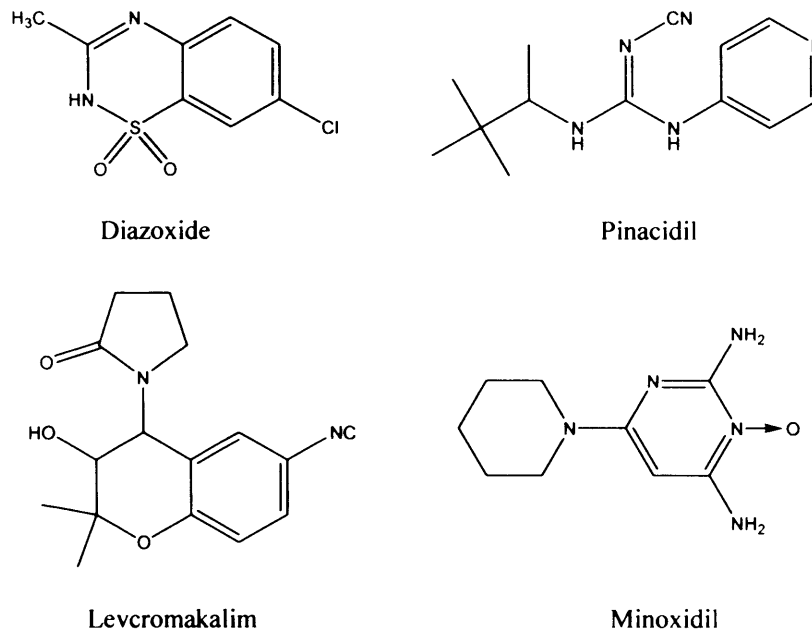
Figure 3.2 **Structures of the K$_{ATP}$ channel openers.**

The structure of the pore-forming subunits of K$_{ATP}$ channels is similar to that of the inward-rectifier K^{+} channels, consisting of two transmembrane-spanning domains with a highly conserved pore-forming loop similar to that of the K$_{Ca}$ channels. A large C-terminus domain is thought to act as a lining of β sheets and regulates inward rectification by Mg^{2+}, and causes conformational changes to the pore in the closed state (Kuo et al., 2003; Nishida & MacKinnon, 2002; Yang et al., 1995). The K$_{IR}$6.x subunits alone do not form functional K^{+}-conducting pores, but must be associated with regulatory sulphonylurea receptor (SUR) subunits, together forming an octameric channel complex in the stoichiometric ratio (K$_{IR}$6.x/SUR)$_4$. ER retention motifs on both K$_{IR}$6.x and

SUR subunits prevent membrane surface expression unless one is associated with the other (Zerangue *et al.*, 1999). SUR subunits are members of the ATP-binding cassette protein family and structurally consist of 17 transmembrane domains arranged into three groups of 6, 6 and 5, with 2 nucleotide-binding domains NBD1 and NBD2, which appear to be important for KCO and Mg-nucleotide binding.

There are two known genes for $K_{IR}6.x$ forming two distinct subunit types which have different electrophysiological properties. These are $K_{IR}6.1$ and $K_{IR}6.2$. The SUR subunit type can also be genetically separated into SUR1 and SUR2, the latter of which also has two known variants labelled as SUR2A and SUR2B. The SUR composition of the K_{ATP} channels determines their pharmacology.

K_{ATP} subunit composition has been shown to be tissue specific (Ashcroft & Gribble, 2000). The pore-forming subunit in most tissues appears to be $K_{IR}6.2$, except in some smooth muscle, such as vascular smooth muscle, in which it is $K_{IR}6.1$ (Sakura *et al.*, 1995; Inagaki *et al.*, 1995). The SUR subunit specificity is more diverse, and SUR1 appears dominant in β cells and some neurones (Aguilar-Bryan *et al.*, 1995; Liss *et al.*, 1999), whilst SUR2A is regulatory in cardiac and skeletal muscle cells (Chutkow *et al.*, 1996), whereas SUR2B takes precedence in smooth muscle and some neurones (Chutkow *et al.*, 1996; Isomoto *et al.*, 1996). The combinations of $K_{IR}6.x$/SUR subunits make the pharmacology of K_{ATP} channels complex, and therefore tissue-specific

responses are found to KCOs, inactivators and modulators. For example, pinacidil is known to activate channels built with SUR2 but not SUR1, and the effect is greater for SUR2B than for SUR2A (Babenko *et al.*, 2000), whereas diazoxide binds to and activates via SUR1 and SUR2B (Gribble *et al.*, 1997; Shyng *et al.*, 1997), but does not cause activation via SUR2A although it can increase activity in the presence of MgADP (D'hahan *et al.*, 1999).

Although the K$_{IR}$6.x/SUR pharmacology is complex, the electrophysiology matches it in this regard and different subunit combinations with modulator binding differentials result in channel conductances seemingly anywhere between the smaller conductance K$_{IR}$6.1 and larger conductance K$_{IR}$6.2 in heteromultimers.

3.1.3 K channels have important roles in proliferation

The evidence for a functional role for K$^+$ channels in cell proliferation is growing, but mechanisms are poorly understood. Hyperpolarisation of the cell membrane by activation of K$_{ATP}$ channels is thought to be necessary for early stage progression between the G$_1$ growth phase and the S phase of the cell cycle (Wonderlin & Strobl, 1996), and K$_{ATP}$ channels have been implicated in cancer cell proliferation (Woodfork *et al.*, 1995; Wondergem *et al.*, 1998). Maxi-K channels may also have an important role in proliferation, as reported by Wondergem *et al.* (1998) who show increased HTB-9 human bladder carcinoma cell proliferation by presumed inactivation of maxi-K channels with CTX and IbTX.

Direct increases in cell number have been reported with pinacidil on nephron epithelial tubules (Braun *et al.*, 2002) and diazoxide on bladder carcinoma cells (Wondergem *et al.*, 1998), and increases in DNA synthesis with pinacidil, cromakalim/levcromakalim and diazoxide (Braun *et al.*, 2002; Malhi *et al.*, 2000; Wondergem *et al.*, 1998). The K_{ATP} channel opener minoxidil has also been shown by others to increase DNA synthesis (Malhi *et al.*, 2000) and to increase proliferation of various cell-types including fibroblasts, keratinocytes and stimulate hair follicles (Messenger & Rundegren, 2004). Other K_{ATP} openers have also been shown to increase hair growth (rate & thickness) including pinacidil (Goldberg *et al.*, 1988), diazoxide (Burton *et al.*, 1975) and cromakalim (Bulh *et al.*, 1993), and minoxidil is a medicine licensed for use in androgenetic alopecia.

The roles of maxi-K and K_{ATP} channels in bone cells are relatively unexplored, but these channels do appear to be involved in osteocalcin secretion by osteoblasts (Moreau, *et al.*, 1997).

3.1.4 Chapter hypothesis, aims and experimental strategies

The chapter hypothesis is (i) that the maxi-K and K_{ATP} channels will be expressed and active in human osteoblast-like cell lines and primary osteoblasts, and (ii) that K_{ATP} ligands will have a functional role in MG63 cell proliferation.

This chapter aims to establish the patch-clamp technique with MG63 and SaOS-2 cells, to demonstrate the abundance and activity of K$^+$ channels in MG63 and SaOS-2 osteoblast-like cell membranes, and show some of the first important data demonstrating that K$^+$ channels are also active in primary human osteoblasts. RT-PCR will be used to confirm the expression of the maxi-K channel α and β1-4 subunits and K$_{ATP}$ channel K$_{IR}$6 and SUR subunits. The putative roles of K$_{ATP}$ channels in osteoblast proliferation will also be explored, with the objective of testing whether K$_{ATP}$ channels are important in osteoblast cell growth by means of haemocytometry and MTS dye-conversion assays.

3.2 Methods

3.2.1 Electrophysiology

MG63, SaOS-2 and HOB-c cells were seeded at densities of between 3,000 and 5,000 cells per coverslip and incubated for at least 24 hours before patch-clamp recording. Stock solutions of drugs were prepared in distilled water unless otherwise stated, and were obtained from Sigma. HOB-c primary human osteoblasts with passage numbers between 4 and 10 were used.

The patch-clamp methods described in chapter 2 (2.4) were used, with freshly-pulled electrodes with a resistance of between 4 and 8 MΩ (measured with High K⁺ in the pipette and Locke solution in the bath). Criteria for successful seals included a seal resistance of > 1 GΩ, low variance of noise when channels were closed (RMS noise < 1), and stability over a range of holding potentials.

3.2.1.1 Single channel analysis

Using Strathclyde electrophysiology Software WinEDR v2.8.2, recordings were initially scanned at low resolution by eye for potentially interesting events, anomalies, etc. followed by software construction of distribution of current amplitude histograms for all digitised points to determine single-channel current amplitudes and the number of channels active in the patch. Peaks were fitted with Gaussian probability density functions using the least squares method to estimate the mean current for the peak. From the Gaussian

curve, estimates of the single channel open probability could be made from area under the curve, corresponding to the percentage of time spent in that current state, and provided that only one channel appeared in the patch.

Occasionally, in recordings from less-stable patches, or where current states were close together, the all points histogram was not successful at resolving current peaks, and the Patlak average method (Patlak, 1988) was used to construct current amplitude histograms. This method allows effective resolution of peaks by averaging a sequence of digitised data points (user defined from 2 - 256) and excluding averages with a standard deviation that exceeds the variance of a portion of closed state record. This effectively excludes transitional states, allowing construction of resolved peaks.

Transition detection was used to measure the transitions from channel closed to open states, and the dwell times in these states. This was achieved by placing a threshold at 50% of the open single channel current level. This provided valuable open probability data (as NP$_o$) and the dwell times for kinetic analysis. Logarithmic dwell time histograms (as described by Sigworth & Sine, 1987) were constructed to determine how the length of open and closed states of the maxi K channel varied with changes in potential. Histograms were fitted with exponential probability density functions (least squares method) to reveal open (τ_o) or closed (τ_o) time components.

3.2.1.2 Filtering

The recording apparatus made use of in-built filters to decrease the amount of

random electrical noise in the recordings. However, though filtering can be a

very useful tool, heavy filtering may erase short-duration channel openings and

in doing so, decrease the quality of the data record. Also, in some cases rather

than complete erasure of short-duration openings, filtering results in failure to

record the full amplitude of a channel current, which has clear consequences

for I/V plots and conductance calculations. Therefore, filtering has to be a

payoff between improved signal/noise and minimising loss of data quality.

The effective cut-off frequency of filtering used in the experimental apparatus

for the single-channel recordings detailed in this chapter can be calculated by

the following equation (Colquhoun, 1994):

$$1/f_c^2 = 1/f_1^2 + 1/f_2^2 \ldots + 1/f_n^2$$

where f_c is the effective cut-off frequency and f_1, f_2 and f_n are the cut-off

frequencies of each filter in the system. Thus, in the system used here with a 20

kHz filter and a 5 kHz filter, the calculated effective cut-off is 4.85 kHz.

Another way to describe the level of filtering is by the rise time, which is the

time taken for a signal to rise from 10% of its low value to 90% of its

maximum value. The rise time, t_r, is given by (Colquhoun, 1994):

$$t_r = 0.3321 / f_c$$

Therefore, a 4.85 kHz filter has a rise time of 68 μs. The f_c and t_r values are important in determining the minimum duration of an event which can be detected at a specified fraction of its full amplitude, which is often called the minimum resolvable event. Colquhoun & Sigworth (1983) showed that for the errors in duration of events caused by filtering to become negligible and for the signal to reach at least 90% of its full amplitude, the minimum event duration needs to be above $1.3t_r$ and for a reliable amplitude measurement, an opening must be above $2t_r$.

The minimum resolvable event for an opening at 90% of its full amplitude for the 4.85 kHz effective filter is given by $1.3t_r$ which is 88 μs. Event durations shorter than double this value (for greater confidence), i.e. shorter that 176 μs, were not included in the kinetic analysis.

3.2.2   Cell growth assays

For proliferations and growth assays, cells were seeded at densities of 3,000 cells per well for 96-well plates and 50,000 cells per well for 6-well plates. Assays were generally read, unless otherwise stated in the results, after 72 hours for 96 well-plates by MTS/PMS dye conversion and absorption measurements, and for 6-well plates assays were read at the intervals indicated by haemocytometry. See section 2.2.2 for details of the assay method. Stock solutions of pinacidil and tolbutamide were prepared in ethanol, and diazoxide, levcromakalim and glibenclamide were prepared in DMSO. Vehicle

concentrations were kept to a minimum and vehicle controls were run alongside the test compounds during assays.

3.2.3 RT-PCR

General RT-PCR methods are detailed in Chapter 2: Materials and Methods, section 2.4.1.

3.2.3.1 Oligonucleotide primers: K_{ATP} channels and associated SUR subunits

Oligonucleotide primers for ATP-dependent potassium channel (K_{ATP}) subunits $K_{IR}6.1$ (KCNJ8) and $K_{IR}6.2$ (KCNJ11), and associated sulphonylurea receptor (SUR) subunits SUR1 (ABCC8) and SUR2B (ABCC9), as used by Curley *et al.* (2002) (see table 3.1 and Figure 3.3), were obtained from Invitrogen.

Table 3.1 **Oligonucleotide primer details for K_{ATP} channels and associated SUR subunits**

Primer	Sequence	Product size	Location	Acc. No.
$K_{IR}6.1$	F: CATCTTTACCATGTCCTTCC R: GTGAGCCTGAGCTGTTTTCA	334	560-893	NM_004982
$K_{IR}6.2$	F: ACTCCAAGTTTGGCAACACC R: CTGCTGAGGCCAGAAATAGC	353	1198-1550	D50582
SUR1	F: ATGAGGAAGAGGAGGAAGAG R: TCGATGGTGTTACAGTCAGA	493	2941-3433	L78207
SUR2B	F: TGGGAACACATTTTCTGCAA R: CGCATGGGTCACAAATGTAG	150	1528-1677	NM_020297

Figure 3.3   **K$_{ATP}$ and SUR subunit primers and amplification sequences.**
Target primer sequences are shown in red.

K$_{IR}$6.1

```
481 agaacatccg tgagcaagga cgctttctac aggacatctt caccaccttg gtggacctga
541 aatggcgcca cacgctggtc atctttacca tgtccttcct ctgcagctgg ctgctcttcg
601 ctatcatgtg gtggctggtg gcctttgccc atggggacat ctatgcttac atggagaaaa
661 gtggaatgga gaaaagtggt ttggagtcca ctgtgtgtgt gactaatgtc aggtctttca
721 cttctgcttt tctcttctcc attgaagttc aagttaccat tgggtttgga gggaggatga
781 tgacagagga atgccctttg gccatcacgg ttttgattct ccagaatatt gtgggtttga
841 tcatcaatgc agtcatgtta ggctgcattt tcatgaaaac agctcaggct cacagaaggg
901 cagaaacttt gattttcagc cgccatgctg tgattgccgt ccgaaatggc aagctgtgct
```

K$_{IR}$6.2

```
1081 tggaaaccac gggcatcacc acccaggccc gcacctccta cctggccgat gagatcctgt
1141 ggggccagcg ctttgtgccc attgtagctg aggaggacgg acgttactct gtggactact
1201 ccaagtttgg caacaccatc aaagtgccca caccactctg cacggcccgc cagcttgatg
1261 aggaccacag cctactggaa gctctgaccc tcgcctcagc ccgcgggccc ctgcgcaagc
1321 gcagcgtgcc catggccaag gccaagccca agttcagcat ctctccagat tccctgtcct
1381 gagccatggt ctctcgggcc ccccacacgc gtgtgtacac acggaccatg tggtatgtag
1441 cccagccagg gcctggtgtg aggctgggcc agcctcagct cagcctcccc ctgctgctca
1501 tccaggggtgt tacaaggcac ttgtcactat gctatttctg gcctcagcag gaacctgtac
1561 tgggttatttt ttgtccctgc tcctcccaac ccaatttagg actggctcac ccctctcccc
```

SUR1

```
2881 ccacagagcc accccagggc ctatctcgtg ccatgtcctc gagggatggc cttctgcagg
2941 atgaggaaga ggaggaagag gaggcagctg agagcgagga ggatgacaac ctgtcgtcca
3001 tgctgcacca gcgtgctgag atcccatggc gagcctgcgc caagtacctg tcctccgccg
3061 gcatcctgct cctgtcgttg ctggtcttct cacagctgct caagcacatg gtcctggtgg
3121 ccatcgacta ctggctggcc aagtggaccg acagcgccct gacccgacc cctgcagcca
3181 ggaactgctc cctcagccag gagtgcaccc tcgaccagac tgtctatgcc atggtgttca
3241 cggctgtctg cagcctgggc attgtgctgt gcctcgtcac gtctgtcact gtggagtgga
3301 cagggctgaa ggtggccaag agactgcacc gcagcctgct aaaccggatc atcctagccc
3361 ccatgaggtt ttttgagacc acgccccttg ggagcatcct gaacagattt tcatctgact
3421 gtaacaccat cgaccagcac atcccatcca cgctggagtg cctgagccgc tccaccctgc
3481 tctgtgtctc agccctggcc gtcatctcct atgtcacacc tgtgttcctc gtggccctct
```

SUR2B

```
1441 cagaaaagta cacttgatta ttccactgag agactcaaga aaacaaatga aatattgaaa
1501 ggcatcaaac ttctaaaatt gtatgcctgg gaacacattt tctgcaaaag tgtggaggaa
1561 acaagaatga aagaactatc tagtctcaaa accttt gcac tatatacatc actctccatc
1621 ttcatgaatg cagcaattcc catagcagct gttcttgcta catttgtgac ccatgcgtat
1681 gccagtggaa acaatctgaa acctgcagag gcctttgctt cactgtctct cttccatatc
```

3.2.3.2 Oligonucleotide primers: Maxi-K channel α and β subunits

Oligonucleotide primers for maxi-K (BK$_{Ca}$) channel pore subunit α (KCNMA1) and associated β1 - β4 subunits (KCNMB1, KCNMB2, KCNMB3 and KCNMB4) were designed from human mRNA coding sequence (CDS) as follows:

The National Center for Biotechnology Information's (NCBI) nucleotide database was searched for the above maxi-K channel subunit genetic sequences in the human genome. mRNA sequences were copied into the 'source sequence box' of the web-based Primer3 primer design software (Rozen & Skaletsky, 2000). The software selected left and right primers for the given sequence without modification of the default software settings. Primer3-suggested primers were checked against the complete genetic sequence using Ensembl web-based software (Hubbard *et al.*, 2007) to look for intron-spanning primers (i.e. where forward and reverse primer sequences are in different exons), which would also enable detection of unwanted genomic DNA in the reactions by larger amplicon size. Primers (see table 3.2 and Figure 3.4) were obtained from Invitrogen.

Table 3.2   **Oligonucleotide primer details for maxi-K channel subunits**

Primer	Sequence	Product size	Location	Acc. No.
KCNMA1	F: ACGCAATCTGCCTCGCAGAGTTG R: CATCATGACAGGCCTTGCAG	408	1640-2047	AAA85104
KCNMB1	F: CTGTACCACACGGAGGACACT R: GTAGAGGCGCTGGAATAGGAC	189	668-856	NM_004137
KCNMB2	F: CATGTCCCTGGTGAATGTTG R: TTGATCCGTTGGATCCTCTC	237	808-1044	NM_181361
KCNMB3	F: AACCCCCTTTTCATGCTTCT R: TCTTCCTTTGCTCCTCCTCA	277	1404-1680	NM_171830
KCNMB4	F: GTTCGAGTGCACCTTCACCT R: TAAATGGCTGGGAACCAATC	245	648-892	NM_014505

Figure 3.4   **Maxi-K channel α and β1 - β4 subunit primers and amplification sequences.** Target primer sequences are shown in red.

KCNMA1

```
1561 atcatcactc aaatgctgca gtatcacaac aaggcccatc tgctaaacat cccgagctgg
1621 aattggaaag aaggtgatg                          aagttggg cttcatagcc
1681 cagagctgcc tggctcaagg cctctccacc atgcttgcca acctcttctc catgaggtca
1741 ttcataaaga ttgaggaaga cacatggcag aaatactact tggaaggagt ctcaaatgaa
1801 atgtacacag aatatctctc cagtgccttc gtgggtctgt ccttccctac tgtttgtgag
1861 ctgtgttttg tgaagctcaa gctcctaatg atagccattg agtacaagtc tgccaaccga
1921 gagagccgta tattaattaa tcctggaaac catcttaaga tccaagaagg tactttagga
1981 tttttcatcg caagtgatgc caaagaagtt aaaagggcat tttttta
2041        aca tcacagatcc caaaagaata aaaaaatgtg gctgcaaacg gcttgaagat
2101 gagcagccgt caacactatc accaaaaaaa aagcaacgga atggaggcat gcggaactca
```

KCNMB1

```
601  gggcaagaag gtgccccagt acccatgcct gtgggtcaac gtgtcagctg ccggcaggtg
661  ggctgtg                              cg ggaccagaac cagcagtgct cctacatccc
721  aggcagcgtg gacaattacc agacggcccg ggccgacgtg gagaaggtca gagccaaatt
781  ccaagagcag caggtcttct actgcttctc cgcacctcgg gggaacgaaa ccagc
841                           gggc cccaggccct cctcttctcc ctcttctggc ccaccttcct
901  gctgaccggt ggcctcctca ttatcgccat ggtgaagagc aaccagtacc tgtccatcct
```

KCNMB2

```
721  gctcctcctc taccacacag aagagacaat aaaaatcaat cagaagtgct cctatatacc
781  taaatgtgga aaaaattttg aagaatc                         tca tggaaaactt
841  caggaagtat caacacttct cctgctattc tgacccagaa ggaaaccaga agagtgttat
901  cctaacaaaa ctctacagtt ccaacgtgct gttccattca ctcttctggc caacctgtat
961  gatggctggg ggtgtggcaa ttgttgccat ggtgaaactt acacagtacc tctccctact
1021 atgt                              tagata aatgcaaaaa tggataaaat aatttttgtt
1081 aaagctcaaa tactgttttc tttcattctt caccaaagaa ccttaagttt gtaacgtgca
```

KCNMB3

```
1321 tacacaccta agtgccacca agatagaaat gatttgctca acagtgctct ggacataaaa
1381 gaattcttcg atcacaaaaa tgg                          acagtcc agccagccaa
1441 tctgaagatg tcattcttat aaaaaagtat gaccaaatgg ctatcttcca ctgtttattt
1501 tggccttcac tgactctgct aggtggtgcc ctgattgttg gcatggtgag attaacacaa
1561 cacctgtcct tactgtgtga aaaatatagc actgtagtca gagatgaggt aggtggaaaa
1621 gtaccttata tagaacagca tcagttcaaa ctgtgcatta
1681 gcagagaaat cttaagacgg tggccaaatt aaagtgctgg ccttcagatg tctgtgattt
```

KCNMB4

```
541  gtgtcgctct tcatcttcgg cttctgctgg ctgagtcccg cgctgcagga tctgcaagcc
601  acggaggcca attgcacggt gctgtcggtg cagcagatcg gcgaggt                  
661          gtg gcgccgactg caggggcacc tcgcagtacc cctgcgtcca ggtctacgtg
721  aacaactctg agtccaactc tagggcgctg ctgcacagcg acgagcacca gctcctgacc
781  aaccccaagt gctcctatat ccctccctgt aagagagaaa atcagaagaa tttggaaagt
841  gtcatgaatt ggcaacagta ctggaaagat ga                         cttgctat
901  tttaatcaac atcaaagacc agatgatgtg cttctgcatc gcactcatga tgagattgtc
```

3.2.3.3 RT-PCR reaction compositions and conditions

K_{ATP} channels and associated SUR subunits

RT-PCR was carried out using MG63 (passage number 72) mRNA and the reaction compositions and conditions were optimised and are detailed in tables 3.3 and 3.4 respectively. Reactions of 12.5 µl were routinely performed and negative controls using nuclease-free water or no-RT reaction products from reverse transcription were run alongside reactions with cDNA. The PCR amplification products were analysed by gel electrophoresis in 1 % to 3.5 % agarose gels stained with ethidium bromide, in 1× TAE buffer*. K_{ATP} subunit products were not sequenced to confirm identity.

Table 3.3 PCR reaction composition (K_{ATP} and SUR primers)

Components	Final concentrations	Volumes
5× Green GoTaq® Flexi Buffer	1×	2.5 µl
MgCl₂, 25 mM	1.5 mM	0.75 µl
PCR nucleotide (dNTP) mixture	200 µM each dNTP	1.25 µl
Forward primer (sense)	0.4 µM	0.5 µl
Reverse primer (antisense)	0.4 µM	0.5 µl
GoTaq® DNA polymerase (5u/µl)	0.3125u	0.0625 µl
cDNA (or H₂O, or No-AMV.RT)		0.5 µl
Nuclease-free H₂O		to 12.5 µl

Table 3.4 PCR reaction conditions (K_{ATP} and SUR primers)

Step	Temperature °C	Time	No. of cycles
Initial denaturation	95	10 min	1
Denaturation	95	30 s	
Annealing	55	45 s	30
Extension	72	1 min	
Final extension	72	10 min	1
Soak	4	Indefinite	

---

* Tris-Acetate-EDTA

Maxi-K channel α and β subunits

RT-PCR was carried out using MG63 (passage number 34) osteoblast-like cell mRNA and the reaction compositions and conditions were optimised and are detailed in tables 3.5 and 3.6 respectively. Reactions of 12.5 μl were routinely performed and negative controls using nuclease-free water or no-RT reaction products from reverse transcription were run alongside reactions with cDNA. The PCR amplification products were analysed by gel electrophoresis in 2 % agarose gels stained with ethidium bromide, in 1× TAE buffer*. Bands were cut from gels, stored in 50 μl sterile nuclease-free water, and cDNA eluted into the water was sequenced using the Big Dye® Terminator V 3.1 Cycle Sequencing Kit (Applied Biosystems, UK) by Central Biotechnology Services at Cardiff University.

Table 3.5 **PCR reaction composition (Maxi-K α and β subunit primers)**

Components	Final concentrations	Volumes
5× Green GoTaq® Flexi Buffer	1×	2.5 μl
MgCl₂, 25 mM	1.5 mM	0.75 μl
PCR nucleotide (dNTP) mixture	200 μM each dNTP	1.25 μl
Forward primer (sense)	0.4 μM	0.5 μl
Reverse primer (antisense)	0.4 μM	0.5 μl
GoTaq® DNA polymerase (5u/μl)	0.3125u	0.0625 μl
cDNA (or H₂O, or No-AMV.RT)		0.5 μl
Nuclease-free H₂O		to 12.5 μl

Table 3.6 **PCR reaction conditions (Maxi-K α and β subunit primers)**

Step	Temperature °C	Time	No. of cycles
Initial denaturation	95	10 min	1
Denaturation	95	30 s	
Annealing	55	45 s	40
Extension	72	1 min	
Final extension	72	10 min	1
Soak	4	Indefinite	

* Tris-Acetate-EDTA

3.2.4 Statistical methods

Distributions of current histograms from patch recordings were fitted with Gaussian distributions, the means of which were taken as the zero level or channel current for each peak. Exponential probability density functions (PDFs) were fitted to dwell-time histograms according to best fit, to derive channel dwell time values. Statistical significance at the 0.05 level was tested using appropriate student t-tests, or analysis of variance with Bonferroni's mean comparison test to identify significantly different groups. Data shown are mean $\pm$ SEM.

3.3 Results

3.3.1 Ion channel activity in osteoblasts and osteoblast-like cells

Analysis of single channel data from patch-clamp experiments reveals distinct channel currents which indicates that a variety of ion channels are present and active in MG63 osteoblast-like cells, SaOS-2 osteoblast-like cells, HOB-c human primary osteoblasts and LNCaP and DU145 prostate cancer cells (data not shown for the latter two cell lines). For the purposes of analysis and discussion, these will be categorised into large conductance, intermediate conductance and small conductance channels.

3.3.1.1 The large-conductance channel

By far the most prevalent channel observed, particularly in the osteoblasts and osteoblast-like cells, was a large conductance, voltage-dependent channel. With high K solution in the electrode, this channel was observed in 98% (n = 49/50) of successful cell-attached (*i.e.* > 1 GΩ seal, RMS noise < 1.0) MG63 patches, 72% (n = 18/25) of SaOS-2 patches and 100% (n = 17) of HOB-c patches. Conductance values were obtained by linear regression over the linear portion of the current-voltage plots.

3.3.1.1.1   Cell-attached

The large conductance channel was rarely spontaneously active at 0 mV holding potential, and no recordings were possible in the few instances of channel activity. This channel type became active on depolarisation ≥ 90 mV,

but once 'primed' the channel remained active over the voltage range -100 mV to +200 mV.

The mean single channel conductance in MG63 cells with high K solution in the electrode and Locke as the bathing solution was 198.7 ± 9 pS (n = 8) with a corrected reversal potential (E_{rev}) (adjusted for junction potential - see methods 2.4.6) of 60.7 ± 7.7 mV. In the same cell-type, changing the bathing solution to sodium gluconate Locke resulted in channels with a mean conductance of 212.5 ± 15 pS (n = 6) and a corrected E_{rev} of 56.18 ± 6.7 mV (see Figure 3.5, for example). When the electrode solution and bathing solution were both sodium gluconate Locke the unitary conductance of the channel was 221.8 pS (n = 1) and the curve was shifted to the left with a real E_{rev} of 7.8 mV.

There was no significant difference between mean single channel conductances ($p < 0.05$) for the three different combinations of electrode/bathing solutions, but the E_{rev} for the channel in the sodium gluconate Locke electrode/sodium gluconate Locke bathing solution was significantly different ($p < 0.05$) from the E_{rev} values with the other combinations of solutions (Figure 3.6).

Observational data from HOB-c cells (n = 2) indicated the presence of a 239.5 ± 6.4 pS channel, $E_{rev} = 68.6 \pm 4.8$ mV in High K electrode solution and Locke bathing solution.

In many patches more than one large conductance channel was active, particularly at depolarising patch potentials above 140 mV. Figure 3.5 shows data records with 3 and 4 channels opening together in MG63 cells. Channel open probability (P_{open}) increased with each increase in patch potential, showing that this channel-type is voltage dependent. As there were often two or more channels active per patch, NPo was used as a measure of open probability, in which N is the number of channels in the patch and Po is the open probability of the channel. 20 mM TEA applied to the outside of cell-attached patches in the electrode solution (n = 13 patches) resulted in a complete absence of maxi-K channel activity in these patches, at a patch potential (120 mV) where the channel was previously active in other cell-attached patches (n = 41). A χ^2 test showed statistical significance between the control and TEA groups for channel activity ($p < 0.001$).

In all cell-attached recordings in all three osteoblast and osteoblast-like cell-types used, the channel current increased linearly with increasing potential up to around 140 mV. Further increases in potential, between around 140 mV and 200 mV, resulted in a decrease in single channel current but at the same time a marked increase in channel open probability. This I/V 'tailing' at high potentials was seen in all cell-attached patch recordings of this channel type (Figure 3.7).

3.3.1.1.2   Excised inside-out

This patch configuration often displayed active large conductance channels at 0 mV patch potential. Current amplitudes decreased with depolarising potentials and dropped to zero for potentials higher than around 50 mV, but increased with hyperpolarising potentials.

In MG63 cells, with High K solution in the electrode and Locke solution bathing the cells, the mean slope conductance from excised inside-out recordings was 154.2 ± 4.7 pS (n = 8) and the extrapolated corrected mean E_{rev} of these channels by polynomial curve fitting was 43.9 ± 4.7 mV (see Figure 3.8 for an example). In experiments where sodium gluconate Locke was substituted for Locke solution, the mean conductance was 129.8 ± 4.9 pS (n = 2) with a corrected mean E_{rev} of 59.78 ± 12.6 mV.

Calculating using the Goldman-Hodgkin-Katz equation (equation 3.8), the channel was selectively permeable for potassium over sodium by between 4: 1 (minimum E_{rev}) and 24: 1 (maximum E_{rev}) with High K / Locke, and by between 8: 1 and 30: 1 with High K / Na gluconate Locke.

$$E = 58 \log \frac{P_K [K]_i + \alpha [Na]_i}{P_K [K]_o + \alpha [Na]_o}$$

Eqn. 3.8

where E is the reversal potential and α is the channel selectivity ratio P_K/P_{Na}.

In the excised inside-out patches, 20 mM TEA applied to the external side of the patch (in the patch electrode) resulted in an absence of channel activity at potentials where channel activity was previously seen (n = 9) (Figure 3.8).

For HOB-c cells, inside-out patch recordings revealed I/V plots with channel conductances of 180.2 ± 4.2 pS (n = 3) with extrapolated slopes revealing a corrected mean E_{rev} of 44.5 ± 6.5 mV with High K solution in the electrode and Locke solution bathing the cells. All of these patches had two or more active large conductance channels, and the example given in Figure 3.9 shows at least 6 channels active. The channel was selective for potassium over sodium by between 5: 1 and 19: 1.

In SaOS-2 cells, a single I/V plot yielded a slope conductance of 193.9 pS and with a corrected E_{rev} of 35.9 mV with High K solution in the electrode and Locke as the bathing solution (Figure 3.10). From this recording, the channel was selective for potassium over sodium by 5: 1.

3.3.1.1.3   Similar characteristics in MG63, SaOS-2 and HOB-c cells

Figure 3.11 demonstrates that the large conductance channels are electrophysiologically similar in all three osteoblast or osteoblast-like cell types, both in the cell-attached and excised inside-out configurations, although the mean cell-attached conductance value for HOB-c cells was higher than for MG63 cells (244 ± 10.3 pS, n = 3 vs. 199 ± 5.1 pS, n = 12). Patch membrane

reversal potentials (E_{rev}) were similar for all three cell lines in both cell-attached and inside-out mode.

3.3.1.1.4   Large conductance channel kinetics

Log-square distribution plots of open and closed times were constructed (Figure 3.12) for MG63 cell large conductance single-channel data at 90 mV, 110 mV and 140 mV to determine if increases in P_{open} with increasing potential were due to more short openings, or longer periods of channel openings. Open and closed time distribution peaks were fitted with exponential probability density function curves where possible. The slower components of the closed dwell time curve fits (τ_c) decreased with increasing potential from 34 ± 2.1 ms at 90 mV to 8.549 ± 0.43 ms at 140 mV. The open dwell time fast component τ_{o1} did not appear to change with increasing potential, but the slow component τ_{o2} increased from 1.343 ± 0.157 ms at 90 mV to 5.514 ± 0.3 ms at 140 mV.

3.3.1.1.5   Maxi-K activation following application of glutamate

A short series of experiments was conducted in MG63 cells to test the Ca^{2+}-activation of the large conductance channel reported above, and to further confirm the identity of this channel. Applications of glutamate were made to Mg^{2+}-free bathing solution (Locke) of cell-attached patches, held at 100 mV depolarising potential, to give final concentrations of 2 μM glutamate or 100 μM glutamate (Figure 3.13). Coverslips of cells were changed between each application, so all cells recorded were naïve to glutamate. Patches selected were considered to have maxi-K channel activity at +100 mV before glutamate

application by measurement of the channel current ($\geq$ 8 pA). 2 μM glutamate caused a delayed increase in channel activity (delayed between 25 and 50 seconds) in 4/7 patches (in the remaining 3 patches the seal became unstable and broke during or immediately after glutamate application). Application of 100 μM glutamate (to different cells) caused marked and almost immediate increases in maxi-K activity in 6/8 patches (again, in the remaining 2 patches the seals were broken on glutamate application).

3.3.1.2 The 149 pS conductance channel

This channel type was recorded in 12% of successful MG63 cell-attached patches with High K solution in the electrode. From these recordings, I/V plots were created and slope conductances were derived from 3 patches. The mean single channel conductance was 149.9 $\pm$ 2.31 pS (n = 3) with a mean reversal potential, E_{rev}, of 55 $\pm$ 8.96 mV. Channel activity was voltage-dependent over depolarising potentials. A representative example is shown in Figure 3.14.

3.3.1.3 The 45 pS conductance channel

This channel was recorded in 3 cell-attached patches with High K solution in the electrode (1 HOB-c cell, 2 MG63 cells) and had a mean single channel conductance of 45.46 $\pm$ 1.1 pS (n = 3) and a mean E_{rev} of 52.5 $\pm$ 4.8 mV. This channel-type did not appear to be voltage dependent over the hyperpolarising and depolarising potentials used, but was densely packed in each patch with at least 6 or 7 channels active per patch (Fig 3.16). The channel displayed inward rectification at depolarising potentials.

Table 3.x Summary of Chapter 3 patch-clamp findings
Categorised into 3 groups according to channel conductance, from the data for which
I/V plots could be constructed. (c/a: cell-attached, i/o: inside-out).

	MG63			HOB-c	SaOS-2
	High K / Locke	High K / Na gluconate	Na gluconate / Na gluconate	High K / Locke	High K / Locke
c/a	198.7 ± 9 pS E_{rev} 60.7 ± 7.7 mV (n = 8)	212.5 ± 15 pS E_{rev} 56.2 ± 6.7 mV (n = 6)	221.8 pS E_{rev} 7.8 (n = 1)	239.5 ± 6.4 pS E_{rev} 68.6 ± 4.8 mV (n = 2)	
i/o	154.2 ± 4.7 pS E_{rev} 43.9 ± 4.7 mV P_K/P_{Na} = 14:1 (n = 8)	129.8 ± 4.9 pS E_{rev} 59.8 ± 12.6 mV P_K/P_{Na} =19:1 (n = 2)		180.2 ± 4.2 pS E_{rev} 44.5 ± 6.5 mV P_K/P_{Na} = 12:1 (n = 3)	193.9 pS E_{rev} 35.9 mV P_K/P_{Na} = 5:1 (n = 1)
c/a	149.9 ± 2.31 pS E_{rev} 55 ± 8.96 mV (n = 3)			149.8 pS E_{rev} 37.6 mV (n = 1)	
c/a	43.7 ± 0.7 pS E_{rev} 48.2 ± 1.4 mV (n = 2)			49 pS E_{rev} 61.1 mV (n = 1)	

3.3.2 Extracellular calcium and serum concentration changes

affect MG63 cell growth

Small adjustments to the free calcium concentrations $[Ca^{2+}]_o$ of DMEM culture

medium (Invitrogen) by chelation with EGTA appeared to result in growth

differentials of MG63 osteoblast-like cells after chronic exposure (days). Wells

with 1.2 mM $[Ca^{2+}]_o$ contained significantly more cells at days 9, 12 and 13 (p

> 0.05) compared to wells containing the standard (control) 1.8 mM $[Ca^{2+}]_o$

(see Figure 3.16). Between 2 and 8 days there were no significant differences

between cell numbers. Wells containing 0.6, 2.4 or 3.0 mM $[Ca^{2+}]_o$ were not

significantly different from the control wells. MG63 cells grown in DMEM

with foetal bovine serum concentrations of 0 %, 0.1%, 0.5 %, 1 % and 5 %

showed increased cell numbers with increasing serum concentrations after 72

hours exposure (Figure 3.17). This may possibly be due to chelation of the calcium, the effects of which would be larger in the smaller concentrations of serum. The above effects of free-Ca^{2+} dependent proliferation probably share a common mechanism, which is likely to be mediated by the calcium-sensing receptor (see discussion).

3.3.3   Effect of K_{ATP} ligands on MG63 cell growth

The K_{ATP} channel-blocking sulphonylureas glibenclamide and tolbutamide, and the K_{ATP} channel openers pinacidil (cyanoguanidine-type), diazoxide (benzothiadiazine-type) and levcromakalim (benzopyran-type) were tested at various concentrations against the proliferation of MG63 osteoblast-like cells over a period of days (72 hours).

After 72 hours of exposure, pinacidil significantly increased MG63 cell numbers (P < 0.05, n = 3) at 30 μM, 100 μM and 300 μM compared to vehicle control wells (Figure 3.18). Neither diazoxide 0.1 – 300 μM (Figure 3.19), nor levcromakalim 0.1 – 100 μM (Figure 3.20), had any significant effect on cell numbers after 72 hours exposure.

The sulphonylurea glibenclamide significantly decreased cell numbers at 100 μM and 300 μM (P < 0.05) whereas lower concentrations had no significant effect during the same time. Similarly, tolbutamide significantly decreased cell numbers at 300 μM (P < 0.05) but had no significant effect at lower concentrations (Figure 3.21).
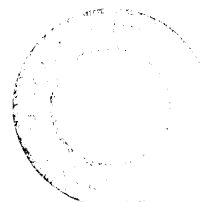
In an attempt to begin to map out the pharmacology of the pinacidil-induced proliferation of MG63 cells, low non-growth inhibiting doses of glibenclamide (10 µM) or tolbutamide (10 µM) were exposed to the cells in combination with pinacidil (0.1 – 300 µM). After 72 hours exposure, neither glibenclamide nor tolbutamide blocked the proliferative effects of pinacidil, and significant increases ($P < 0.05$) in cell numbers were observed at 30, 100 and 300 µM pinacidil with either tolbutamide or glibenclamide (Figure 3.22).

3.3.4 RT-PCR: K channels in MG63 cells

3.3.4.1 MG63 osteoblast like cells contain mRNA for K_{ATP} channel & SUR subunits

The expression of K_{ATP} channels Kir6.1 (KCNJ8) and Kir6.2 (KCNJ11) and associated sulphonylurea receptor subunits SUR1 (ABCC8) and SUR2B (ABCC9) in MG63 cells was confirmed by RT-PCR as shown in Figure 3.23.

3.3.4.2 MG63 osteoblast-like cells contain mRNA for maxi-K channel subunits

RT-PCR confirms the presence of the maxi-K channel α pore-forming subunit KCBMA1 and all four known associated β subunits KCNMB1, KCNMB2, KCNMB3 and KCNMB4 in MG63 osteoblast-like cells (Figure 3.24). Sequencing of the products confirmed the identity of all five maxi-K channel subunits.

3.4 Discussion

3.4.1 Channel activity

3.4.1.1 The large conductance channel

The large conductance, voltage-dependent channel has the hallmarks of the maxi-K channel. Channel characteristics were very similar for the primary human HOB-c osteoblasts and the MG63 and SaOS-2 human osteoblast-like cell lines, in either cell attached or excised inside out configuration, with cell attached conductances of 244 pS (n = 3) in HOB-c cells and 199 pS (n = 12) in MG63 cells. Single channel I/V plots showed that replacement of 140 mM K^+ in the electrode with 150 mM Na^+ (as sodium gluconate) shifted the curve to the left. This shift was probably due to maxi-K channel outward rectification caused by the potassium differential across the membrane and the selectivity of the channel for K^+, but there are no data at less positive potentials to prove this.

The voltage-dependent inactivation of the maxi-K channels (i.e. the tailing effect of I/V curves) at high depolarising potentials has been identified previously and is a hallmark of the maxi-K channel. Yellen (1984a; 1984b) reports that the effect is due to internal Na^+ blockade of the channel pore, but Goodwin *et al.* (1998) report observations of this phenomenon in excised patches of fibroblasts in the absence of Na^+ and suggest an intrinsic channel gating mechanism. Goodwin *et al.* (1998) also report the maxi-K channel 'priming' shown here.

The maxi K channel was seen in so many patches of osteoblasts and osteoblast-like cells, and in such numbers per patch, that it must be densely packed in the cell membrane and fairly evenly distributed rather than in tight clusters. If we were to calculate the approximate number of channels per cell from these single channel data, we might take an average of three channels per 1 μm^2 patch of membrane (which is perhaps erring on the conservative side) and calculate channel number per cell (membrane) as follows: an osteoblast of diameter 30 μm, assuming spherical shape for ease of calculation, will have a surface area of $4\pi r^2$:

$$4\pi \times 15^2 = 2827.4 \ \mu m$$

$$\therefore \quad 2827.4 \times 3 \text{ channels} \cong 8482 \text{ channels per cell}$$

This is clearly not an insignificant number of maxi-K channels. If we were to calculate the total conducting capacity of the channels in the membrane, taking a value of 220 pS per channel:

$$8482 \times 220 \times 10^{-12} = 1.866 \ \mu S \text{ per cell.}$$

Although maxi K is not active at rest in osteoblasts, the channel may contribute to plasma membrane potential following cytosolic calcium dumping, and the channel may have other important regulatory roles in these cells. A series of

whole-cell experiments could be carried out in future studies to confirm the above figures and the contribution of the channel to membrane potential.

The glutamate-induced current activation in MG63 cells provides further evidence that this large-conductance channel is indeed maxi-K. Osteoblasts, including the MG63 cell-line, have been previously reported to express functional neuronal-type N-methyl-D-aspartate (NMDA) receptors (Mason *et al.*, 1997; Gu *et al.*, 2000; Laketic-Ljubojevic *et al.*, 1999), which are known to be blocked by Mg^{2+} in MG63 cells in a voltage-insensitive way (Gu *et al.*, 2002), and also several alpha-amino-3-hydroxy-5-methyl-4-isoxazolepropionic acid (AMPA) and kainate glutamate receptor subtypes (see Taylor, 2002a/b for review). By applying glutamate to these cells in Mg^{2+}-free solution, the NMDA-type glutaminergic receptors, or the AMPA/kainate receptors, presumably allow Ca^{2+} influx as previously reported which therefore results in Ca^{2+}-activation of large conductance channels. This effectively shows that the osteoblastic large conductance channel reported in this Thesis is Ca^{2+}-activated and is supportive of the conclusion that this belongs to the maxi-K channel type.

3.4.1.2 The 45 pS conductance channel

This channel (45.46 ± 1.1 pS; n = 3), although only seen in a small number of patches, is active at rest and hyperpolarising potentials, seemingly inwardly rectifies in the cell-attached configuration in 140 mM K^+ and is voltage-independent. Although not seen often enough to begin to create a

pharmacological profile using patch clamping, it is possible that this channel belongs in the inward-rectifier (K$_{IR}$) family of K$^+$ channels, and possibly is of the K$_{ATP}$ subtype although ATP-sensitivity has not been systematically tested here.

3.4.1.3 The 149 pS conductance channel

This channel (149.9 ± 2.31 pS; n = 3) was voltage-sensitive and activated by depolarising potentials, after which it remained active below reversal potential and at hyperpolarising potentials. During recording, the channel appeared to behave as a maxi-K channel might and although the conductance is rather low and quite different from maxi-K channels discussed in 3.4.1.1, this channel might yet be maxi-K as it remains in the very broad window of conductance values for this channel type. Alternatively, the channel could be another member of the SLO K$^+$ channel family, such as SLO2.2 – a putative Na$^+$-activated K$^+$ channel with a conductance range of 100 – 180 pS. However, SLO2.2 is much more weakly voltage-sensitive than maxi-K (also known as SLO1) due to the positive charges on the maxi-K S4 domain of the α subunit being absent, and replaced with two negative charges. Also, it has been suggested in a review by Salkoff, et al. (2006) and by Joiner et al. (1998) that heteromultimerisation of the α subunits of maxi-K (SLO1) and other members of the SLO family might occur, resulting in functional and pharmacological diversity.

Due to a lack of evidence, it is impossible to make any meaningful conclusions about the identity of this channel and the intermediate conductance channel will not be discussed further in this thesis. Further experimentation with pharmacological agents would be useful to identify this channel in future work.

3.4.2 Extracellular calcium concentration affects MG63 growth

These experiments demonstrated that small <1 mM changes in $[Ca^{2+}]_o$ made to the cell culture medium can be detected by osteoblast-like cells. Decreasing $[Ca^{2+}]_o$ from the standard 1.8 mM Ca^{2+} of DMEM culture medium to 1.2 mM caused significant cell proliferation. The detection of such small changes in $[Ca^{2+}]_o$ are thought to be due to surface membrane calcium-sensing receptors (CaR) which have been shown to be expressed in osteoblast-like cells (Dvorak *et al.*, 2004). Foreman *et al.* (2006) have also reported a role for extracellular calcium in proliferation and differentiation of primary bone marrow stromal cells, in the form of calcium oscillations which can be evoked by serum-containing medium. There is no evidence to date that the maxi-K channel is able to directly detect extracellular calcium concentration in the physiological range 1 – 3 mM, although the HERG channel (human ether-a-go-go related gene, or K$_v$11.1) does have an extracellular calcium sensor which has been shown to have the ability to detect within this narrow range (Johnson *et al.*, 1999; Johnson *et al.*, 2001) and Hofer (2005) has reviewed the evidence, indicating that extracellular Ca^{2+} signalling and detection may be more significant and diverse than previously thought.

3.4.3 Effect of K$_{ATP}$ ligands on MG63 cell growth

While the ATP-sensitive potassium channel openers diazoxide and levcromakalim had no effect on MG63 proliferation (cell numbers) over the concentrations and durations of exposure tested, the third opener, pinacidil, caused definite and significant increases in cell numbers at higher concentrations which were not attenuated by growth-uninhibiting concentrations of the sulphonylureas. These data alone begin to paint a confusing picture of what the K$_{IR}$6.x/SUR channel compositions might be in osteoblast-like cells as the SUR subunits and splice variants identified to date are each thought to be able to bind several KCOs in different combinations and with different affinities. It is possible that although pinacidil is the only agent that caused proliferation, other KCOs might have affected signalling pathways or secretions not explored by this work, as has been reported with diazoxide which did not increase cell number but increased protein accumulation in bladder carcinoma cells (Wondergem *et al.*, 1998). Alternatively, proliferation induced by pinacidil might involve a different, unknown mechanism from K$_{ATP}$ activation.

In MG63 cells, the sulphonylureas alone inhibited growth at higher concentrations, similar to those reported on other cell- and tissue-types with serum-containing media (Braun *et al.*, 2002; Malhi *et al.*, 2000; Wondergem *et al.*, 1998). The growth inhibiting concentrations ($\geq$ 100 μM) are higher than reported channel blocking concentrations (1 – 10 μM), but as sulphonylureas are well documented to bind to plasma proteins in serum-containing medium

resulting in lower free sulphonylurea concentrations, this is hardly surprising. The consequences of sulfonylurea-plasma protein binding on growth inhibiting concentrations have also been reported previously by Wondergem *et al.* (1998).

These data add yet more weight to the argument that K^+ channels have an important role in the cell cycle, promoting proliferation in human osteoblasts.

3.4.4   RT-PCR: K channels in MG63 cells

3.4.4.1 Expression of K_{ATP} subunits

The expression of mRNAs for both pore-forming $K_{IR}6.1$ and $K_{IR}6.2$ subunits, and for SUR1 and the SUR2B splice variant (of SUR2) adds weight to the proliferation data and the single channel data. From the semi-quantitative band intensities of the ethidium bromide-stained gel, $K_{IR}6.1$ and $K_{IR}6.2$ mRNAs appear to be fairly equally expressed. Heteromultimers of $K_{IR}6.1$ and $K_{IR}6.2$ subunits forming the pore may be responsible for the 44 pS value of the conductance for the presumed K_{ATP} channel, derived from a combination of conductance values from homomultimeric $K_{IR}6.1$ channels at 33 – 40 pS and homomultimeric $K_{IR}6.2$ channels at 65 – 80 pS in 140 mM K^+. The expression of SUR1 and SUR2B should result in channel sensitivity to all the KCOs and blockers used, although the membrane protein-expressed $K_{IR}6.x$/SUR subunit combinations remain unknown.

3.4.4.2 Expression of maxi-K subunits

MG63 cells express mRNA for the pore-forming α subunit and all four associated β subunits which determine the channel pharmacology. While $\beta2$, $\beta3$ and $\beta4$ show similar levels of expression, $\beta1$ band intensities remained low even with 40 cycles of PCR. The RT-PCR data confirms maxi-K channel presence in MG63 cells and suggests that if heteromultimers were to form, that more likely combinations would include $\beta2$, $\beta3$ and $\beta4$ subunits than $\beta1$.

3.4.5 Chapter conclusions and future work

Parts (i) and (ii) of the hypothesis were both deemed to be true. Both maxi-K and K_{ATP} channels have been identified in human osteoblast-like cells, and for the first time the BK_{Ca} channel is shown to be expressed in primary human osteoblasts. There is evidence of a proliferative role for K_{ATP} channels in human osteoblasts cells as demonstrated by the K_{ATP} opener pinacidil, and maxi-K channels may also have a regulatory role in bone cell growth, possibly by $[Ca^{2+}]_o$ detection or regulation of the cell resting membrane potential following calcium dumping. The surface membrane maxi-K channel β subunit composition in osteoblasts is yet to be discovered, but mRNAs for all four β subunits are expressed. Similarly, K_{ATP} channel subunit composition requires attention in these cells to begin to understand pharmacology of the channel and the mechanisms behind the proliferative effects. Extracellular calcium concentration also appears to be important in bone cell growth and minor concentration changes can be detected at the cellular level. In summary, this

chapter delivers the fullest description yet of the maxi-K channel in bone and therefore may be a useful reference for future work in this area.

The results presented in this chapter open up many further questions that require addressing in future work, but some immediate suggestions for follow-up investigations include:

- the determination of the maxi-K channel subunit composition at protein level in osteoblasts, and the consequences of this for maxi-K pharmacology in these cells with various known K channel openers and blockers

- clarifying the role maxi K channels play in osteoblastic signalling pathways involving cytosolic and extracellular calcium

- the role of maxi-K channels in the functions of osteoblasts, considering the abundance of the channel in the plasma membrane, and the consequences of maxi K gene knockout on bone, taking advantage of recent developments in tissue-specific gene knockout technologies

- further work on the identification of the intermediate conductance K channel observed in osteoblasts, including building a pharmacological profile of the channel and importantly determining ATP sensitivity

- in conjunction with the previous suggestion, further investigate the interesting effects of pinacidil on osteoblasts including proliferation and mineralisation, extending the work to other similar KCOs (such as nicorandil and minoxidil)
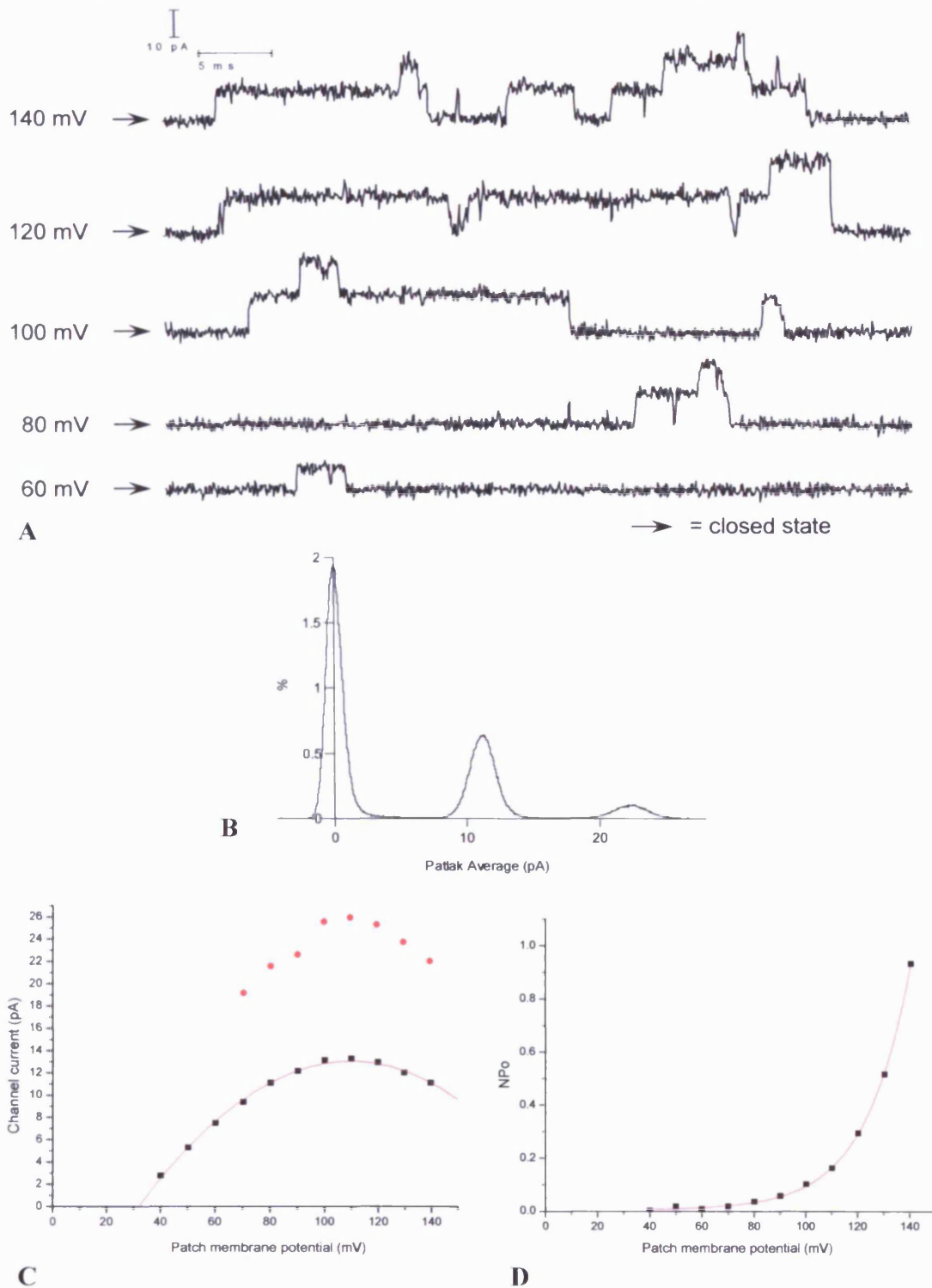
Figure 3.5 **Large conductance (maxi-K) channel in MG63 cell cell-attached patch.** (High K pipette, Na gluconate bath) **(A)** Raw data showing at least 3 channels in this patch (140 mV) **(B)** Patlak average distribution of current histogram from data record at 140 mV, showing peaks at 11.12 pA and 22.27 pA. **(C)** I/V plot from these data recordings. Single channel conductance $\gamma = 207.4$ pS (40 to 80 mV), $R^2 = 0.99417$. **(D)** NPo/V plot shows that these channels increase in activity with increasing potential.
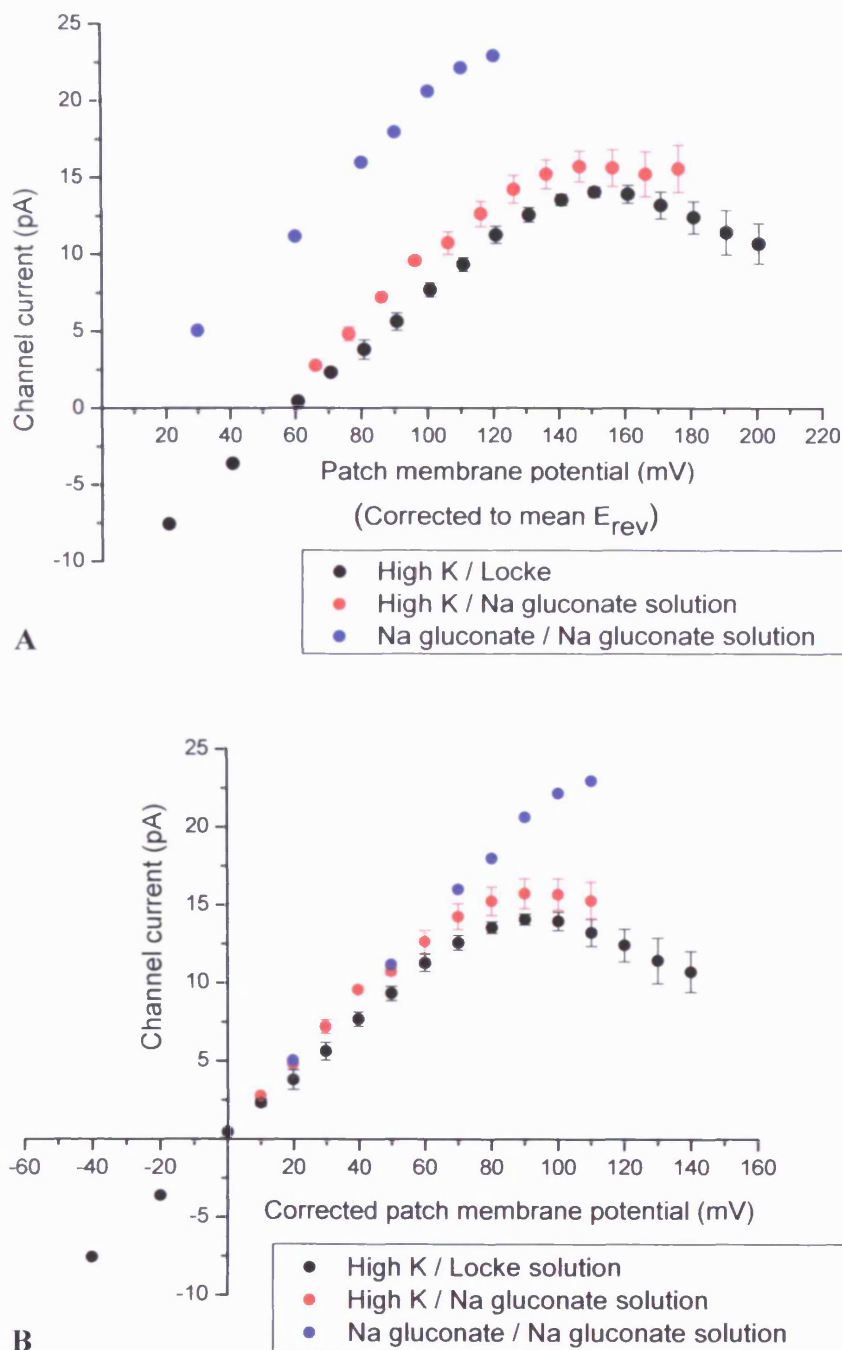
Figure 3.6 **Large conductance (maxi-K) channels in MG63 cells.** Recorded in the cell-attached configuration. **(A)** shows mean I/V plots for patches with different solution combinations in the electrode and bathing the cells respectively, according to the key. Plots are adjusted to mean E_{rev} for each curve and are corrected for calculated junction potentials. • n = 7, E_{rev} = 60.7 ± 7.7 mV; • n = 3, E_{rev} = 56.18 ± 6.7 mV; • n = 1, E_{rev} = 7.8 mV. **(B)** Same data as for A, with E_{rev} values corrected to 0 mV for each curve for comparison and superimposition. Mean slope conductances are very similar: • γ = 186.7 pS; • γ = 191.5 pS; • γ = 221.8 pS.
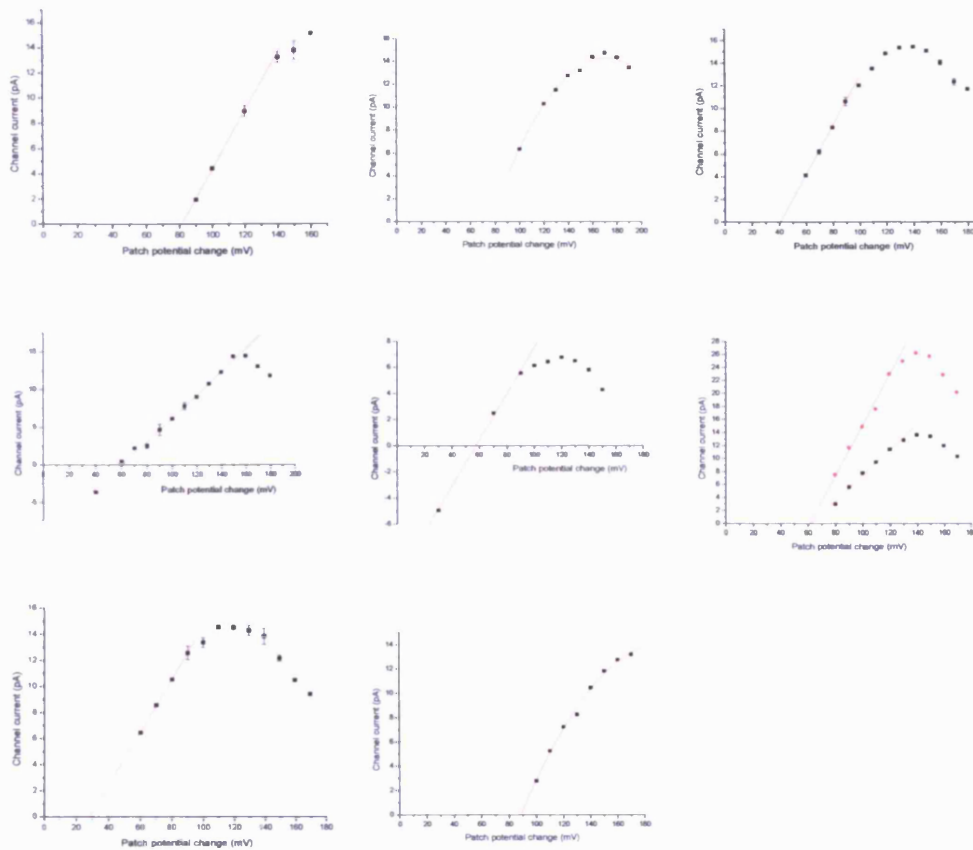
Figure 3.7 **Examples of maxi-K I/V curves with slopes tailing-off at high potentials.** These examples are typical of all maxi-K channels seen and recorded. Current increases linearly with potential at first, but a point is reached after which the current begins to decrease with further increases of potential. This is accompanied by a further rise in P_{open}.
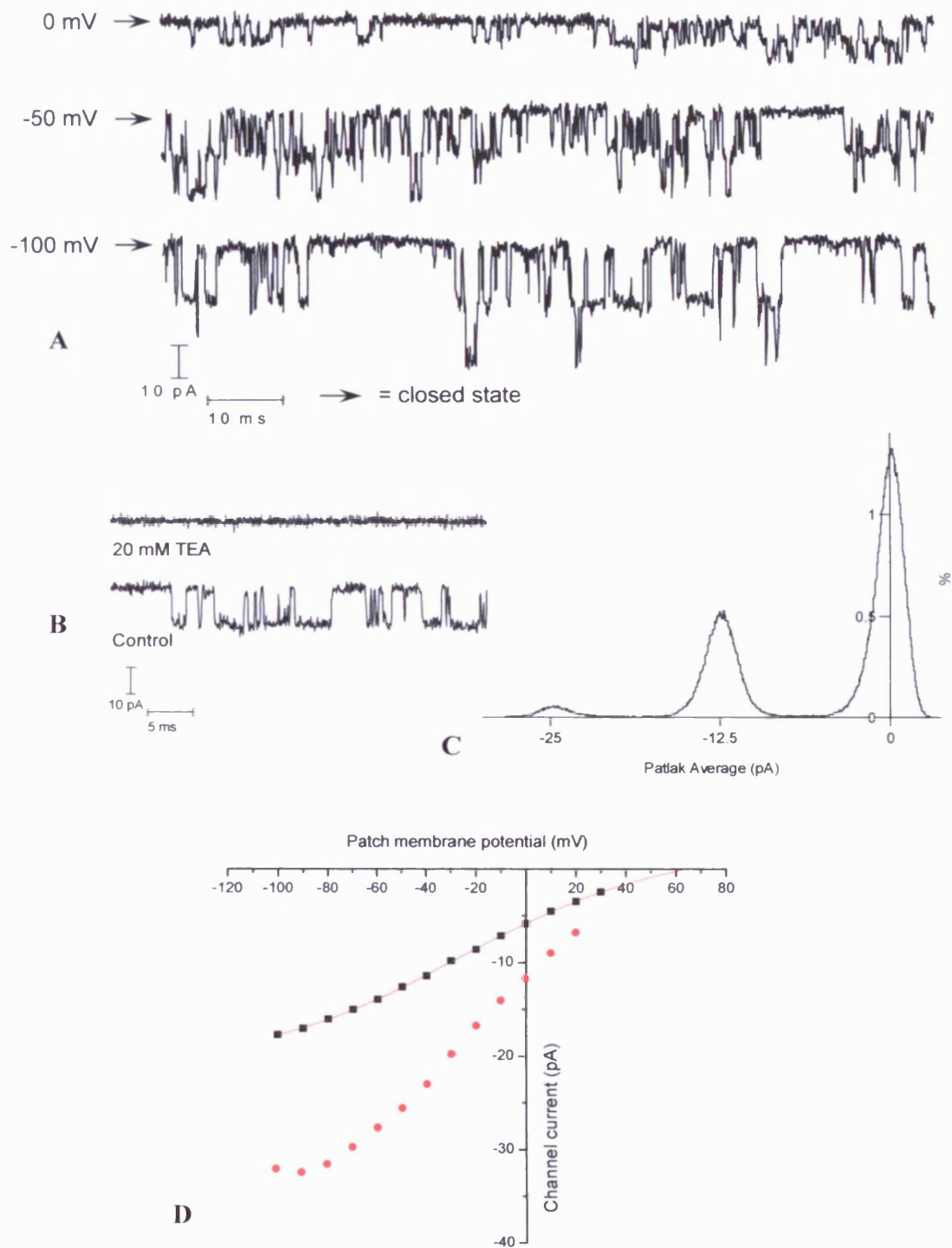
Figure 3.8 **Large conductance (maxi-K) channels in MG63 excised inside-out patch.** (High K pipette, Locke bath). **(A)** Raw data records show at least 2 channels in the patch. **(B)** 20 mM external TEA blocks this channel (at -60 mV) **(C)** Patlak average distribution of current histogram at -50 mV shows current peaks at -12.64 pA and -25.6 pA. **(D)** I/V plot showing inward rectification and uncorrected E_{rev} = 64.2 mV. Single channel conductance γ = 136 pS (R^2 = 0.99936). Junction potential-corrected E_{rev} = 64.2 + 4.5 = 68.7 mV.
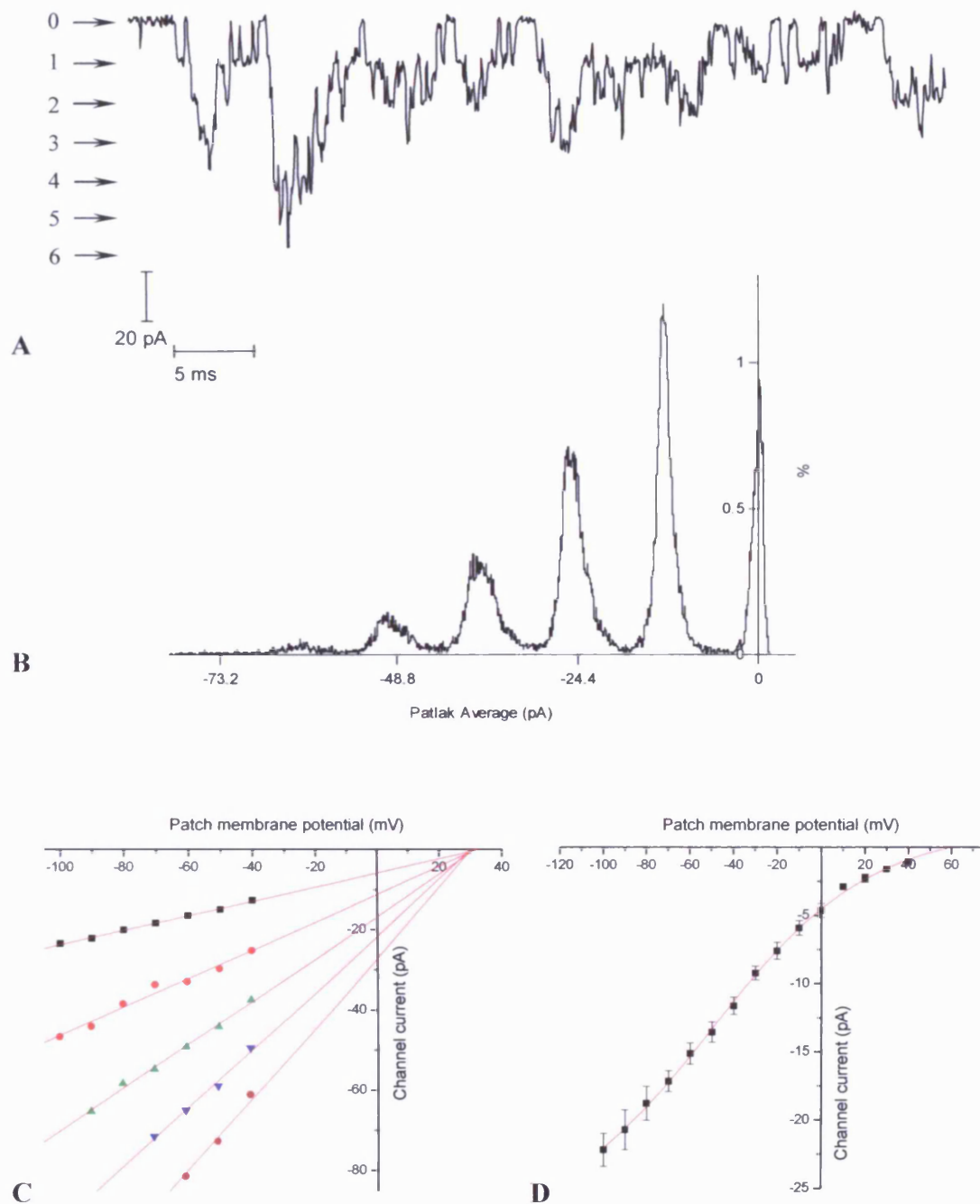
Figure 3.9 **Maxi-K channel data from HOB-c cell excised inside-out patch.** (High K pipette, Locke bath). **(A)** Data recording at -40 mV patch potential. 6 distinct current levels indicate at least 6 ion channels in the patch. **(B)** Patlak average distribution of current histogram with peaks at -12.71 pA, -25.18 pA, -37.42 pA, -49.42 pA and -61.01 pA. **(C)** I/V plot showing slope conductances (linear regression, -100 mV to -40 mV) of 178.3 pS (R^2 = 0.997), 351 pS (R^2 = 0.976), 553.3 pS (R^2 = 0.994), 717.8 pS (R^2 = 0.998) and 900 pS (R^2 = 0.993). **(D)** I/V plot (n = 3 cells) showing E_{rev} = 60 mV. When corrected for junction potential, E_{rev} = 60 + 4.5 = 64.5 mV.

110
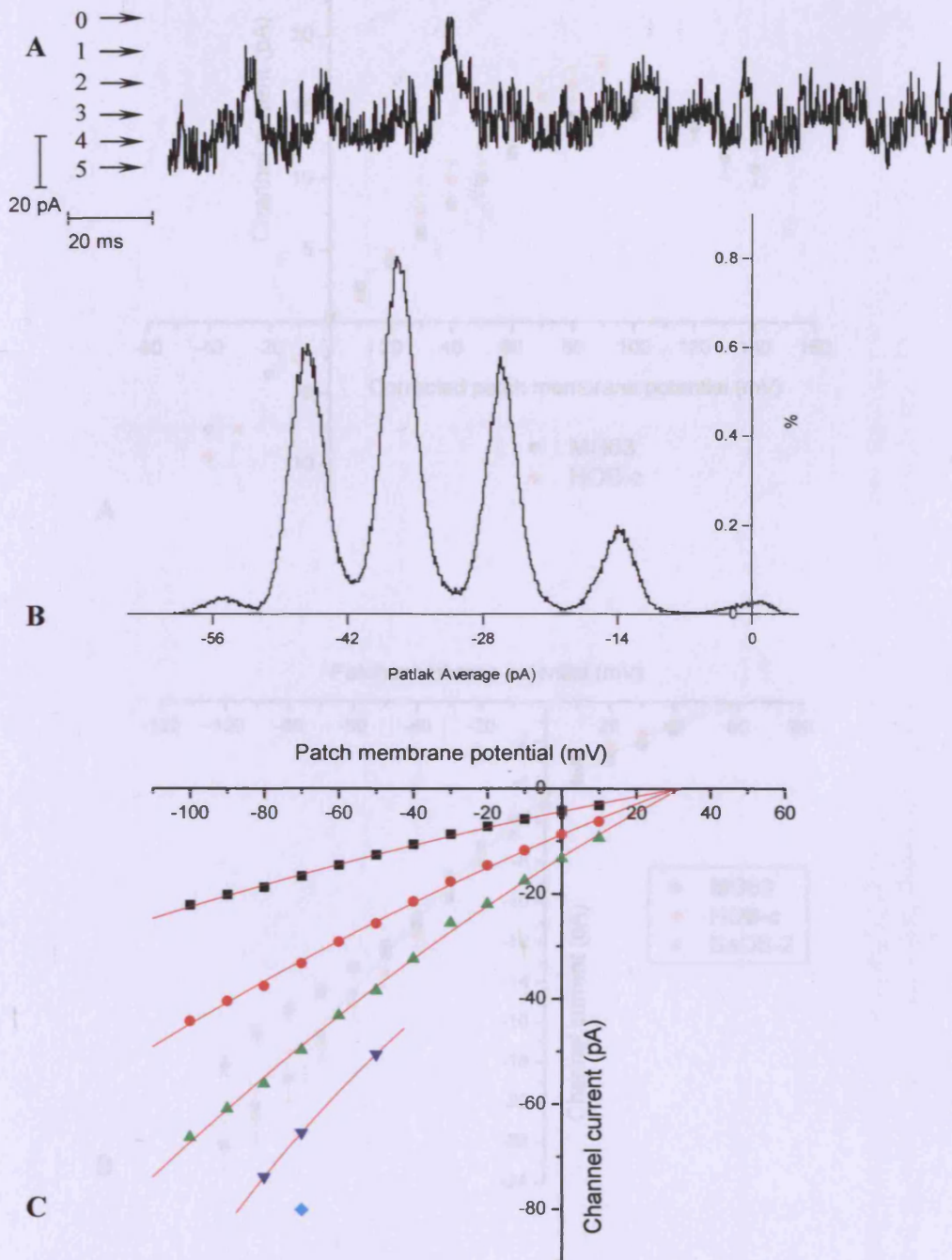
Figure 3.10 **Maxi-K channel data from an SaOS-2 cell excised inside-out patch.** (High K pipette, Locke bath). **(A)** Data recording at -50 mV patch potential. 5 distinct current levels indicate at least 5 ion channels in the patch. **(B)** Patlak average distribution of current histogram, at -50 mV, with peaks at -13.91 pA, -25.99 pA, -36.65 pA, -46.17 pA and -54.85 pA. **(C)** I/V plot showing channel reversal potential E_{rev} = 31.4 mV, corrected for junction potentials to E_{rev} = 31.4 + 4.5 = 35.9 mV. Slopes (linear regression, -100 mV to -40 mV) reveal conductance states of 193.9 pS (R^2 = 0.99812), 380.7 pS (R^2 = 0.99834), 572.1 pS (R^2 = 0.99844) and 775 pS (R^2 = 0.99902).

111
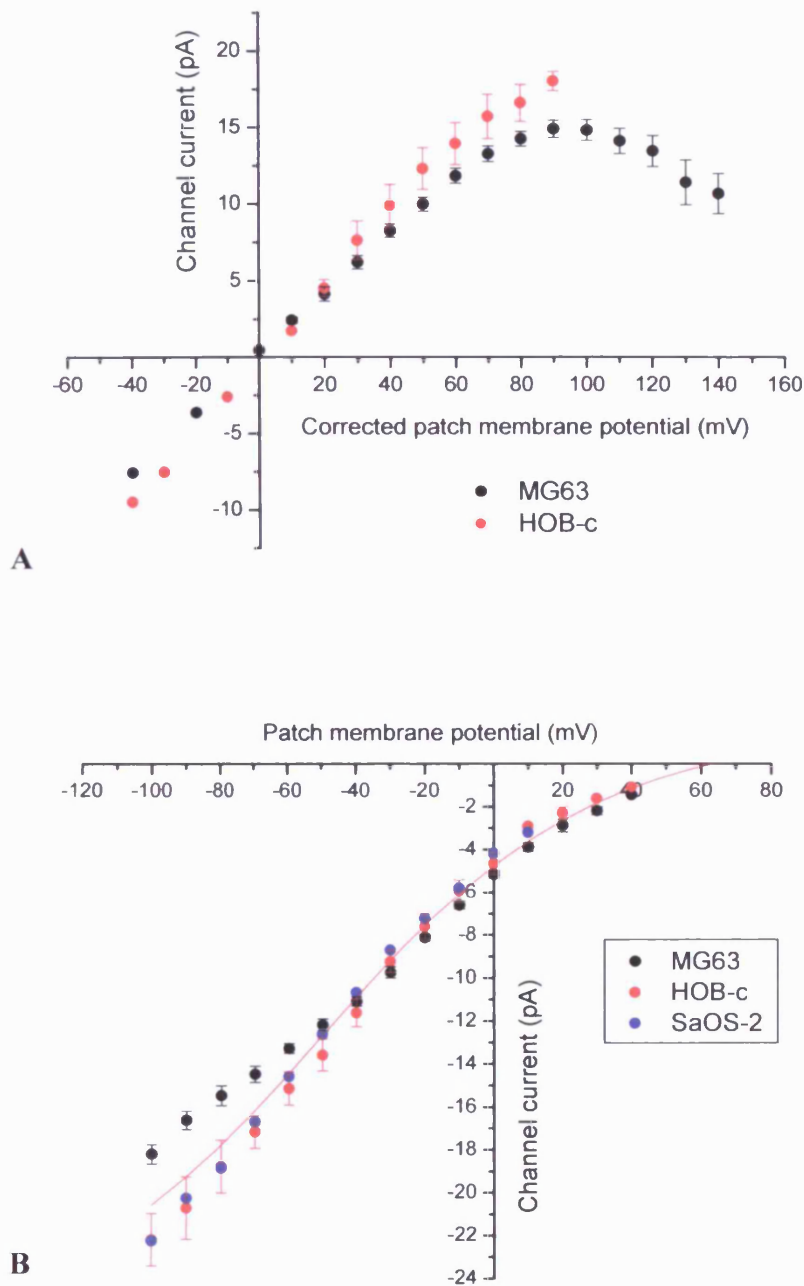
Figure 3.11 **Comparison of maxi-K channels in MG63, SaOS-2 and HOB-c cells.** (High K pipette, Locke bath). **(A)** I/V plot from cell-attached patches of MG63 (n = 12) and HOB-c (n = 3) cells, adjusted to E_{rev} = 0. Mean MG63 maxi-K conductance γ = 199 pS (R^2 = 0.999); mean HOB-c maxi-K conductance γ = 244 pS (R^2 = 0.999). **(B)** I/V plot from excised inside-out patches of MG63 (n = 9), HOB-c (n = 3) and SaOS-2 (n = 1). E_{rev} = 63.1 mV from mean of the slopes by Boltzmann curve fit, corrected for junction potentials to E_{rev} = 63.1 + 4.5 mV = 67.6 mV and P_K/P_{Na} = 23.

$\tau_c = 34 \pm 2.106$ ms

$\tau_{c1} = 0.1387 \pm 0.01$ ms
$\tau_{c2} = 23.35 \pm 0.6579$ ms

$\tau_{c1} = 0.1737 \pm 0.006$ ms
$\tau_{c2} = 8.549 \pm 0.4313$ ms

A

B

C

$\tau_{o1} = 0.1062 \pm 0.01$ ms
$\tau_{o2} = 1.343 \pm 0.157$ ms

$\tau_{o1} = 0.1393 \pm 0.01$ ms
$\tau_{o2} = 2.805 \pm 0.1909$ ms

$\tau_{o1} = 0.1228 \pm 0.006$ ms
$\tau_{o2} = 5.514 \pm 0.3$ ms
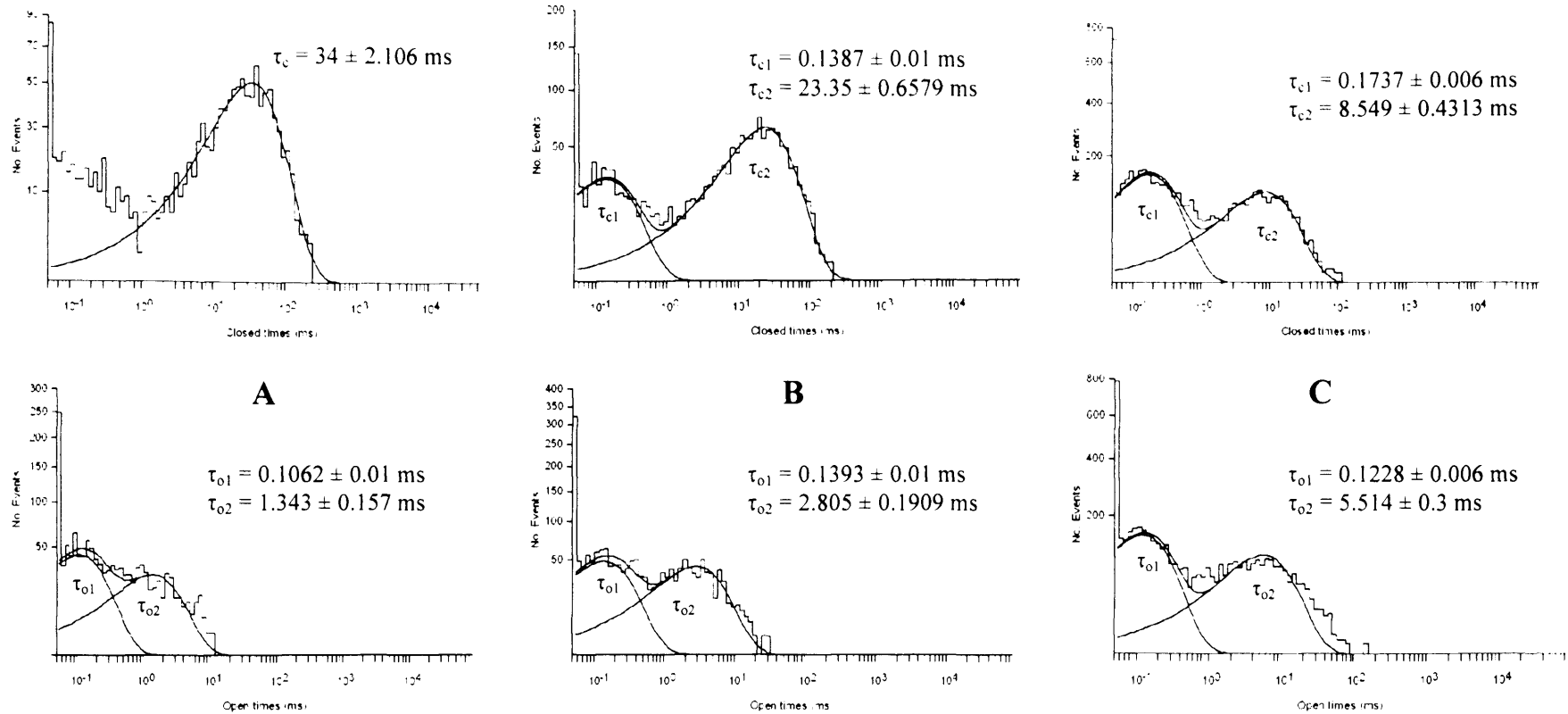
Figure 3.12 **Dwell time histograms** demonstrating that increase in P_{open} in maxi-K cell-attached patches of MG63 cells is due to longer states of channel opening, and not just more short openings. Patch holding potentials are (**A**) +90 mV, (**B**) +120 mV and (**C**) +140 mV.
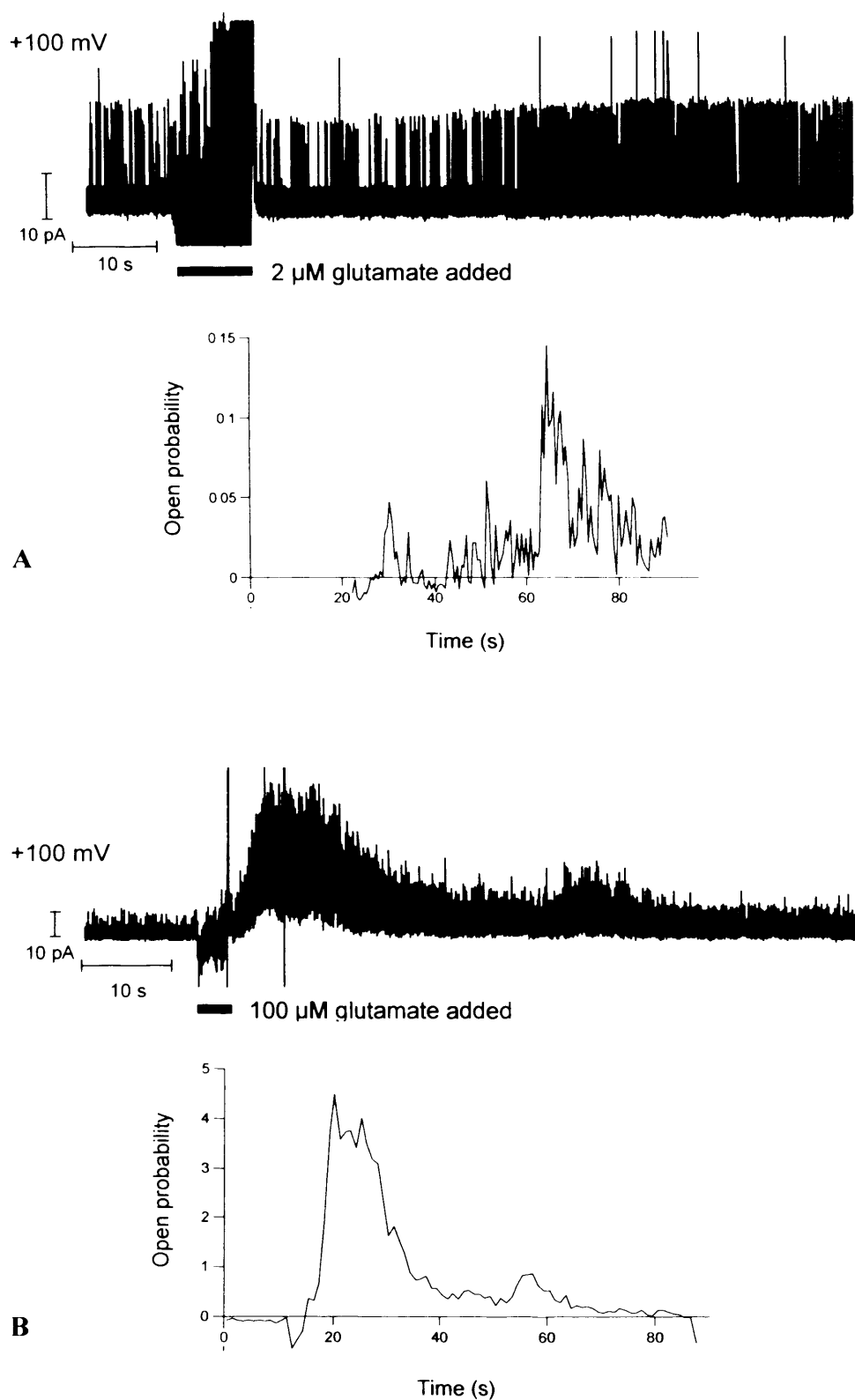
Figure 3.13 **Glutamate enhances maxi-K channel activity in MG63 cells. A** at +100 mV patch potential, 2 μM glutamate increases maxi K channel activity after 40 s. **B** also at +100 mV patch potential, 100 μM glutamate markedly increases maxi-K channel activity almost immediately after application. The mechanism is presumably that glutamate-induced Ca^{2+} influx through NMDA channels causes Ca^{2+}-activation of the maxi-K channel. Data shown are representative examples of experimental results.
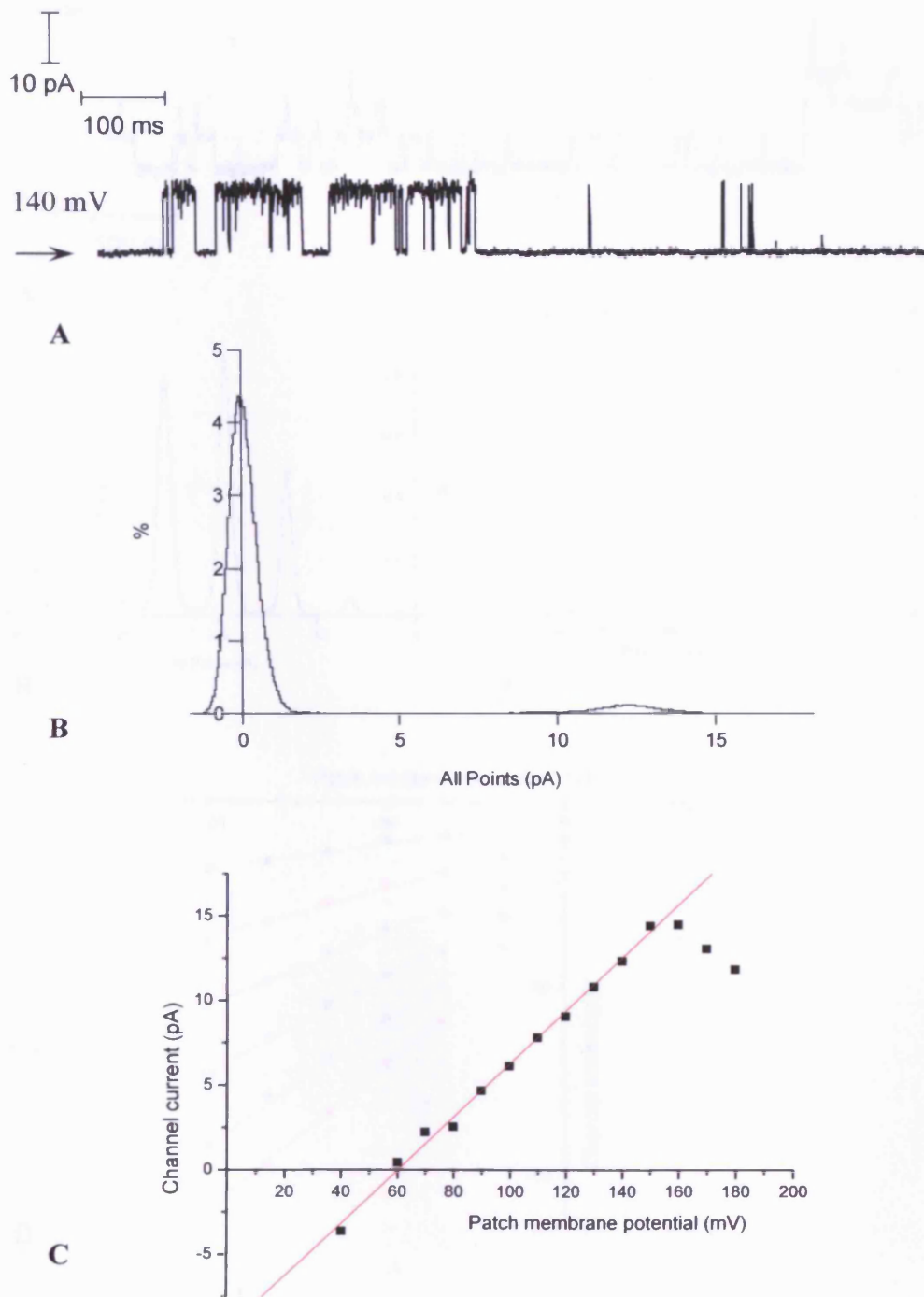
Figure 3.14 **An example of the intermediate conductance channel recorded in MG63 cells** (High K pipette, Locke bath). **(A)** A sample of data record showing channel openings at +140 mV. **(B)** Distribution of current histogram at the same patch potential showing a current peak at 12.34 pA. **(C)** I/V plot fitted with a line of best fit by linear regression over 40 to 150 mV giving a conductance of 154 pS ($R^2 = 0.994$) and an E_{rev} of 60 mV, corrected for junction potentials to $E_{rev} = 60 + 4.5 = 64.5$ mV.

A

B

All Points (pA)

C

Patch membrane potential (mV)

NPo

D

Patch membrane potential (mV)
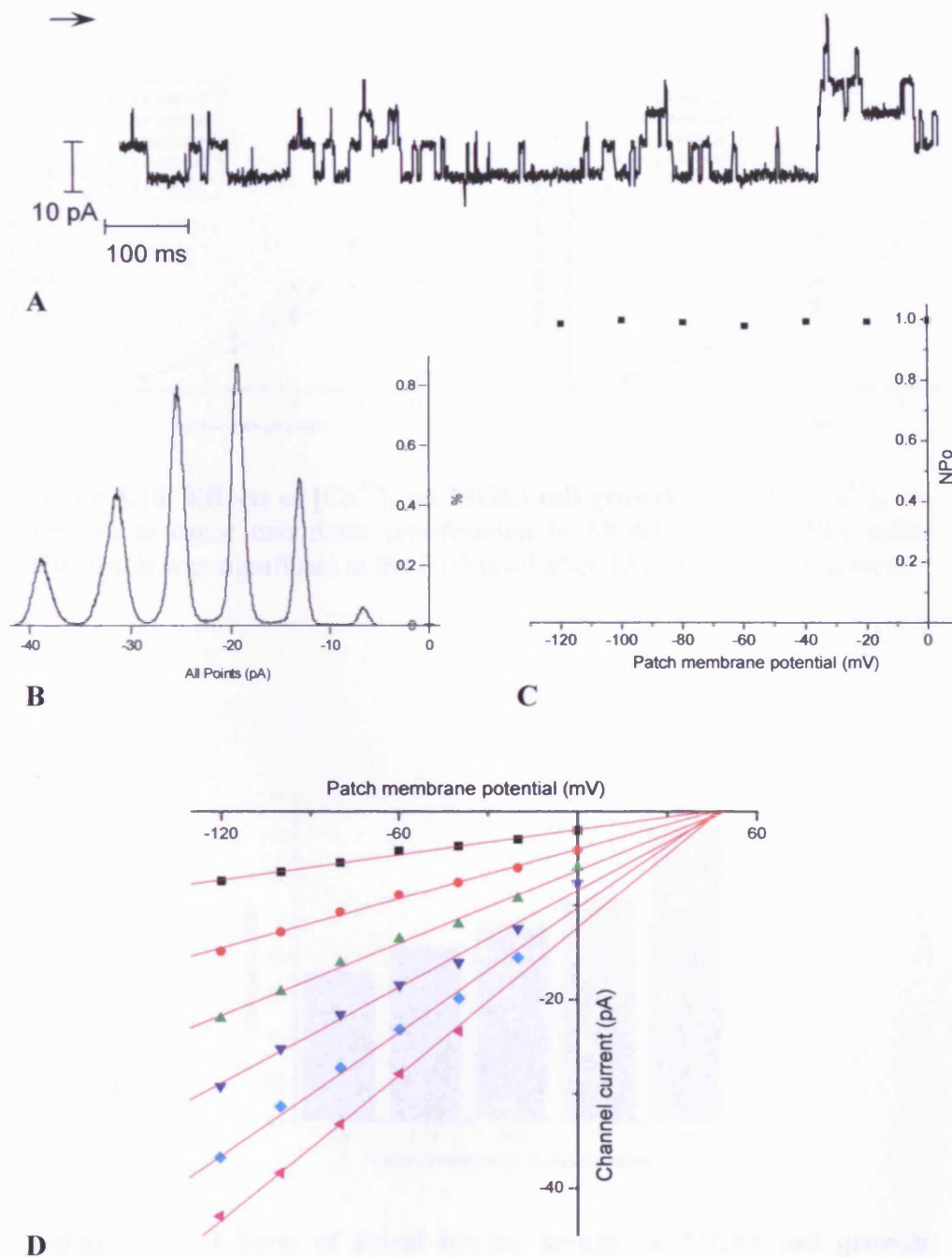
Channel current (pA)

Figure 3.15   **A representative example of the small conductance channels in MG63 osteoblast-like cell-attached patches. (A)** shows the density and activity of this channel type, with at least 6 current states shown in the data record at -100 mV patch potential. **(B)** is a distribution of current histogram displaying 6 current states which are multiples of -6.432 pA. **(C)** NPo/V plot showing this channel type is not voltage dependent over the range shown. **(D)** I/V plot from the 6 current states giving a single channel conductance of 44.4 pS from the slope by linear regression (R^2 = 0.99).

116
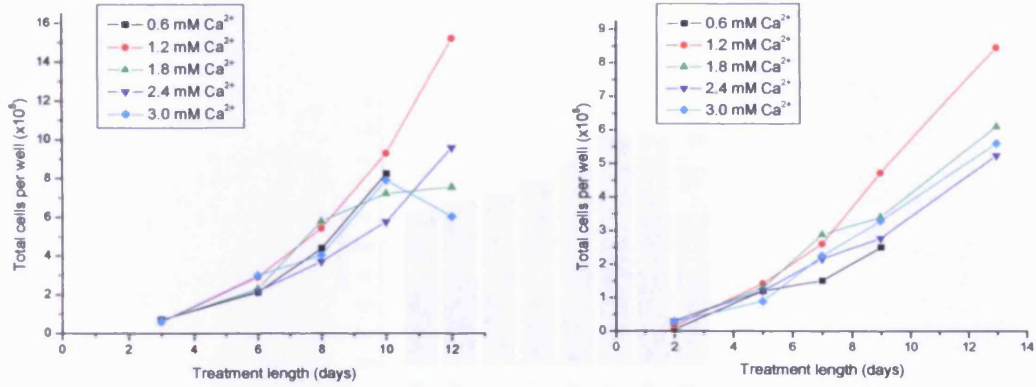
Figure 3.16 **Effects of [Ca^{2+}]$_o$ on MG63 cell growth.** 1.2 mM [Ca^{2+}]$_o$ -●- appears to cause maximum proliferation in MG63 osteoblast-like cells. This result was significant at the 0.05 level after 12 and 13 days treatment.
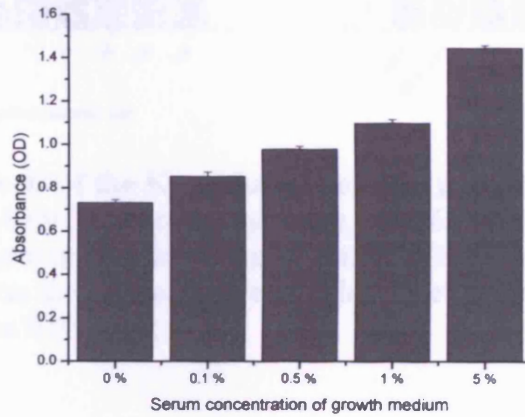
Figure 3.17 **Effects of foetal bovine serum on MG63 cell growth.** Proliferation of MG63 cells is shown to be serum-dependent.

117
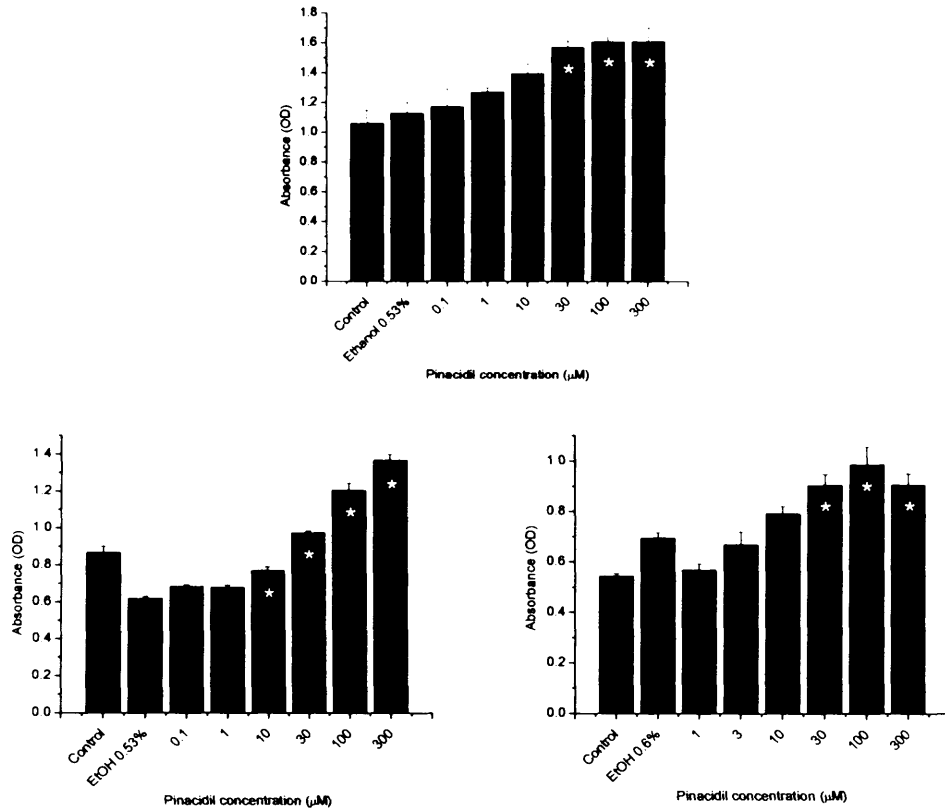
Figure 3.18 **Effects of the K_{ATP} channel opener pinacidil on MG63 cell proliferation.** After 72 hours exposure, MG63 cell numbers were significantly greater at concentrations of pinacidil between 30 μM and 100 μM (n = 3. Figures are representative of at least 6 experiments). * indicates significance at the 0.05 level.
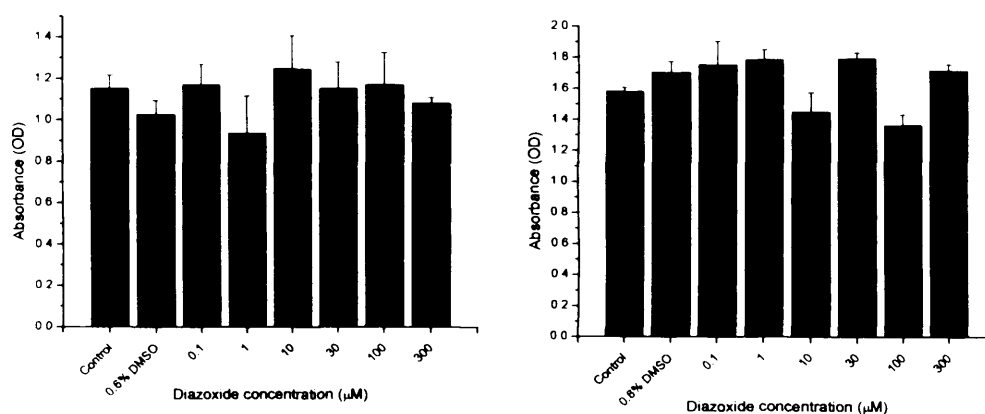
Figure 3.19 **Effects of diazoxide on MG63 cell numbers.** Diazoxide did not significantly affect MG63 cell numbers over the concentration range and exposure times tested (n = 2).
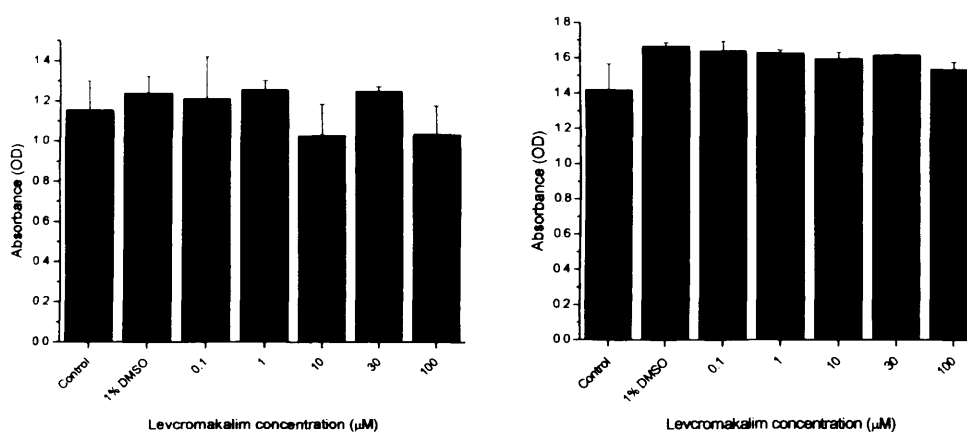
Figure 3.20 **Effects of levcromakalim on MG63 cell numbers.** Levcromakalim did not significantly affect MG63 cell numbers over the concentration range and exposure times tested (n = 2).
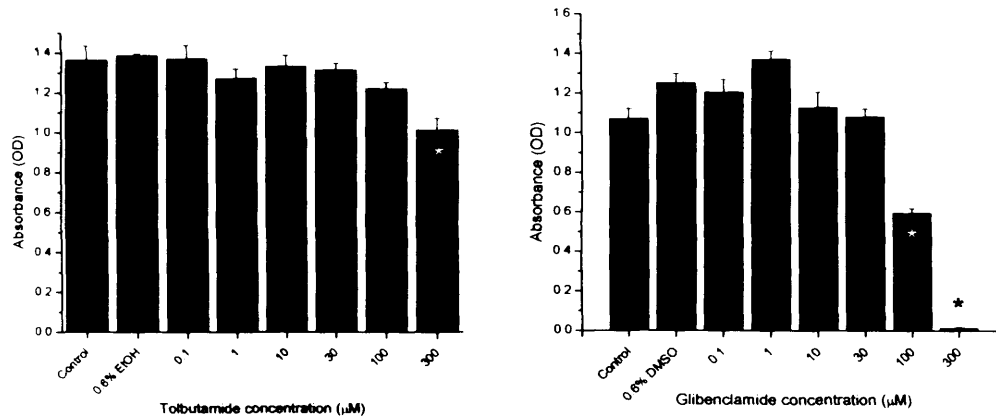
Figure 3.21 **Effects of sulphonylureas on MG63 cell numbers.** 300 µM tolbutamide and ≥ 100 µM glibenclamide significantly reduced MG63 cell proliferation after 72 hours exposure (figures are representative of 3 experiments per sulphonylurea). * indicates significance at the 0.05 level.
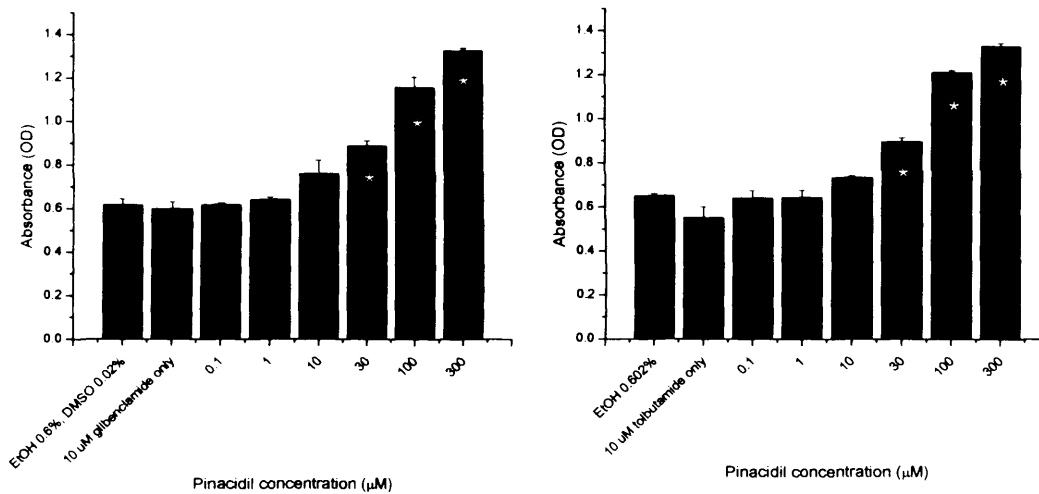
Figure 3.22 **Effects of pinacidil + sulphonylureas on MG63 cell numbers.** Low concentrations of sulphonylureas did not attenuate pinacidil-induced increases in MG63 proliferation. Figures are representative of 3 experiments per sulphonylurea. * indicates significance at the 0.05 level.

120
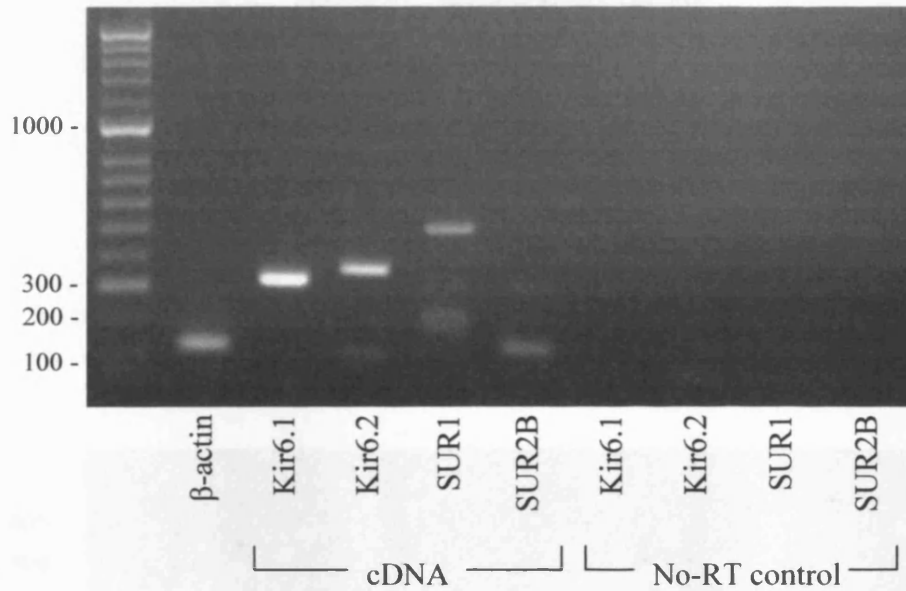
Figure 3.23 **RT-PCR confirms presence of K$_{ATP}$ channels in MG63 cells.** The two pore-forming subunits Kir6.1 and Kir6.2, and the associated sulphonylurea receptor subunits SUR1 and the splice variant SUR2B are expressed. Kir6.1 = 334 bp, Kir6.2 = 353 bp, SUR1 = 493 bp, SUR2B = 150 bp.
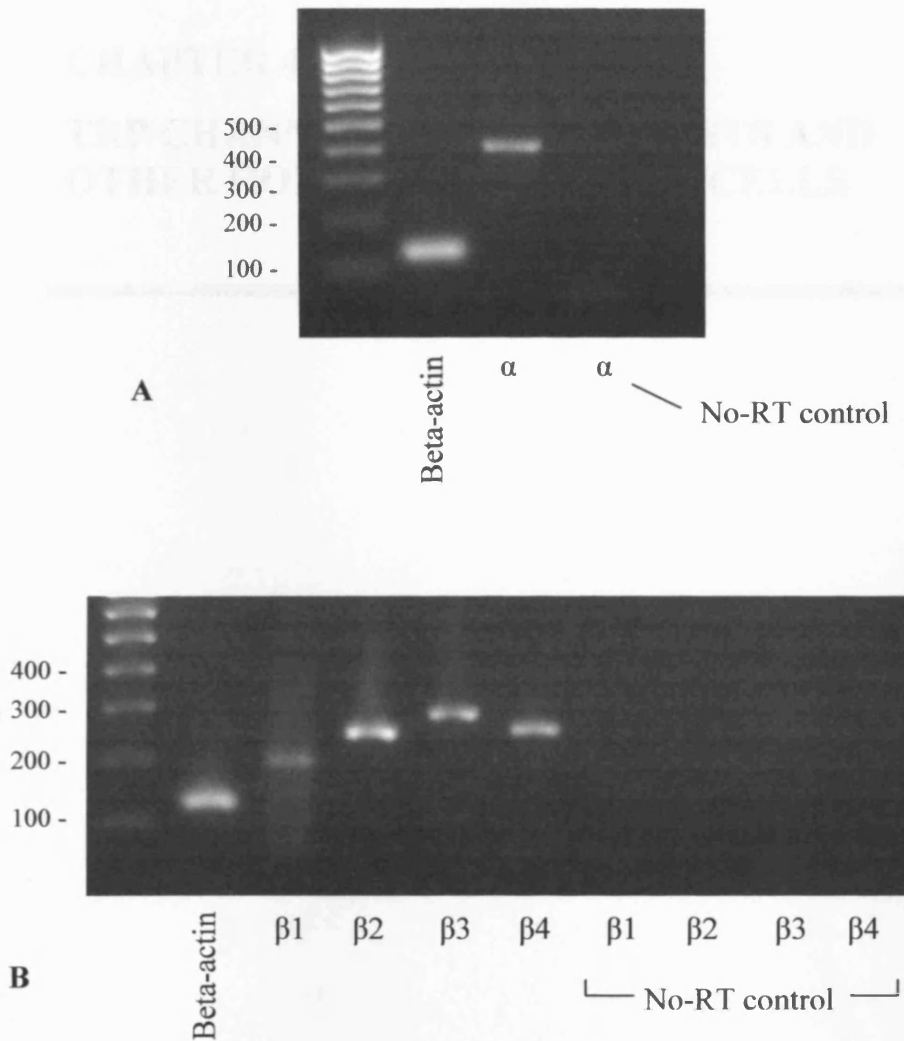
Figure 3.24 **RT-PCR confirms the presence of maxi-K channel subunits in MG63 osteoblast-like cells**. **(A)** The pore-forming α subunit KCNMA1, and **(B)** all four known associated β subunits, KCNMB1-4, are expressed. α = 407 bp, β1 = 189 bp, β2 = 236 bp, β3 = 276 bp, β4 = 245 bp.

CHAPTER 4:

TRP CHANNELS IN OSTEOBLASTS AND OTHER HORMONE-SENSITIVE CELLS

4 TRP CHANNELS IN OSTEOBLASTS AND OTHER HORMONE-SENSITIVE CELLS

4.1 Introduction

Since the discovery of the defining transient receptor potential (TRP) channel

in *Drosophila*, an entire superfamily of ion channels has been described which

have an ever-increasing remit of roles within cells, as these become known.

Functions are diverse and range from taste receptors (Zhang *et al.*, 2003) to

pain receptors (Cahalan *et al.*, 1997) and regulators of cell Ca^{2+} and Mg^{2+} (den

Dekker *et al.*, 2003; Nadler *et al.*, 2001). A general overview of the TRP

channel superfamily is given in the introduction to this thesis (section 1.4). As

with the K^+ channels in chapter 3, what is curious is the expression of TRP

channels that were originally identified in excitable cells, with clearly defined

roles such as temperature sensation and nociception (e.g. Cahalan *et al.*, 1997;

McKemy *et al.*, 2002), being discovered in non-excitable cells such as prostate

and breast cells (Sanchez *et al.*, 2001; Tsavaler *et al.*, 2001; Fixemer *et al.*,

2003).

Cancers of the prostate and breast will often metastasise to the bone (Buijs &
van der Pluijm, 2008) and therefore these tissues must share some common
signalling factors and receptors, which might include some of the TRP
channels that have been identified in prostate and breast cancers, as discussed
below. Identification of TRP channels which are common to these tissues will
act as a basis for the electrophysiological exploration of a chosen channel or
channels in osteoblasts, as bone is currently a tissue in which TRP channels are
relatively unexplored and uncharacterised.

4.1.1 Bone metastases: the 'seed and soil' hypothesis

Whilst it is well known that localised primary breast and prostate cancer
tumours eventually become much more aggressive and invasive, and that these
tumour cells migrate to, and thrive particularly well in bone, the reasons for
this remain only partially understood. The 'seed and soil' hypothesis (Paget,
1889), which is more than 100 years old, describes the early concept of a
relationship between the tumour cells (seed) and metastatic site (soil) enabling
the tumour to thrive in a non-native environment, and that certain 'soils' are
better for particular 'seeds'. But why should breast or prostate cancer cells find
the bone environment particularly attractive?

Breast cancer metastases in bone tend to be osteolytic, and parathyroid
hormone-related peptide (PTHrP) is thought to be one responsible factor as
PTHrP levels are increased in breast cancer metastases of the bone (Powell *et
al.*, 1991; Brydon *et al.*, 2002). PTHrP secreted by breast cancer cells acts on

bone PTH receptors, stimulating RANKL (receptor activator of nuclear factor-κB ligand) production which ultimately stimulates osteoclastic bone resorption and therefore relinquishes space for breast tumour cells to proliferate (Mundy, 2002).

Prostate cancer metastases, on the other hand, tend to be osteoblastic (osteogenic) and osteoblast proliferation may be stimulated by growth factors such as EGF (endothelin growth factor) (Mundy, 2003; Yin *et al.*, 2003), TGF-β (transforming growth factor) (Marcelli *et al.*, 1990) and FGF (fibroblast growth factor) (Izbicka *et al.*, 1996). Tumour progression from androgen-dependence to more aggressive androgen-independence may be mediated by interleukin-6 (IL-6) (Wallner *et al.*, 2006).

4.1.2 TRP channels in bone metastases

It is now recognised that a variety of ion channels may have important roles in tumour survival and progression, including K_{ATP} channels (Klimatcheva *et al.*, 1999), L-type calcium channels (Wang *et al.*, 2000), chloride channels (Shuba *et al.*, 2000), IK_{Ca} channels (Parihar *et al.*, 2003), EAG K channels (Farias *et al.*, 2004; Pardo *et al.*, 1999), K_v channels (Wang, Z. *et al.*, 2004), maxi-K channels (Bloch *et al.*, 2005) and various others as described in a review by Kunzelmann (2005). TRP channels also have putative roles in cancer cell function. The cold-sensitive channel TRPM8 is known to be highly expressed in early stage androgen-sensitive prostate cancer compared with normal tissue and down-regulates in line with androgen receptor expression, and therefore

androgen-sensitivity, and metastasis (Bidaux *et al.*, 2005; Tsavaler *et al.*, 2001;

Zhang & Barritt, 2006). More recently, TRPV6, a highly calcium-selective

cation channel, has been recognised as playing a part in prostate cancer

proliferation (Lehen'kyi *et al.*, 2007) and as TRPV6 expression is regulated by

vitamin D (Taparia *et al.*, 2006), channel expression in bone could have

implications for calcium regulation. Bianco *et al.*, 2007 show that TRPV6

appears to play a role in calcium homeostasis of the bone. TRPV1 has also

been shown to express differently in prostate and bladder cancers compared to

normal tissues/cells (Lazzeri *et al.*, 2005; Sanchez *et al.*, 2005) and capsaicin

appears to inhibit androgen-sensitive prostate cancer progression (Mori *et al.*,

2006).

Table 4.1 TRP channel expressions in cancers

TRP channel	Expression in cancer	Changes in expression in cancer	References
TRPV1	Prostate, colon, pancreas, bladder	Increased expression in prostate, colon and pancreatic cancers. Decreased expression in later stage bladder cancer.	Dömötör *et al.*, 2005 Hartel *et al.*, 2006 Lazzeri *et al.*, 2005 Sanchez *et al.*, 2005
TRPV6	Prostate, breast, colon, thyroid, ovary	Generally increased expression.	Fixemer *et al.*, 2003 Peng *et al.*, 2000 Peng *et al.*, 2001 Wissenbach *et al.*, 2004a Zhuang *et al.*, 2002
TRPM8	Prostate, Pancreas	Increased expression in later stage prostate cancer – linked to androgen receptor expression.	Bidaux *et al.*, 2005 Tsavaler *et al.*, 2001 Mergler *et al.*, 2007 Zhang & Barritt, 2004

Adapted and updated from Prevarskaya *et al.*, 2007

4.1.3 TRP channel expression and activity in osteoclasts

Whilst the literature covering TRP channels in osteoblasts was notably absent at the beginning of this thesis (early 2005), there was some new evidence that TRP channels had important roles in osteoclasts. The highly calcium-selective TRPV5 channel was found to be expressed in osteoclasts and seemingly 'essential' for osteoclastic function (van der Eerden *et al.*, 2005). In 2006, the heat-activated channel TRPV1 was shown to be expressed in human osteoclasts with a putative role in resorption activity (Brandao-Burch *et al.*, 2006). Arnett (2008) has extensively researched the effects of pH changes on osteoclast and osteoblast activity, and TRPV1 is now emerging as a candidate for the sensor of extracellular pH changes in these cells.

4.1.4 Evidence of functional TRP channels in bone

At the start of the work for this thesis in 2005, there were some early indications that some members of the TRP channel superfamily might populate bone cells and have important roles in the functions of these cells. Mice bred with the TRPV5 gene deleted showed reduced bone thickness and hypercalciuria (Hoenderop *et al.*, 2003b) which implied that TRPV5 was involved in bone cell function. TRPM7 was also emerging as a potentially interesting channel in bone, as zebrafish with a mutant TRPM7 channel had defective skeletal growth (Elizondo *et al.*, 2005).

Given that there are now 28 known mammalian TRP channels, a selection of five TRP channels were chosen for investigation based on the information

discussed above. These were TRPV1, TRPV6 and TRPM8 based on their expressions in prostate and breast cancers, TRPV5 as this channel co-assembles with TRPV6 and shares many characteristics including its Ca^{2+} selectivity and sensitivity to parathyroid hormone and vitamin D3, and finally TRPM7 due to its putative roles in skeletogenesis and cell proliferation (Hanano *et al.*, 2004).

4.1.5 Chapter hypotheses, aims and experimental strategies

The first hypothesis of this chapter was that all five of the selected TRP channels TRPV1, TRPV5, TRPV6, TRPM7 and TRPM8 would be expressed at mRNA level in human osteoblasts, and breast and prostate cancer cell lines, for the reasons discussed immediately above.

The second hypothesis, born from the results of the first hypothesis, was that TRPV1 would be expressed as a channel in the plasma membrane of MG63, SaOS-2 and primary human osteoblasts, and meet the criteria set out below.

A number of essential criteria were used to determine whether channel currents recorded were due to TRPV1 activation, based on the channel characteristics summarised by Alexander *et al.* (2004). These four criteria were:

- the channel should be activated by the defining TRPV1 agonist capsaicin within the concentration range 1 – 10 μM (EC_{50} has been reported as 0.48 in HEK cells at pH 7.4 (Ryu *et al.*, 2007)) and blocked by 1 μM capsazepine.

- the activation of the channel by capsaicin should be potentiated by protons (by decreasing the extracellular pH with HCl), by measure of increasing channel open probability at a particular capsaicin concentration with decreasing pH.

- the channel conductance should be around 80 pS in physiological solutions at depolarising potentials, as measured from the slope of I/V plots.

- the channel should display voltage-dependent outward rectification around 0 mV patch potential.

Experimental aims and strategies were: to show the expressions of the above TRP channel messages in MG63, SaOS-2, LNCaP, DU145, MCF-7 and HOB-c cells using the Trizol® RNA extraction method, and RT-PCR followed by ethidium bromide-stained gel electrophoresis; to use the single-channel patch-clamp technique (Hamill *et al.*, 1981) to activate and record the TRPV1 channel in human osteoblasts; and to use RT-PCR to establish the presence of any TRPV1 splice variants.

4.2 Methods

4.2.1 Electrophysiology

Patch-clamp recording methods and analysis were as described in the methods

(chapter 2, section 2.3) and the previous chapter (chapter 3, section 3.2.1).

4.2.2 RT-PCR

General RT-PCR methods are detailed in the methods (chapter 2, section

2.4.1).

4.2.2.1 TRP oligonucleotide primer design

Oligonucleotide primers for five TRP channel mRNA sequences (TRPV1,

TRPV5, TRPV6, TRPM7 and TRPM8) were designed from human mRNA

CDS, as described in section 3.2.3.1 of chapter 3 for maxi-K primer design.

Primers (see table 4.2 and Figure 4.1 for details) were obtained from

Invitrogen.

Table 4.2 **Oligonucleotide primer details for TRP channels.**

Primer	Sequence	Product size	Location	Acc. No.
TRPV1	F: GCCTGGAGCTGTTCAAGTTC R: TCTCCTGTGCGATCTTGTTG	177	2062-2238	NM_018727
TRPV5	F: GGAGCTTGTGGTCTCCTCTG R: GAAACTTAAGGGGGCGGTAG	185	1143-1327	NM_019841
TRPV6	F: TTGAGCATGGAGCTGACATC R: TCTGCATCAGGTGCTGAAAC	237	764-1000	NM_018646
TRPM7	F: TGGGAAGGCTGAATATGAGG R: TTCCATGGGGATCTCTTCTG	197	2481-2677	NM_017672
TRPM8	F: CATTGTGTGTTTTGCCCAAG R: TTGACGGCAGAAGATGTCAG	165	940-1104	NM_024080

Figure 4.1 **TRP channel primers and amplification sequences.** Target
primer sequences are shown in red.

TRPV1

```
1981 cgtctgagtc cacgtcgcac aggtggcggg ggcctgcctg caggcccccc gatagctcct
2041 acaacagcct gtactccacc tgcctggagc tgttcaagtt caccatcggc atgggcgacc
2101 tggagttcac tgagaactat gacttcaagg ctgtcttcat catcctgctg ctggcctatg
2161 taattctcac ctacatcctc ctgctcaaca tgctcatcgc cctcatgggt gagactgtca
2221 acaagatcgc acaggagagc aagaacatct ggaagctgca gagagccatc accatcctgg
2281 acacggagaa gagcttcctt aagtgcatga ggaaggcctt ccgctcaggc aagctgctgc
```

TRPV5

```
1081 ctgacctcca ttctctacga cctcacagag atcgactcct ggggagagga gctgtccttc
1141 ctggagcttg tggtctcctc tgataaacga gaggctcgcc aaattctgga acagacccca
1201 gtgaaggagc tggtgagctt caagtggaac aagtatggcc ggccgtactt ctgcatcctg
1261 gctgccttgt acctgctcta catgatctgc tttaccacgt gctgcgtcta ccgcccccctt
1321 aagtttcgtg gtggcaaccg cactcattct cgagacatca ccatcctcca gcaaaaacta
1381 ctacaggagg cctatgagac acgtgaagat atcatcaggc tggtggggga gctggtgagc
```

TRPV6

```
 661 ggcactgcct tccgccgtag tccctgcaac ctcatctact ttggggagca ccctttgtcc
 721 tttgctgcct gtgtgaacag tgaggagatc gtgcggctgc tcattgagca tggagctgac
 781 atccgggccc aggactccct gggaaacaca gtgttacaca tcctcatcct ccagcccaac
 841 aaaacctttg cctgccagat gtacaacctg ttgctgtcct acgacagaca tggggaccac
 901 ctgcagcccc tggacctcgt gcccaatcac cagggtctca ccccttttcaa gctggctgga
 961 gtggagggta acactgtgat gtttcagcac ctgatgcaga agcggaagca cacccagtgg
1021 acgtatggac cactgacctc gactctctat gacctcacag agatcgactc ctcaggggat
```

TRPM7

```
2401 ccttaagtta gcagtttctt caagacttag accttttgta gctcacacct gtacacaaat
2461 gttgttatct gatatgtgga tgggaaggct gaatatgagg aaaaattcct ggtacaaggt
2521 catactaagc attttagttc cacctgccat attgctgtta gagtataaaa ctaaggctga
2581 aatgtcccat atcccacaat ctcaagatgc tcatcagatg acaatggatg acagcgaaaa
2641 caactttcag aacataacag aagagatccc catggaagtg tttaaagaag tacggatttt
2701 ggatagtaat gaaggaaaga atgagatgga gatacaaatg aaatcaaaaa agcttccaat
```

TRPM8

```
 841 tcatggacat cccactgtcg aagcaaagct ccggaatcag ctagagaagt atatctctga
 901 gcgcactatt caagattcca actatggtgg caagatcccc attgtgtgtt ttgcccaagg
 961 aggtggaaaa gagactttga aagccatcaa tacctccatc aaaaataaaa ttccttgtgt
1021 ggtggtggaa ggctcgggcc agatcgctga tgtgatcgct agcctggtgg aggtggagga
1081 tgccctgaca tcttctgccg tcaaggagaa gctggtgcgc tttttacccc gcacggtgtc
1141 ccggctgcct gaggaggaga ctgagagttg gatcaaatgg ctcaaagaaa ttctcgaatg
```

4.2.2.2 TRPV1 splice variant oligonucleotide primer design

Oligonucleotide primers were designed for TRPV1 channel mRNA using methods described above, and by selecting primer sequences that flanked the region of interest (exon 7) that was thought to be spliced. In this way, primers were selected so that products would be intron-spanning. Primer details are given in table 4.3 and Figure 4.2.

Table 4.3 **Oligonucleotide primers for TRPV1 splice variants.**

Primer	Sequence	Product sizes	Location	Acc. No.
TRPV1b	F: GGAGCTCACCAACAAGAAGG R: AGAAGATGCGCTTGACGAAT	146 & 326	2062-2238	NM_018727

Figure 4.2 **TRPV1 and splice variant primers and amplification sequence.** Target primer sequences are shown in red, and the region expected to be spliced out in TRPV1b is shown in blue.

TRPV1
```
 901 gacaacacga agtttgtgac gagcatgtac aatgagattc tgatcctggg ggccaaactg
 961 cacccgacgc tgaagctgga ggagctcacc aacaagaagg gaatgacgcc gctggctctg
1021 gcagctggga ccgggaagat cggggtcttg gcctatattc tccagcggga gatccaggag
1081 cccgagtgca ggcacctgtc caggaagttc accgagtggg cctacgggcc cgtgcactcc
1141 tcgctgtacg acctgtcctg catcgacacc tgcgagaaga actcggtgct ggaggtgatc
1201 gcctacagca gcagcgagac ccctaatcgc cacgacatgc tcttggtgga gccgctgaac
1261 cgactcctgc aggacaagtg ggacagattc gtcaagcgca tcttctactt caacttcctg
1321 gtctactgcc tgtacatgat catcttcacc atggctgcct actacaggcc cgtggatggc
```

4.2.2.3 RT-PCR reaction composition and conditions

RT-PCR was carried out using mRNAs from 6 human cell-types: MG63 (passage number 34) osteoblast-like cells, SaOS-2 (passage number 27) osteoblast-like cells, HOB-c (passage number 3) primary osteoblasts, DU145 prostate cancer cells, LNCaP (passage number 18) prostate cancer cells, and MCF7 (passage number 20) breast cancer cells. The reaction composition and conditions were optimised and are detailed in tables 4.4 and 4.5 respectively. Reactions of 12.5 µl were routinely performed and negative controls using nuclease-free water or no-RT reaction products from reverse transcription were run alongside reactions with cDNA. The PCR amplification products were analysed by gel electrophoresis in 2 % or 3 % agarose gels stained with ethidium bromide, in 1× TAE buffer*.

Table 4.4 **PCR reaction composition**

Components	Final concentrations	Volumes
5× Green GoTaq® Flexi Buffer	1×	2.5 µl
MgCl₂, 25 mM	1.5 mM	0.75 µl
PCR nucleotide (dNTP) mixture	200 µM each dNTP	1.25 µl
Forward primer (sense)	0.4 µM	0.5 µl
Reverse primer (antisense)	0.4 µM	0.5 µl
GoTaq® DNA polymerase (5u/µl)	0.3125u	0.0625 µl
cDNA (or H₂O, or No-AMV.RT)		0.5 µl
Nuclease-free H₂O		to 12.5 µl

Table 4.5 **PCR reaction conditions**

Step	Temperature °C	Time	No. of cycles
Initial denaturation	95	10 min	1
Denaturation	95	30 s	
Annealing	55	45 s	40
Extension	72	1 min	
Final extension	72	10 min	1
Soak	4	Indefinite	

* Tris-Acetate-EDTA

4.2.2.4 RT-PCR product sequencing

RT-PCR bands were cut from ethidium bromide stained agarose gels under UV

light. Each cut-out was placed into a separate 0.5 ml microcentrifuge tube and

a small volume of nuclease-free water was added (typically 10 - 20 μl per tube)

to keep the product concentrated. The gel was broken up in the water by gently

mashing with a pipette tip and stored in the refrigerator for at least 24 hours to

allow the PCR products to leach out of the gel. cDNA eluted into the water was

sequenced using the Big Dye® Terminator V 3.1 Cycle Sequencing Kit

(Applied Biosystems, UK) by Central Biotechnology Services at Cardiff

University.

4.3   Results

4.3.1   TRP channel expression in osteoblasts and other hormone-sensitive cells

Breast and prostate cancers tend to metastasize to the bones, which provide a suitable environment for the tumour cells to thrive. These three tissues may express similar complements of receptors and signalling factors that allow the different cell types to communicate and co-habit. Therefore, the expressions of five TRP channels were compared in osteoblastic, breast and prostate cells. RT-PCR revealed that the human osteoblast-like cells, prostate cancer cells and breast cancer cells have different complements of TRPV5, TRPV6 and TRPM8 messenger signals (Figures 4.3 and 4.4), but all cells expressed mRNA for TRPV1 and TRPM7, and the osteoblasts also expressed a splice variant of TRPV1.

Results shown (Figure 4.3) are representative of at least three RT-PCR reactions showing the same expressions. Whilst mRNA expressions of TRPV1 and TRPM7 were consistent across all the cells (MG63 and SaOS-2 osteosarcoma cells, DU145 and LNCaP prostate cancer cells, and MCF-7 breast cancer cells) indicating that these channels may have potentially important roles, there were some interesting differences between the messenger signals for TRPV5, TRPV6 and TRPM8. Both prostate cancer LNCaP and DU145 cell lines expressed all five TRP channel messengers, including TRPM8, whereas the breast cancer cell line MCF7 expressed all except

TRPM8. Interestingly, The MG63 and SaOS-2 osteosarcoma cells expressed

different complements of TRP messengers: MG63 cells expressed all except

TRPM8, whereas the SaOS-2 cells expressed TRPM8, but not TRPV5 or

TRPV6. Table 4.6 summarizes the different TRP messenger complements in

the above cells

To confirm the true expression of the above TRP channels in human

osteoblasts, RT-PCR was carried out on primary human osteoblasts (passage

number 3). Figure 4.4, which is representative of n = 3 PCR reactions, shows

that the primary osteoblasts expressed mRNA for TRPV1 and TRPM7 only,

and not TRPV5, TRPV6 or TRPM8. The primary cells are fully functioning

mineralising osteoblasts (confirmed by PromoCell for 15 passages) which

appear not to require these latter three TRP channels, but conserve the

expressions of TRPV1 and TRPM8, as with all the above cells tested.

4.3.2   Patch clamping: the search for TRPV1 channels in osteoblasts

TRPV1 was shown to be expressed in all three osteoblastic cells by RT-PCR,

and as the pharmacology of TRPV1 is well described with various known

agonists and antagonists, the patch-clamp technique was used to investigate the

electrophysiological characteristics of this channel in human osteoblasts.

Various physiological solutions were used as described in table 2.1 in chapter

2. Of more than 100 successfully sealed cell-attached patches with > 1 GΩ seal

resistance, and more than 40 excised inside-out patches in total, most of the

channel openings observed and recorded were not consistent with reported

channel conductances or other TRP channel characteristics. In the few recordings where channel openings did begin to match reported characteristics for TRPV1, there was no significant difference ($p < 0.05$) in open probabilities between channels exposed to agonists and controls. This is true for MG63 cells, SaOS-2 cells and HOB-c primary osteoblasts.

4.3.2.1 Electrophysiology fails to identify TRPV1

The TRPV1 agonists capsaicin (1 – 10 μM) and resiniferatoxin (100 nM – 1 μM) did not in general appear to increase channel activity in MG63, SaOS-2 or HOB-c cells. There were occasional recordings of channel openings in the presence of capsaicin or resiniferatoxin and of these very few were good enough to plot I/V curves. Out of 44 successful seals on MG63 cells with Na gluconate TRP solution and 1 μM capsaicin in the electrode, just 2 patches had channel activity good enough to enable I/V plots to be constructed from the data. The I/V plot for the first channel was linear at both depolarising and hyperpolarising potentials and slope conductance was calculated as 24.1 pS, with an E_{rev} of 18.5 mV, which is not consistent with previous reports of TRPV1. This channel appeared to display voltage-sensitivity, as channel activity increased with depolarising potential. In the second patch, the channel was activated by depolarising potentials, had a slope conductance of 72 pS and an extrapolated E_{rev} of around 0 mV (Figure 4.5A). It is not known if this channel displayed any degree of rectification as patch stability was lost during recording, but it appeared to display some voltage-sensitivity as measured by increased open probability of the channel with increasing depolarising

potentials. With 100 nM resiniferatoxin in the electrode, channel activity was observed in 1/16 patches over a range of potentials. This channel had a slope conductance of 189.7 pS at patch potentials > 40 mV, and the I/V slope appeared linear with an extrapolated E_{rev} of 27 mV positive to resting membrane potential (Figure 4.5B). Due to very short opening bursts over the range of potentials, the extent of voltage dependency of this channel is unclear.

Seal success rate for the human primary osteoblasts, HOB-c, with Na gluconate TRP solution or Na gluconate Locke in the bath and electrode, with or without capsaicin, was 67/75 (89 %). However, many seals became unstable within 2 - 3 minutes and therefore recordings of channel activity were, in general, of poor quality making data analysis difficult and therefore I/V plots could not be constructed. In patches with good seal resistances (> 1 GΩ) and low RMS noise (< 1.0), I/V plots revealed channels of different conductances, E_{rev} values and varying degrees of voltage-sensitivity. Channel activity was observed/recorded in the following proportion of patches: control (no agonist) 15/28 patches; capsaicin in electrode 6/23; 1 µM capsaicin applied to the bath 3/11; and resiniferatoxin in electrode 0/5.

A small number of channels in MG63 cells did show some degree of outward-rectification, meaning that the inward current is smaller than the outward current and is defined by a change in slope conductance around a particular patch potential. This is a feature of the TRPV1 channel which outwardly rectifies around 0 mV in physiological solutions. The first example (Figure

4.6A), the only one of its kind out of > 30 cell-attached patches under similar conditions, displayed pronounced outward rectification around 0 mV patch potential with Na gluconate TRP solution in the bath and electrode (no TRPV1 agonist) with a slope conductance of 174 pS at depolarising potentials, and < 5 pS at hyperpolarising potentials. The channel current appeared to decrease with increasing depolarising potentials greater than 100 mV. The second example (Figure 4.6B), observed in 1/17 cell-attached patches with High K solution and 1 μM capsaicin in the electrode and Na gluconate Locke in the bath, displayed pronounced outward rectification around 25 mV patch potential cell-attached. Channel conductance was approximately 90 pS at depolarising potentials and 17 pS at hyperpolarising potentials. As with the channel in Figure 4.6A the I/V curve tails off at potentials > 140 mV. The third example (Figure 4.6C), again with 1 μM capsaicin and High K solution in the electrode and Na gluconate Locke in the bath but in the excised inside-out configuration, showed outward-rectification around 10 mV and a slope conductance of 142 pS at depolarising potentials and around 6 pS at hyperpolarising potentials.

4.3.2.2 Acidification of bathing solution

TRPV1 channel activation by capsaicin or resiniferatoxin is potentiated by protons. Therefore, attempts were made to activate the TRPV1 channel in MG63 and HOB-c cells by decreasing the pH of the electrode and bathing solutions to pH 6.1 with HCl, but this also did not prove fruitful. Seal success rate was 13/14 for MG63 cells, and 14/21 for HOB-c cells with Na gluconate TRP solutions or Na gluconate Locke and 1 μM capsaicin in the electrode

pipette. In MG63 cells, small conductance channels of < 23 pS were observed and recorded from 4/13 cell-attached patches, and similarly recordings from HOB-c cell-attached patches (4/14) contained small conductance channels of $\sim$ 24 pS, each of which had different reversal potentials. None of these channel characteristics matched the criteria for TRPV1.

4.3.2.3 Electrophysiology finds small conductance channels

Of > 25 successfully sealed patches in MG63 cells in the excised inside-out configuration with Na gluconate TRP solution in the electrode and bath, channel activity was recorded in 8 patches. The channels seen in each case were of small conductance (22.4 ± 1.26 pS, n = 8) and in all 8 recordings there were multiple channels per patch. In 5/8 cases, with 1 μM capsaicin in the electrode solution, I/V plots revealed a channel conductance of 23.96 ± 1.28 pS and a mean E_{rev} of 0.64 ± 6.4 mV, calculated from the mean of the I/V slopes (Figure 4.7A). In 1/8 recordings, with 1 μM capsaicin and 20 mM TEA in the electrode solution, channel conductance was 17.8 pS with an E_{rev} of -5 mV (Figure 4.7B). The channel activity in the presence of TEA implies that this is not a voltage-gated K^+ channel. I/V plots constructed with channel data from the final 2/8 control recordings revealed a channel conductance of 20.9 ± 3 pS and an E_{rev} of 2.5 ± 4.1 mV, calculated from the mean of the two slopes (Figure 4.7C).

Channel open probability was not increased in patches exposed to capsaicin compared to control patches over the range of depolarising and hyperpolarising

potentials, indicating that the channel was not capsaicin-activated. Figure 4.8 shows superimposed mean I/V data from the three above scenarios for comparison, and the mean I/V slopes are closely matched in conductance and reversal potential with no significant differences (p < 0.05).

4.3.2.4 Is the TRPV1 channel active in osteoclasts?

The electrophysiological data collected do not appear to show TRPV1 activity in osteoclasts. Rat primary osteoclasts were grown on coverslips and patched within two days of seeding. Cells were much larger than osteoblasts (4-5× diameter) and high resistance seals > 1 GΩ were difficult to achieve, with a success rate of 15/43 with Na gluconate TRP solution in the electrode and bath. Only 3/15 patches showed channel activity: cell-attached recordings were made in 2/3 cases with the above solutions in the electrode/bath and 1/3 patches contained 1 μM capsaicin in the electrode. Channel activity was low in the first two patches and channel conductance for one of these was estimated (by calculation of I/V) at 45 pS. The patch exposed to capsaicin contained active channels with channel currents at +60 mV of 3.05 pA and 5.97 pA, corresponding to a single channel conductance of 33.4 pS and a double channel conductance of 60.1 pS, with an E_{rev} of -30 mV (Figure 4.9). The channel was voltage-sensitive, and activated by depolarising potentials. However, once again, this channel is probably not TRPV1.

4.3.3 Further molecular biology uncovers a TRPV1 splice variant

Following the failure to identify TRPV1 channel activity using electrophysiology, the evidence for expression of this channel was re-explored. A splice variant of TRPV1 was found to be co-expressed along with the complete receptor, at both messenger and protein level in osteoblast cell membranes. RT-PCR was carried out using oligonucleotide primers flanking a previously reported splice variant sequence of the TRPV1 gene, termed TRPV1b. Gel electrophoresis revealed three different sized bands each for MG63, SaOS-2 and HOB-c mRNA (Figure 4.10). The largest band size at > 300 bp is the most intense and corresponds to the predicted band size of 326 bp for TRPV1. The smallest band size at around 150 bp corresponds to the predicted TRPV1b splice variant band of 146 bp. The intermediate band at approximately 300 bp was not predicted and the mRNA sequence remains unknown.

4.3.3.1 Sequencing of suspected TRPV1 and splice variant gel bands

Sequencing confirmed that the identity of the largest band was TRPV1 (Figure 4.11). The sequence of the smallest 150 bp band was short of 180 base pairs from the full TRPV1 sequence, which matched the mRNA sequence for exon 7 of this gene. Therefore the smallest band is confirmed as the splice variant TRPV1b (Figure 4.11). For confirmation, the deleted sequence also matches that reported by Lu *et al.* (2005) (Figure 4.12). The intermediate band remains unidentified despite attempts to sequence due to poor quality/small quantity of PCR product. Occasional point mutations appear to occur in the TRPV1

sequence, particularly either side of the exon 7 sequence shown by dashed red

underline in Figure 4.11, and one point mutation within exon 7 (adenine

instead of guanine). This mutation therby formed the amino acid triplet code

GAA instead of GAG. Both these triplets code for glutamic acid, so the point

mutation is silent.

4.4 Discussion

4.4.1 TRP channel expression in hormone-sensitive cells

The RT-PCR data enable a partial expression profile to be built for TRP channel proteins in sex hormone-sensitive cells. Interestingly, TRPV1 and TRPM7 messenger signals were expressed in all cells, supporting an argument for putative roles for these channels in important cellular processes such as proliferation, and in carrying Ca^{2+} and Mg^{2+} currents across the plasma membrane. In support of these findings, there have been a number of key reports within the last three years on the importance of TRPM7 and TRPV1 expression. TRPM7 is considered a key regulator of cell Mg^{2+} levels (Schlingmann et al., 2007) and possibly other divalent cations (Wei et al., 2007) in a variety of cells, and is essential for mast cell survival (Wykes et al., 2007) and the proliferation of some cancers (Jiang et al., 2007). The messenger signal has also been detected in rat prostate tissue (Wang et al., 2007). In bone the links between TRPM7 channel expression and human osteoblast proliferation (Abed & Moreau, 2007) and MG63 cell Ca^{2+} and Mg^{2+} regulation (Lévesque et al., 2008) have been further strengthened from the early work by Elizondo et al. (2005) in zebrafish skeletogenesis. Similarly, evidence is beginning to emerge of important roles for TRPV1 in non-excitable cells, including putative functional roles in prostate, pancreatic, colon and bladder cancers (Sanchez et al., 2005; Hartel et al., 2006; Dömötör et al., 2005; Lazzeri et al., 2005) and in the regulation of fat metabolism (Motter et al., 2008) and adipocyte differentiation (Zhang et al., 2007). In bone, TRPV1 may have a

putative functional role as a pH detector and regulator of osteoblastic and osteoclastic activity (Arnett, 2008).

The different expressions of the other three TRP channels must be due to tissue-dependent requirements for the channels. Both prostate cancer cell lines (LNCaP and DU145) express all five of the TRP mRNAs including TRPM8. As described in the introduction to this chapter, TRPM8 expression has been reported to be linked with androgen receptor expression in prostate tissue (Bidaux *et al.*, 2005; Tsavaler *et al.*, 2001) and for this reason TRPM8 expression would be expected in androgen-sensitive tissues such as prostate and possibly bone, and may be a diagnostic marker for androgen-sensitive early-stage prostate cancer. The absence of TRPM8 expression in MCF7 breast cancer cells could be explained by the relative androgen insensitivity of this cell type. The TRPV6 channel also shows increased expression in some cancers, including prostate and breast cancers (Fixemer *et al.*, 2003; Bolanz *et al.*, 2008) and is known to heteromultimerise with TRPV5 to form channels with different characteristics (Weber *et al.*, 2001).

In the osteoblast cells, the apparent expressions of TRPV5, TRPV6 and TRPM8 are curiously different in each of the cell lines. It is worthy of note that MG63 and SaOS-2 cells are, of course, human osteosarcoma cell lines and not primary osteoblast cells and functional characteristics may be slightly different (Pautke *et al.*, 2004). For example, MG63 cells do not mineralise in culture, whereas SaOS-2 cells will extensively mineralise under the correct conditions

(McQuillan *et al.*, 1995). Therefore, SaOS-2 cells may be considered more mature osteoblasts (Rodan *et al.*, 1987), phenotypically closer to true osteoblasts than MG63 cells with more similar gene and protein expressions. But from the RT-PCR data, it is clear that the messenger RNA expressions do not support this argument for the TRP channels. The Ca^{2+} selective channels TRPV5 and TRPV6 are targets for calciotropic hormones such as parathyroid hormone and vitamin D3 (Schoeber *et al.*, 2007; van der Graaf *et al.*, 2004; Meyer *et al.*, 2006), and therefore these channels would be expected to be found in bone cells. However, the primary osteoblast cells apparently do not require these channels to function and instead presumably rely more heavily on the parathyroid hormone receptor (e.g. Ahlstrom *et al.*, 2008) and vitamin D3 receptor (Jurutka *et al.*, 2007) for signalling by these hormones.

In summary, TRPV1 and TRPM7 stand out as potentially important channel proteins in these hormone-sensitive cells, whereas TRPV5, TRPV6 and TRPM8 appear to have heterogeneous roles that may relate to the malignant or non-malignant status of the cells.

4.4.2   Electrophysiology fails to detect TRPV1 in osteoblasts

The search for TRP channels in osteoblasts using the patch-clamp technique concentrated on TRPV1 given its ubiquitous expression and the availability of pharmacological tools. However, despite this expression at messenger level the electrophysiology did not find functionally active TRPV1 channels in MG63, SaOS-2 or HOB-c osteoblastic cells, none of the criteria for identification of

TRPV1 channels were met and therefore the chapter hypothesis was deemed false.

Recordings were made from all three osteoblast cell-types, but the number of patches with active channels was low and ion channel characteristics were disparate with no conformity even on attempts to activate TRPV1 with well-recognised and documented channel openers. Agonist applications were made external to the channel/cell as the evidence shows this is effective: resiniferatoxin has been found to bind and activate at an extracellular site (Chou *et al.*, 2005), whereas capsaicin appears to bind to an intracellular domain of the channel. However, due to the lipophilic nature of capsaicin, the molecule readily crosses through the cell membrane to act intracellularly (Jung *et al.*, 1999). It has been shown by others (Jordt *et al.*, 2000) that acidification of the extracellular environment can potentiate the agonistic effect of capsaicin to greatly increase activity of TRPV1, but in MG63 and HOB-c cells the evidence in this thesis for this is lacking. There is no clear evidence that any of the channels recorded are TRPV1 (or any other TRP channel) but they could be non-selective channels. This is in stark contrast to the wealth of K^+ channel data collected and presented in chapter 3, some of the experiments for which were run in parallel demonstrating that the cells were viable and ion channel rich.

Due to the difficulty in activating TRPV1 in osteoblasts, experiments were carried out in an attempt to activate the channel in rat osteoclasts. TRPV1 has

been reported to be expressed in human osteoclasts where it may function as a

pH sensor and regulator of osteoclastic activity (Brandao-Burch *et al.*, 2006).

However, in the experiments here the single example of ion channel activity in

rat osteoclast cells in the presence of capsaicin does not display the classical

channel rectification that would be exected of TRPV1, and single channel

conductance is much lower than reported TRPV1 conductances in other cell

types under similar conditions (see for example, Premkumar *et al.*, 2002;

Raisinghani *et al.*, 2005). Therefore, despite being the only truly active channel

observed over a wide range of potentials in the presence of capsaicin, this

channel is probably not TRPV1, but could be a non-selective cation channel.

Whether or not this channel is capsaicin sensitive requires future attention, but

as n = 1 only (1/43), the activity in the presence of capsaicin may well be

coincidental.

4.4.3 TRPV1 splice variant expression. A possible explanation for channel inactivity?

The lack of evidence for functional TRPV1 channels from the

electrophysiology prompted a return to the molecular biology in search for an

emerging splice variant of mammalian TRPV1 protein, which is reportedly

insensitive to capsaicin, protons and heat (Schumacher *et al.*, 2000; Xue *et al.*,

2001). The RT-PCR data and sequencing of the PCR gel bands showed the co-

expression at messenger level of TRPV1 and the splice variant of this channel

now known as TRPV1b in human osteoblasts. A recent report of this splice

variant supports the findings of Schumacher and Xue (ibid.) and shows that

TRPV1b has a total deletion of exon 7 forming part of the N-terminus, thought to be the location of the capsaicin-binding site (Lu *et al.*, 2005). Importantly, the TRPV1b splice variant subunit is thought to be dominant over the full TRPV1 subunit, and therefore TRPV1 channels comprising heteromultimers of TRPV1 and TRPV1b may be less sensitive to capsaicin and other TRPV1 agonists, and protons (Vos *et al.*, 2006; Wang, C. *et al.*, 2004). This could explain the difficulty in finding any active TRPV1 channels in the osteoblasts with patch-clamping. Whilst the largest and smallest amplicons have been confirmed by sequencing, the unidentified band (at around 300 bp) is possibly due to non-specific amplification, and therefore primers should be redesigned to eliminate this, and/or further sequencing should be carried out to identify this product.

4.4.4 Chapter conclusions and future work

The first hypothesis in this chapter that the osteoblasts, breast and prostate cancer cells would share the same expression of selected TRP channels was shown to be false. However, TRPV1 and TRPM7 are expressed by all cell types and are potentially important players in key functions of these cells. The unexpected findings of mixed TRPV5 and TRPV6 channel expressions in the osteoblasts raises questions which would be worthy of address in future work (see below).

The second hypothesis, born from the RT-PCR findings, that the TRPV1 channel would active in osteoblasts and sensitive to capsaicin, also tested false.

Despite the osteoblasts being richly decorated with K^+ channels (see chapter 3) proving the patch-clamp setup was established and working well, and despite the RT-PCR evidence for TRPV1 expression, TRPV1 channel activity was not seen in these cells. However, the apparent co-expression of the functionally dominant-negative splice variant TRPV1b may explain this inactivity. It is likely that heteromultimers of TRPV1 and TRPV1b co-assemble in the plasma membrane of osteoblasts and that TRPV1b negatively modulates the activity of the channel in response to the classical agonists. This raises another question: if the TRPV1/TRPV1b protein is not active as an ion channel in osteoblasts, is the protein functional and if so, what does it do? In summary, this chapter shows for the first time the various expressions of a number of TRP channels in osteoblast, breast-cancer and prostate-cancer cells, and that TRPV1 and TRPM7 are commonly expressed in all of these cell-types. Also shown for the first time is the mRNA expression of the splice variant TRPV1b in osteoblasts, including primary human osteoblasts, which may have important consequences for channel function in these cells.

These findings raise a number of interesting questions which require addressing. Some suggestions for points requiring more immediate attention in future work include:

- Further investigations into the reasons for the different expressions of TRP channels, particularly TRPV5 and TRPV6, in the osteosarcoma cell lines and primary osteoblasts.

- Whole-cell patch clamp experiments to try to activate whole membrane TRPV1 currents using capsaicin, acid conditions and heat > 44 °C.

- Cloning and transfection of the osteoblast TRPV1 channel into (for example) HEK-293 cells in large quantities, in TRPV1 homomultimers, TRPV1b homomultimers and TRPV1/TRPV1b heteromultimers to determine the electrophysiological characteristics of these channels.

- Identification of the 'unknown' 300 bp amplicon identified in MG63, SaOS-2 and HOB-c cells by sequencing, and primer redesign to establish if this amplicon is a true variant of TRPV1 or due to non-specific amplification.

- Western blotting and immunocytochemistry to find if TRPV1 and any splice variants are expressed as proteins in the cell plasma membrane, or other fractions of the cytoskeleton.

- The recent reports of functional roles for TRPM7 in bone are very interesting, and channel expression in human osteoblasts was shown by the findings of this thesis. Future work on the functions of TRPM7 in human osteoblasts or osteoclasts would be beneficial to the story of TRP channels in bone.
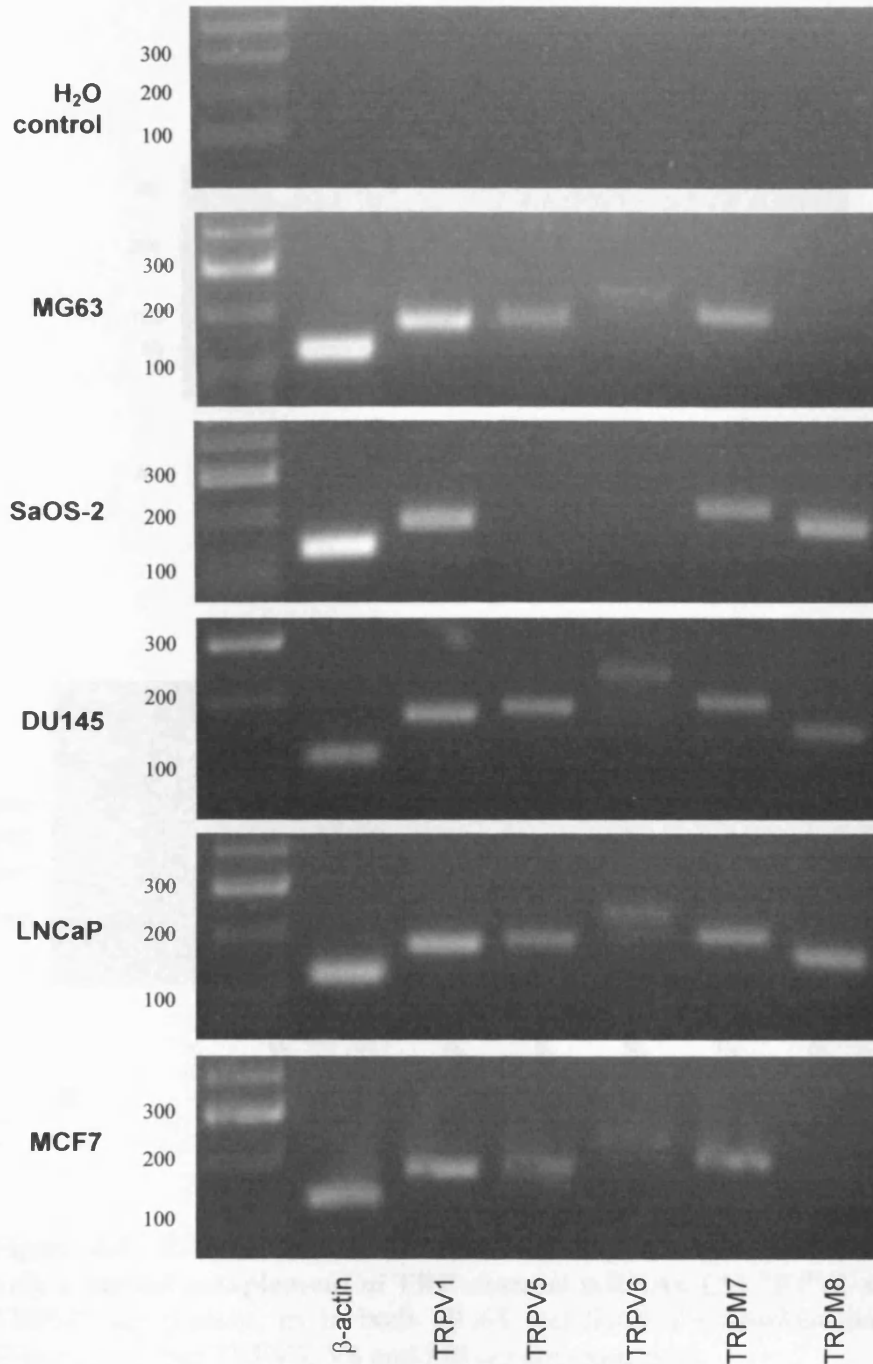
Figure 4.3 **RT-PCR for several TRP channel mRNAs in various hormone-sensitive cell-types**. TRPM8 band is absent for MG63 cells but not for SaOS-2, whereas bands for TRPV5 and V6 are absent for SaOS-2 cells. Prostate cancer derived LNCaP and DU145 cells have the full complement of TRP mRNAs tested for, whereas MCF-7 breast cancer cells do not contain TRPM8 mRNA.

Product sizes

β-actin 126 bp
TRPV1 177 bp
TRPV5 185 bp
TRPV6 237 bp
TRPM7 197 bp
TRPM8 165 bp
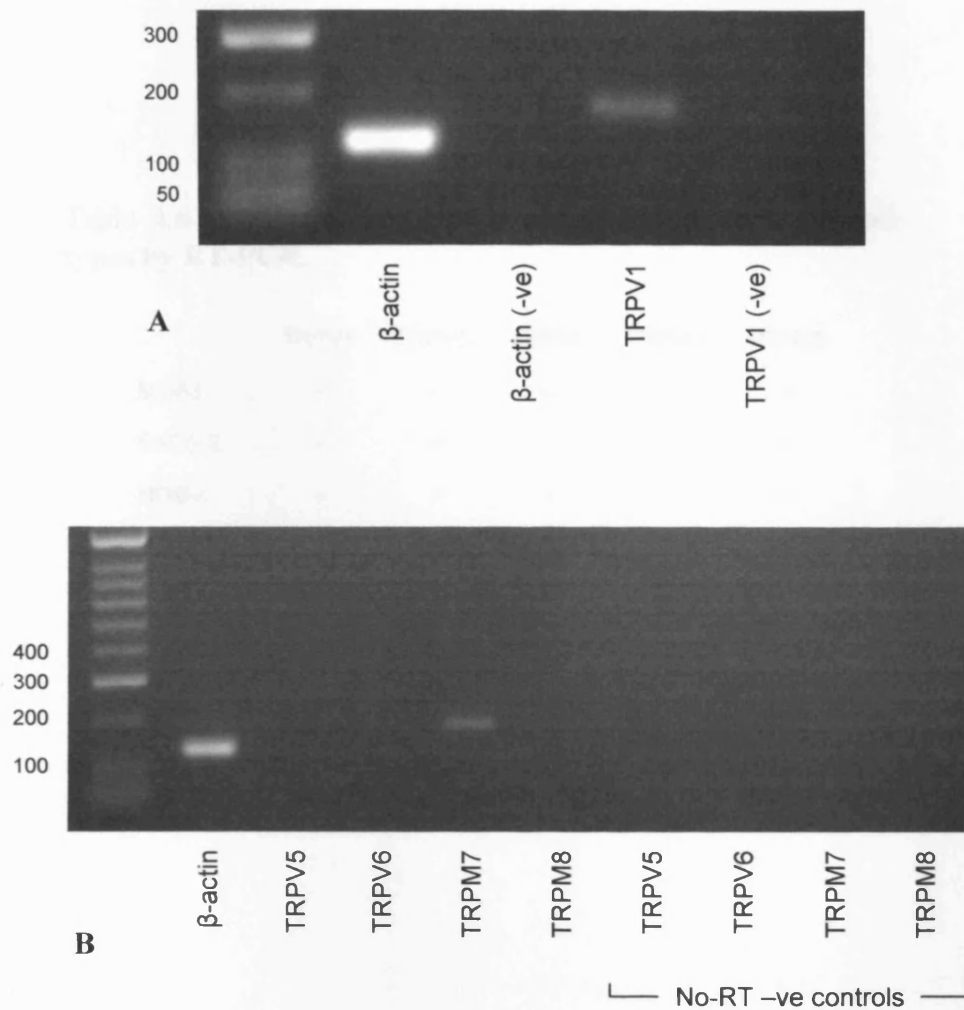
Figure 4.4   **RT-PCR shows HOB-c human primary osteoblasts have only a partial complement of TRP channel mRNAs. (A)** TRPV1 and **(B)** TRPM7 are present, as in both MG63 and SaOS-2 osteoblast-like cells (Figure 4.4), but TRPV5, V6 and M8 are not expressed.

Table 4.6 **TRP channel mRNAs identified in various cell-types by RT-PCR.**

	TRPV1	TRPV5	TRPV6	TRPM7	TRPM8
MG63	✓	✓	✓	✓	✗
SaOS-2	✓	✗	✗	✓	✓
HOB-c	✓	✗	✗	✓	✗
LNCaP	✓	✓	✓	✓	✓
DU145	✓	✓	✓	✓	✓
MCF7	✓	✓	✓	✓	✗
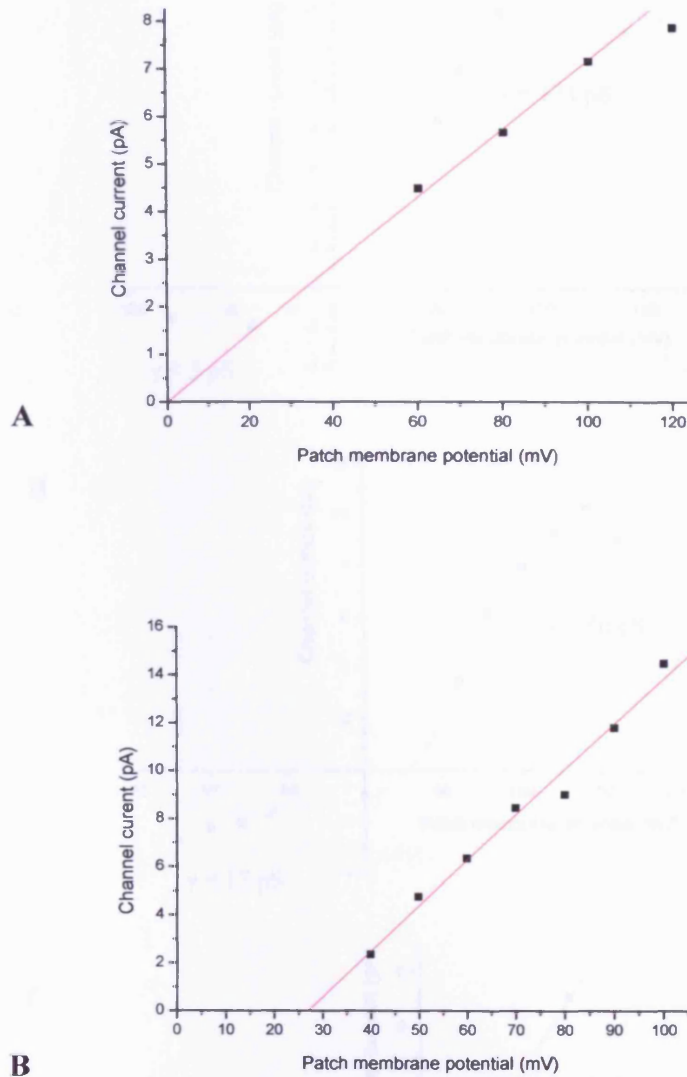
Figure 4.5 **MG63 cell-attached I/V plots in the presence of capsaicin or resiniferatoxin**, with Na gluconate TRP solutions in the bath and electrode. **(A)** With 1 μM capsaicin in the electrode, γ = 72 pS (R^2 = 0.9954), and E_{rev} = 0 mV. **(B)** With 100 nM resiniferatoxin in the electrode, γ = 189.7 pS (R^2 = 0.9821), and E_{rev} = +27 mV.
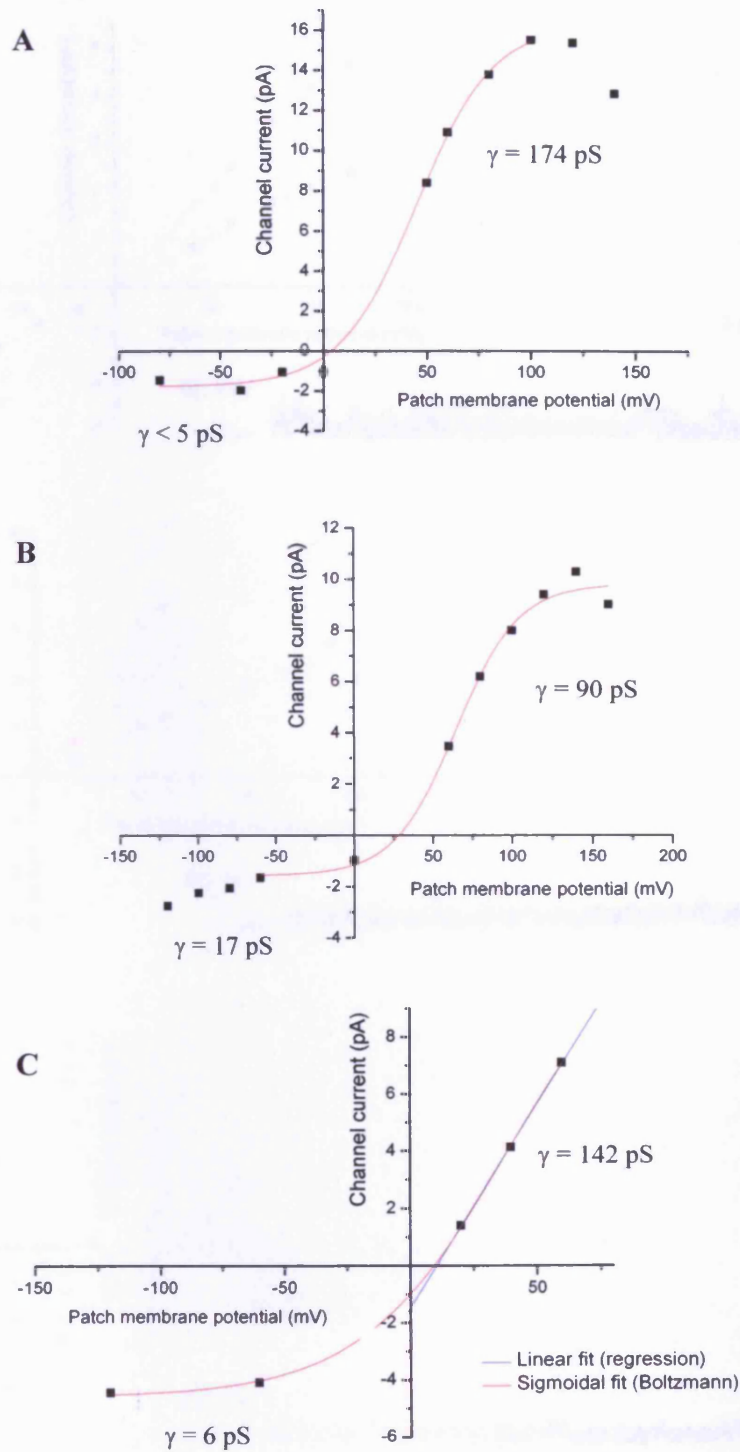
Figure 4.6 **MG63 cell outwardly rectifying channel I/V plots. (A)** Cell attached, with Na gluconate TRP solution in the bath and electrode, $\gamma = 174.3$ pS ($R^2 = 0.97776$) at depolarising potentials and $E_{rev} = +2.5$ mV. **(B)** Cell-attached, with High K solution and 1 μM capsaicin in the electrode, and Na gluconate solution in the bath, $E_{rev} = +26$ mV. **(C)** Inside-out, with High K solution and 1 μM capsaicin in the electrode and Na gluconate solution in the bath, $E_{rev} = +9.7$ mV.
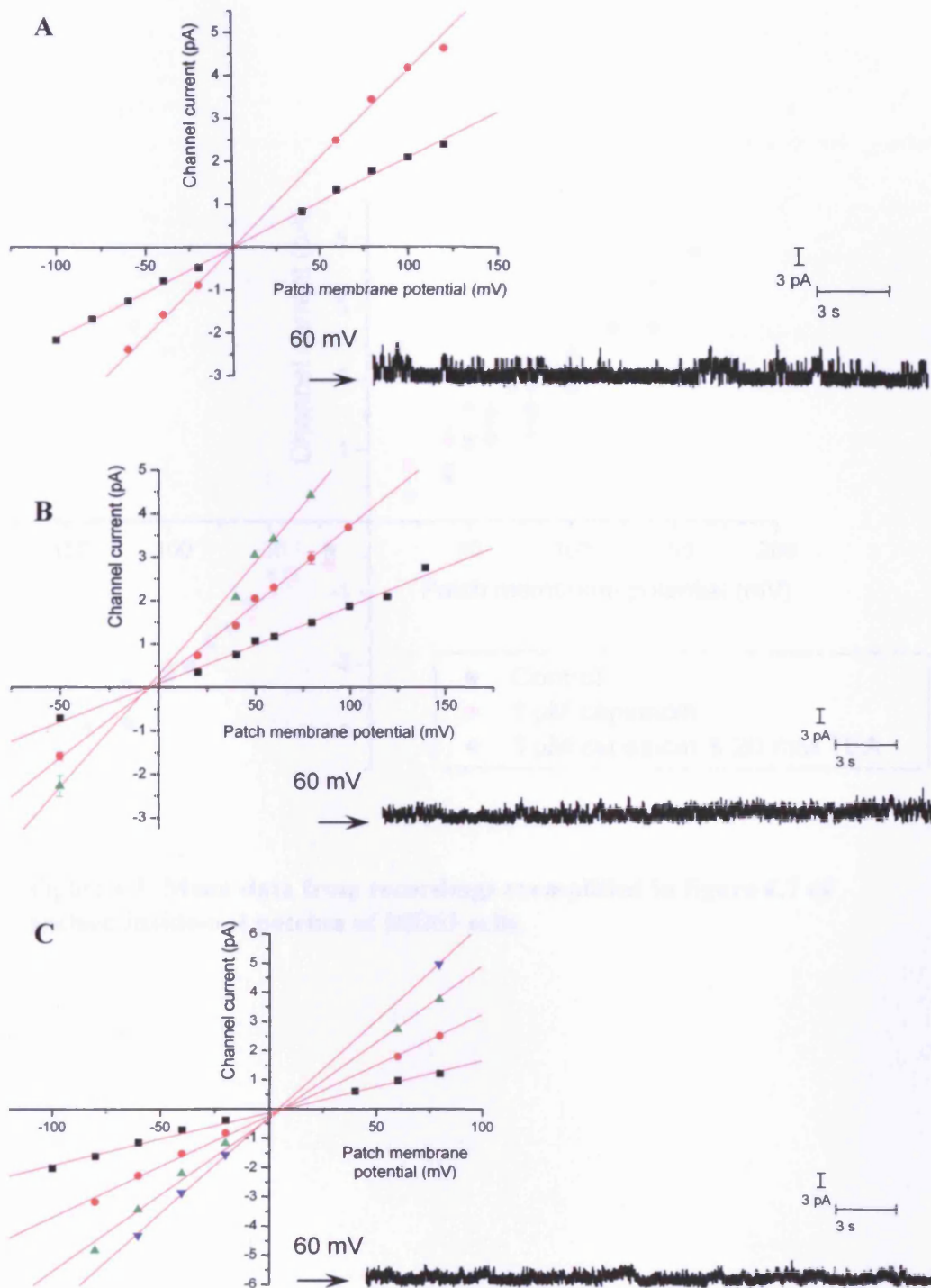
Figure 4.7   **Exemplar I/V plots and single channel data from excised inside-out patches of MG63 cells**. Recordings were with Na gluconate TRP solution in the bath and electrode. **(A)** 1 μM capsaicin in the electrode. γ = 21 pS (R^2 = 0.998) and 41.5 pS (R^2 = 0.999). E_{rev} = 0 mV. **(B)** 1 μM capsaicin and 20 mM TEA in the electrode. γ = 17.8 pS (R^2 = 0.991), 35.4 pS (R^2 = 0.997) and 51.6 pS (R^2 = 0.996). E_{rev} = -5 mV. **(C)** Control. γ = 17.9 pS (R^2 = 0.995), 34.6 pS (R^2 = 0.998) and 52.2 pS (R^2 = 0.997). E_{rev} = +6.7 mV.

158
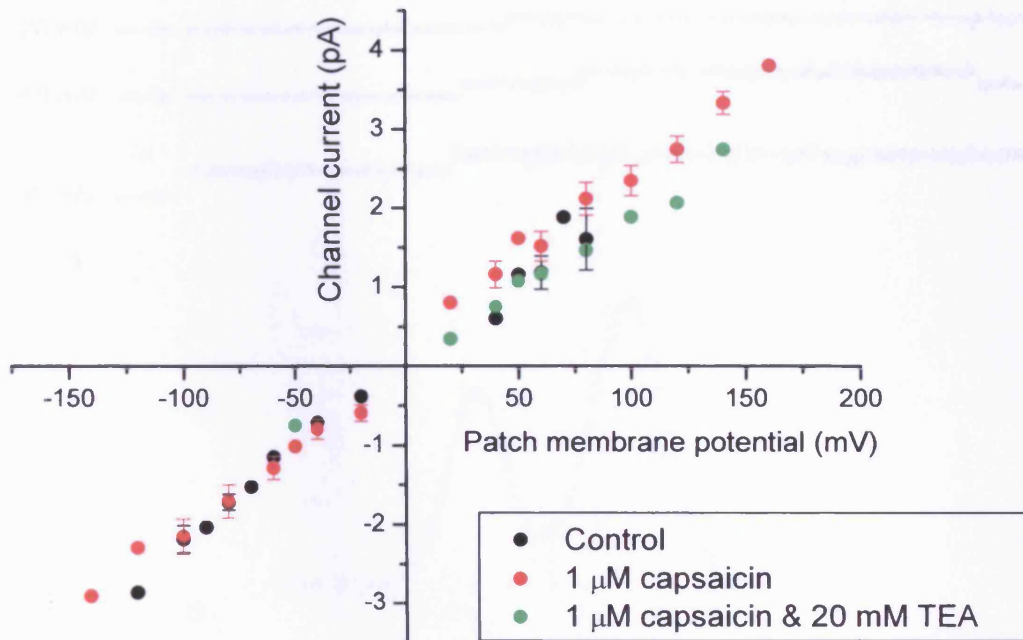
Figure 4.8 **Mean data from recordings exemplified in figure 4.7 of
excised inside-out patches of MG63 cells.**
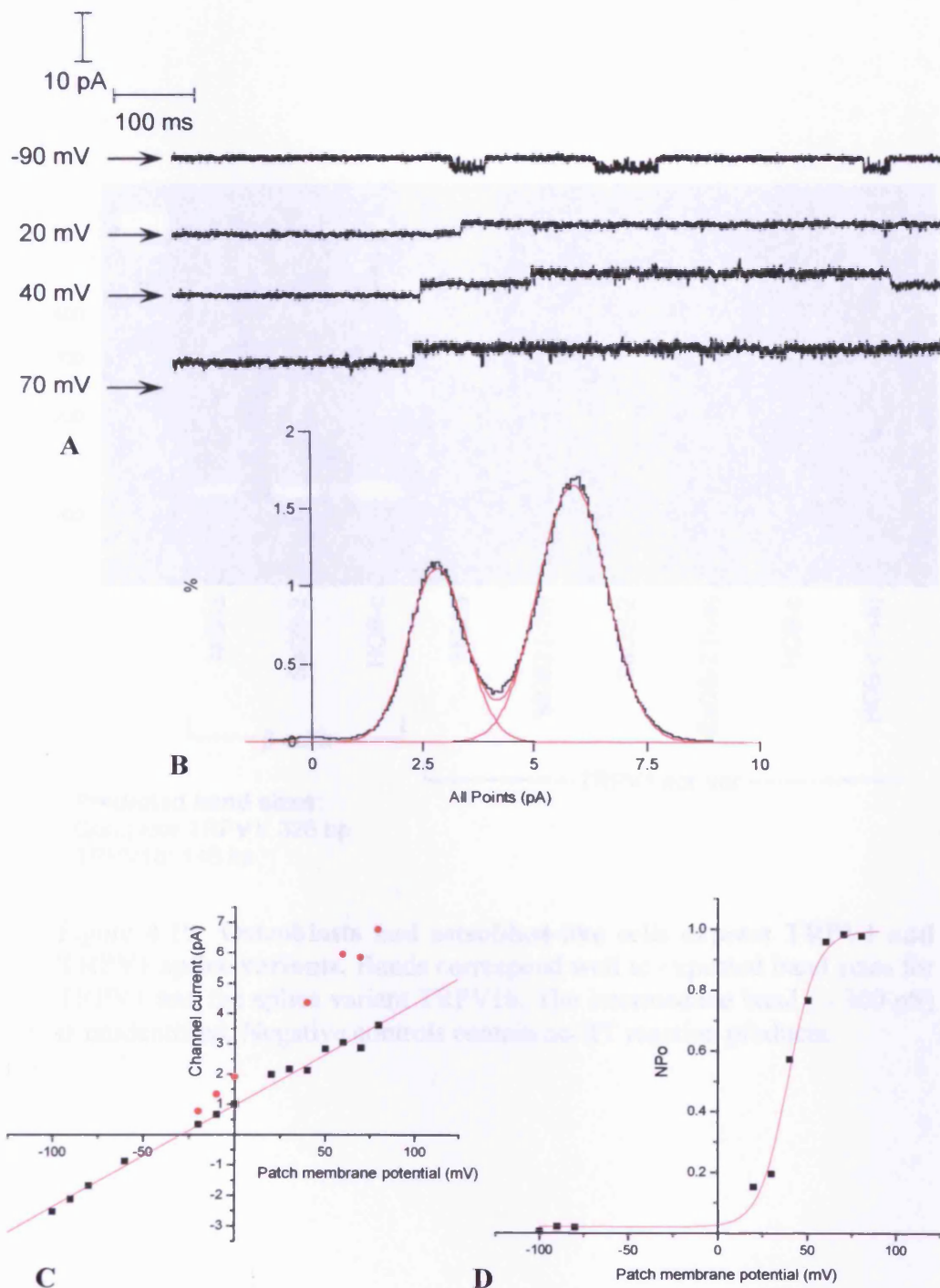
Figure 4.9 **Data from cell-attached recording of rat osteoclast**. Na gluconate solution in bath and electrode, with 1 μM capsaicin in the electrode. **(A)** Single channel data shows channel activity at + and − potentials. **(B)** Current distribution histogram, with Gaussian fits over peaks giving mean currents of 3.05 pA and 5.968 pA. **(C)** I/V plot showing slopes for single and double openings. Single channel γ = 33.4 pS and double channel γ = 60.1 pS. **(D)** NPo/V plot showing channel is voltage dependent and activity increases markedly with depolarising potentials.
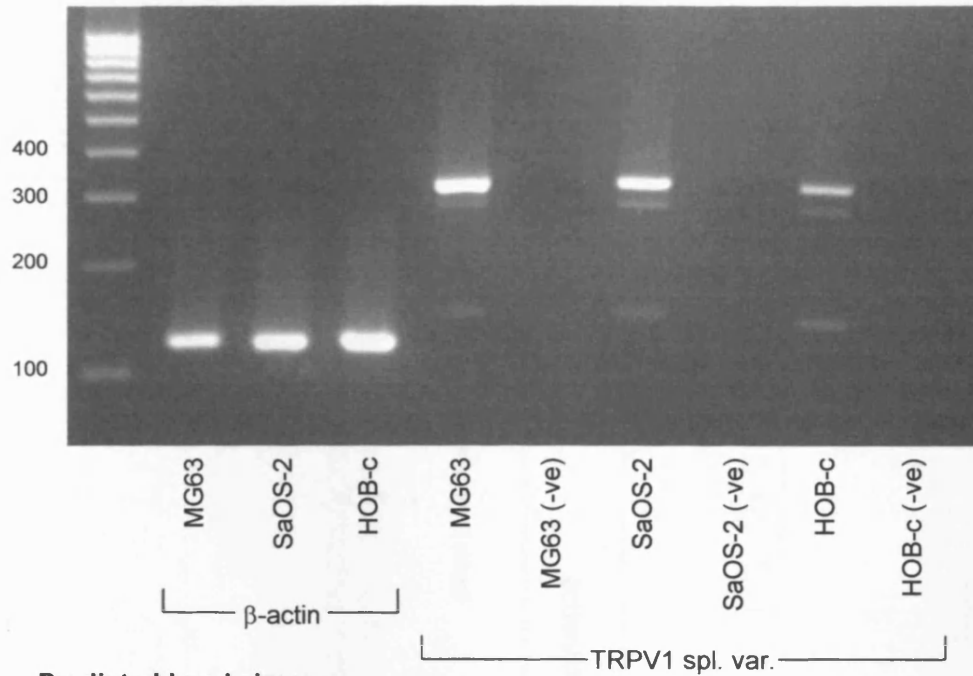
Predicted band sizes:
Complete TRPV1: 326 bp
TRPV1b: 146 bp

Figure 4.10 **Osteoblasts and osteoblast-like cells express TRPV1 and TRPV1 splice variants.** Bands correspond well to expected band sizes for TRPV1 and the splice variant TRPV1b. The intermediate band (~ 300 pS) is unidentified. Negative controls contain no-RT reaction products.
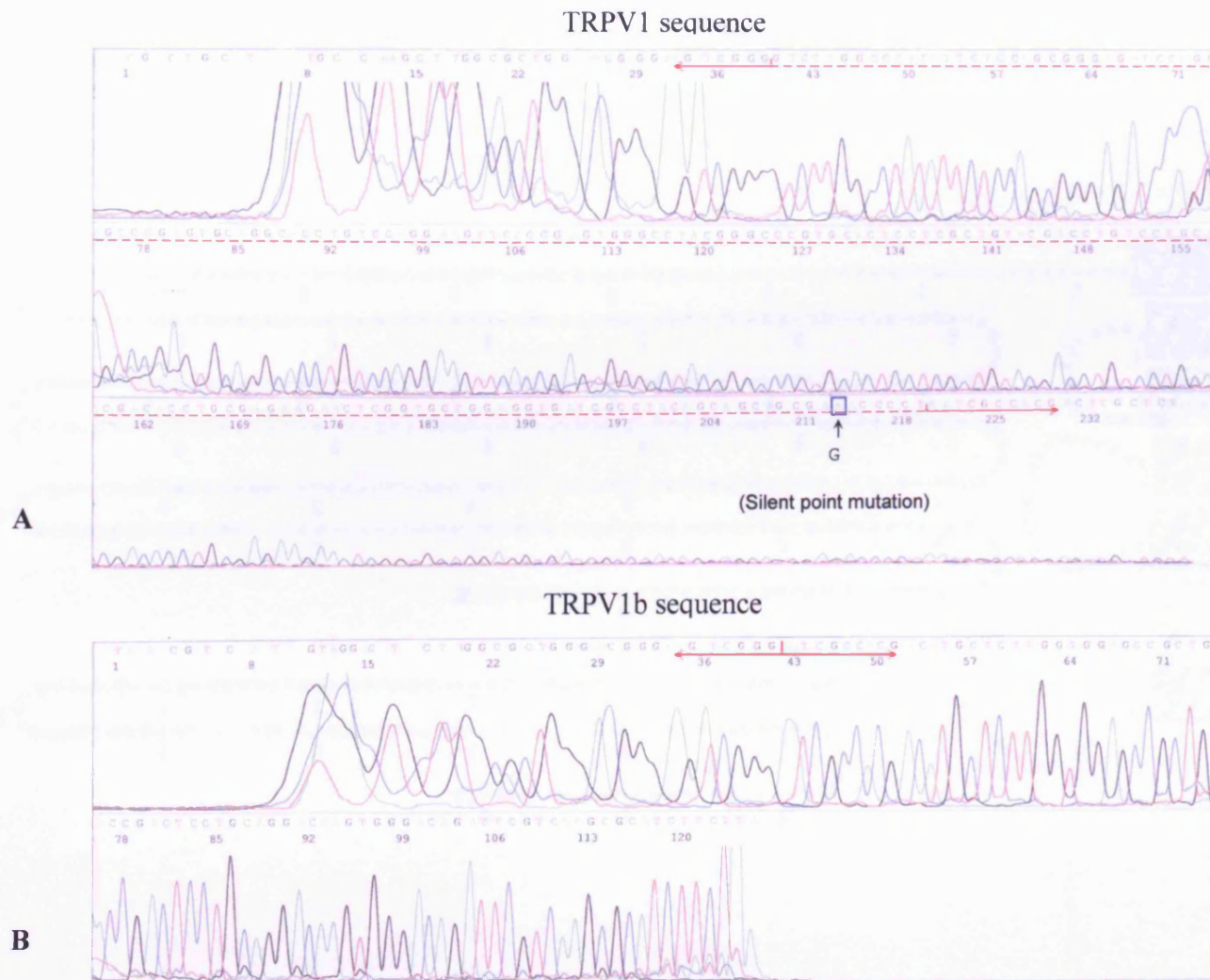
Figure 4.11 **RNA sequencing of TRPV1 bands** (from figure 4.11) confirms expression of (**A**) TRPV1 and (**B**) TRPV1b. Red dashed line indicates sequence missing from TRPV1b splice variant.
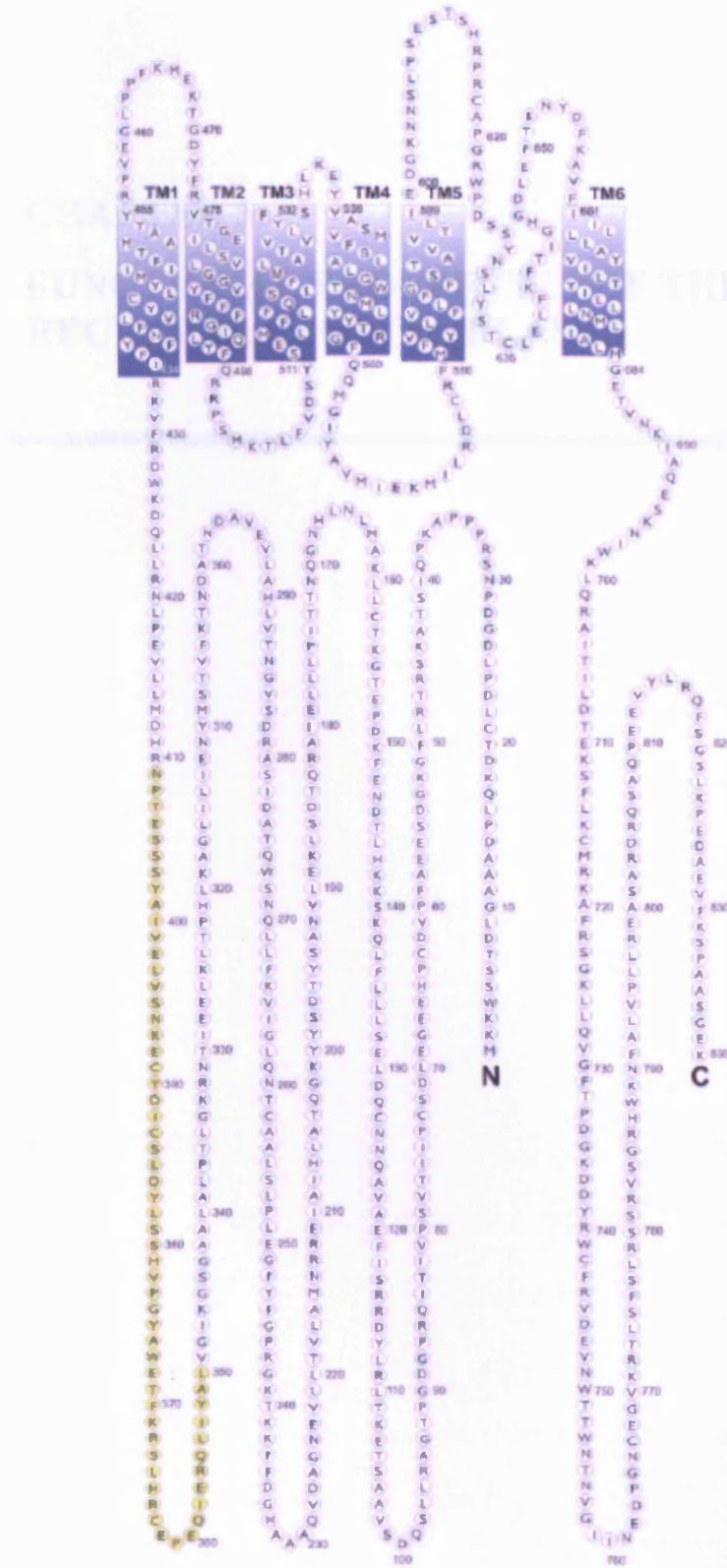
Figure 4.12 **TRPV1 amino acid sequence**. The osteoblast TRPV1 splice variant identified in figure 4.12 has the same 60 amino acid deletion in the N terminus (shown here in yellow) as reported for the human TRPV1b receptor (figure from Lu *et al.*, 2005).

163

CHAPTER 5:

FUNCTIONAL PROPERTIES OF THE TRPV1 RECEPTOR IN OSTEOBLASTS

5 FUNCTIONAL PROPERTIES OF THE TRPV1 RECEPTOR IN OSTEOBLASTS

5.1 Introduction

In the previous chapter, the case was presented for the differential expressions of five TRP channels in hormone-sensitive prostate, breast and osteoblast cells and showed that one TRP channel, TRPV1, expresses in osteoblasts in at least two variant forms: the 'conventional' TRPV1 subunit, and a shorter splice variant which is known as TRPV1b. The lack of evidence in chapter 4 for TRPV1 ion channel activity was possibly due to the expression of the dominant negative TRPV1b subunit which confers capsaicin insensitivity to the channel. The work presented in this chapter will seek to determine any longer-term effects of various TRP ligands on osteoblast cell growth and function, to begin to map out the role of TRPV1 in osteoblasts.

5.1.1 Evidence of putative functional roles for TRP channels in bone

Several members of the TRP channel superfamily are beginning to attract increasing interest in the field of bone function research due to emerging putative roles in osteoblast proliferation, mineralisation and differentiation.

The highly calcium-selective channels TRPV5 and TRPV6 are involved in bone growth. TRPV5 appears to be essential for normal bone turnover and it has been shown that TRPV5 knockout (TRPV5$^{-/-}$) mice have 'reduced bone thickness' (Hoenderop et al., 2003b) due to the diminished active Ca^{2+} resorption by the kidney nephrons, for which TRPV5 has been called the 'gatekeeper' of transepithelial renal Ca^{2+} transport. The same knockout mouse model shows increased osteoclast cell numbers and cell size, but much diminished resorptive activity compared to TRPV5$^{+/+}$ mice (van der Eerden et al., 2005). Therefore TRPV5 is required in the kidney for renal Ca^{2+} resorption and in osteoclasts for bone resorption. The second highly Ca^{2+} selective TRP channel, TRPV6, which shares more than 70% homology with TRPV5, has been shown to have a role in cell proliferation, and is upregulated particularly in later stage prostate and breast tumours that are metastasising (Schwarz et al., 2006; Prevarskaya et al., 2007). It has been implied by Nijenhuis et al. (2003a) that as TRPV6 expression has been identified in osteoblasts, this channel might play a role in mineralisation. TRPV5 and TRPV6 channels may be targets for the well-known bone regulator 1,25(OH)$_2$D$_3$ or vitamin D$_3$ (Hoenderop et al., 2002; Weber et al., 2001), and possibly also targets for oestrogens (Van Abel

et al., 2002) as TRPV5 expression was stimulated by 17β-oestradiol in ovariectomised rats.

TRPM7 has been shown by Elizondo *et al.* (2005) to be important for normal skeletogenesis in the dwarf zebrafish model, in which the mutant *nutria*^{j124e2} has different tissue expressions of TRPM7 compared to wild-type. Consequently the *nutria*^{j124e2} mutant zebrafish is phenotypically much smaller and differently shaped to the wild-type dwarf zebrafish. Abed and Moreau (2007) found that in human osteosarcoma cell lines MG63, SaOS-2 and U-2OS, TRPM7 was important for osteoblast proliferation. Cells treated with siRNAs targeted at TRPM7 showed 60 – 75% reduction in proliferation compared to untreated TRPM7-'normal' cells.

The cold-sensitive channel TRPM8 is upregulated in a variety of malignant tumours including prostate, breast, colon, lung and skin (Tsavaler *et al.*, 2001; Zhang *et al.*, 2004; Zhang *et al.*, 2006), many of which metastasize to bone. In chapter 4, the expression of TRPM8 in human osteoblast-like cell lines was shown to be low. The expression of TRPM8 in prostate cancer is known to be linked to androgen receptor expression – the tumour becomes more aggressive and begins to metastasize at the same time as androgen-sensitivity of the tumour is lost, and TRPM8 expression is down-regulated (Zhang *et al.*, 2004). The transition from TRPM8 high-expression to low-expression may be necessary for tumour seeding and proliferation in the bone environment.

5.1.1.1 Current evidence for TRPV1 function in bone

TRPV1 has been shown to be expressed in osteoblasts and osteoclasts and appears to have several functional roles:

Proliferation and mineralisation

TRPV1 activation is known to be sensitive to pH and reduced pH (increased number of protons) increases the activity of this channel by potentiation (Ryu *et al.*, 2003). Bone is a pH sensitive tissue and small changes in pH may have consequences for bone mineralisation or absorption. A decrease in extracellular pH *in vitro* from 7.4 to 6.9 abolishes mineralisation by osteoblasts, and is associated with an 8× reduction in osteoblast alkaline phosphatase production (a marker for mineralising osteoblasts) and a significant rise in the expression of matrix Gla protein, which is a calcium-binding protein that inhibits mineralisation (Brandao-Burch *et al.*, 2005). The same change in conditions stimulates osteoclasts to maximum resorptive activity, whereas at pH 7.4 resorptive activity is minimal (Arnett, 2008). The author (ibid) argues that TRPV1 might well be the cellular sensor for pH in osteoblasts and osteoclasts, and therefore has a vital role in normal bone turnover.

Differentiation

The association between decreased bone mineral density and increased bone marrow or trabecular bone adipocyte content is well known, and occurs with aging (Parfitt *et al.*, 1992; Rozman *et al.*, 1989), non-weight bearing osteoporosis (Jee *et al.*, 1983), glucocorticoid-induced osteoporosis (Kwai *et*

al., 1985), ovariectomy-induced osteoporosis (Martin & Zissimos, 1991) and

general osteoporosis of all ages (Gimble *et al.*, 1996; Meunier *et al.*, 1971;

Nuttall *et al.*, 1998). It is presumed that adipocyte formation takes place at the

expense of osteoblast maturation and that these cell types have a common

ancestor (Gimble *et al.*, 1996; Thompson *et al.*, 1998). The mechanisms that

control the differentiation of osteoblast and adipocyte precursors are poorly

understood, but clearly pharmacological intervention could provide a future

treatment for pathologies.

An emerging putative role for TRPV1 in bone is in differentiation. It has been

shown that TRPV1 activation by capsaicin prevents adipogenesis in 3T3-L1-

preadipocytes (a non-bone precursor) and that this effect is lost when TRPV1 is

knocked-down (Zhang *et al.*, 2008). Furthermore, the authors also showed that

during regular adipogenesis in 3T3-L1-preadipocytes, TRPV1 expression is

downregulated, but exposure to capsaicin maintains TRPV1 expression levels.

Therefore, it is clear that TRPV1 expression and activation is pivotal in

determining whether precursor cells differentiate into adipocytes. These very

interesting findings of the above two studies beg further investigation, with the

obvious and important next step being to determine whether TRPV1 activation

in osteoblastic-precursors can discourage adipogenesis and promote

osteoblastogenesis. Osteoblast-precursor differentiation has clear implications

for osteogenesis and diseases such as osteoporosis (Griffith *et al.*, 2008;

Griffith *et al.*, 2005; Justesen *et al.*, 2001; Kha *et al.*, 2004).

5.1.2 Cannabinoids as TRPV1 ligands

5.1.2.1 Cannabinoid receptors are functional in bone

Firstly, it is pertinent to recognise that the expression of cannabinoid receptors CB_1 or CB_2 influences bone cell function. CB_1 receptors have been shown to be involved in the regulation of bone mass and bone turnover, but CB_1 receptors are expressed only at low levels in osteoblastic precursors, mature osteoblasts and in osteoclasts (Tam et al., 2006) but high expression is found in trabecular bone sympathetic nerve fibres. As noradrenaline release from these nerve fibres decreases osteoblastic activity but increases osteoclastic bone resorption, the likely mechanism of bone regulation by CB_1 receptor stimulation is downstream sympathetic signalling (Bab et al., 2008; Bab & Zimmer, 2008; Tam et al., 2008). In contrast, CB_2 receptors, which are also expressed only at very low levels in osteoblast precursors, increase in expression as cells mature into true osteoblasts in line with increasing expressions of markers of osteoblast activity including alkaline phosphatase (Zhou et al., 2004), parathyroid hormone receptor (Zhang et al., 1995) and runt-related transcription factor 2 (RUNX2) (Araujo et al., 2004; Bab & Zimmer, 2008). CB_2 also shows high expression in osteoclasts (Bab et al., 2008; Ofek et al., 2006). CB_2 stimulation by the endogenous cannabinoid anandamide results in increased osteoblastic activity and reduced osteoclastic absorption, both directly and by increased osteoblastic RANKL expression, thereby increasing bone mass, whereas $CB_2^{-/-}$ mice display significantly decreased bone mass (Ofek et al., 2006).

5.1.2.2 Cannabinoid ligands as TRPV1 channel agonists

It is evident that the endocannabinoid system plays an important part in the regulation of bone mass and metabolism, but it is becoming clear that endocannabinoids – in particular anandamide – can be endogenous activators of TRPV1 and may therefore partake in a different mechanism for bone regulation. Smart *et al.* (2000) recognised that anandamide is a full agonist of TRPV1 producing similar inward currents to those induced by capsaicin, and evoking $[Ca^{2+}]_i$ increases in the same manner. The potency of anandamide at the TRPV1 receptor was weaker than that of capsaicin, and was approximately 20× weaker than its binding affinity at the cannabinoid receptor (Smart *et al.*, 2000; Devane *et al.*, 1992).

The chemical structure of anandamide resembles that of many vanilloids (Pertwee, 1997; Szallasi & Blumberg, 1999) and one of the vanilloids, olvanil, has been shown to inhibit the facilitated diffusion of anandamide via carrier proteins, thus maintaining high levels of anandamide for CB receptor activation (Di Marzo *et al.*, 1998). In addition to TRPV1 activation by anandamide, a second endocannabinoid ligand, palmitoylethanolamide (Pertwee, 1997), has been shown to activate TRPV1, but is less potent than anandamide at the same receptor site (Smart *et al.*, 2000). Figure 5.1 shows the structural similarities between some selected vanilloids and an endocannabinoid as an example.
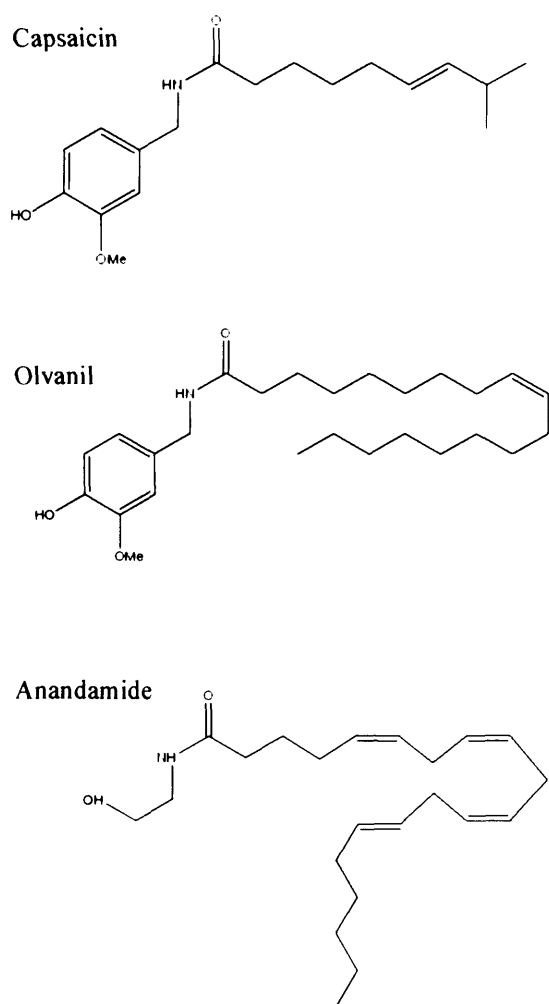
Figure 5.1 **Chemical structures of vanilloids and an endocannabinoid for comparison.**

5.1.3 Chapter hypothesis, aims and experimental strategies

Given the evidence, the hypothesis of this chapter is that the TRPV1 channel

has a functional role in (i) the proliferation, (ii), mineralisation and (iii)

differentiation of osteoblasts.

The aims of this chapter are:

- to test whether known TRPV1 agonists and antagonists, and also

  cannabinoid ligands, have any effect on the growth (proliferation) of

  MG63 cells, using haemocytometry and MTS dye absorption

  measurements.

- to test whether TRPV1 agonists and antagonists affect the mineralisation

  of human SaOS-2 and mouse 7F2 osteoblasts.

- to test whether the differentiation of mouse 7F2 osteoblast precursors into

  either mature osteoblasts or adipocytes is affected by TRPV1 and

  cannabinoid ligands.

- to investigate the effects of capsaicin and other TRPV1 ligands on the

  isolated guinea pig ileum, as a model for the short-term effects of

  capsaicin and other TRPV1 ligands, including anandamide and other

  cannabinoids.

5.2 Methods

5.2.1 Cell culture and counting

Cells were cultured and numbers counted as described in chapter 2, sections 2.1 and 2.2 respectively.

5.2.2 Drug solutions

Drugs and chemicals used in experiments were obtained from Sigma (Sigma-Aldrich Co. Ltd., Dorset, UK) unless otherwise stated. Anandamide, methanandamide and abnormal cannabidiol were obtained from Tocris (Tocris Cookson Ltd., UK). Stock solutions of menthol, capsaicin, capsazepine, anandamide, methanandamide, abnormal cannabidiol, thapsigargin, SB366791, resiniferatoxin and pinacidil were prepared in absolute ethanol (99.8% certified AR grade) (Fisher Scientific, Ltd.). Stocks of ruthenium red and all other chemicals were prepared in in-house distilled H_2O, unless explicitly stated for each drug/chemical.

5.2.3 RT-PCR: Mouse TRPV1

General RT-PCR methods are detailed in Chapter 2: Materials and Methods, section 2.4.1. Products obtained from RT-PCR with mouse 7F2 cells have not been sequenced to confirm identity.

5.2.3.1 Oligonucleotide primer design

Oligonucleotide primers for mouse TRPV1 and β-actin mRNA sequences were designed from *Mus musculus* mRNA coding sequence, as described in section 3.2.3.1 of chapter 3 for maxi-K primer design. Primers (see table 5.1 and Figure 5.2 for details) were obtained from Invitrogen.

Table 5.1 **Oligonucleotide primer details for TRP channels.**

Primer	Sequence	Product size	Location	Acc. No.
TRPV1	F: agcgagttcaaagacccaga R: ttctccaccaagagggtcac	233	439 - 671	NM_001001445
β-actin	F: tgttaccaactgggacgaca R: tctcagctgtggtggtgaag	392	304 - 695	NM_007393

Figure 5.2   **TRPV1 and β-actin primers and amplification sequences.** Target primer sequences are shown in red.

TRPV1

```
361 gctgtggctc agagcaactg ccaggagctg gagagcctgc tgtccttcct gcagaagagc
421 aagaagcgcc tgactgacag cgagttcaaa gacccagaga cgggaaagac ctgtctgctc
481 aaagccatgc tcaatctgca caatgggcag aacgacacca ttgctctgct cctggacatt
541 gcccggaaga cagatagcct gaagcagttt gtcaatgcca gctacacaga cagctactac
601 aagggccaga cagcattaca cattgccatt gaaaggcgga acatggcact ggtgaccctc
661 ttggtggaga atggagcaga tgtccaggct gctgctaacg gggacttctt caagaaaacc
721 aaagggaggc ctggcttcta ctttggtgag ctgcccctgt ccctggctgc gtgcaccaac
```

β-actin

```
241 gggtgacgag gcccagagca agagaggtat cctgaccctg aagtacccca ttgaacatgg
301 cattgttacc aactgggacg acatggagaa gatctggcac cacaccttct acaatgagct
361 gcgtgtggcc cctgaggagc accctgtgct gctcaccgag gcccccctga accctaaggc
421 caaccgtgaa aagatgaccc agatcatgtt tgagaccttc aacaccccag ccatgtacgt
481 agccatccag gctgtgctgt ccctgtatgc ctctggtcgt accacaggca ttgtgatgga
541 ctccggagac ggggtcaccc acactgtgcc catctacgag ggctatgctc tccctcacgc
601 catcctgcgt ctggacctgg ctggccggga cctgacagac tacctcatga agatcctgac
661 cgagcgtggc tacagcttca ccaccacagc tgagagggaa atcgtgcgtg acatcaaaga
721 gaagctgtgc tatgttgctc tagacttcga gcaggagatg gccactgccg catcctcttc
781 ctccctggag aagagctatg agctgcctga cggccaggtc atcactattg caacgagcg
841 gttccgatgc cctgaggctc ttttccagcc ttccttcttg ggtatggaat cctgtggcat
```

5.2.3.2 RT-PCR reaction compositions and conditions

RT-PCR was carried out using 7F2 (passage number 24) mRNA and the reaction compositions and conditions were optimised and are detailed in tables 5.2 and 5.3 respectively. Reactions of 25 µl were routinely performed and negative controls using no-RT reaction products from reverse transcription were run alongside reactions with cDNA. The PCR amplification products were analysed by gel electrophoresis in 2 % agarose gels stained with ethidium bromide, in 1× TAE buffer[*].

Table 5.2 **PCR reaction composition (mouse TRPV1 & β-actin)**

Components	Final concentrations	Volumes
5× Green GoTaq® Flexi Buffer	1×	5 µl
MgCl₂, 25 mM	1.5 mM	1.5 µl
PCR nucleotide (dNTP) mixture	200 µM each dNTP	2.5 µl
Forward primer (sense)	0.4 µM	1 µl
Reverse primer (antisense)	0.4 µM	1 µl
GoTaq® DNA polymerase (5u/µl)	0.625 u	0.125 µl
cDNA (or H₂O, or No-AMV.RT)		1 µl
Nuclease-free H₂O		to 25 µl

Table 5.3 **PCR reaction conditions (mouse TRPV1 & β-actin)**

Step	Temperature °C	Time	No. of cycles
Initial denaturation	95	10 min	1
Denaturation	95	30 s	
Annealing	55	45 s	30
Extension	72	1 min	
Final extension	72	10 min	1
Soak	4	Indefinite	

[*] Tris-Acetate-EDTA

5.2.4 Statistics and graphing

Statistical significance at the 0.05 level was determined by one-way analysis of variance, with post hoc comparisons of means by the Bonferroni method. Graphs were plotted using Origin® 7 software (OriginLab Corp.). Data are presented as mean ± SEM. Graph bars marked with * indicates a statistically significant difference to the control at the 0.05 level.

5.3   Results

5.3.1   Effects of TRP channel ligands on MG63 cell numbers

MG63 cells were incubated in various known TRPM8 and TRPV1 ligands and Ca^{2+} channel ligands, including the SERCA pump inhibitor thapsigargin, for a period of 72 hours to investigate the chronic effects of these drugs on osteoblast cell numbers, in a preliminary attempt to elucidate roles for these channels in osteoblast proliferation or cell death. While many of the drugs tested caused a concentration-dependent decrease in cell numbers following the treatment period, none of the compounds tested induced proliferation of the MG63 cells within the experimental time limits. In addition, osteoblast cell proliferation is shown to be pH-dependent.

The cold-sensitive TRPM8 agonist menthol had no significant effect on MG63 cell number within the concentration range 10 μM – 1 mM after 72 hours exposure (n = 3) and the application of the TRPV1/TRPM8 antagonist capsazepine at a concentration of 1 μM did not make any difference to the cell number after exposure of the cells to the same concentration range of menthol (n = 3) (Figure 5.3). These initial findings do not indicate a role for TRPM8 in osteoblast proliferation.

The TRPV1 agonist capsaicin caused a concentration dependent (0.3 μM – 100 μM) reduction in MG63 cell numbers after 72 hours exposure, and the effects of the highest concentrations 30 μM and 100 μM capsaicin were significantly

reduced cell numbers (p < 0.05; n = 3). Similarly, the TRPV1 antagonist capsazepine caused a concentration-dependent reduction in cell numbers (0.1 µM – 100 µM), with the effects of 30 µM and 100 µM capsazepine being statistically significant (p < 0.05; n = 4) (Figure 5.4). 1 µM capsazepine, which did not cause a change in cell numbers (Figure 5.4), curiously prevented the effects of the higher concentrations of capsaicin (30 µM and 100 µM) resulting in a much smaller effect on cell numbers by capsaicin, which was statistically insignificant (p > 0.05; n = 3) (Figure 5.5). Therefore 1 µM capsazepine may be blocking the effects of higher concentrations of capsaicin on MG63 cell numbers, which points towards TRPV1-channel mediated cell death.

MG63 cell number was not increased by any of the three cannabinoids (1 – 100 µM anandamide and 0.1 – 100 µM methanandamide or abnormal cannabidiol), but was significantly decreased after 72 hours exposure by ≥ 10 µM anandamide (p < 0.05; n = 3), ≥ 10 µM methanandamide (p < 0.05; n = 3), and ≥ 30 µM abnormal cannabidiol (p < 0.05; n = 3) (Figure 5.6). These effects are likely attributable to cannabinoid receptor stimulation, but this has not been systematically explored in this thesis.

Thapsigargin, the SERCA pump inhibitor, caused a concentration-dependent decrease in MG63 cell numbers after 72 hours exposure over the concentration range 10 – 1000 nM, which was statistically significant over this range (p < 0.05; n = 4) (Figure 5.7). Ruthenium red, a non-specific Ca^{2+}-channel blocker,

also caused a significant concentration-dependent decrease in MG63 cell

numbers at 30 μM and 100 μM (p < 0.05; n = 2) (Figure 5.8).

A short pilot study investigating the effects of pH on osteoblastic cell number

revealed a significant decrease in cell number at pH 6.91 compared to control

pH 7.4 (n = 1). This was not explored further, but could be investigated in

future experiments.

5.3.2 The effects of TRPV1 ligands on the mineralisation of SaOS-2 and 7F2 osteoblast-like cells

Induction of true osteoblast mineralisation in the human SaOS-2 osteoblasts

was inconclusive. Up to 14 days after initiation of the mineralisation treatment

in SaOS-2 osteoblast-like cells, the alizarin red-stained wells appeared to show

saturation of mineralisation, possibly due to non-specific (non-osteoblast-like)

mineralisation, excessive cell number, or time-scale of the assay, in all

controls, 1 and 10 μM capsaicin, and 1 and 10 μM capsazepine (Figure 5.9).

True osteoblastic mineralisation of mouse 7F2 cells appeared to be more

successful as shown in Figure 5.10. However, although there appears to be

little visual difference in mineralisation with 10 μM capsaicin or 100 μM of the

K_{ATP} opener pinacidil after 10 days treatment, elution of the dye to quantify

mineral deposition would be required to draw any firm conclusions from these

experiments.

5.3.3 The effects of TRPV1 ligands on the differentiation of osteoblast precursors into adipocytes

Results show that 7F2 osteoblast precursors can be prevented from differentiating into adipocytic cells, and persuaded along the osteoblastic pathway, by stimulation of TRPV1 with known TRPV1 agonists and the cannabinoid anandamide. TRPV1 antagonists do not prevent differentiation. Therefore, TRPV1 appears to have an important role in osteoblast precursor cell differentiation.

Control wells showed that induction of adipogenesis in 7F2 cells was successful. Lipid droplets were visible in induced cells after approximately 3 days, and the differentiation of 7F2 cells appeared to slow cell division as can be seen when comparing the control wells of induced and non-induced cells (10 days) in Figure 5.11. Non-induced cells appear much more densely packed, whereas induced adipogenic cells are more sparse with visible lipid droplets (stained red). After 10 days treatment and oil red O staining, the TRPV1 agonists capsaicin (1 μM) and resiniferatoxin (100 nM) both appeared to have reduced adipogenesis compared to control wells, whereas the non-specific TRPV1 antagonist capsazepine (1 μM) and the selective TRPV1 antagonist SB366791 (100 nM) each had no apparent effect on adipogenesis compared to controls. Also interestingly, the endocannabinoid anandamide (1 μM) appeared to have reduced adipogenesis compared to controls, in a similar fashion to capsaicin and resiniferatoxin. The TRPV1 antagonists were able to block the preventative effects of capsaicin, resiniferatoxin and also anandamide resulting

in differentiation to adipogenic cells. Figure 5.11 shows representative images

from 1 of 3 experiments.

5.3.4 RT-PCR confirms expression of TRPV1 in mouse osteoblast precursors

30 cycles of RT-PCR showed that TRPV1 is expressed in mouse 7F2

osteoblastic cells at the mRNA level, revealing a band between 200 and 300

bp, corresponding well with an expected band size of 233 bp (Figure 5.12).

5.4   Discussion

5.4.1   TRP and Ca^{2+} channel ligands on osteoblast cell number

The results show that after a 72-hour treatment, none of the TRP ligands tested promoted proliferation of MG63 cells. The insignificant effects of up to 1 mM menthol on MG63 cell numbers is not surprising given the very low expression of TRPM8 in these cells, as shown by RT-PCR in chapter 4. Others have shown that 100 μM menthol activates TRPM8 channel currents in transfected HEK-293 cells (Thebault *et al.*, 2005) so the concentration range used is presumably appropriate. Given these results, and the low expression of TRPM8 in osteoblasts, it is likely that these cells do not utilise TRPM8 in a major role in cell proliferation.

Hui *et al.* (2003) have reported that the binding of capsaicin at the TRPV1 receptor occurs with a K_d of around 0.6 μM with the increase in channel activity peaking at around 3 μM in TRPV1-tranfected *Xenopus* oocytes. In MG63 osteosarcoma cells, 0.3 - 10 μM capsaicin did not significantly affect the number of cells after 72 hours, but 30 μM and 100 μM capsaicin significantly reduced cell numbers with signs of cell death. Caterina *et al.* (1997) showed that TRPV1-transfected HEK-293 cells were killed by prolonged (7 hours) exposure to 3 μM capsaicin whilst non-transfected cells remained healthy, and suggested that TRPV1 mediates capsaicin-induced necrosis rather than apoptosis due to the absence of nuclear fragmentation in the dead cells. As demonstrated in previous chapters, TRPV1 expressed in

MG63 cells is seemingly much more difficult to activate, arguably due to the expression of the dominant negative TRPV1b splice variant which renders TRPV1b subunit-containing channels much less sensitive to capsaicin. Therefore, it would seem reasonable that higher concentrations of capsaicin may be required to have the same effect, which may be TRPV1-mediated necrosis, in MG63 cells. However, it is most likely that death of MG63 cells by high concentrations of capsaicin may be due to necrotic non-specific toxicity. Interestingly, the fact that the capsaicin-induced effects at 30 and 100 μM were blocked by 1 μM capsazepine confuses the matter by indicating that these effects were specific and mediated by capsaicin on the TRPV1 channel, but this should be further repeated for confirmation. Future work such as apoptosis assays are suggested to determine the mechanism of cell death.

The growth-arresting and apoptotic/necrotic effects of the cannabinoids anandamide, methanandamide and abnormal cannabidiol at micromolar concentrations have been shown previously in various cells, and these effects occur either via the cannabinoid CB_1 and CB_2 receptors and the TRPV1 channel (Ligresti et al., 2003; McKallip et al., 2002; Maccarrone et al., 2000; Siegmund et al., 2005), or independently of these receptors (Biswas et al., 2003; Sarker et al., 2003). Siegmund et al. (2005) report that 1 – 10 μM anandamide blocked proliferation of human hepatic stellate cells and dose-dependently induced cell death at concentrations > 25 μM. This is consistent with the effects of anandamide on MG63 cells reported in this thesis. Siegmund et al. (2005) also showed that the growth-arresting and cell death

effects of anandamide were unaffected by selective blockade of CB_1 and CB_2 receptors or TRPV1 receptors. Although untested here, this may mean that in MG63 cells the cannabinoid agonists cause growth-arrest and cell death by non-specific means.

Thapsigargin, a selective inhibitor of the sarcoplasmic/endoplasmic reticulum Ca^{2+}-ATPase (SERCA) pump, prevents replenishment of the ER with Ca^{2+} and leads to cytosolic $[Ca^{2+}]$ increases as Ca^{2+} leaks out of the ER. Cells undergoing apoptosis are known to have depleted thapsigargin-sensitive Ca^{2+} stores, suggesting Ca^{2+} movement within the cell (Jan et al., 2000; Distelhorst et al., 1996; Baffy et al., 1993). In osteoblasts, thapsigargin-induced apoptosis has been previously reported (Labelle et al., 2007; Jan et al., 2000; Mentaverri et al., 2003) and the dose-dependent thapsigargin toxicity on MG63 cells presented in this thesis is consistent with the dose-dependent apoptosis of MC3T3E1 osteoblast cells over the range 1 – 100 nM reported by Chae et al. (1999), although apoptosis was not systematically confirmed in this thesis. Labelle et al. (2007) also show that thapsigargin-induced ER depletion of Ca^{2+} causes capacitative Ca^{2+} entry (CCE) through the plasma membrane, which is associated with osteoblast proliferation and may involve TRPC channels, as observed in other tissues (Golovina et al. 2001; Sweeney et al. 2002; Liu et al. 2003; Wang, X. et al. 2004), but not TRPV1 (Wisnoskey et al., 2003).

The Ca^{2+} channel blocker ruthenium red caused growth arrest but not cell death at 30 and 100 µM, which is consistent with reports of similar effects at the

same concentrations in cerebella astrocytes and neurons, and in cortical neurons (Tapia & Velasco, 1996). The presumed mechanism of cell death by ruthenium red is by inhibiting Ca^{2+} movement within the cell from ER stores and via mitochondrial ryanodine receptors, and by inhibiting mitochondrial Ca^{2+} uptake (Hajnóczky et al., 2006).

Much of the reduced MTS absorbance signals from the highest concentrations of compounds used in these experiments are probably due to necrotic, rather than apoptotic cell death. In contrast to the majority of data shown, the thapsigargin concentration-effect is perhaps more likely to be due to apoptosis rather than necrosis due to the nature of the concentration dependence within an appropriate concentration range for SERCA pump antagonism. Cells observed under the microscope appeared healthy at all concentrations of thapsigargin, although numbers were reduced at higher concentrations, whereas for many of the other compounds the cells at the highest concentrations had detached from the plates.

5.4.2 Mineralisation experiments

The mineralisation of SaOS-2 osteosarcoma cells was unsuccessful as the alizarin red stain showed saturation, as described in the results. Future experiments with these cells should use a lower cell density, a reduced assay time-scale and/or possibly a reduced supplementation of β-glycerophosphate, although ideally a true osteoblastic cell-type should be employed, rather than a sarcoma to reduce the possibility of non-specific mineralisation. The data from

7F2 cells are inconclusive and these assays should be repeated in future studies followed by elution of the dye to quantify mineral deposition, and establish whether or not there are any differences in mineral deposition due to the compounds used. Edge-effects, due to the exposure of those wells around the perimeter of plates to gaseous exchange during incubation, could be avoided in future experiments by either avoiding perimeter wells in multiwell plates, or by using 6-well plates where the bias is removed from the experiments.

5.4.3 The effects of TRPV1 ligands on 7F2 osteoblast differentiation

The results presented here are further evidence of the remarkable ability of this cell line, which otherwise displays all the markers of mature osteoblasts, to differentiate and divert from the osteoblast pathway into lipid-producing adipocytes. The novel data presented here are a beginning in closing the link between this phenomenon, as originally described by Thompson *et al.*, (1998), and the role TRPV1 plays in the differentiation of 3T3-L1-preadipocytes into mature adipocytes (Zhang *et al.*, 2007) showing for the first time that the TRPV1 channel appears to play a role in regulating the differentiation of immature osteoblasts either into mature osteoblasts or into adipocytes.

Whereas Zhang *et al.* (2007) recently showed that capsaicin as an agonist of TRPV1 prevented differentiation along the adipocyte pathway, the results shown in this thesis demonstrate that both capsaicin and resiniferatoxin have the same effect on immature osteoblasts, and of further interest are the data showing that anandamide also has the same effect. This adds strength to the

suggestion that anandamide is a putative endogenous agonist of human TRPV1

(Smart *et al.*, 2000). The TRPV1 antagonists capsazepine and the specific

ligand SB366791 did not prevent differentiation to adipocytes, which is

consistent with the reports by Zhang (op. cit.) that capsazepine does not

prevent adipogenesis and that TRPV1 is downregulated along the pathway to

adipocyte differentiation. In support of this, it is interesting to note that

capsazepine and SB366791 were each separately able to antagonise the anti-

adipogenic effects of capsaicin, resiniferatoxin and anandamide, in each case

resulting in differentiation along the adipocyte pathway. These

pharmacological data show that the apparent anti-adipogenic (or pro-

osteoblastic) effects of anandamide are mediated by TRPV1 and not the

cannabinoid receptors.

The consequences of osteoblast differentiation into adipocytic cells are

pathologically important and the data presented here highlight a target for

pharmacological intervention in the TRPV1 channel, and bring to our attention

a very interesting functional role for TRPV1 in bone.

5.4.4 RT-PCR confirms TRPV1 expression in mouse 7F2 osteoblasts

Confirmation that the TRPV1 channel is expressed in 7F2 cells is given by the

RT-PCR data. The results discussed above are indicative of a functional

channel that is receptive and responsive to capsaicin. Human TRPV1 and

mouse TRPV1 share 86.5% sequence identity and as with the human TRPV1

channel, a splice variant of mouse TRPV1 (mTRPV1) has been identified

which is unresponsive to capsaicin, protons or heat, and has been termed

mTRPV1β (Wang, C. *et al.*, 2004). The variant form has a deletion of 10

amino acids from exon 7 forming part of the N terminus and is dominant /

negative when heteromultimers of mTRPV1 and mTRPV1β are expressed.

Along with human TRPV1b expression, this is also consistent with reports of

N terminal exon 7 deletions in rat TRPV1 sequences, forming splice variants

known as SIC, VR.5'sv and VR1L2, each of which are unresponsive to

capsaicin and form non-functional channels (Sharif Naeini *et al.*, 2006; Eilers

et al., 2007; Tian *et al.*, 2006). However, Wang, C, *et al.* (2004) have shown

that the tissue expression of mouse mTRPV1β is heterogeneous, and largely

confined to brain, skin, DRG, stomach and tongue. The expression of a mouse

TRPV1 splice variant has not been systematically tested in this thesis.

5.4.5 Chapter conclusions and future work

The chapter 5 hypothesis was that the TRPV1 channel has a functional role in

(i) the proliferation, (ii), mineralisation and (iii) differentiation of osteoblasts.

The data presented in this chapter show that part (iii) of the hypothesis appears

to be true, but parts (i) and (ii) appear false. The proven part of the hypothesis

is very interesting: if the functional role of TRPV1 in osteoblast differentiation

is real, as evidenced in this thesis, TRPV1 could become an important target

for new drugs, or novel indications for drugs currently under investigation, in

the battle against osteoporosis and particularly glucocorticoid- and age-related

osteoporosis where osteoblast production is seemingly sacrificed for

adipocytes.

Some of the data presented in this chapter are preliminary and were intended to be exploratory in nature in the search for TRPV1 receptor functions in osteoblasts, and to create dose-response curves in order to select appropriate drug concentrations for experimentation. Some of these preliminary data require future attention, including further work on the growth-arresting effects of pH on MG63 cells which contrasts with data in the literature, and development of the findings of the effects of thapsigargin and ruthenium red, and the use of these drugs as pharmacological tools in the characterisation of TRPV1 and its functions in osteoblasts. Recommendations for more immediate investigation include:

- further evidence of the anti-adipogenic effects of TRPV1 activation with the use of a larger pharmacological artillery, to include adenosine as a putative TRPV1 antagonist and cannabinoids (agonists and antagonists) to further investigate the action of anandamide and more conclusively distinguish its effects of TRPV1 from cannabinoid receptors.

- the effects of acidification on the differentiation of 7F2 cells, both alone and in combination with TRPV1 agonists.

- further work on the protective effects of capsazepine on capsaicin toxicity in osteoblasts, to determine whether TRPV1 antagonist by other ligands has the same protective effect, and whether this can also protect against the toxic effects of other TRPV1 agonists.

- proliferation, apoptosis, mineralisation and differentiation assays using primary human osteoblasts as the gold standard.
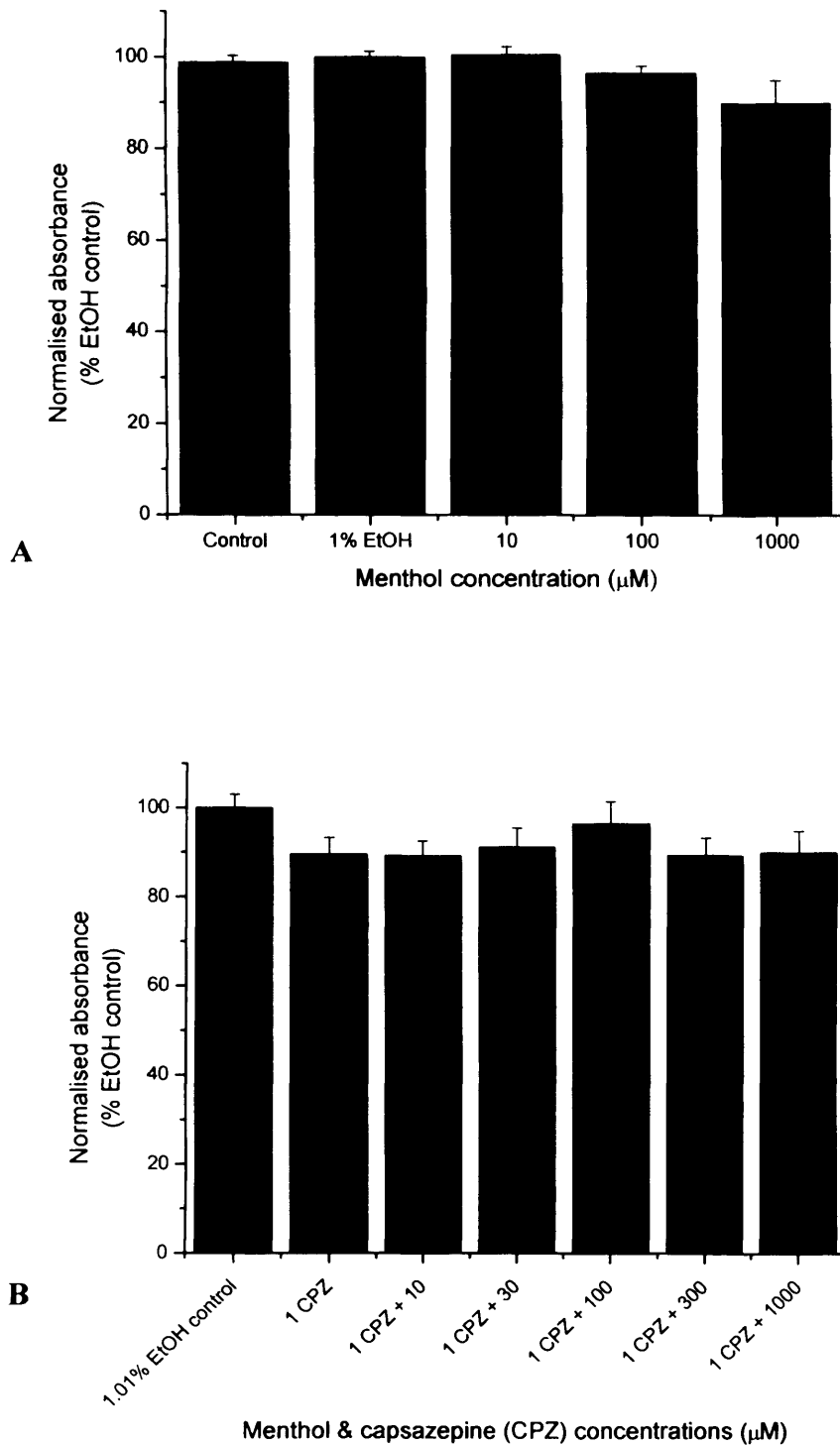
Figure 5.3 **(A) The TRPM8 agonist menthol had no significant effect on MG63 cell number** after 72 hours treatment ($p < 0.05$) either **(A)** alone over the range 10 µM to 1 mM (n = 3), or **(B)** in combination with 1 µM capsazepine over the same menthol concentration range (n = 3).
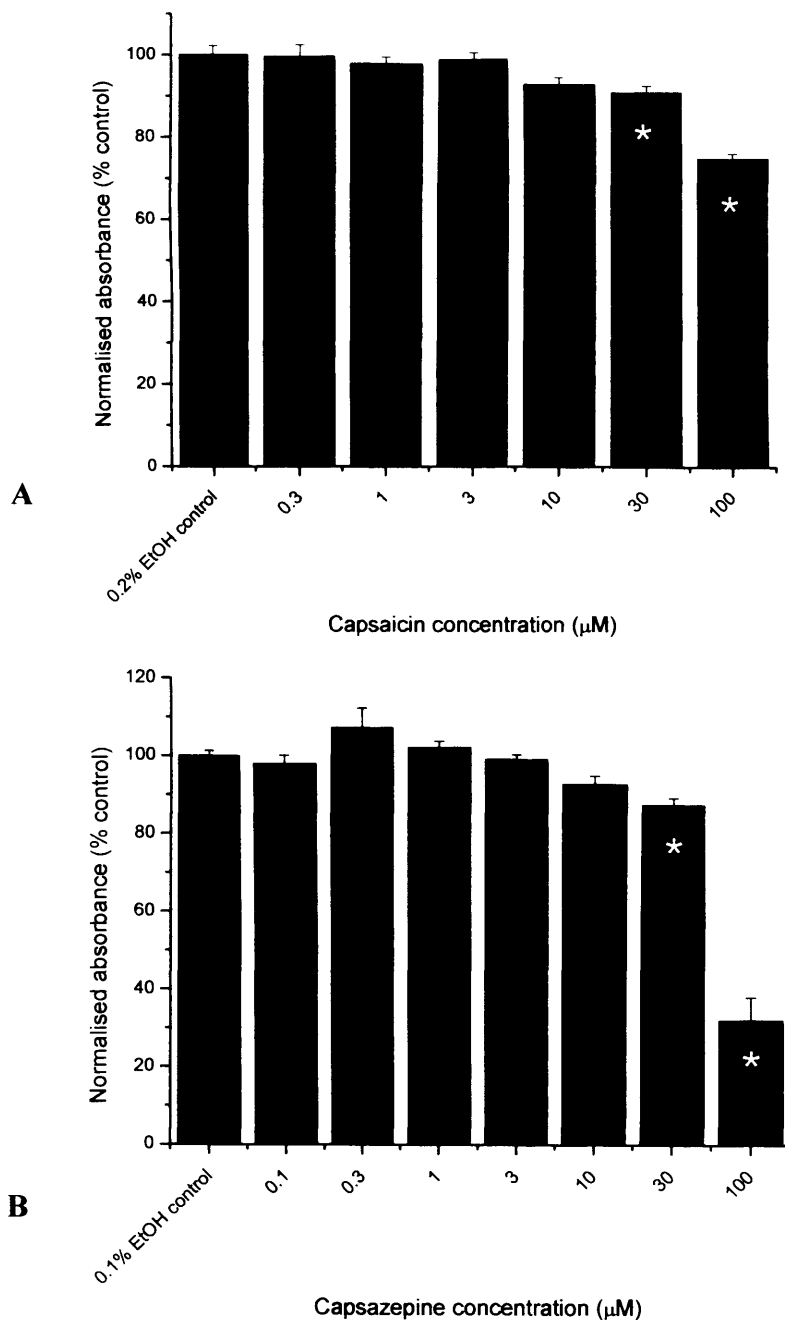
Figure 5.4   **Effects of capsaicin and capsazepine on MG63 cell numbers.** After 72 hours treatment, **(A)** the TRPV1 agonist capsaicin caused a significant decrease ($p < 0.05$) in MG63 cell numbers at 30 μM and 100 μM ($n = 3$), and **(B)** the non-specific TRPV1 antagonist capsazepine also caused a significant decrease ($p < 0.05$) in MG63 cell numbers at 30 μM and 100 μM ($n = 4$). * indicates significant difference from control.
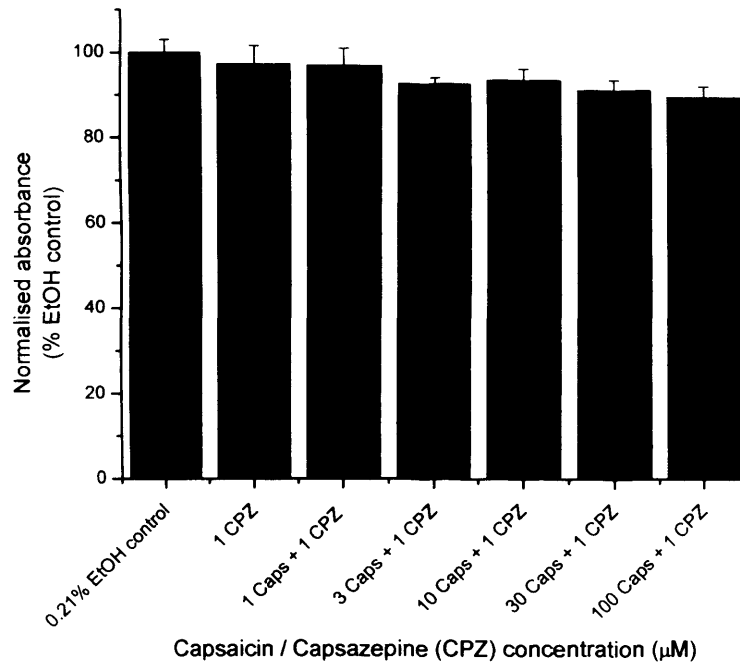
Figure 5.5 **Effects of capsaicin vs. capsazepine on MG63 cell numbers.** After 72 hours treatment, 1 μM capsazepine (which had no significant effect on MG63 cell number) prevented the cell number decreases caused by 30 μM and 100 μM capsaicin, seen in figure 5.4 (n = 3).
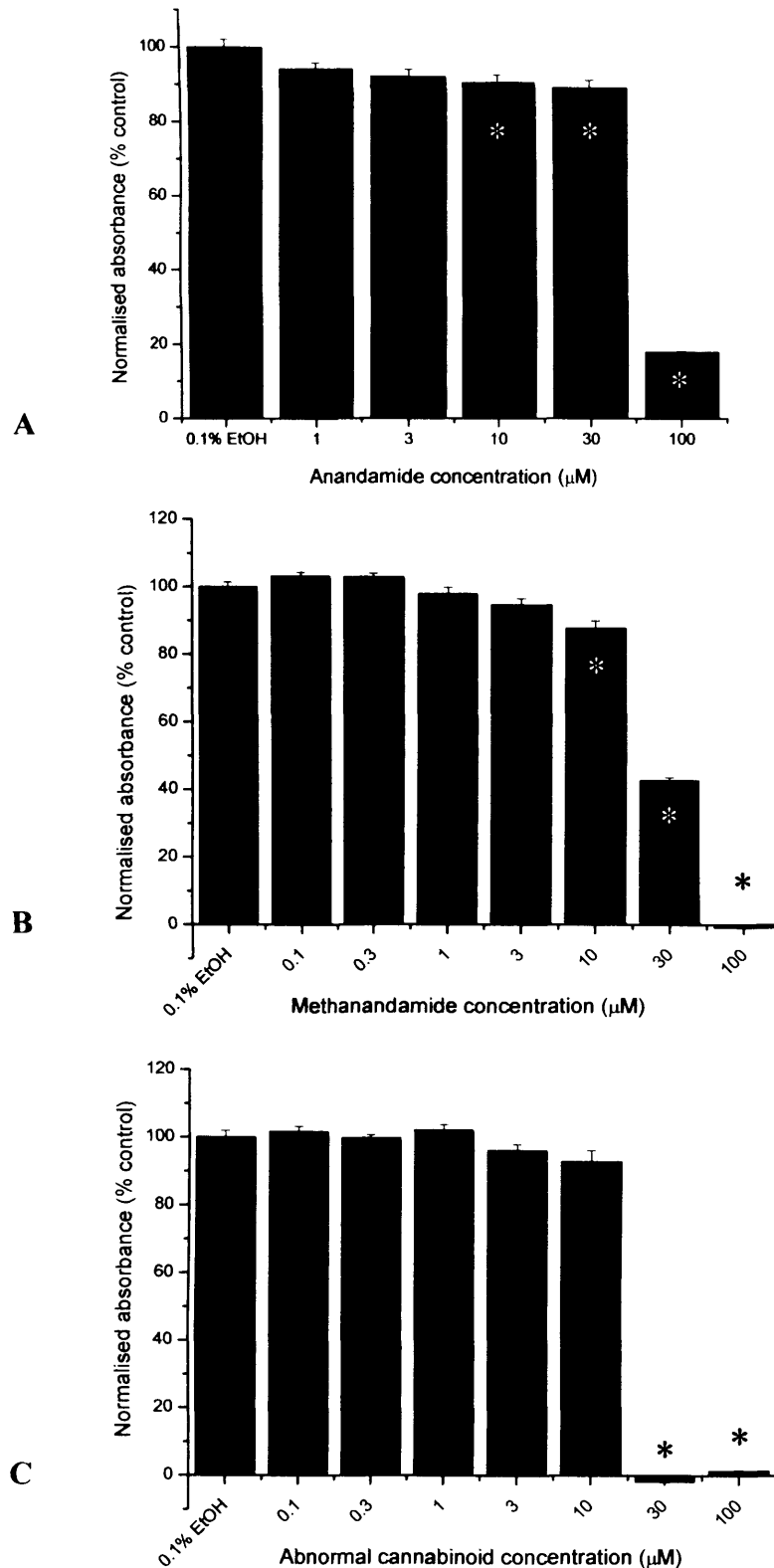
Figure 5.6 **Effects of different cannabinoids on MG63 growth.** All 3 agonists caused concentration-dependent reduction of cell numbers after 72 hours treatment, which were significantly different from controls at **(A)** 10, 30 and 100 μM anandamide (n = 3), **(B)** 10, 30 and 100 μM methanandamide (n = 3), and **(C)** 30 and 100 μM abnormal cannabinoid (n = 3). * indicates significant difference from control ($p < 0.05$).

Thapsigargin concentration (nM)
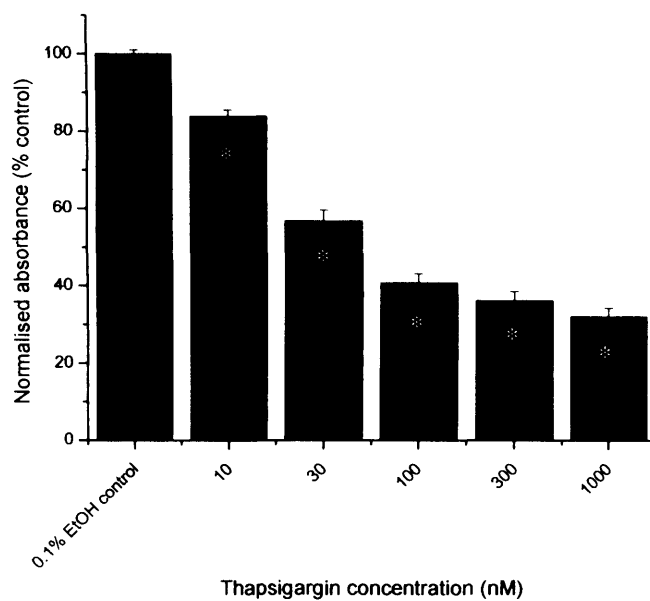
Figure 5.7 **Effects of thapsigargin on MG63 cell numbers**. The SERCA pump inhibitor thapsigargin caused a concentration-dependent decrease in MG63 cell numbers after 72 hours treatment over the concentration range 10 – 1000 nM, which was statistically significant from control over this entire range ($p < 0.05$; $n = 4$).
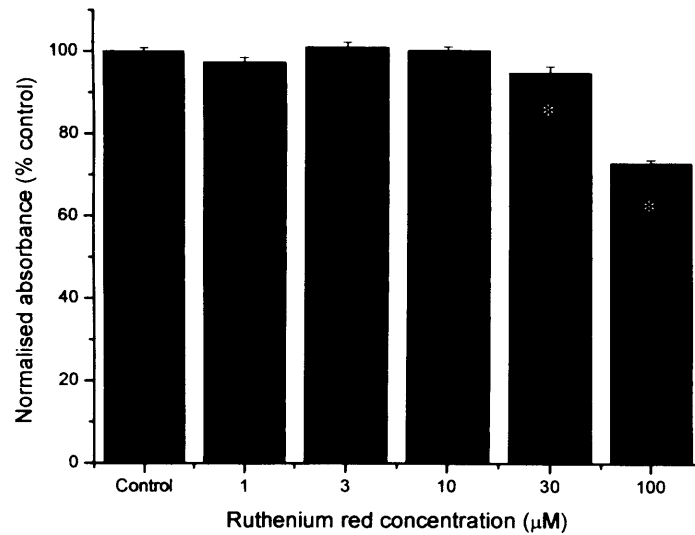
Figure 5.8 **Effects of ruthenium red of MG63 cell numbers.** The non-specific Ca^{2+}-channel blocker ruthenium red caused a concentration-dependent decrease in MG63 cell numbers at 30 μM and 100 μM, which was significantly different from control ($p < 0.05$; $n = 2$).

Capsaicin

Capsazepine

Figure 5.9 **Mineralisation assay of SaOS-2 human osteosarcoma cells.**
Mineralisation appears to be saturated, and therefore results are
inconclusive (n = 2).
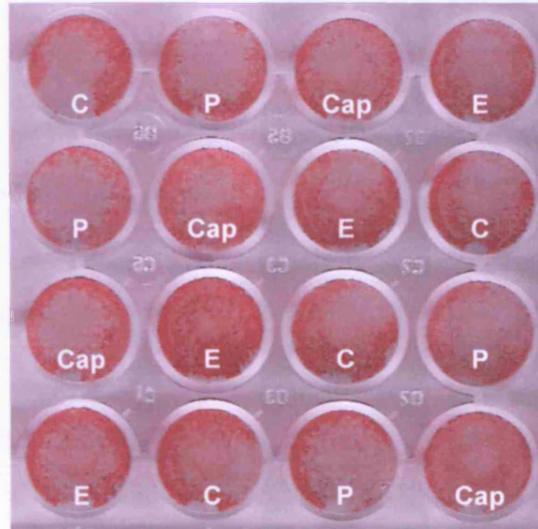
Key

C	Control
E	Ethanol vehicle control
Caps	Capsaicin (10 µM)
P	Pinacidil (100 µM)

Figure 5.10 **Mineralisation assay of 7F2 mouse osteoblasts.** Alizarin red staining shows osteoblastic mineralisation appears successful after 10 days treatment (n = 3). However, dye elution is required in future repeats to quantify mineral deposition and allow any differences to be measured.
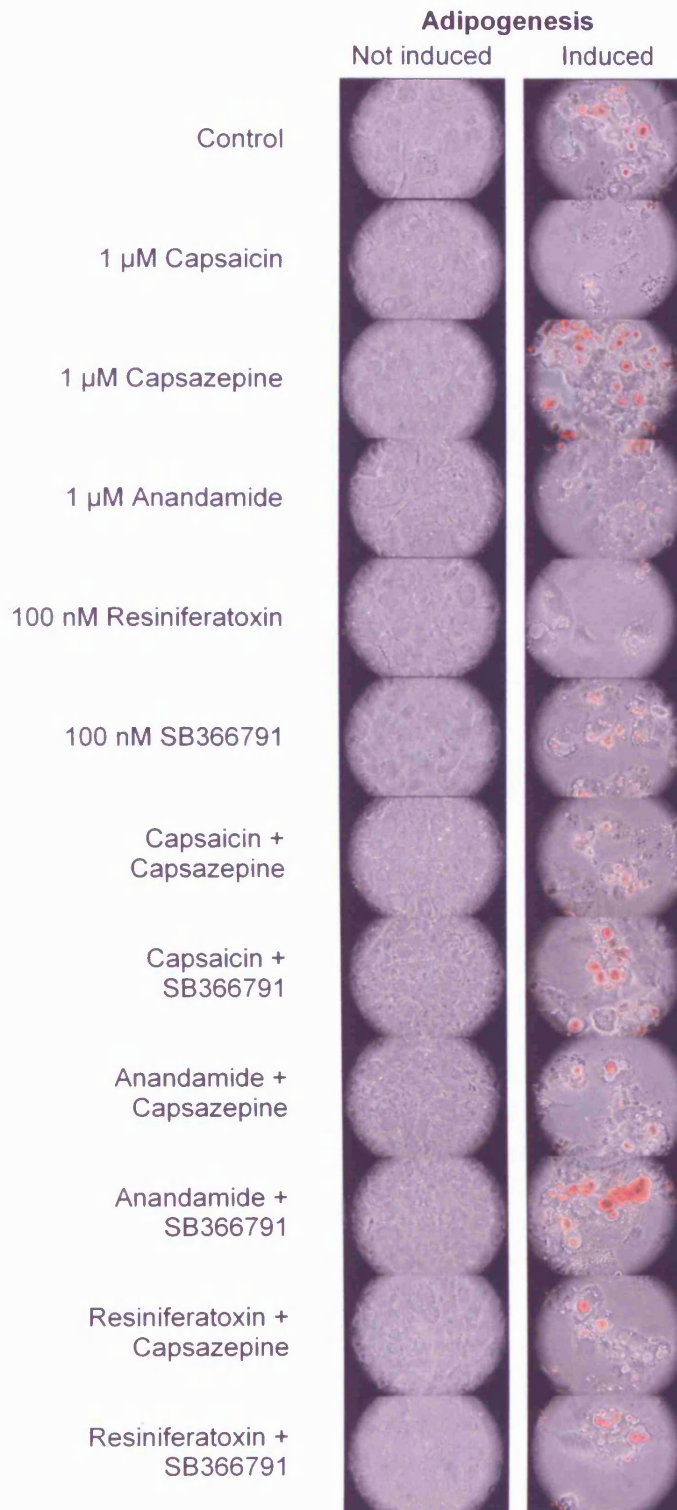
Figure 5.11 **Adipogenesis assays** (n = 3) with lipids stained red, showing that TRPV1 agonists capsaicin (1 µM) and resiniferatoxin (100 nM) prevented adipogenesis of induced 7F2 cells, and anandamide (1 µM) also appeared to do the same. The TRPV1 antagonists capsazepine and SB366791 did not prevent adipogenesis, but did appear to block the effects of the above agonists.
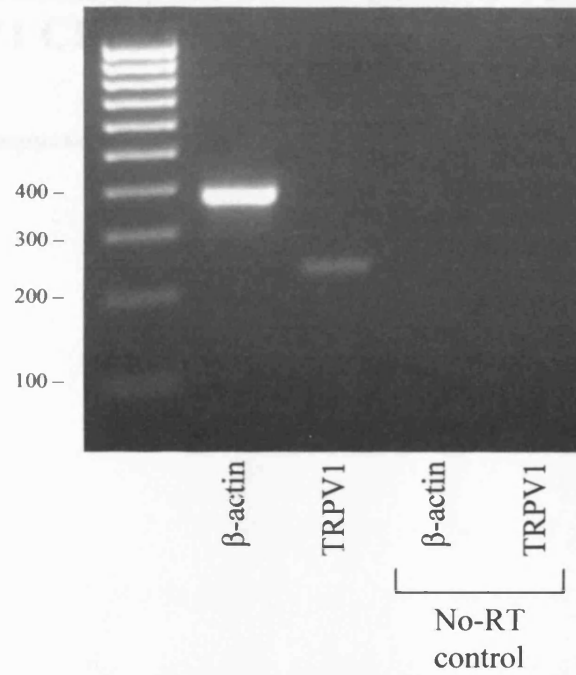
Figure 5.12 **RT-PCR confirms mRNA expression of TRPV1 in mouse 7F2 osteoblasts.** β-actin = 392 bp and TRPV1 = 233 bp.

CHAPTER 6:

CAPSAICIN-INDUCED CALCIUM SIGNALLING IN MG63 CELLS VIA THE TRPV1 CHANNEL

6 CAPSAICIN-INDUCED CALCIUM SIGNALLING IN MG63 CELLS VIA THE TRPV1 CHANNEL

6.1 Introduction

In chapter 4, it was shown that the TRPV1 channel is expressed at the messenger level in MG63 osteosarcoma cells and other human osteoblasts (including primary osteoblasts) and at the protein level in MG63 cell membranes. Importantly, the splice variant TRPV1b was also shown to be expressed at both messenger and protein level, which may, at least in part, account for the difficulty in gathering electrophysiological data of TRPV1 activation (chapter 4) as TRPV1b is a putative inhibitory subunit, meaning that any TRPV1 channel which contains TRPV1b subunits (homologous or heterologous) is insensitive to capsaicin (1 μM), protons (pH 5.0) and heat (50 °C) (Vos *et al.*, 2006). However, in chapter 5, TRPV1 was found to be functional in mouse 7F2 osteoblasts, specifically being important in differentiation, regulating progression of osteoblast-precursors to mature osteoblasts or to adipocytes, despite the expression of TRPV1b. Another

demonstrable criterion of TRPV1 functionality is channel activation by known

agonists (e.g. capsaicin, protons) in order to cause an increase in intracellular

Ca^{2+} concentration via the TRPV1 channel.

This chapter aims to address this final point to further confirm the presence and

functional status of the TRPV1 channel in osteoblasts, and to show whether or

not TRPV1 channel activation by capsaicin induces a Ca^{2+} signal in these cells.

6.1.1   Calcium signalling

Calcium signalling is the term given to the process by which cytoplasmic free

Ca^{2+} ions act in a signal transduction cascade either following influx from

extracellular fluid via plasma membrane ion channels, or as second messengers

following activation of an indirect pathway, such as G protein-coupled receptor

activation (Campbell, 1983). Intracellular sources of Ca^{2+} are the endoplasmic

reticulum (ER) and mitochondria, which act as internal Ca^{2+} stores, although

mitochondrial stores are transient. Ca^{2+} ions are pumped against their

concentration gradient into these stores to maintain a 'resting' cytosolic $[Ca^{2+}]$

of around 100 nM (Campbell, 1983; Baker, 1972). Activation of specific

receptors on the ER, the vast majority of which are ryanodine receptors and

inositol triphosphate (IP$_3$) receptors, allows release of Ca^{2+} ions into the

cytoplasm, increasing free $[Ca^{2+}]_i$ to as much as 5 – 10 μM (as much as 50 μM

Ca^{2+} may actually be released, but the majority is bound to cytoplasmic

proteins and organelles) (Campbell, 1983). This cytosolic Ca^{2+} regulates an

array of important physiological processes, including enzyme activity and ion

channels/pumps.

On the plasma membrane, ion channels which allow Ca^{2+} influx to the cytosol

include the voltage-gated Ca^{2+} channels, which are generally associated with

excitable tissue (neurons, myocytes, etc.) but are also found in non-excitable

cells such as osteoblasts (L-type) (Grygorczyk *et al.*, 1989; Meszaros *et al.*,

1996), and ligand-gated Ca^{2+} channels, including TRP channels (Clapham *et

al.*, 2005; Harteneck *et al.*, 2000) and store-operated channels (Clapham *et al.*,

2005; Parekh & Putney, 2005). TRP channel signalling has already been

reviewed (section 1.6.4.1), and store-operation may be a mechanism featured

by some TRP channels (such as the TRPC channels: see below). However, the

general theory that all TRP channels are store-operated channels is now widely

accepted as wrong.

6.1.1.1 Store-operated channels

The idea that cellular Ca^{2+} entry across the plasma membrane could be, at least

in part, controlled by intracellular Ca^{2+} store depletion following signalling in

order to replete these stores has been building for over more than 20 years

(Putney, 1986; Putney, 1990). This is now known as store operated Ca^{2+} entry

(SOCE) and the best described of the SOCE currents is that which is known as

the Ca^{2+} release activated Ca^{2+} current, I_{CRAC} (Lewis & Cahalan, 1989;

Matthews *et al.*, 1989; Penner *et al.*, 1988). However, there is now evidence to

show that SOCs do more than simply replete internal stores, but also create

Ca^{2+} signals which regulate cellular processes such as gene expression, cell metabolism and exocytosis (Parekh & Putney, 2005; Lewis, 2007).

The best described, by far, of the store-operated channels (SOCs) is the Ca^{2+} release activated Ca^{2+} (CRAC) channel which carries I_{CRAC} (Hoth & Penner, 1992). The messenger linking intracellular Ca^{2+} release and plasma membrane (PM) SOCs has long been unknown, but recent breakthroughs have identified STIM1, a primarily ER-bound transmembrane protein, as the Ca^{2+} store sensor, and CRACM1 (also known as Orai1), a plasma transmembrane protein, as the putative CRAC channel pore-forming subunit (Feske *et al.*, 2006; Li *et al.*, 2007; Vog *et al.*, 2006; Zhang *et al.*, 2005; Zhang *et al.*, 2006; Potier & Trebak, 2008). Verification occurs with artificial co-expression of STIM1 and CRACM1, which results in CRAC-like currents exhibiting all the features of CRAC (Mercer *et al.*, 2006; Peinelt *et al.*, 2006; Soboloff *et al.*, 2006). The proposed mechanism of interaction is that on store-depletion, STIM1 accumulates in regions of the ER close to the PM (Wu *et al.*, 2006), but whether there is direct protein-protein interaction between STIM1 and CRACM1 (Muik *et al.*, 2008; Yeromin *et al.*, 2006), or whether there are intermediate signalling proteins (Csutora *et al.*, 2008; Wu *et al.*, 2006), is currently an issue of contention.

6.1.1.2 Is there a role for TRP channels in store-operated Ca^{2+} entry?

Whether or not some TRP channels have a role in SOCE remains a hot topic, but TRPC channels remain controversial candidates (Parekh & Putney, 2005;

Smyth *et al.*, 2006; Alicia *et al.*, 2008). TRP channels began to emerge as

candidates for SOCs due their Ca^{2+} permeability and selectivity, and the

predicted topology of TRP channels was similar to that of VDCCs (Hardie &

Minke, 1993). But as it emerged that the Drosophila TRP channel was

activated by downstream products of PLC, such as diacyl glycerol (DAG) or

polyunsaturated fatty acids (PUFAs) (Hardie, 2003; Montell, 2003) the notion

that all TRPs and SOCs were one and the same suffered a setback. However, it

should be noted that whilst understanding of the CRAC channel (see above)

signalling mechanism may be progressing fruitfully, CRAC is just one

component of SOC currents, the remainder of which are poorly understood.

Whilst TRPC channels may not be CRAC channels, some authors believe

TRPC channels may yet reveal themselves as SOCs. Worley *et al.* (2007)

propose in one article that TRPC1 is a STIM1-regulated SOC, whilst in another

the authors go further and believe all TRPC channels (except TRPC7) to be

SOCs which are heteromultimerised by STIM1 (Yuan *et al.*, 2007). Therefore

the answer to the above question is: possibly, but there is a lot to do before a

definite answer can be given. In addition to the TRPC subgroup, TRPV6 (Den

Dekker *et al.*, 2003; Vennekens *et al.*, 2000; Voets *et al.*, 2001) has shown

some early promise as a SOC, but is not the I_{CRAC} channel as this has a Ca^{2+}

selectivity over Na^+ (P_{Ca}/P_{Na}) of > 1000:1 and a conductance of < 1 pS (Broad

et al., 1999), compared to P_{Ca}/P_{Na} > 130:1 and 58 - 79 pS conductance for

TRPV6 (Alexander *et al.*, 2004).

6.1.1.3 The calcium-sensing receptor (CaR)

The extracellular calcium-sensing receptor was first cloned from bovine parathyroid by Brown et al. (1993) and is a PM-bound non-ion channel receptor, characteristic of the GPCR family. The receptor is particularly sensitive to extracellular Ca^{2+} and other polyvalent cations and therefore the authors (ibid) proposed that the CaR on parathyroid and other calcium-sensitive tissues is the extracellular calcium-sensor in the regulation of Ca^{2+} metabolism, and report that the receptor responds to changes of $[Ca^{2+}]_o$ in the millimolar range. The receptor is a 7-transmembrane protein receptor with a large extracellular domain, containing multiple Ca^{2+}-binding sites (Brown et al., 1993). $[Ca^{2+}]_o$ changes are detected by the CaR, which then modulates multiple signalling pathways of G-protein coupling via G_i (inhibiting adenylate cyclase) (de Jesus Ferreira et al., 1998), G_q (activating phospholipase C) (Kifor et al., 1997) and possibly $G_{12/13}$ (activating Rho-mediated phospholipase D) (Huang et al., 2004), to alter $[Ca^{2+}]_i$. However, there is also good evidence for CaR responses via non-G-protein coupling pathways, including direct CaR-induced phospholipase induction (Kifor et al,. 1997), CaR-induced Ca^{2+}_i oscillations (Breitwieser et al., 2001; Miki et al., 2005), and PKC-mediated CaR phosphorylation (Bai et al., 1998; Meggio et al., 1995). However, the full detail of the CaR downstream signalling mechanisms remain unresolved to date (van den Hurk et al., 2008).

Detection of changes in $[Ca^{2+}]_o$ by the parathyroid gland is presumably the mechanism by which the parathyroid regulates the secretion of parathyroid

hormone (PTH). Parathyroid hormone action on bone cells results in calcium

resorption into the blood from the bone by stimulating osteoblasts to increase

their release of RANKL, which stimulates osteoclast development. The CaR

has also been identified in osteoblasts (Dvorak *et al.*, 2004; Chattopadhyay *et*

al., 2004) and osteoclasts (Kameda *et al.*, 1998) and may directly regulate bone

turnover. Osteoblasts have been shown in this Thesis (see section 3.3.2, and

Figure 3.17) to detect and respond to small changes in extracellular calcium

concentration within the physiological range 0.6 – 3.0 mM, which is likely due

to CaR sensing.

6.1.2 The role of TRPV1 in modulating intracellular free Ca^{2+} concentration

The TRPV1 channel has for some time been recognised as a Ca^{2+}-permeable

ion channel with high expression in peripheral sensory neurones and dorsal

root ganglia (Caterina *et al.*, 1997). Plasma membrane TRPV1 activation is a

known means of Ca^{2+} influx from extracellular free Ca^{2+}, and also $[Ca^{2+}]_i$

elevation by Ca^{2+} release from internal stores in dorsal root ganglia (Savidge *et*

al., 2001) and various other non-excitable tissue- and cell-types (e.g. Liu *et al.*,

2000; Sanchez *et al.*, 2005), and is outwardly rectifying with a conductance of

around 80 pS and a P_{Ca}/P_{Na} of around 10: 1. The relatively defined

pharmacology of the TRPV1 channel compared to other TRP channels has

enabled the elucidation of mechanisms of activation of Ca^{2+} entry. The channel

is directly activated by the specific agonist capsaicin (Caterina *et al.*, 1997) and

the endocannabinoid anandamide (Smart *et al.*, 2000) which evoke $[Ca^{2+}]_i$

increases in various cell types, and blocked by the synthetic compound capsazepine (Bevan *et al.*, 1992). Perhaps rather surprisingly, the TRPV1 antagonist capsazepine on its own evokes a rise in $[Ca^{2+}]_i$ in MG63 cells similar to that seen with capsaicin in other cell types (Teng *et al.*, 2004. Capsazepine in other cell types inhibits Ca^{2+} signals (Piper *et al.*, 1999), although recently another group has reported $[Ca^{2+}]_i$ increases in prostate cancer cells in response to capsazepine (Huang *et al.*, 2006). Teng *et al.* (2004) speculate that the capsazepine-induced $[Ca^{2+}]_i$ rise in MG63 cells may be via a separate mechanism exclusive of TRPV1. Capsazepine is now well documented to be non-selective for TRPV1; it also blocks voltage-dependent Ca^{2+} channels (VDCCs) (Docherty *et al.*, 1997), and interestingly capsazepine activates the amiloride-sensitive epithelial Na^+ channel (ENaC) in human epithelial cells (Yamamura *et al.*, 2004).

More recently, the nucleoside adenosine has been shown to block the Ca^{2+} signalling effect of capsaicin (Puntembekar *et al.*, 2004) and therefore is a putative endogenous antagonist of TRPV1, and interestingly Zhang *et al.* (2007) have shown the importance of the Ca^{2+} signal by capsaicin-induced TRPV1 activation in adipocyte cell differentiation. What appears lacking in the literature is evidence of $[Ca^{2+}]_i$ signals in human osteoblasts in response to capsaicin and other TRPV1 agonists.

6.1.3 Is TRPV1 involved in SOCE?

TRPV1 does not have any of the characteristics that could realistically make it

a SOC, other than the fact that as a Ca^{2+} permeable channel it allows Ca^{2+} entry

across the plasma membrane which may contribute to Ca^{2+} store repletion.

There is plenty of evidence against TRPV1 being the CRAC channel. For

instance, 2-aminoethoxydiphenylborane (2-APB), a ligand that was used to

discriminate I_{CRAC} as a selective blocker (although now known not to be

selective at all) *activates* TRPV1, TRPV2 and TRPV3 channels (Hu *et al.*,

2004; Chung *et al.*, 2004). Also, and importantly in this argument, capsaicin

blocks I_{CRAC} in Jurkat T-cells (Fischer *et al.*, 2001) whereas capsaicin is the

defining TRPV1 agonist (Cahalan *et al.*, 1997). TRPV1 agonists have been

shown to release Ca^{2+} from internal stores via activation of endoplasmic

reticulum TRPV1 channels, but this failed to activate SOCs on the plasma

membrane, which indicates that TRPV1 is also not involved in SOCE

signalling (Wisnoskey *et al.*, 2003).

6.1.4 Desensitisation of capsaicin-induced Ca^{2+} flux in excitable cells

The capsaicin-induced influx of Ca^{2+} ions into excitable cells (dorsal root

ganglionic neurones, peripheral sensory neurones) has been shown to be

desensitising resulting in reduced inward currents on further challenges with

capsaicin and that this desensitisation is capsaicin-, $[Ca^{2+}]_o$- and voltage-

dependent (Piper *et al.*, 1999; Cholewinski *et al.*, 1993; Koplas *et al.*, 1997). A

number of mechanisms of action of desensitisation have been proposed: one is

that TRPV1 is dephosphorylated by calcineurin (protein phosphatase 3 CA –

formerly called protein phosphatase 2B) (Novakova-Tousova *et al.*, 2007) and

another is that desensitisation may be regulated by protein kinase A activation

and calmodulin binding (Bhave *et al.*, 2002; Mohapatra & Nau, 2003;

Numazaki *et al.*, 2003; Rosenbaum *et al.*, 2004). A possible third mechanism

of desensitisation (shown in Figure 6.1) is that Ca^{2+} influx via TRPV1 causes

hydrolysis of phosphatidylinositol 4,5-bisphosphate (PIP$_2$) which deactivates

the channel, as PIP$_2$-binding is thought to be essential for TRPV1 activation

(Liu *et al.*, 2005). Re-synthesis of PIP$_2$ by phosphatidylinositol-4-kinase

(PI4K) rephosphorylates TRPV1 and reverses the capsaicin-desensitisation

(Liu *et al.*, 2005). The authors of this proposed mechanism do not agree with

Mandadi *et al.* (2004) who propose that resensitisation is probably mediated by

protein kinase C, and Liu *et al.* (Ibid) suggest that the 're-sensitisation' seen by

Mandadi *et al.* is due to incomplete desensitisation of TRPV1 following short

bursts of capsaicin exposure, and therefore Ca^{2+} responses were due to

activation of non-desensitised channels following PKC activation.

Much of the evidence for capsaicin-desensitisation is based on experiments

with excitable cells although the same mechanism is presumably responsible

for any TRPV1 desensitization in non-excitable cells, including osteoblasts.
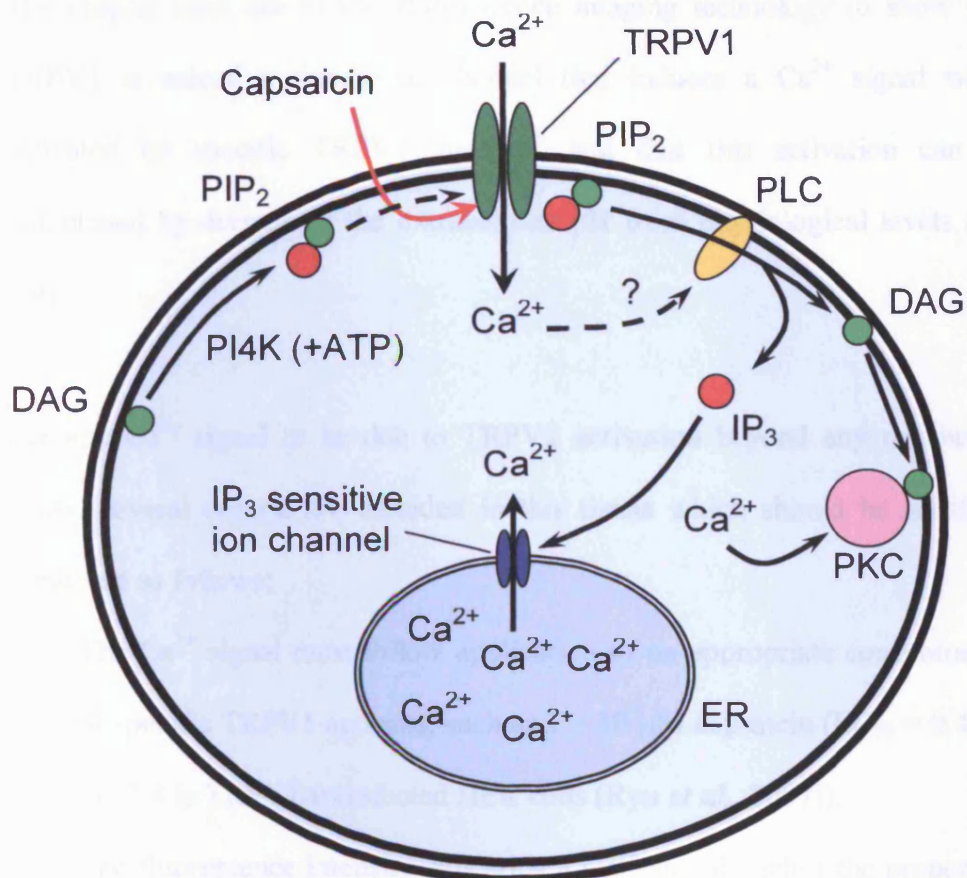
Figure 6.1 **Possible mechanism of desensitisation of TRPV1 by capsaicin.**
Ca^{2+} influx may promote Ca^{2+}-dependent PIP_2 hydrolysis by phospholipase C
(PLC), leading to desensitisation of the channel. Resynthesis of PIP_2 allows
recovery and resensitisation of TRPV1 to capsaicin.

6.1.5 Chapter hypothesis, aims and experimental strategies

The hypothesis in chapter 6 is that applications of TRPV1 agonists, such as

capsaicin and protons, to MG63 osteosarcoma cells will cause intracellular free

Ca^{2+} to rise due to activation of the TRPV1 channel, thus fulfilling the 5th key

aim of the thesis, as listed in the introduction (section 1.7).

The chapter aims are to use fluorescence imaging technology to show that TRPV1 is indeed a functional channel that induces a Ca^{2+} signal when activated by specific TRPV1 agonists, and that this activation can be potentiated by decreasing the extracellular pH from physiological levels (pH 7.4).

For any Ca^{2+} signal to be due to TRPV1 activation beyond any reasonable doubt, several criteria are included in this thesis which should be satisfied. These are as follows:

1   The Ca^{2+} signal must follow application of an appropriate concentration of specific TRPV1 agonists, such as 1 – 10 µM capsaicin (EC_{50} = 0.48 at pH 7.4 in TRPV1-transfected HEK cells (Ryu et al., 2007)).

2   The fluorescence intensity indicating a Ca^{2+} signal, and/or the proportion of cells fluorescing, in response to a TRPV1 agonist should increase when the extracellular pH is decreased to show potentiation of the channel-activation by protons.

3   A decrease in pH itself should not induce a Ca^{2+} signal in the absence of any TRPV1 agonists.

4   Capsaicin-desensitisation should be apparent following the initial application of capsaicin. Further applications should not induce a Ca^{2+} signal at the same pH.

5   The Ca^{2+} signal should be due to direct activation of TRPV1, and not secondary Ca^{2+} signalling due to TRPV1-stimulated glutamate release. Therefore, glutamatergic Ca^{2+} signalling should either be absent in

213

response to application of glutamate, *or* glutamate receptor antagonists

should not impair any capsaicin-induced Ca^{2+} signal.

6.1.5.1 Experimental strategy

In order to achieve the above aims, calcium imaging experiments made use of

the fluorescent Ca^{2+} indicator fluo-3. This chemiluminescent compound was

first introduced by Minta *et al.* (1989) and has the advantage of producing a

large increase in fluorescence with Ca^{2+} chelation.

6.2 Methods

6.2.1 Cell culture

MG63 cells (passage number 11) were cultured, counted and seeded as described in chapter 2, sections 2.1, 2.2 and 2.5, and calcium imaging experiments were conducted as described in section 2.5.

6.2.2 Ca^{2+} imaging protocol

MG63 cells were cultured in 35 mm culture dishes with a 10 mm diameter glass-bottom of standard thickness 1.0 (MatTek Corporation, Ashland, MA, USA) and incubated for two to three days in DMEM supplemented with 5 % FBS and penicillin-streptomycin 1000: 1000. Cells were loaded in culture medium with 5 μM Fluo-3 acetoxymethyl (Molecular Probes, Invitrogen, Eugene, OR, USA) prepared with 20 % pluronic F127 (Molecular Probes) in DMSO (Sigma) for 20 minutes at 37 °C in the dark. Cells were then washed in culture medium and again incubated for 20 minutes at 37 °C in the dark for the loaded dye to de-esterify. For the experiments, the culture medium was replaced with sodium 'Locke' solution (mM: 150 NaCl, 3 KCl, 2 $CaCl_2$, 2 $MgCl_2$, 10 HEPES, 10 D-glucose) and additions were made directly to the dish with a variable volume pipettor. All drugs were prepared in sodium 'Locke' solution, where possible, at 10× final concentrations.

Experiments were carried out using a laser scanning confocal microscope (Zeiss LSM 510) with a C-Apochromat 63×/1.2 n.a. water-immersion lens for

high resolution imaging. The fluorescent dye was excited by the 488 nm line of an argon/2 laser running at 1 % power, and emitted light was collected with a bandpass IR filter of between 500 and 550 nm. Images of 512 × 512 pixels were acquired with a pixel dwell-time of 2.56 µs, resulting in an acquisition rate of 1.576 seconds per frame.

Image data were saved as Zeiss .lsm files in databases and later converted from .lsm sequences to .avi movie file sequences using Zeiss LSM Image Browser (version 4,2,0,121). Movie file sequences were then analysed with Photek IFS32 (C-Vision/Im32 Version 5.25 X3.1490) software by drawing Odd Area Profiles (OAP) around cells and extracting Odd Area Set (OAS) intensity data for the entire set of images in the movie sequence. These values were then plotted against time using Origin 7 software (OriginLab®).

6.2.3 Interpretation of data

Image fluorescence intensity was measured for each frame of the odd area set (OAS) of cells in each 512 × 512 pixel area recorded (see Figure 6.2, and as described in section 2.5) over time courses of around 550 to 750 seconds (364 to 481 frames, with 1.576 seconds between frames). Data were copied into Microsoft Office Excel 2003 and the first 10 frames of each odd area profile (OAP) were averaged to get a baseline intensity value (FI_0). The relative fluorescence intensity was calculated for each frame of each OAP by dividing each measured intensity value (FI) by the averaged baseline value (FI/FI_0).
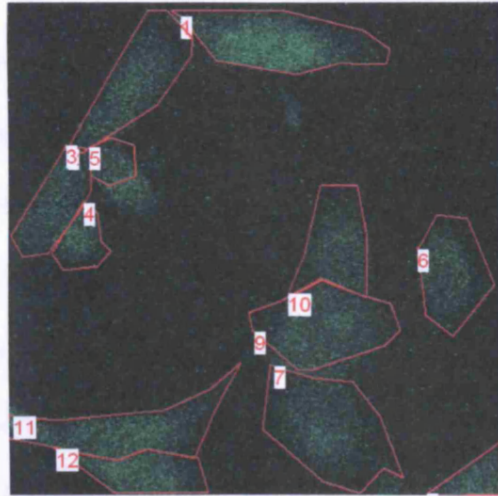
Figure 6.2 **Example of a 512 × 512 pixel frame showing Odd Area Profiles** (OAP) drawn around MG63 cells, collectively forming an Odd Area Set (OAS). Intensity data were measured for each OAP in each frame.

Relative fluorescence intensity values were copied to Origin software and average values for all cells in each frame were plotted against time. Increases in fluorescence intensity with fluo-3 stained cells indicates increases in $[Ca^{2+}]_i$ of these cells.

6.3   Results

6.3.1   Optimisation of fluorescent dye loading

Adjustments to the fluo-3 loading protocol described in the methods section were required to achieve optimised loading. The loading protocol reported by Labelle *et al.* (2007) which uses 2 μM fluo-3 (with pluronic F127) incubating for 45 minutes followed by washing and 45 minutes in Locke solution to allow the dye to de-esterify resulted in poor dye loading into the MG63 cells. Increasing fluo-3 concentrations to 5 μM and 10 μM and incubating for 20 minutes, with a 20 minute wash/de-esterification period resulted in improved dye-loading and this amended protocol, with 5 μM fluo-3, was therefore followed for all the experiments.

6.3.2   Capsaicin pH-dependently induces a calcium signal

The TRPV1 agonist capsaicin induced calcium signals in the MG63 cells, which were potentiated by a decrease in pH from 7.4 to 6.3, thereby meeting criteria 1 and 2 for TRPV1-mediated Ca^{2+} signalling (see 6.1.4). On application of 1 μM or 10 μM capsaicin at physiological pH (7.4), increases in cell fluorescence intensity corresponding to increased $[Ca^{2+}]_i$ were heterogeneous, with just 50% or less of cells showing detectably increased fluorescence intensity. Figure 6.3 shows no increase in fluorescence intensity (0/8 cells produced calcium responses) when challenged with 1 μM or 10 μM capsaicin, whereas in Figures 6.4 and 6.5 in naïve cells, 3/6 and 2/12 cells respectively

displayed 1.1 and 1.4 increased fluorescence intensity within 2 - 5 seconds

of challenge with 1 μM capsaicin.

The $[Ca^{2+}]_i$ increase in response to 1 μM capsaicin appeared to be transient

rather than sustained, and after quickly reaching maximum fluorescence in

approximately 10 seconds, the intensity decreased steadily over a period of

approximately 100 seconds before levelling out at pre-capsaicin intensity

values in the 3/6 cells that responded (Figure 6.4).

Decreasing the extracellular pH from 7.4 to 6.3 with HCl appeared to

potentiate the $[Ca^{2+}]_i$ response of the cells to capsaicin as expected (Figures

6.4, 6.5 and 6.6). As demonstrated by Figure 6.4, the capsaicin-induced $[Ca^{2+}]_i$

rise at pH 7.4 was mixed, with only 3/6 of the cells showing increased

fluorescence intensity (overall intensity increased 1.1×), and following a pH

drop to 6.3 the capsaicin response was homogeneous (6/6 cells) with a greater

fluorescence intensity increase to 1.4× the relative fluorescence intensity (RFI).

Figure 6.5 also shows that in the presence of 1 μM capsaicin, decreasing the

extracellular pH to 6.3 without further application of capsaicin causes $[Ca^{2+}]_i$ to

rise above the initial response to capsaicin at pH 7.4 (1.4× increase overall;

2/12 cells), to around 3.6× the RFI (12/12 cells).

To show that protons alone do not lead to $[Ca^{2+}]_i$ rises, extracellular pH was

decreased after 75 seconds recording at pH 7.4 to pH 6.3 as a challenge to

naïve cells and, as expected, the cells (0/10) did not display any detectable

change in fluorescence intensity (Figure 6.6). On application of 1 μM capsaicin following pH decrease, the fluorescence intensity of 3/10 cells increased transiently to a total RFI of 1.2×, indicating a TRPV1-mediated calcium signal. The fact that protons do not induce a Ca^{2+} signal in the absence of capsaicin shows that the above responses are due to capsaicin, and these responses are simply potentiated by decreased pH. This satisfies criterion 3 for TRPV1-mediated calcium signals in osteoblasts (see 6.1.4).

6.3.3 Desensitisation of the capsaicin-response

Multiple applications of capsaicin revealed that initial capsaicin-induced calcium signals were non repeatable at the same pH (n = 3, Figures 6.4 - 6.6), indicating a mechanism for capsaicin-desensitisation. This satisfies the 4th criterion for osteoblastic TRPV1-mediated calcium signals (see 6.1.4).

At physiological pH (7.4), a single application of 1 μM capsaicin to the MG63 cells induced a calcium signal in 3/6 cells (total RFI 1.1×), but a second application of 10 μM capsaicin produced no response (Figure 6.4) indicating capsaicin-desensitisation. However, following pH change to 6.3 (with HCl) a third application of capsaicin (10 μM) induced a large calcium signal in 6/6 cells, with a total RFI increase to 1.4× from background. This shows that at physiological pH, capsaicin-desensitisation occurs, but can seemingly be reversed by acidifying the extracellular environment. But does capsaicin-desensitisation also occur at pH 6.3?

Figure 6.5 shows that it does. An initial application of 1 µM capsaicin at pH 7.4 induced a small total change (1.4×) in fluorescence signal, corresponding to 2/12 cells. With the capsaicin still in the bath, HCl was added to decrease the pH to 6.3 and a much larger calcium signal can be seen at around 3.6× change in fluorescence intensity (from background), due to a homogeneous cellular calcium response (2/12 cells). A further application of 1 µM capsaicin produced no response at the same pH.

In Figure 6.6, the bathing solution was acidified to pH 6.3 prior to exposure to capsaicin. The initial 1 µM capsaicin application induced a calcium signal (1.2× RFI increase, corresponding to 3/10 cells), but a second 10 µM application of capsaicin produced no response, again showing capsaicin-desensitisation.

6.3.4   No calcium response to challenges with L-glutamate

Application of L-glutamate produced no detectable calcium responses in the MG63 cells at the concentrations used (n = 5, representative data shown in Figures 6.3 and 6.7), which indicates that capsaicin-induced Ca^{2+} signals are probably not due to the effects of osteoblastic TRPV1-stimulated glutamate release acting on NMDA receptors (see Medvedeva *et al.*, 2008; Lappin *et al.*, 2006), or glutamate-induced TRPV1 activation (Ahern *et al.*, 2006) thus satisfying the 5th and final criterion for TRPV1-induced Ca^{2+} signalling (see 6.1.4). When various concentrations of L-glutamate (sodium salt, Sigma) from 30 µM to 100 µM were added to the bath, there was no detectable increase in

fluorescence in the MG63 cells up to 140 seconds post addition (Figures 6.3

and 6.7). In both examples shown, the cells were naïve to challenges by other

drugs and increases in fluorescence were demonstrated with 100 mM $CaCl_2$

applied to the bath as a positive control.

6.3.5   KCl causes $[Ca^{2+}]_i$ to increase

KCl causes an increase in intracellular calcium, which is probably due to

membrane depolarisation and Ca^{2+} entry via VDCCs. This effect was used as a

positive control at the end of each experiment to show that the fluo-3 loading

had worked effectively and did not affect cell viability. Application of 50 mM

KCl to the bath (final concentration) caused a small $[Ca^{2+}]_i$ increase (RFI

increased by 1.1×; n = 2), reaching a sustained maximum after 10-30 seconds

from the initial response (Figures 6.4 and 6.7). The $[Ca^{2+}]_i$ maximum was

sustained for at least 130 seconds before challenge with $CaCl_2$. Figure 6.4B

shows a decrease in fluorescence intensity in response to 50 mM KCl when

measuring fluorescence over total cell area as drawn at time = 0. This conflicts

with the effects seen in Figures 6.3 and 6.7, but on closer inspection the cells in

Figure 6.4 shrink on application of KCl. If the fluorescence intensity is

measured for the entire time course based on cell area *after* cell shrinkage, the

fluorescence intensity of the cells increases in response to KCl, as shown in

Figure 6.4C.

6.4 Discussion

6.4.1 Optimisation of fluorescent dye loading

Dye loading was optimised by amending the protocol fluo-3 concentration and incubation times. Although the same cell line was used for these experiments, the dye was incubated with the cells in culture medium whereas Labelle *et al.* incubated the cells in a less complex (by number of ingredients) HEPES-buffered saline solution. It is noted that the product information given for fluo calcium indicators (Molecular Probes, Invitrogen) states that in addition to using the non-ionic detergent Pluronic® F127 as a dispersing agent to facilitate dye loading into cells, BSA or FBS may also facilitate cell loading. Therefore it is possible that a shorter loading time may be required when using culture medium containing FBS than for a buffer solution. However, in the experiments discussed in this thesis, all media contained 5% FBS and no attempt was made to investigate this systematically.

However, the recommendations also state that a loading buffer free of primary and secondary amines is used to minimise extracellular hydrolysis of fluo-3 acetoxymethyl esters. DMEM does contain amines and the use of this medium as a loading buffer may explain the need to increase the fluo-3 loading concentration due to dye ester hydrolysis.

Although the dye-loading protocol used for this thesis deviates slightly from the manufacturers' recommendations and that of Labelle *et al.* (2007), slight

modifications resulted in good dye-uptake and low background (baseline)

fluorescence giving good signal-noise ratio fluorescence intensities during

experiments.

6.4.2 Capsaicin-induced calcium signals

6.4.2.1 Effects of capsaicin are potentiated by acidification

At pH 7.4 the intracellular free calcium responses to capsaicin were

heterogeneous, whereas at pH 6.3 all cells showed increased $[Ca^{2+}]_i$. It is

recognised that TRPV1 channel activation is potentiated by protons, resulting

in a lower EC_{50} of capsaicin in more acid conditions: at pH 7.4, $EC_{50} = 0.48 \pm$

0.03 µM and at pH 6.5, $EC_{50} = 0.05 \pm 0.004$ µM (Ryu et al., 2007) making

capsaicin approximately 1 order of magnitude more potent at pH 6.5.

Puntambekar et al. (2004), for example, have reported that capsaicin causes

$[Ca^{2+}]_i$ increases in TRPV1-transfected Xenopus laevis oocytes, and many

groups have shown that small reductions in pH potentiates activation of

TRPV1 by capsaicin and resiniferatoxin (e.g. Caterina et al., 1997; Jordt et al.,

2000; Ryu et al., 2007). However, the expression of TRPV1b either as a

heteromultimer or a homomultimer has been shown to negatively regulate the

channel, rendering it much less responsive to capsaicin or protons (Lu et al.,

2005; Schumacher et al., 2000; Vos et al., 2006; Wang, C. et al., 2004).

It would seem reasonable, given the data shown here, to draw the conclusion

that TRPV1 homomultimers must be expressed in MG63 cells as $[Ca^{2+}]_i$ is

increased by capsaicin, and the effect is clearly enhanced by reducing the

extracellular pH. If the conclusions drawn by Lu, Schumacher, Vos and Wang

(ibid) are to be believed then the MG63 cell membranes cannot be populated

by TRPV1b/TRPV1 heteromultimers or TRPV1b homomultimers alone.

6.4.2.2 Desensitisation of capsaicin-evoked $[Ca^{2+}]_i$ increases

The fact that $[Ca^{2+}]_i$ responses to capsaicin challenge were not repeatable at the

same pH shows that desensitisation of the TRPV1 channel occurs in

osteoblasts. Following desensitisation by capsaicin, depolarisation of the cell

membrane by KCl does still cause $[Ca^{2+}]_i$ to rise, showing that the capsaicin-

desensitisation is specific and exclusive of other mechanisms of cytosolic free

calcium-entry. This capsaicin desensitisation in MG63 cells is very much like

the desensitisation seen in dorsal root ganglia and thus it is tempting to propose

a common underlying mechanism.

The capsaicin-induced MG63 cell TRPV1 activation and $[Ca^{2+}]_i$ response at pH

6.3, following apparent capsaicin-desensitisation at pH 7.4 (normal), can

probably be explained yet again by the potentiating effects of protons on

capsaicin-evoked TRPV1 activation. The results show that only a small

proportion of cells display increased fluorescence intensity on application of

capsaicin at pH 7.4, but all cells light up at pH 6.3 in the presence of 1 μM

capsaicin. So why do some cells respond at pH 7.4 when others do not? There

are a variety of possible explanations for this, such as heterogeneous

expression levels of TRPV1 across the cells, different phosphorylation states of

TRPV1 channels in different cells, TRPV1/TRPV1b heteromultimer

expression level differentials, and cells at various stages of the cell cycle, to name but a few. It is likely that at pH 7.4, 1 µM capsaicin produces a submaximal response resulting in desensitisation of those channels that were activated, but at pH 6.3 the proton-potentiated homogeneous response was at or near the maximum due to reduction in EC_{50} concentrations of capsaicin and was therefore followed by homogeneous desensitisation of TRPV1.

6.4.3 Calcium signal not due to downstream glutamate action

Fluorimetric measurements of $[Ca^{2+}]_i$ showed that glutamate did not cause a rise in $[Ca^{2+}]_i$ of cells bathed in Locke solution at concentrations between 30 µM and 100 µM. However, as fluorescence intensity increases were observed on application of capsaicin, calcium signals must be directly due to Ca^{2+} influx via TRPV1 channels rather than a secondary effect due to TRPV1-stimulated glutamate release. Primary osteoblasts and osteoblast-like cells such as MG63 and SaOS-2 are recognised to express a variety of metabotropic and ionotropic glutamate receptors including NMDA receptors and glutamate has been shown to cause increases in $[Ca^{2+}]_i$ in these cells (Gu et al., 2002; Laketić-Ljubojević et al., 1999). The authors recognise that these $[Ca^{2+}]_i$ increases could be effected by any glutamate receptor type, but report that 1 mM extracellular Mg^{2+} caused partial channel block and changed the I/V curve shape (Gu et al., 2002) and in $0-Mg^{2+}$ extracellular solution glutamate caused $[Ca^{2+}]_i$ to rise. Laketić-Ljubojević et al. (1999) similarly report complete inhibition of $[Ca^{2+}]_i$ increase with 3 mM extracellular Mg^{2+}. Blockade by Mg^{2+} ions is a recognised distinguishing characteristic of NMDA receptors which differs from other

glutamate receptor types: therefore $[Ca^{2+}]_i$ rises shown by Gu and Laketić-Ljubojević were probably due to activation of NMDA receptors.

The Locke solution used to bathe the MG63 cells for experiments in this thesis contained 2 mM $MgCl_2$. It is likely that the lack of calcium responses to glutamate was therefore due to NMDA receptor Mg^{2+} blockade. If this is true, it also suggests that other glutamate receptor types express at low levels or not at all.

6.4.4 KCl-induced $[Ca^{2+}]_i$ increases

Application of 50 mM KCl to the bath, in order to depolarise the cell membrane, caused $[Ca^{2+}]_i$ to increase. It should be noted that depolarisation here simply means that cell membrane potential becomes more positive than the resting membrane potential, and in inexcitable cells there is no threshold potential, after which in excitable cells an action potential would follow. The mechanism of depolarisation by external KCl application and the resultant increased intracellular Ca^{2+} signal can be explained due to a disruption of the Gibbs-Donnan equilibrium. There is a resultant change in the Nernst potential of the membrane for K^+, from -85.5 mV $([5]_o/[140]_i)$ to -23.9 mV $([55]_o/[140]_i)$. This is a clear positive shift in the membrane potential, and therefore the membrane is said to be depolarised.

In turn, cell membrane depolarisation causes voltage-dependent Ca^{2+} channels (VDCCs) to open, and this is the presumed route of Ca^{2+} entry into the

osteoblasts, leading to increased intracellular Ca^{2+} concentration as shown by the experimental data (Figures 6.3, 6.4 and 6.7). Although the expression of VDCCs is said to define an excitable cell (Hille, 2001), evidence is emerging for lower levels of expression of members of this ion channel group in inexcitable cells, recently including skeletal tissue (Shao *et al.*, 2005; Mancilla *et al.*, 2007) and osteoblasts (Cox, personal communication, 2007).

In the data presented in this thesis, the KCl-induced $[Ca^{2+}]_i$ increase was used as a positive control to show that the fluo-3 dye was present and able to chelate calcium in the cells in which $[Ca^{2+}]_i$ was not changed by other drugs. A clear $[Ca^{2+}]_i$ response is seen after application of KCl in Figure 6.7, whereas a much smaller $[Ca^{2+}]_i$ response is seen in Figure 6.3 but is nevertheless detectable. In Figure 6.4 the fluorescence vs. time graph appears to show a decrease in $[Ca^{2+}]_i$ on application of KCl but this is due to cell shrinkage which reduced the fluorescing region of the odd area set (OAS) measured and intracellular free calcium actually increased as shown in Figure 6.4C. The cell shrinkage observed is probably due to a hyperosmotic extracellular solution and a cell membrane that is relatively impermeable to Cl^-, resulting in water passing from the cytosol into the extracellular environment, as described by Boyle and Conway (1941) and Hodgkin and Horowicz (1959), according to:

$$[K]_o[Cl]_o = [K]_i[Cl]_i$$

6.4.5 Possible consequences of acid-potentiation of TRPV1 activation on bone *in vivo*

The effects of acid pH on osteoblasts and osteoclasts are known to be opposite. Reduction of pH from 7.4 to < 7.0 effectively switches osteoclasts on, with maximum bone mineral absorption taking place by osteoclasts at around pH 6.9 (Arnett, 2007). At the same time, acid conditions cause osteoblasts to be switched off – growth, differentiation and mineralisation are all reduced or inhibited. Arnett (2007) believes that TRPV1 is a candidate for H^+ ion detection and has a regulatory role in bone metabolism. In this chapter, capsaicin-induced $[Ca^{2+}]_i$ increases in MG63 cells are shown to be potentiated by acidic conditions, and therefore TRPV1 activation may be important as a switch for osteoblast growth and function.

6.4.6 Chapter conclusions and future work

The chapter hypothesis that TRPV1 channel activation by capsaicin induces a Ca^{2+} signal in osteoblasts, and that this signal can be potentiated by protons, is therefore proven correct. TRPV1 channels are proven for the first time to be expressed and functional as Ca^{2+}-permeant ion channels in human osteosarcoma cells, and presumably also in primary human osteoblasts.

The data presented here are a beginning in the understanding of the Ca^{2+} signal evoked by TRPV1 activation in osteoblasts by capsaicin, and the potentiation of this channel by acidic extracellular conditions, where the apparent channel expression is the full-length TRPV1 and the dominant negative splice variant

TRPV1b. There is plenty of scope for a more comprehensive study in this area,

but some of the more immediate questions that require future attention include:

- Do other TRPV1 agonists such as resiniferatoxin or anandamide evoke the Ca^{2+} signal in osteoblasts, and does an acidic extracellular environment potentiate the $[Ca^{2+}]_i$ signal with these agonists?

- Is the capsaicin-induced (and potentially other TRPV1 agonists-induced) $[Ca^{2+}]_i$ increase blocked by TRPV1 antagonists, such as capsazepine and SB366791?

- Can the putative endogenous agonist anandamide and antagonist adenosine effectively mimic the effects of capsaicin and a TRPV1 antagonist on the Ca^{2+} signal?

- Can further increases in proton concentration, by further decreases in extracellular pH, activate the TRPV1 channel alone (i.e. no agonists) to induce a $[Ca^{2+}]_i$ increase?

- And importantly, is the Ca^{2+} entry route via TRPV1 alone, or do other Ca^{2+}-permeable channels (e.g. VDCCs) contribute? Establish using antagonists of other Ca^{2+} cha-nnels, such as dihydropyridines.
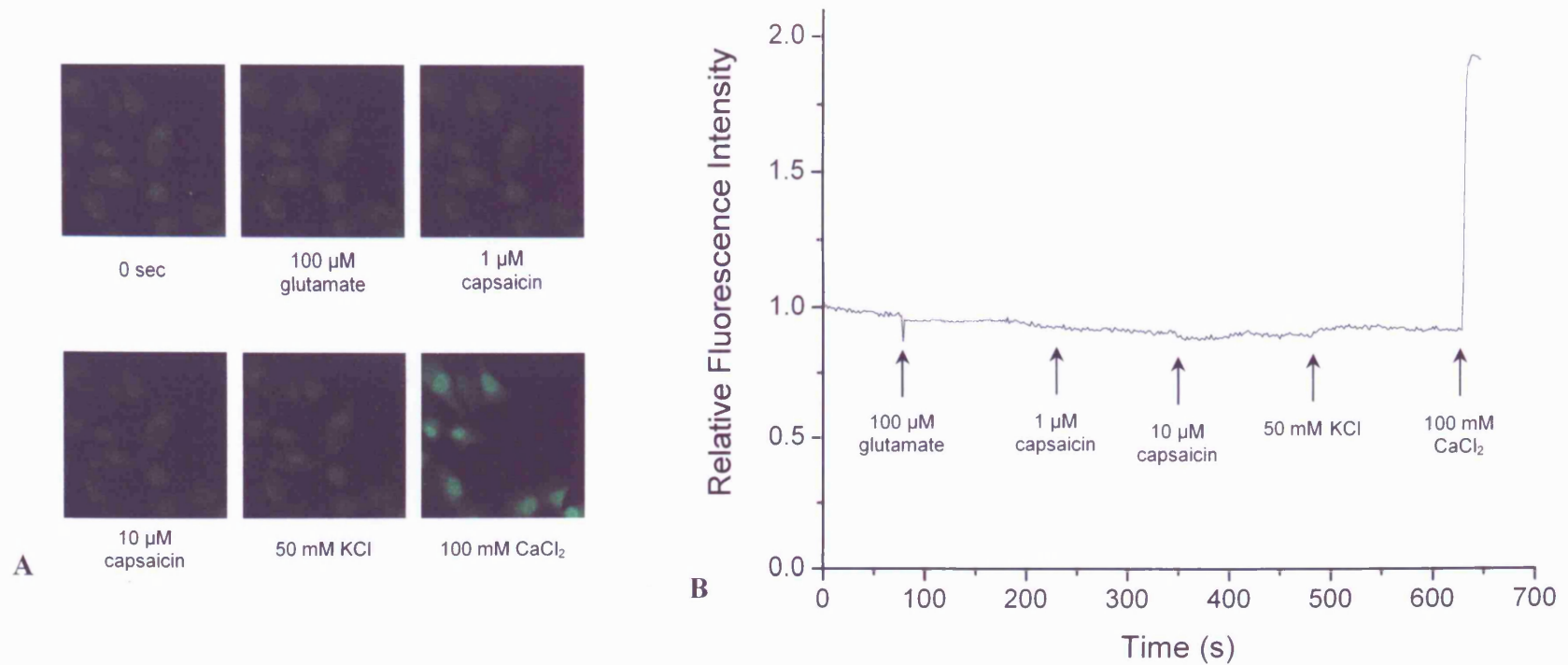
Figure 6.3 **Glutamate and capsaicin do not cause $[Ca^{2+}]_i$ to increase at physiological pH. (A)** As also observed in figure 6.7, glutamate does not increase $[Ca^{2+}]_i$ and $1 - 10 \ \mu M$ capsaicin also does not detectably increase $[Ca^{2+}]_i$. Application of 50 mM KCl causes a slight increase in fluorescence in some cells, whereas 100 mM $CaCl_2$ causes all cells to fluoresce brightly. **(B)** Averaged relative fluorescence intensity data from all cells showing effects of drug challenges on $[Ca^{2+}]_i$.
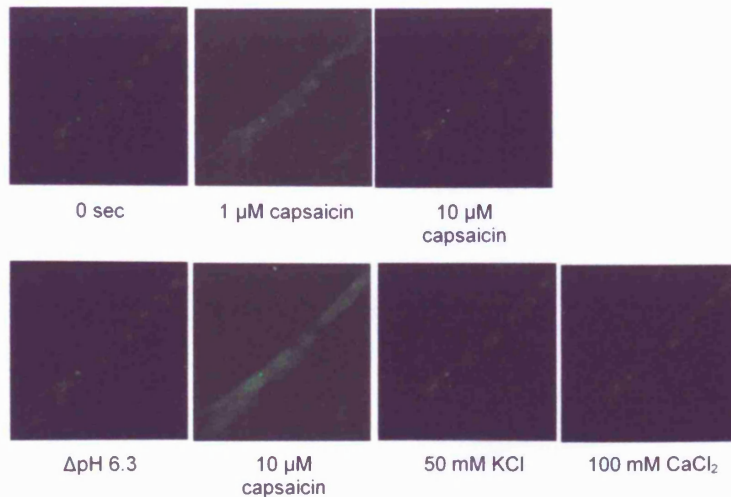
A

Figure 6.4 **Decreasing pH potentiates $[Ca^{2+}]_i$ increases due to capsaicin. (A)** At pH 7.4, 1 μM capsaicin causes a small increase in fluorescence. At pH 6.3 10 μM capsaicin causes a much larger increase. **(B)** Averaged RFI data showing that the $[Ca^{2+}]_i$ increase due to capsaicin cannot be repeated by a higher concentration at the same pH, but after reducing pH to 6.3, a much larger calcium response is seen to 10 μM capsaicin. The drop in fluorescence on application of KCl is due to cell shrinkage as demonstrated in **(C)** where shrinkage can be seen in the fluorescence images, and a $[Ca^{2+}]_i$ increase is seen if the OAS is decreased to fit the shrunken cell as highlighted in red.

B

C
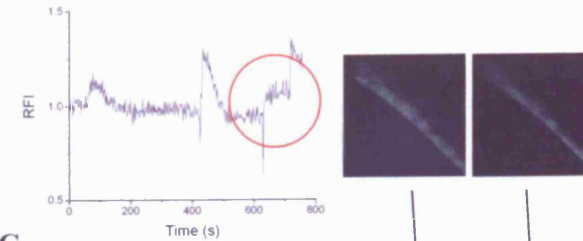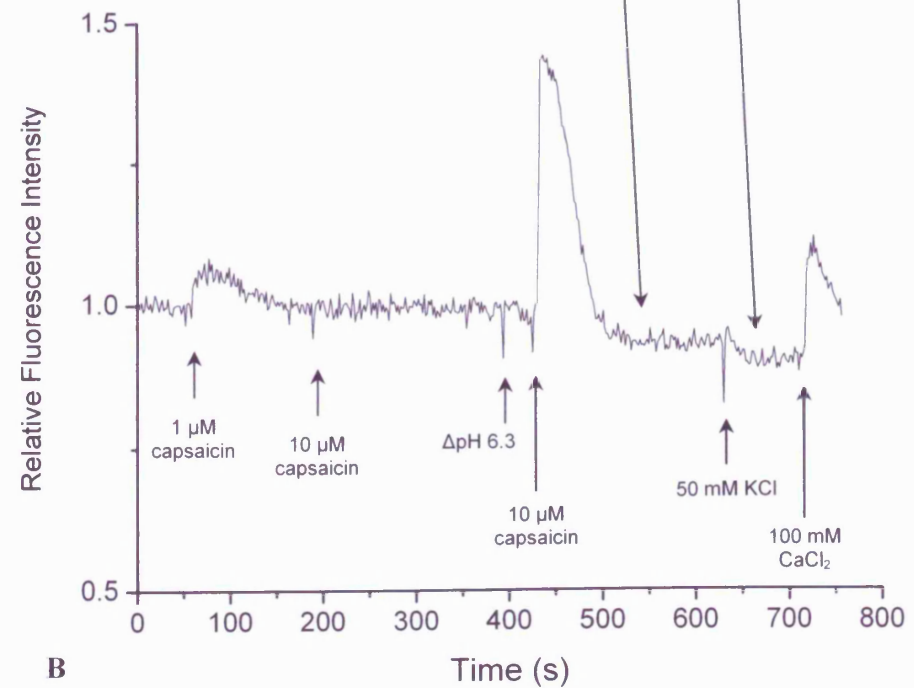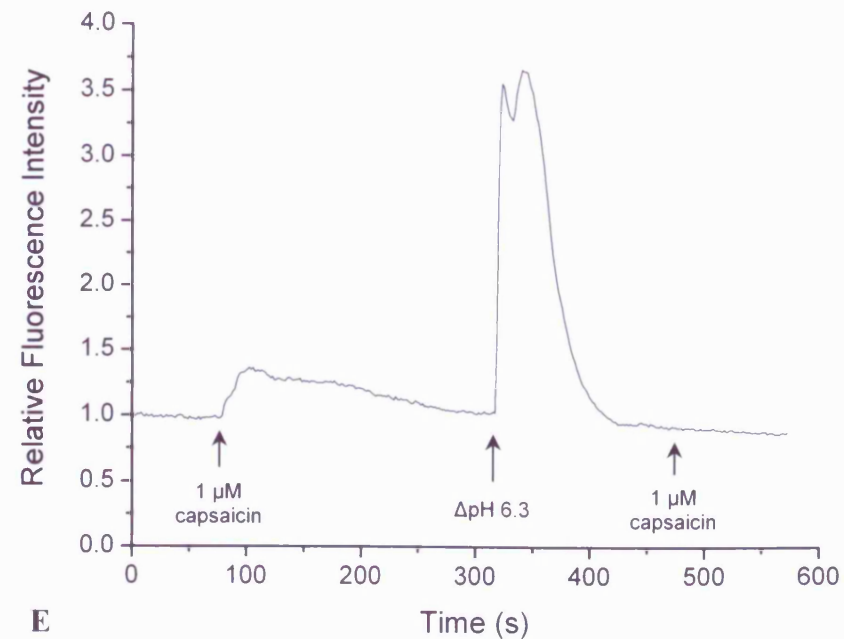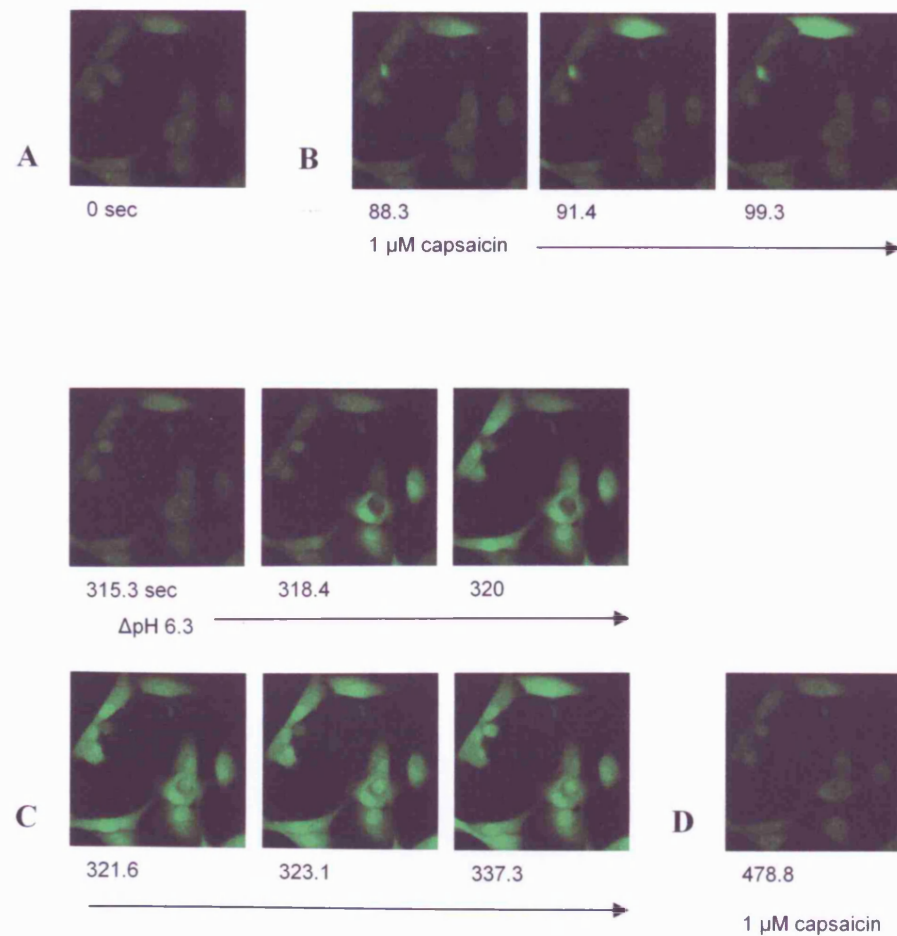
Figure 6.5 **Decreasing pH in the presence of capsaicin causes a large $[Ca^{2+}]_i$ increase. (A)** Time frames (with seconds shown) show initial fluorescence, **(B)** two cells responding to 1 μM capsaicin at pH 7.4, **(C)** all cells responding in the presence of capsaicin when pH is reduced to 6.3 and **(D)** that further capsaicin challenges have no effect. **(E)** Averaged RFI values for all cells showing the above plotted against time.
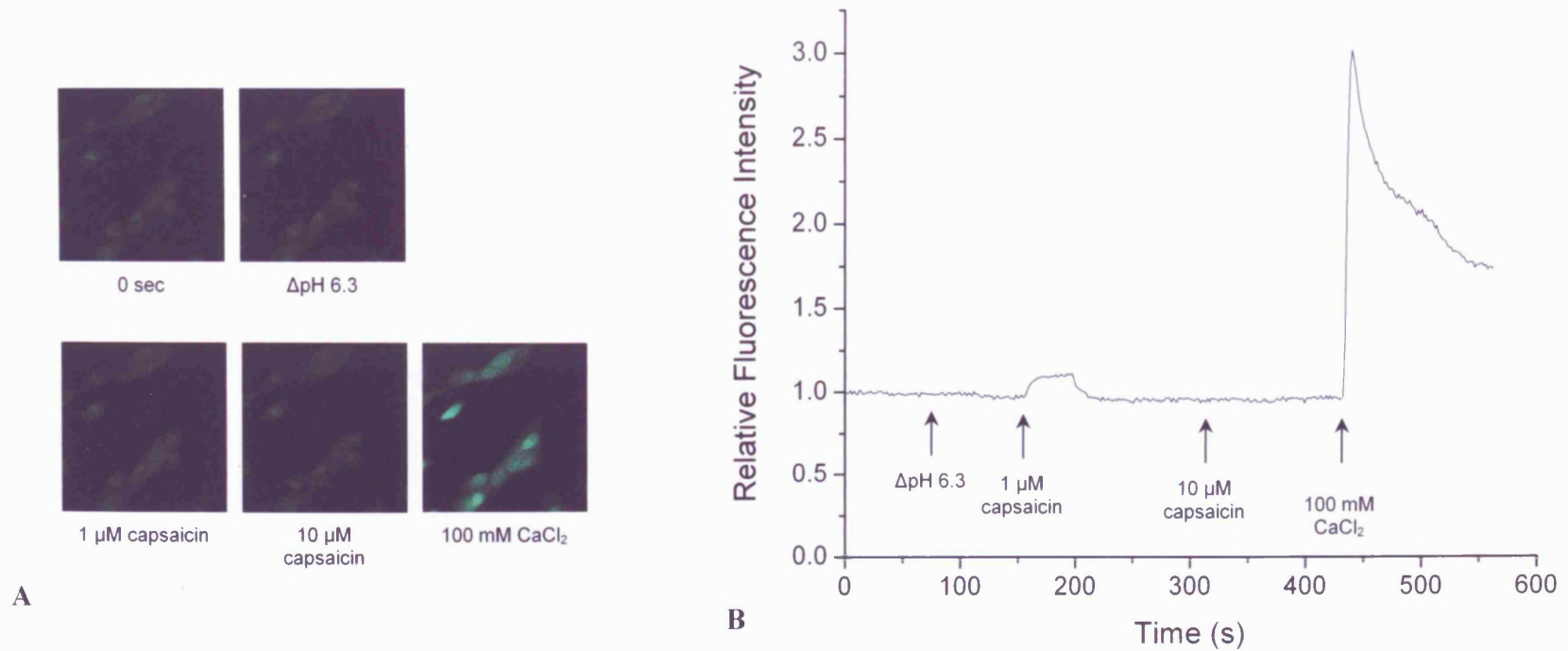
Figure 6.6 **Protons do not increase [Ca²⁺]ᵢ alone, but potentiate calcium responses to capsaicin**. (A) Fluorescence imaging frames showing no [Ca²⁺]ᵢ increase after reducing pH to 6.3, but a slight increase at this pH when 1 μM capsaicin is applied. The capsaicin-induced [Ca²⁺]ᵢ increase cannot be repeated even with 10 μM concentration after the initial response during the time recorded. (B) Averaged RFI vs. time plot showing the above.
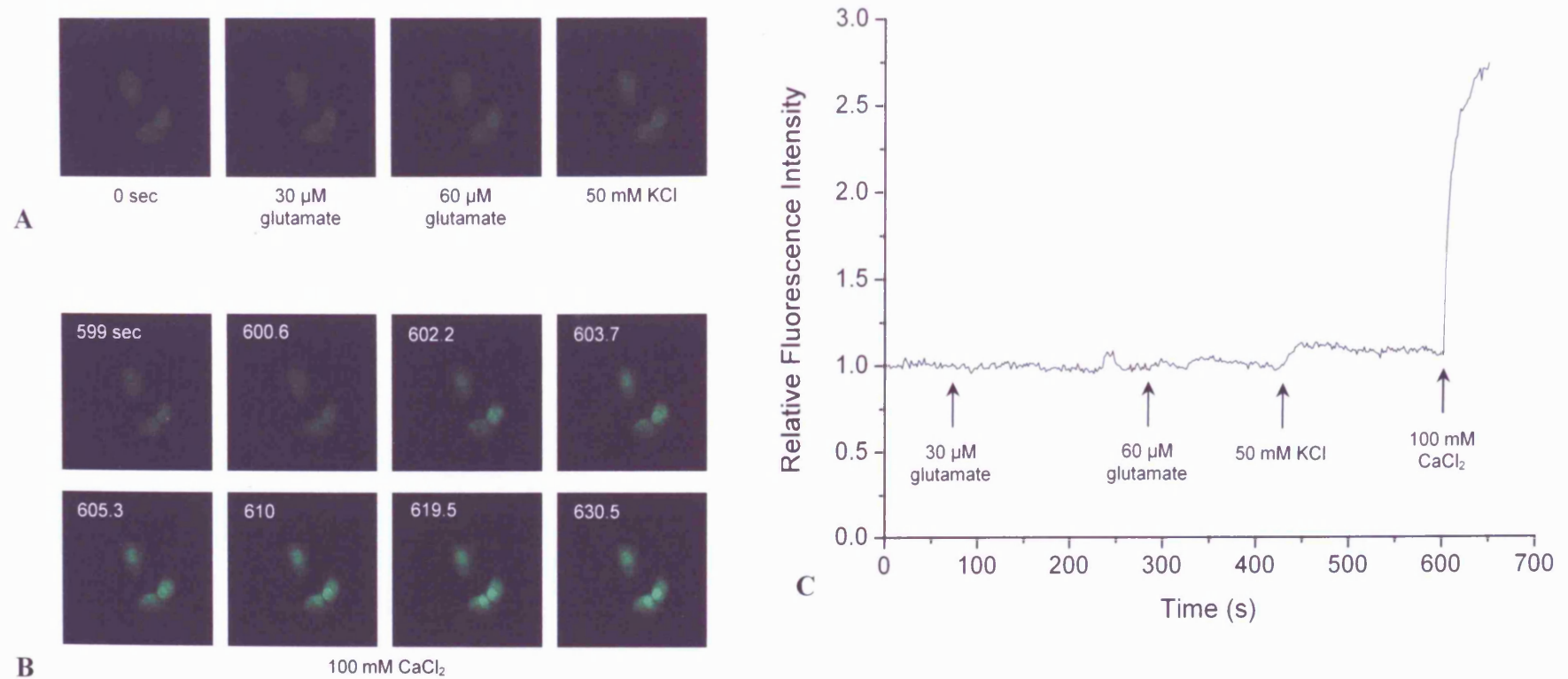
Figure 6.7 **No calcium response to glutamate challenge in MG63 cells**. (A) Neither 30 μM glutamate nor 90 μM (total concentration) caused a detectable change in $[Ca^{2+}]_i$. 50 mM KCl caused an small increase in $[Ca^{2+}]_i$ which can be seen as a slight increase in fluorescence. (B) Eight frames showing the large increase in fluorescence caused by application of 100 mM $CaCl_2$. The increase is rapid and uniform (both cytoplasm and nucleus light up together). (C) Averaged relative fluorescence intensity data from all cells showing effects of drug challenges on $[Ca^{2+}]_i$. Times are shown for each frame in seconds.

CHAPTER 7:
GENERAL DISCUSSION & CONCLUSIONS

7 GENERAL DISCUSSION & CONCLUSIONS

7.1 Discussion

The evolution of ion channels is thought to have begun soon after the encapsulation of primitive life forms by a phospholipid barrier, separating the inner workings of the cell from the surrounding environment. The incarceration of the organelles in this manner, although advantageous as a collective and protective consequence, prevented the transport of ionised particles into or out of the cell. Therefore, mechanisms evolved to overcome this problem, allowing the passage of selected ionised particles across the membrane. The pioneering, Nobel prize-winning work by Hodgkin and Huxley (1952) demonstrating their theory of the electrical mechanism of nerve conduction, showed the importance of ionic exchange across cell membranes, and although carrier proteins were originally the favoured theory of ion transport, ion channels were confirmed as the accepted mechanism following the establishment of Neher and Sakmann's patch-clamp technique (Neher & Sakmann, 1976; Hamill *et al.*, 1981). It is now recognised that mammalian ion channel homologues stretch far back in the evolutionary tree, with *Caenorhabditis elegans* expressing voltage-gated

Na^+ and K^+ channels, TRP channels, mechanosensitive Cl^- channels, and many other ion channels homologous to those found in much more recently evolved organisms. Mammalian cells of all types have been shown to express a huge variety of ion channels, which are not necessarily limited to obvious functions: e.g. voltage-gated channels that have a clear purpose in excitable cells, such as the conduction of action potentials in neurons, are also to be found in many non-excitable cells where their purpose is less easily identifiable in the first instance. As the expression of so many ion channels is conserved in such a diverse range of tissues and cells, then the real question turns to their purpose in these systems. If channel proteins are found to be present, are they simply redundant entities awaiting the brokers yard of evolution, or are they fully functional either as ion channels or as enzymes or coupling proteins, for example, serving an important role in cellular processes?

This Thesis picks up on that very question and has attempted to firstly confirm the expression of a selection of ion channels (K^+ and TRP channels) in human osteoblastic cells, and then to go some way towards characterising the channels and testing the hypothesis that the proteins have key functions in these cells.

The osteoblast cell-lines and primary osteoblast cultures were new to the laboratory. However, the cells were found to be hardy and doubled at an approximate rate of once every 24 hours, and when cell husbandry protocols were established and optimised the routine maintenance of these cells became straightforward. The expressions of maxi-K channel subunits α and $\beta 1-4$

(KCNMA1 and KCNMB1-4), K_{ATP} subunits $K_{IR}6.1$, $K_{IR}6.2$, SUR1 and

SUR2B, and TRP channels TRPV1 and TRPM7, were confirmed at messenger

level in human MG63 and SaOS-2 osteosarcoma cells and primary osteoblasts.

The expressions of TRPV5, TRPV6 and TRPM8, however, were not

ubiquitous in the osteoblasts, or across a panel of prostate cancer and breast

cancer cells, indicating that these proteins have functions that are more specific

to different cell-types or to different stages in cell differentiation. These

expression data laid the foundations for subsequent characterisation of the

ubiquitously expressed channels in human osteoblasts using the patch-clamp

technique, and raised the question stated above on the possibility of functional

roles in osteoblasts.

The osteoblastic cells were amenable to single-channel patch-clamping, and

high-resistance seal formation was readily achievable. Patch-clamping showed

that MG63 and SaOS-2 cells expressed a large-conductance channel with the

hallmarks of the K_{Ca} channel of large conductance, known as maxi-K,

consistent with the RT-PCR data. The channels were large conductance (> 180

pS), activated with depolarising voltage, were calcium-activated (as evidenced

by glutamate application), displayed voltage-dependent deactivation at large

depolarising potentials, and were blocked by TEA. The powerful and highly-

sensitive patch-clamp technique illustrated that this channel-type, previously

identified in osteoblasts as having neuronal type-II characteristics (Moreau *et

al.*, 1996), was found to be in abundance in MG63 and SaOS-2 cells, often with

5 or 6 channels per patch. Importantly, this Thesis describes some of the first

examples of work characterising the maxi-K channel in primary human osteoblasts, which also have an abundance of maxi-K channels in the plasma membrane. The data presented show that MG63 and SaOS-2 cells are good models for primary osteoblasts in terms of maxi-K channel character and expression. This work also provides what is probably the first maxi-K channel kinetic data in osteoblasts, showing that voltage-activation increases open probability by increasing open burst duration rather than simply increasing burst number.

Possible roles for the maxi-K channel in osteoblasts were not systematically explored in this Thesis, but work elsewhere in the laboratory has provided clues that some pharmacological compounds which target maxi-K, such as the plant alkaloid tetrandrine, have putative proliferative effects in osteoblasts (Li *et al.*, 2007 abstract). Excitingly, the K^+ channel blocker tetraethylammonium (TEA) appears to increase osteoblast mineralisation in SaOS-2 cells and HOB-c primary osteoblasts (Evans, B.A.J., 2008 and Li, B., 2008, personal communications), although it is not known if this effect is due to maxi-K blockade or another target of this promiscuous ligand. Finally, there are emerging data that the specific maxi-K channel blocker iberiotoxin may also have an enhancing effect on osteoblast mineralisation (Li, 2008, personal communication).

The K_{ATP} channels have not been electrophysiologically characterised in this Thesis, but the proliferative effects of pinacidil may indicate that these

channels have an important functional role in osteoblasts. The mechanism of this proliferative effect is untested here, but if it is indeed due to K_{ATP} channel activation, as is likely, then either membrane potential change or cell volume change are two often-cited hypotheses. K^+ channels in the plasma membrane are well recognised to regulate cell division in many, if not all, cell types (Dubois *et al.*, 1993; Nilius & Droogmans, 1993; Wonderlin & Strobl, 1996) by one of the two hypotheses suggested above: in the membrane potential hypothesis K^+ channel inhibitors cause electrochemical rundown and Ca^{2+}-entry decreases, preventing mitogenesis, whereas in the cell volume hypothesis K^+ channel modulators affect ion transport across the membrane and therefore the osmotic potential of the cell, with volume changes resulting in intracellular concentration changes (of other components) and cytoskeletal reorganisation. It is likely, of course, that the mechanisms described in these two hypotheses are not separate but linked, as a change in one will almost certainly affect the other. But whatever the mechanism, the effect of pinacidil-induced osteoblast proliferation is interesting and warrants further investigation in future work (see below).

Of the TRP channels identified in osteoblasts by RT-PCR, the TRPV1 channel was selected for further investigation due to the advantage of previously described channel pharmacology. However, the patch-clamp technique did not prove fruitful when attempting to find and characterise the TRPV1 channel in osteoblasts, despite its apparent expression at mRNA level in the MG63 cells. Generally, the electrophysiology data collected and reported here do not

support the hypothesis that TRPV1 proteins are functional as channels in osteoblasts. It is worth noting here that attempts were made in this thesis to find *native* TRPV1 channels in osteoblasts, without attempting up-regulation or transfection of the channel. In contrast, previous reports characterising the TRPV1 channel electrophysiology by other groups have been conducted in either excitable cells (particularly dorsal root ganglionic cells) (e.g. Caterina *et al.*, 1997; Raisinghani *et al.*, 2005) where TRPV1 is highly expressed, or TRPV1-transfected non-excitable cells with high channel expression levels (e.g. Hui *et al.*, 2003; Jung *et al.*, 2002). Of course, it could be argued in hindsight that the choice of the single-channel technique was perhaps less appropriate than the macroscopic alternative, which is whole-cell membrane current recording. The advantage of this would be that ionic currents flowing through the entire population of TRPV1 channels in the plasma membrane could be recorded, solving the problem of having to find individual TRPV1 channel currents. As a possible explanation of the single-channel negative findings, further RT-PCR experiments identified for the first time in any bone cells the expression of the dominant negative splice variant TRPV1b, which markedly reduces the affinity of the channel for capsaicin (and possibly other similar ligands). Although the co-expression of TRPV1b with TRPV1 in other cells does not appear to prevent ion channel function (only activation by certain ligands is affected), the effect in osteoblasts is unknown.

In contrast to the patch-clamp data, the Ca^{2+} fluorescence imaging experiments show that TRPV1 is functional as an ion channel in the plasma membrane, and

is involved in Ca^{2+} signalling within osteoblastic cells. Although it is possible that another mechanism for Ca^{2+} entry may be present, for example TRPV1-activation of plasma membrane Ca^{2+} channels by coupling or downstream signalling, evidence points to Ca^{2+} entry via TRPV1 channels. The capsaicin-induced $[Ca^{2+}]_i$ signals were desensitised on repeated exposure to capsaicin, and were pH sensitive with greater fluorescence (indicating higher $[Ca^{2+}]_i$ levels) in more acidic conditions. In this way, the responses displayed some of the hallmarks of the TRPV1 channel and these data fit with previous reports of capsaicin-induced calcium signals in other cell-types (e.g. Puntambekar *et al.*, 2004). However, TRPV1 channels are normally associated with the detection of pain and heat in sensory pathways, so what might be the role or roles of TRPV1 channels in osteoblasts?

One very exciting discovery in this Thesis is that TRPV1 may be involved in osteoblast differentiation, regulating the pathway taken by osteoblastic precursor cells to either mature osteoblasts or to adipocytes. Stimulation of the TRPV1 channel by various agonists prevented the differentiation of the osteoblastic precursors into adipocytes, despite promotion of the adipocytic route with adipocyte-differentiation medium. TRPV1 antagonists did not prevent adipocyte differentiation, and were able to block the anti-adipogenic effects of the TRPV1 agonists. The mechanism of this function is presumably linked with the Ca^{2+} entry following TRPV1 channel activation, which must interrupt the intracellular signalling processes leading to adipocyte differentiation. These very interesting findings begin to fill in the gap created

by the works of Thompson *et al.* (1998) who reported on osteoblastic precursor differentiation to adipocytes and Zhang *et al.* (2008) who reported that TRPV1 stimulation could prevent adipogenesis from pre-adipocyte cells. These findings fit into the osteoporosis story very nicely: osteoporosis has long been associated with increased adipocyte content of the bones, presumably at the expense of osteoblasts via this very differentiation pathway. Therefore, this is an exciting preliminary finding which potentially provides a lead for future drug development and treatment of osteoporosis.

7.2   Recommendations for further work

The findings presented in this thesis raise some interesting questions and provide several new avenues for further research. The following is a series of suggestions and ideas for future investigation, which due to the constraints of time were not possible to pursue here.

The role of K^+ channels in osteoblasts

Given the preliminary data presented here, a more complete investigation into the characterisation and roles of K^+ channels in osteoblasts is recommended. In particular, the abundance of the maxi-K channel in osteoblasts implies an important functional role, which surely begs to be discovered. However, pertinent to this implied functional importance is the apparent lack of maxi-K activity at rest in these cells. It would perhaps be fair to argue that as these cells are not excitable, and therefore probably do not undergo large fluctuations in plasma membrane potential, maxi-K would remain inactive or 'dormant' in the

plasma membrane being superfluous for use as an excitatory braking mechanism for Ca^{2+} influx following action potential firing, which is an important regulatory mechanism in neuronal cells, but of course not required in non-excitable cells. Therefore, if maxi-K is presumed not to be activated by membrane depolarisation in osteoblasts, is there another activating mechanism? Can intracellular Ca^{2+} levels rise high enough to activate the channel alone? Or maybe the maxi-K channel has a functional role in osteoblasts that does not depend on channel gating by Ca^{2+} or voltage? For example, the long cytoplasmic C-terminus of the α-subunit may have folds or loops which confer enzymatic activity, leading to active substrates. Furthermore, the maxi K channel in osteoblasts needs to be characterised in terms of β subunit composition. Whilst this Thesis shows that all four known β subunit messages are expressed, the translated protein composition that locates to the plasma membrane is unknown, but ultimately determines the pharmacology of the channel. Sausbier et al. (2004) describe a $BK_{Ca}^{-/-}$ mouse model, which would provide useful data on the phenotypic consequences of the loss of maxi-K function in bone, and further down the line a 'conditional knockout' of maxi-K from bone, meaning a tissue-specific gene deletion, would be a very powerful tool for determining maxi-K function in bone.

Further work is also suggested on the putative proliferative role for K_{ATP} channels in osteoblasts, as demonstrated in this Thesis with pinacidil, using other similar KCOs such as minoxidil and nicorandil which are in clinical use (see above for suggested mechanisms of K_{ATP}-regulated proliferation). A full

characterisation of K_{ATP} channel electrophysiology in these cells is also required, and again, knowledge of the channel-protein subunit composition would be useful for pharmacological characterisation.

TRPV1 channel characterisation in osteoblasts

It is recommended that future work concentrating on characterising the TRPV1 channel in osteoblasts should either use the whole-cell patch-clamp technique to record macroscopic membrane currents, or use TRPV1-transfected osteoblasts so that the density of TRPV1 channels in the plasma membrane is high and therefore allowing successful single-channel patch-clamp recording. In addition, Western blotting and immunocytochemistry should be carried out to search for TRPV1 and splice-variant protein expression in the osteoblast plasma membranes, and as the expression of the TRPV1b splice variant in other cells putatively limits the use of pharmacological tools, the cells/membrane patches should be subjected to heat (> 42 °C) as an activator of the TRPV1 channel. Whichever methods are used, the electrophysiological characterisation of TRPV1 and its splice variant(s) are an important part of the understanding of the channel in osteoblasts. The Ca^{2+} signalling experiments, which served here to show that TRPV1 is able to carry calcium currents across the plasma membrane, require further work to help in establishing a more complete picture of the pharmacology of the channel in osteoblasts. As discussed above, Ca^{2+} signalling presumably plays a role in TRPV1-regulation of osteoblast differentiation, but it is likely that Ca^{2+} entry via TRPV1 has other roles in these cells, for example in proliferation or secretion.

The role of TRPV1 in differentiation

Although it is fair to say that the role postulated here for TRPV1 in osteoblastic differentiation is based on somewhat tentative findings, given the small number of experiments carried out, the findings are nevertheless very interesting and provide a potentially useful lead for further investigation. Such work should concentrate on further repeats of the same, perhaps with longer periods of treatments to try to enhance the inhibitory effect of the TRPV1 agonists. In addition, quantitative measurements of lipid production would enable graphic representation of the results, and allow the data to be tested for statistical significance. Taking a step further, a carefully planned series of experiments using an *in vivo* model for osteoporosis which displayed increased adipocyte content of the bone, would perhaps serve to show whether adipocyte differentiation is decreased in individuals treated with TRPV1 agonists, and importantly whether bone mineral density is higher in these individuals than in controls or those treated with TRPV1 antagonists. The use of tissue-specific TRPV1$^{-/-}$ animals, with the knockout targeted at bone, would serve as a particularly useful tool in determining the true *in vivo* role of this channel in bone and possibly highlight any pathophysiological consequences of TRPV1 modulation.

7.3 Conclusions

In conclusion, the findings of this thesis confirm the expression of maxi-K, K_{ATP}, TRPV1 and TRPM7 channels in osteoblasts and go some way towards

testing the hypothesis that these ion channels have functional roles in osteoblasts, as reiterated by the points below.

- RT-PCR confirms the expression of maxi-K channel α and $\beta1$-4 subunits, K_{ATP} channel $K_{IR}6.1/6.2$ and SUR1/2B subunits, TRPV1 and TRPM7 channel subunits.

- Electrophysiology further confirms the expression of a large-conductance ($>$ 180 pS) Ca^{2+}- and voltage-activated channel which displays the characteristic electrophysiological hallmarks of the maxi-K channel. This channel is abundantly expressed in the plasma membranes of MG63 and SaOS-2 osteosarcoma cells and HOB-c human primary osteoblasts, and activated with depolarised voltages. Channel kinetic data shows that voltage activation increases open burst length rather than increasing the number of shorter open bursts.

- The K_{ATP} channel opener pinacidil significantly promotes proliferation of osteoblastic cells in culture, and this effect is not blocked by glibenclamide or tolbutamide.

- Despite the lack of electrophysiological evidence for TRPV1 activity in osteoblasts, the Ca^{2+} fluorescence imaging data shows that the TRPV1 channel carries Ca^{2+} currents into the cell, and that this Ca^{2+}-entry is capsaicin and pH sensitive, and becomes desensitized to capsaicin following multiple exposures.

- RT-PCR shows that TRPV1 and the splice-variant TRPV1b are expressed at messenger level in human primary osteoblasts and osteosarcoma cell

lines, and therefore this may result in reduced channel sensitivity to capsaicin and protons.

- 7F2 osteoblastic precursor cells treated with adipocyte-inducing medium undergo complete differentiation into adipocytes, rather than mature mineralising osteoblasts. Stimulation of these cells with the TRPV1 agonists capsaicin, resiniferatoxin or the cannabinoid anandamide prevents differentiation along the adipocyte pathway, whereas TRPV1 antagonists capsazepine and SB366791 themselves do not prevent adipogenesis, but are able to antagonise the effects of the TRPV1 agonists. This implies an important functional role for the TRPV1 channel in osteoblastic differentiation.

8   APPENDICES

APPENDICES

8.1 Publications relevant to this thesis

Peer-reviewed meeting abstracts

Li, B., **Henney, N.C.**, Evans, B.A.J. & Wann, K.T. (2007) Large conductance potassium channel in human osteoblast cells. *Proceedings of the British Pharmacological Society* at http://bps.conference-services.net/viewPDF.asp?conferenceID=1175&abstractID=177854

Henney, N.C., Evans, B.A.J., Campbell, A.K. & Wann, K.T. (2007) TRP channels are both present and functional in human osteoblast-like cells. *J Bone Miner Res.* 22(suppl 1): T022

Li, B., **Henney, N.C.**, Evans, B.A.J., Reviriego, P., Campbell, A.K. & Wann, K.T. (2007) BK channels in human osteoblast-like cells - properties and function. *J Bone Miner Res.* 22(suppl 1): W045

Henney, N.C., Evans, B.A., Campbell, A.K. & Wann, K.T. (2007) Make no bones about TRP channels. *Proc Life Sciences.* PC231

Li, B., **Henney, N.C.**, Evans, B.A., Reviriego, P., Campbell, A.K. & Wann, K.T. (2007) BK channels are expressed and functional in human osteoblast-like cells. *Proc Life Sciences.* PC162

Henney, N.C., Li, B., Evans, B.A.J., Hall, E.J. & Wann, K.T. (2006) Potassium channel subunits in human osteoblast-like cells. *J Bone Miner Res.* 21(7): 1169

8.2 Cell culture media formulae

MINIMAL ESSENTIAL MEDIUM (MEM) ALPHA

COMPONENTS	MW	Concentration (mg/L)
Amino Acids		
Glycine	75	50
L-Alanine	89	25
L-Arginine	211	105
L-Asparagine-H_2O	150	25
L-Aspartic acid	133	30
L-Cysteine hydrochloride-H_2O	176	100
L-Cystine	313	31
L-Glutamic Acid	147	75
L-Glutamine	146	292
L-Histidine	155	31
L-Isoleucine	131	52.4
L-Leucine	131	52
L-Lysine	183	73
L-Methionine	149	15
L-Phenylalanine	165	32
L-Proline	115	40
L-Serine	105	25
L-Threonine	119	48
L-Tryptophan	204	10
L-Tyrosine	181	36
L-Valine	117	46
Vitamins		
Ascorbic Acid	176	50
Biotin	244	0.1
Choline chloride	140	1
D-Calcium pantothenate	477	1
Folic Acid	441	1
Niacinamide	122	1
Pyridoxal hydrochloride	204	1
Riboflavin	376	0.1
Thiamine hydrochloride	337	1
Vitamin B12	1355	1.36
i-Inositol	180	2
Inorganic Salts		
Calcium Chloride ($CaCl_2$-$2H_2O$)	147	264
Magnesium Sulfate ($MgSO_4$) (anhyd.)	120	97.67
Potassium Chloride (KCl)	75	400
Sodium Bicarbonate ($NaHCO_3$)	84	2200
Sodium Chloride (NaCl)	58	6800
Sodium Phosphate monobasic (NaH_2PO_4-$2H_2O$)	156	158
Other Components		
D-Glucose (Dextrose)	180	1000
Lipoic Acid	206	0.2
Phenol Red	376.4	10
Sodium Pyruvate	110	110

RPMI 1640 MEDIUM

COMPONENTS	MW	Concentration (mg/L)
Amino Acids		
Glycine	75	10
L-Arginine	174	200
L-Asparagine	132	50
L-Aspartic acid	133	20
L-Cystine	240	20
L-Glutamic Acid	147	20
L-Glutamine	146	300
L-Histidine	155	15
L-Hydroxyproline	131	20
L-Isoleucine	131	50
L-Leucine	131	50
L-Lysine hydrochloride	183	40
L-Methionine	149	15
L-Phenylalanine	165	15
L-Proline	115	20
L-Serine	105	30
L-Threonine	119	20
L-Tryptophan	204	5
L-Tyrosine	181	20
L-Valine	117	20
Vitamins		
Biotin	244	0.2
Choline chloride	140	3
D-Calcium pantothenate	477	0.25
Folic Acid	441	1
Niacinamide	122	1
Para-Aminobenzoic Acid	137	1
Pyridoxine hydrochloride	206	1
Riboflavin	376	0.2
Thiamine hydrochloride	337	1
Vitamin B12	1355	0.005
i-Inositol	180	35
Inorganic Salts		
Calcium nitrate ($Ca(NO_3)_2$ $4H_2O$)	236	100
Magnesium Sulfate ($MgSO_4$-$7H_2O$)	246	100
Potassium Chloride (KCl)	75	400
Sodium Bicarbonate ($NaHCO_3$)	84	2000
Sodium Chloride (NaCl)	58	6000
Sodium Phosphate dibasic (Na_2HPO_4) anhyd.	142	800
Other components		
D-Glucose (Dextrose)	180	2000
Glutathione (reduced)	307	1
Phenol Red	376.4	5

DULBECCO'S MODIFIED EAGLE MEDIUM (D-MEM)

COMPONENTS	MW	Concentration (mg/L)
Amino Acids		
Glycine	75	30
L-Arginine hydrochloride	211	84
L-Cystine 2HCl	313	63
L-Glutamine	146	580
L-Histidine hydrochloride-H2O	210	42
L-Isoleucine	131	105
L-Leucine	131	105
L-Lysine hydrochloride	183	146
L-Methionine	149	30
L-Phenylalanine	165	66
L-Serine	105	42
L-Threonine	119	95
L-Tryptophan	204	16
L-Tyrosine	181	72
L-Valine	117	94
Vitamins		
Choline chloride	140	4
D-Calcium pantothenate	477	4
Folic Acid	441	4
Niacinamide	122	4
Pyridoxine hydrochloride	204	4
Riboflavin	376	0.4
Thiamine hydrochloride	337	4
i-Inositol	180	7.2
Inorganic Salts		
Calcium Chloride ($CaCl_2$-$2H_2O$)	147	264
Ferric Nitrate ($Fe(NO_3)_3$-$9H_2O$)	404	0.1
Magnesium Sulfate ($MgSO_4$-$7H_2O$)	246	200
Potassium Chloride (KCl)	75	400
Sodium Bicarbonate ($NaHCO_3$)	84	3700
Sodium Chloride (NaCl)	58	6400
Sodium Phosphate monobasic (NaH_2PO_4-$2H_2O$)	154	141
Other components		
D-Glucose (Dextrose)	180	4500
Phenol Red	376.4	15
Sodium Pyruvate	110	110

8.3 Supplier details

(Amersham Biosciences)
GE Healthcare UK Ltd.
Amersham Place
Little Chalfont
Buckinghamshire HP7 9NA
http://www.gelifesciences.com
Phone: 0870 606 1921
Fax: 01494 544350

Applied Biosystems/Ambion
2130 Woodward St.
Austin, TX 78744-1832
USA
http://www.ambion.com
Phone: (+1) 512 651-0200
Fax: (+1) 512 651-0190

Axon Instruments Inc.
GRI Ltd
Gene House
Queensborough Lane
Rayne
Braintree
Essex CM7 8TF
Phone: 01376 332900
Fax: 01376 344724

Biogene Ltd.
6 The Business Centre
Harvard Way
Kimbolton
Cambridgshire
PE28 0NJ
http://www.biogene.com
Phone: 0845 1300 950
Fax: 0845 1300 960

Bio-Rad Laboratories Ltd.
Bio-Rad House
Maxted Road
Hemel Hempstead
Hertfordshire HP2 7DX
http://www.bio-rad.co.uk
Phone: 0800 181134
Fax: 0208 328 2550

Fisher Scientific UK
Bishop Meadow Road
Loughborough
Leicestershire
LE11 5RG
http://www.fisher.co.uk
Phone: 01509 231166
Fax: 01509 231893

Gibco®, Invitrogen Ltd.
3 Fountain Drive
Inchinnan Business Park
Paisley
UK
PA4 9RF
http://www.invitrogen.com
Phone: 0141 814 6100
Fax: 0141 814 6260

Harvard Apparatus, Ltd.
Fircroft Way, Edenbridge
Kent TN8 6HE
UK
Phone: 01732 864001
Fax: 01732 863356
http://www.harvardapparatus.co.uk

Pierce Biotechnology, Inc.
3747 N. Meridian Rd.
P.O. Box 117
Rockford, IL 61105
USA
http://www.piercenet.com
Phone: (+1)800 874 3723
Fax: (+1)815 968 7316

Promega UK
Delta House
Southampton Science Park
Southampton SO16 7NS
UK
http://www.promega.com/uk
Phone: 023 8076 0225
Fax: 023 8076 7014

PromoCell GmbH
Sickingenstr. 63/65
D-69126 Heidelberg
Germany
http://www.promocell.com
Phone (UK): 0800 960333
Fax (UK): 0800 1698554

Sigma-Aldrich Company Ltd.
Fancy Road
Poole
Dorset
BH12 4QH
http://www.sigma-aldrich.com
Phone: 0800 717181
Fax: 0800 378785

Tocris Cookson Ltd.
Northpoint
Fourth Way
Avonmouth
Bristol
BS11 8TA
http://www.tocris.com
Phone: 0117 916 3333
Fax: 0117 916 3344

Whatman
GE Healthcare UK Ltd.
Amersham Place
Little Chalfont
Buckinghamshire HP7 9NA
England
http://www.whatman.com
Phone: 01622 676670
Fax: 01622 670755

World Precision Instruments
Astonbury Farm Business Centre
Aston
Stevenage
Hertfordshire
SG2 7EG
Phone: 01438 880025
Fax: 01438 880026

9   REFERENCES

REFERENCES

Abed, E. & Moreau, R. (2007) Importance of melastatin-like transient receptor potential 7 and cations (magnesium, calcium) in human osteoblast-like cell proliferation. *Cell Prolif.* 40: 849-865

Aguilar-Bryan, L. Nichols, C.G., Wechsler, S.W., Clement, J.P. 4th, Boyd, A.E. 3rd, González, G., Herrera-Sosa, H., Nguy, K., Bryan, J. & Nelson, D.A. (1995) Cloning of the β cell high-affinity sulfonylurea receptor: a regulator of insulin secretion. *Science.* 268: 423-426

Aguilar-Bryan, L., & Bryan, J. (1999) Molecular biology of adenosine triphosphate-sensitive potassium channels. *Endocrine Reviews.* 20: 101-135

Ahern, G.P., Wang, X. & Miyares, R.L. (2006) Polyamines are potent ligands for the capsaicin receptor TRPV1. *J Biol Chem.* 281(13): 8991-5

Ahlstrom, M., Pekkinen, M., Riehle, U., Lamberg-Allardt, C. (2008) Extracellular calcium regulates parathyroid hormone-related peptide expression in osteoblasts and osteoblast progenitor cells. *Bone.* 42(3): 483-90

Aitken, J.M., Hart, D.M. & Lindsay, R. (1973) Oestrogen replacement therapy for prevention of osteoporosis after oophorectomy. *Br Med J.* 3: 515-518

Alexander, S.P.H., Mathie, A. & Peters, J.A. (2008) Guide to Receptors and Channels (GRAC), 3rd edn. *Br J Pharmacol.* 153(2): S1-S209

Alexander, S.P.H., Mathie, A. & Peters, J.A. (eds.) (2004) Ion channels, in: Guide to Receptors and Channels, 1st edition. *Br J Pharmacol.* 141: S71-91

Ali, S.Y., Sajdera, S.W., & Anderson H.C. (1970) Isolation and characterization of calcifying matrix vesicles from epiphyseal cartilage. *Proc Natl Acad Sci USA.* 67: 1513-1520

Alicia, S., Angelica, Z., Carlos, S., Alfonso, S. & Luis, V. (2008) STIM1 converts TRPC1 from a receptor-operated to a store-operated channel: moving TRPC1 in and out of lipid rafts. *Cell Calcium* (in press). doi: 10.1016/j.physletb.2003.10.071

American Type Culture Collection (ATCC) http: //www.lgcpromochem-atcc.com

Amoroso, S., Schmid-Antomarchi, H., Fosset, M. & Lazdunski, M. (1990) Glucose, antidiabetic sulphonylureas and neurotransmitter release: Role of ATP-sensitive K channels. *Science.* 247: 852-854

Anderson, H.C. (2003) Matrix vesicles and calcification. *Curr Rheumatol Rep.* 5: 222-226

Appendino, G., De Petrocellis, L., Trevisani, M., Minassi, A., Daddario, N., Moriello, A.S., Gazzieri, D., Ligresti, A., Campi, B., Fontana, G., Pinna, C., Geppetti, P. & Di Marzo, V. (2005) Development of the first ultra-potent "capsaicinoid" agonist at transient receptor potential vanilloid type 1 (TRPV1) channels and its therapeutic potential. *J Pharmacol Exp Ther*. 312(2): 561-70

Araujo, A.M., Buschang, P.H. & Melo, A.C. (2004). Adaptive condylar growth and mandibular remodelling changes with bionator therapy - an implant study. *Eur J Orthod*. 26: 515-522

Arnett, T.R. & Dempster, D.W. (1986) Effect of pH on bone resorption by rat osteoclasts in vitro. *Endocrinology*. 119(1): 119-24

Arnett, T.R. (2007) Acid-base regulation of bone metabolism. *Int Cong Ser*. 1297: 255-267

Arnett, T.R. (2008) Extracellular pH regulates bone cell function. *J Nutr*. 138(2): 415S-418S

Ashcroft, F.M. & Gribble, F.M. (2000) Tissue-specific effects of sulphonylureas. Lessons from studies of cloned K_{ATP} channels. *J Diabetes Complications*. 14: 192-196

Bab, I. & Zimmer, A. (2008) Cannabinoid receptors and the regulation of bone mass. *Br J Pharmacol*. 153(2): 182-8

Bab, I., Ofek, O., Tam, J., Rehnelt, J. & Zimmer, A. (2008) Endocannabinoids and the regulation of bone metabolism. *J Neuroendocrinol*. 20(1): 69-74

Babenko, A.P., Gonzalez, G. & Bryan, J. (2000) Pharmaco-topology of sulfonylurea receptors. *J Biol Chem*. 275(2): 717-720

Baffy, G., Miyashita, T., Williamson, J.R., & Reed, J.C. (1993) Apoptosis induced by withdrawal of interleukin-3 (IL-3) from an IL-3-dependent hematopoietic cell line is associated with repartitioning of intracellular calcium and is blocked by enforced Bcl-2 oncoprotein production. *J Biol Chem*. 268: 6511- 6519

Bai, M., Trivedi, S., Lane, C.R., Yang, Y., Quinn, S.J. & Brown, E.M. (1998) Protein kinase C phosphorylation of threonine at position 888 in Ca^{2+}-sensing receptor (CaR) inhibits coupling to Ca^{2+} store release. *J Biol Chem*. 273: 21267-21275

Baker, P.F. (1972) Transport and metabolism of calcium ions in nerve. *Prog Biophys Mol Biol*. 24: 177-223

Barry, P.H. & Lynch, J.W. (1991) Liquid junction potentials and small cell effects in patch-clamp analysis. *J Membr Biol*. 121(2): 101-17. Erratum in: *J Membr Biol*. (1992) 125(3): 286

Bartho, L., Lenard, L., Patacchini, R., Halmai, V., Wilhelm, M., Holzer, P. & Maggi, C.A. (1999) Tachykinin receptors are involved in the "local efferent" motor response to capsaicin in the guinea-pig small intestine and oesophagus. *Neuroscience*. 90: 221-228

Berg, K.M., Kunins, H.V., Jackson, J.L. Nahvi, S., Chaudhry, A., Harris, K.A. Jr., Malik, R. & Arnsten, J.H. (2008) Association between alcohol consumption and both osteoporotic fracture and bone density. *Am J Med*. 121(5): 406-18

Berridge, M.J., Lipp, P. & Bootman, M.D. (2000) The versatility and universality of calcium signalling. *Nat Rev Mol Cell Biol*. 1: 11-21

Bevan, S., Hothi, S., Hughes, G.A., James, I.F., Rang, H.P., Shah, K., Walpole, C.S.J. & Yeats, J.C. (1992). Capsazepine: a competitive antagonist of the sensory neurone excitant capsaicin. *Br J Pharmacol*. 107: 544-552

Bhave, G., Zhu, W., Wang, H., Brasier, D.J., Oxford, G.S. & Gereau, R.W. (2002) cAMP-dependent protein kinase regulates desensitization of the capsaicin receptor (VR1) by direct phosphorylation. *Neuron*. 35: 721-731

Bianco, S.D., Peng, J.B., Takanaga, H., Suzuki, Y., Crescenzi, A., Kos, C.H., Zhuang, L., Freeman, M.R., Gouveia, C.H., Wu, J., Luo, H., Mauro, T., Brown, E.M. & Hediger, M.A. (2007) Marked disturbance of calcium homeostasis in mice with targeted disruption of the TRPV6 calcium channel gene. *J Bone Miner Res.* 22: 274-285

Bidaux, G., Flourakis, M., Thebault, S., Zholos, A., Beck, B., Gkika, D., Roudbaraki, M., Bonnal, J.L., Mauroy, B., Shuba, Y., Skryma, R. & Prevarskaya, N. (2007) Differentiation status of prostate cells determines TRPM8 channel subcellular localization and function: involvement in carcinogenesis. *J Clin Invest.* 117: 1647-1657

Bidaux, G., Roudbaraki, M., Merle, C., Crepin, A., Delcourt, P., Slomianny, C., Thebault, S., Bonnal, J.L., Benahmed, M., Cabon, F., Mauroy, B. & Prevarskaya, N. (2005) Evidence for specific TRPM8 expression in human prostate secretory epithelial cells: functional androgen receptor requirement. Endocr *Relat Cancer.* 12: 367-382

Birder, L.A.(2007) TRPs in bladder diseases. *Biochim Biophys Acta.* 1772(8): 879-84

Biswas, K.K., Sarker, K.P., Abeyama, K., Kawahara, K., Iino, S., Otsubo, Y., Saigo, K., Izumi, H., Hashiguchi, T., Yamakuchi, M., Yamaji, K., Endo, R., Suzuki, K., Imaizumi, H. & Maruyama, I. (2003) Membrane cholesterol but not putative receptors mediates anandamide-induced hepatocyte apoptosis. *Hepatology.* 38: 1167-1177

Bloch, M., Ousingsawat, J., Simon, R., Gasser, T.C., Mihatsch, M.J., Kunzelmann, K. & Bubendorf, L. (2005) KCNMA1 gene amplification promotes tumor cell proliferation in prostate cancer. *Oncogene.* 26(17): 2525-34

BNF 54 (Sept. 2007) 6.6.2: Bisphosphonates. British Medical Association and Royal Pharmaceutical Society of Great Britain: *British National Formulary*, 54: p. 403

Bolanz, K.A., Hediger, M.A. & Landowski, C.P. The role of TRPV6 in breast carcinogenesis. *Mol Cancer Ther.* 7(2): 271-9

Bonaiuti, D., Shea, B., Iovine, R., Negrini, S., Robinson, V., Kemper, H.C., Wells, G., Tugwell, P. & Cranney, A. (2002) Exercise for preventing and treating osteoporosis in postmenopausal women. *Cochrane Database of Systematic Reviews: CD000333*

Bone and Tooth Society of Great Britain, National Osteoporosis Society, Royal College of Physicians (2003) Glucocorticoid-induced Osteoporosis. *London, UK: Royal College of Physicians of London.* ISBN 1-860-16173-1

Boyle, P.J. & Conway, E.J. (1941) Potassium accumulation in muscle and associated changes. *J Physiol.* 100(1): 1-63

Brandao-Burch, A., Utting, J.C., Orriss, I.R. & Arnett, T.R. (2005) Acidosis inhibits bone formation by osteoblasts in vitro by preventing mineralisation. *Calcif Tissue Int.* 77(3): 167-74

Brandao-Burch, A., Utting, J.C., Orriss, I.R., Arnett, T.R. (2006) Capsaicin is a potent activator of human osteoclasts. *Calcif Tissue Int.* 78: S1: S36

Brauchi, S., Orio, P. & Latorre, R. (2004) Clues to understanding cold sensation: thermodynamics and electrophysiological analysis of the cold receptor TRPM8. *Proc Natl Acad Sci U S A.* 101(43): 15494-9

Brauchi, S., Orta, G., Mascayano, C., Salazar, M., Raddatz, N., Urbina, H., Rosenmann, E., Gonzalez-Nilo, F. & Latorre, R. (2007) Dissection of the components for PIP2 activation and thermosensation in TRP channels. *Proc Natl Acad Sci U S A.* 104(24): 10246-51

Braun, G.S., Veh, R.W., Segerer, S., Horster, M.F. & Huber, S.M. (2002) Developmental expression and functional significance of Kir channel subunits in ureteric bud and nephron epithelia. *Pflugers Arch.* 445(3): 321-30

Breitwieser, G.E. & Gama, L. (2001) Calcium-sensing receptor activation induces intracellular calcium oscillations. *Am J Physiol Cell Physiol.* 280: C1412-C1421

Broad, L.M., Armstrong, D.L. & Putney, J.W. Jr. (1999) Role of the inositol 1,4,5-trisphosphate receptor in Ca^{2+} feedback inhibition of calcium release-activated calcium current (I_{CRAC}) *J Biol Chem.* 274: 32881-32888

Bryden, A.A., Hoyland, J.A., Freemont, A.J., Clarke, N.W. & George, N.J. (2002) Parathyroid hormone related peptide and receptor expression in paired primary prostate cancer and bone metastases. *Br J Cancer.* 86: 322-325

Buhl, A.E., Conrad, S.J., Waldon, D.J. & Brunden, M.J. (1993) Potassium channel conductance as a control mechanism in hair follicles. *J Invest Dermatol.* 101: 148S-52S

Buijs, J.T. & van der Pluijm, G. (2008) Osteotropic cancers: From primary tumor to bone. *Cancer Lett.* Published online ahead of print. doi: 10.1016/j.canlet.2008.05.044

Burg, E.D., Remillard, C.V. &Yuan, J.X.-J. (2006) K^+ channels in apoptosis. *J Membr Biol.* 209: 1-18

Burton, J.L., Schutt, W.H. & Caldwell, I.W. (1975) Hypertrichosis due to diazoxide.*Br J Dermatol.* 93: 707-11

Cahalan, D.M. (2001) Cell biology. Channels as enzymes. *Nature.* 411: 542-3

Cahill, C.M., White, T.D. & Sawynok, J. (1993a) Influence of calcium on the release of endogenous adenosine from spinal cord synaptosomes. *Life Sci.* 53(6): 487-96

Cahill, C.M., White, T.D. & Sawynok, J. (1993b) Involvement of calcium channels in depolarization-evoked release of adenosine from spinal cord synaptosomes. *J Neurochem.* 60: 886-893

Campbell, A.K. (1983) Intracellular calcium: Its universal role as a regulator. *John Wiley and Sons: Chichester, UK*

Caterina, M.J., Leffler, A., Malmberg, A.B., Martin, W.J., Trafton, J., Petersen-Zeitz, K.R., Koltzenburg, M., Basbaum, A.I. & Julius, D. (2000) Impaired nociception and pain sensation in mice lacking the capsaicin receptor. *Science.* 288: 306-313

Caterina, M.J., Rosen, T.A., Tominaga, M., Brake, A.J. & Julius, D. (1999) A capsaicin-receptor homologue with a high threshold for noxious heat. *Nature.* 398: 436-41

Caterina, M.J., Schumacher, M.A., Tominaga, M., Rosen, T.A., Levine, J.D. & Julius, D. (1997) The capsaicin receptor: a heat-activated ion channel in the pain pathway. *Nature.* 389(6653): 816-24

Chae, H.J., Chae, S.W., Weon, K.H., Kang, J.S. & Kim, H.R. (1999) Signal transduction of thapsigargin-induced apoptosis in osteoblast. *Bone.* 25(4): 453-8

Chandy, G.K., Wulff, H., Beeton, C., Pennington, M., Gutman, G.A. & Cahalan, M.D. (2004) K^+ channels as targets for specific immunomodulation. *TIPS.* 25: 280-289

Chattopadhyay, N., Yano, S., Tfelt-Hansen, J., Rooney, P., Kanuparthi, D., Bandyopadhyay, S., Ren, X., Terwilliger, E. & Brown, E.M. Mitogenic action of calcium-sensing receptor on rat calvarial osteoblasts. *Endocrinology.* 145: 3451-3462

Cholewinski, A., Buaouss, G.M. & Bevan, S. (1993) The role of calcium in capsaicin-induced desensitization in rat cultured dorsal root ganglion neurons. *Neuroscience.* 55(4): 1015-1023

Chou, M.Z., Mtui, T., Gao, Y.D., Kohler, M. & Middleton, R.E. (2004) Resiniferatoxin binds to the capsaicin receptor (TRPV1) near the extracellular side of the S4 transmembrane domain. *Biochemistry.* 43(9): 2501-11

Chuang, H.H., Prescott, E.D., Kong, H., Shields, S., Jordt, S.E., Basbaum, A.I., Chao, M.V. & Julius, D. (2001) Bradykinin and nerve growth factor release the capsaicin receptor from PtdIns(4,5)P_2-mediated inhibition. *Nature.* 411: 957-62

Chubanov, V., Waldegger, S., Mederos y Schnitzler, M., Vitzthum, H., Sassen, M.C., Seyberth, H.W., Konrad, M. & Gudermann, T. (2004) Disruption of TRPM6/TRPM7 complex formation by a mutation in the TRPM6 gene causes hypomagnesemia with secondary hypocalcemia. *Proc Natl Acad Sci USA.* 101: 2894-9

Chung, M.K., Lee, H., Mizuno, A., Suzuki, M. & Caterina, M.J. (2004) 2-Aminoethoxydiphenyl borate activates and sensitizes the heat-gated ion channel TRPV3. *J Neurosci.* 24: 5177-5182

Chutkow, W.A., Simon, M.C., Le Beau, M.M. & Burant, C.F. (1996) Cloning, tissue expression, and chromosomal localization of SUR2, the putative drug-binding subunit of cardiac, skeletal muscle, and vascular K_{ATP} channels. *Diabetes.* 45: 1439-1445

Clapham, D.E. (2003) TRP channels as cellular sensors. *Nature.* 426(6966): 517-24

Clapham, D.E., Julius, D., Montell, C. & Schultz, G. (2005) International Union of Pharmacology. XLIX. Nomenclature and structure-function relationships of transient receptor potential channels. *Pharmacol Rev.* 57(4): 427-50

Clapham, D.E., Runnels, W.L. & Strubing, C. (2001) The TRP ion channel family. *Nat Rev Neurosci.* 2: 387-96

Colquhoun, D. & Sigworth, F.H. (1995) Fitting and statistical analysis of single-channel records. In: Sakmann, B. & Neher, E. (1995) *Single-Channel Recording, 2nd ed.* New York: Plenum Press. 483-587

Colquhoun, D. (1994) Practical analysis of single channel records. In: Ogden, D. (ed.) (1994) *Microelectrode Techniques: The Plymouth Workshop Handbook.* Cambridge: The Company of Biologists Ltd. 101-139

Corey, D.P. (2003) New TRP channels in hearing and mechanosensation. *Neuron.* 39: 585-588

Csutora, P., Peter, K., Kilic, H., Park, K.M., Zarayskiy, V., Gwozdz, T. & Bolotina, V.M. (2008) Novel role of STIM1 as a trigger for calcium influx factor (CIF) production. *J Biol Chem.* 283(21): 14524-31

D'hahan, N., Moreau, C., Prost, A.L., Jacquet, H., Alekseev, A.E., Terzic, A. & Vivaudou, M. (1999) Pharmacological plasticity of cardiac ATP-sensitive potassium channels toward diazoxide revealed by ADP. *Proc Natl Acad Sci.* 96: 12162-12167

Datta, H.K., Ng, W.F., Walker, J.A., Tuck, S.P. & Varanasi, S.S. (2008) The cell biology of bone metabolism. *J Clin Pathol.* 61(5): 577-87

Davidson, R.M., Lingenbrink, P. & Norton, L.A. (1996) Continuous mechanical loading alters properties of mechanosensitive channels in G292 osteoblastic cells. *Calcif Tissue Int.* 59: 500-504

de Jesus Ferreira, M.C., Héliès-Toussaint, C., Imbert-Teboul, M., Bailly, C., Verbavatz, J.M., Bellanger, A.C. & Chabardès, D. (1998) Co-expression of a Ca^{2+}-inhibitable adenylyl cyclase and of a Ca^{2+}-sensing receptor in the cortical thick ascending limb cell of the rat kidney. Inhibition of hormone-dependent cAMP accumulation by extracellular Ca^{2+}. *J Biol Chem.* 273(24): 15192-15202

Delmas, P. (2004) Polycystins: from mechanosensation to gene regulation. *Cell.* 118: 145-148

Den Dekker, E., Hoenderop, J.G., Nilius, B. & Bindels, R.J. (2003) The epithelial calcium channels, TRPV5 & TRPV6: from identification towards regulation. *Cell Calcium.* 33: 497-507

Department of Health. (1998). Nutrition and bone health: with particular reference to calcium and vitamin D. *London: The London Stationery Office.* 49: 1-124

Di Marzo, V., Bisogno, T., Melck, D., Ross, R., Brockie, H., Stevenson, L., Pertwee, R. & De Petrocellis, L. (1998) Interactions between synthetic vanilloids and the endogenous cannabinoid system. *FEBS Lett.* 436(3): 449-54

Distelhorst, C.W., Lam, M. & McCormick, T.S. (2000) Bcl-2 inhibits hydrogen peroxide-induced ER Ca^{2+} pool depletion. *Oncogene.* 12: 2051-2055

Docherty, R.J., Yeats, J.C. & Piper, A.S. (1997) Capsazepine block of voltage-activated calcium channels in adult rat dorsal root ganglion neurones in culture. *Br J Pharmacol.* 121(7): 1461-7

Dömötör, A., Peidl, Z., Vincze, A., Hunyady, B., Szolcsányi, J., Kereskay, L., Szekeres, G. & Mózsik, G. (2005) Immunohistochemical distribution of vanilloid receptor, calcitonin-gene related peptide and substance P in gastrointestinal mucosa of patients with different gastrointestinal disorders. *Inflammopharmacology.* 13(1-3): 161-77

Dray, A. (2008) Neuropathic pain: emerging treatments. *Br J Anaesth.* 101(1): 48-58; Published online ahead of print. doi: 10.1093/bja/aen107

Dubois, J.M. & Rouzaire-Dubois, B. (1993) Role of potassium channels in mitogenesis. *Prog Biophys Mol Biol.* 59: 1-21

Ducy, P., Zhang, R., Geoffroy, V., Ridall, A.L. & Karsenty, G. (1997). Osf2/Cbfa1: a transcriptional activator of osteoblast differentiation. *Cell.* 89: 747-754

Duncan, L.M., Deeds, J., Hunter, J., Shao, J., Holmgren, L.M., Woolf, E.A., Tepper, R.I. & Shyjan, A.W. (1998) Down-regulation of the novel gene melastatin correlates with potential for melanoma metastasis. *Cancer Res.* 58: 1515-20

Duncan, R.L., & Hruska, K.A. (1994) Chronic, intermittent loading alters mechanosensitive channel characteristics in csteoblast-like cells. *Am J Physiol.* 267(6 Pt 2): F909-16

Dvorak, M.M. & Riccardi, D. (2004) Ca^{2+} as an extracellular signal in bone. *Cell Calcium.* 35(3): 249-55

Dvorak, M.M., Siddiqua, A., Ward, D.T., Carter, D.H., Dallas, S.L., Nemeth, E.F. & Riccardi, D. (2004) Physiological changes in extracellular calcium concentration directly control osteoblast function in the absence of calciotropic hormones. *Proc Natl Acad Sci USA.* 101(14): 5140-5

Eilers, H., Lee, S.Y., Hau, C.W., Logvinova, A. & Schumacher, M.A. (2007) The rat vanilloid receptor splice variant VR.5'sv blocks TRPV1 activation. *Neuroreport.* 18(10): 969-73

Elizondo, M.R., Arduini, B.L., Paulsen, J., MacDonald, E.L., Sabel, J.L., Henion, P.D., Cornell, R.A. & Parichy, D.M. (2005) Defective skeletogenesis with kidney stone formation in dwarf zebrafish mutant for trpm7. *Curr Biol.* 15(7): 667-71

Endoh, H., Sasaki, H., Maruyama, K., Takeyama, K., Waga, I., Shimizu, T., Kato, S. & Kawashima, H.(1997) Rapid activation of MAP kinase by estrogen in the bone cell line. *Biochem Biophys Res Commun.* 235(1): 99-102

Eriksen, E.F. (1986) Normal and pathological remodeling of human trabecular bone: three dimensional reconstruction of the remodelling sequence in normals and in metabolic bone disease. *Endocrinol Rev.* 7: 379-408

European Collection of Cell Cultures (ECACC) http://www.ecacc.org.uk

Evans, B.A., Elford, C., Pexa, A., Francis, K., Hughes, A.C., Deussen, A. & Ham, J. (2006) Human osteoblast precursors produce extracellular adenosine, which modulates their secretion of IL-6 and osteoprotegerin. *J Bone Miner Res.* 21: 228-236

Farias, L.M., Ocana, D.B., Diaz, L., Larrea, F., Avila-Chavez, E., Cadena, A., Hinojosa, L.M., Lara, G., Villanueva, L.A., Vargas, C., Hernandez-Gallegos, E., Camacho-Arroyo, I., Duenas-Gonzalez, A., Perez-Cardenas, E., Pardo, L.A., Morales, A., Taja-Chayeb, L., Escamilla, J., Sanchez-Pena, C. & Camacho, J. (2004) Ether a go-go potassium channels as human cervical cancer markers. *Cancer Res.* 64: 6996-7001

Feske, S., Gwack, Y., Prakriya, M., Srikanth, S., Puppel, S.H., Tanasa, B., Hogan, P.G., Lewis, R.S., Daly, M. & Rao, A. (2006) A mutation in Orai1 causes immune deficiency by abrogating CRAC channel function. *Nature.* 441: 179-185

Fischer, B.S., Qin, D., Kim, K. & McDonald, T.V. (2001) Capsaicin inhibits Jurkat T-cell activation by blocking calcium entry current I_{CRAC}. *J Pharmacol Exp Ther.* 299: 238-246

Fixemer, T., Wissenbach, U., Flockerzi, V. & Bonkhoff, H. (2003) Expression of the Ca^{2+}-selective cation channel TRPV6 in human prostate cancer: a novel prognostic marker for tumour progression. *Oncogene.* 22: 7858-7861

Fleig, A. & Penner, R. (2004) The TRPM ion channel subfamily: molecular, biophysical and functional features. *Trends Pharmacol Sci.* 25: 633-9

Fleisch, H. (2002) Development of bisphosphonates. *Breast Cancer Res.* 4(1): 30-4

Fogh, J. & Trempe, G. (1975) Human tumor cells in vitro. Fogh, J., editor. New York: Plenum Press. 115-159

Foreman, M.A., Smith, J. & Publicover, S.J. (2006) Characterisation of serum-induced intracellular Ca^{2+} oscillations in primary bone marrow stromal cells. *J Cell Physiol.* 206(3): 664-71

Franchimont, N., Wertz, S. & Malaise, M. (2005) Interleukin-6: An osteotropic factor influencing bone formation? *Bone.* 37: 601-606

Frith, J., Mönkkönen, J., Blackburn, G., Russell, R. & Rogers, M. (1997) Clodronate and liposome-encapsulated clodronate are metabolized to a toxic ATP analog, adenosine 5'-(beta, gamma-dichloromethylene) triphosphate, by mammalian cells in vitro. *J Bone Miner Res.* 12(9): 1358-67

Fujimoto, S., Mori, M., Tsushima, H. & Kunimatsu, M. (2006) Capsaicin-induced, capsazepine-insensitive relaxation of the guinea-pig ileum. *Eur J Pharmacol.* 530(1-2): 144-51

Geber, C., Mang, C.F. & Kilbinger, H. (2006) Facilitation and inhibition by capsaicin of cholinergic neurotransmission in the guinea-pig small intestine. *Naunyn Schmiedebergs Arch Pharmacol.* 372(4): 277-83

Ghilardi, R.J., Rohrich, H., Lindsay, H.T., Sevcik, A.M., Schwei, J.M., Kubota, K., Halvorson, G.K., Poblete, J., Chaplan, R.S., Dubin, E.A., Carruthers, I.N., Swanson, D., Kuskowski, M., Flores, M., C., Julius, D. & Mantyh, W.P. (2005) Selective blockade of the capsaicin receptor TRPV1 attenuates bone cancer pain. *J Neurosci.* 25: 3126-31

Gimble, J.M., Robinson, C.E., Wu, X. & Kelly, K.A. (1996) The function of adipocytes in the bone marrow stroma: an update. *Bone.* 19: 421-428

Goldberg, M.R.(1988) Clinical pharmacology of pinacidil, a prototype for drugs that affect potassium channels. *J Cardiovasc Pharmacol.* 12(2): S41-7

Golovina, V.A., Platoshyn, O., Bailey, C.L., Wang, J., Limsuwan, A., Sweeney, M., Rubin, L.J. & Yuan, J.X. (2001) Upregulated TRP and enhanced capacitative Ca^{2+} entry in human pulmonary artery myocytes during proliferation. *Am J Physiol Heart Circ Physiol.* 280: H746-H755

Goodwin, P., Campbell, E.K., Evans, B.A.J. & Wann, K.T. (1998) In vitro patch-clamp studies in skin fibroblasts. *J Pharmacol Toxicol Methods.* 39(4): 229-33

Grandolfo, M., D'Andrea, P., Martina, M., Ruzzier, F. & Vittur, F (1992) Calcium-activated potassium channels in chondrocytes. *Biochem Biophys Res Commun.* 182: 1429-1434

Gribble, F.M., Tucker, S.J. & Ashcroft, F.M. (1997) The essential role of the Walker A motifs of SUR1 in K-ATP channel activation by Mg-ADP and diazoxide. *EMBO J.* 16: 1145-1152

Griffith, J.F., Yeung, D.K., Antonio, G.E., Lee, F.K., Hong, A.W., Wong, S.Y., Lau, E.M. & Leung, P.C. (2005) Vertebral bone mineral density, marrow perfusion, and fat content in healthy men and men with osteoporosis: dynamic contrast-enhanced MR imaging and MR spectroscopy. *Radiology.* 236(3): 945-51

Griffith, J.F., Yeung, D.K., Tsang, P.H., Choi, K.C., Kwok, T.C., Ahuja, A.T., Leung, K.S. & Leung, P.C. (2008) Compromised Bone Marrow Perfusion in Osteoporosis. *J Bone Miner Res*. (Published online ahead of print 25 Feb 2008). DOI: 10.1359/JBMR.080233

Grygorczyk, C., Grygorczyk, R. & Ferrier, J. (1989) Osteoblastic cells have L-type calcium channels. *Bone Miner*. 7(2): 137-48

Gu, Y. & Publicover, S.J. (2000) Expression of functional metabotropic glutamate receptors in primary cultured rat osteoblasts. *J Biol Chem*. 275: 34252-34259

Gu, Y., Preston, M.R., El Haj, A.J., Howl, J.D. & Publicover, S.J. (2001a) Three types of K^+ currents in murine osteocyte-like cells (MLO-Y4). *Bone*. 28(1): 29-37

Gu, Y., Preston, M.R., Magnay, J., El Haj, A.J. & Publicover, S.J. (2001b) Hormonally-regulated expression of voltage-operated Ca^{2+} channels in osteocytic (MLO-Y4) cells. *Biochem Biophys Res Commun*. 282(2): 536-542

Gu, Y., Genever, P.G., Skerry, T.M. & Publicover, S.J. (2002) The NMDA type glutamate receptors expressed by primary rat osteoblasts have the same electrophysiological characteristics as neuronal receptors. *Calcif Tissue Int*. 70: 194-203

Guggino, S.E., Lajeunesse, D., Wagner, J.A. & Snyder, S. (1989) Bone remodelling signalled by a dihydropyridine- and phenylalkylamine-sensitive calcium channel. *Proc Natl Acad Sci USA*. 86: 2957-2960

Hadjidakis, D.J. & Androulakis, I.I. (2006) Bone remodeling. *Ann NY Acad Sci*. 1092: 385-396

Hajnóczky, G., Csordás, G., Das, S., Garcia-Perez, C., Saotome, M., Sinha, Roy. S. & Yi, M. (2006) Mitochondrial calcium signalling and cell death: approaches for assessing the role of mitochondrial Ca^{2+} uptake in apoptosis. *Cell Calcium*. 40(5-6): 553-60

Hamill, O.P., Marty, A., Neher, E., Sakmann, B. & Sigworth, F.J. (1981) Improved patch-clamp techniques for high-resolution current recording from cells and cell-free membrane patches. *Pflugers Arch*. 391(2): 85-100

Han, Y., Cowin, S.C., Schaffler, M.B. & Weinbaum, S. (2004) Mechano-transduction and strain amplification in osteocyte cell processes. *Proc Natl Acad Sci USA*. 101: 16689-94

Hanano, T., Hara, Y., Shi, J., Morita, H., Umebayashi, C., Mori, E., Sumimoto, H., Ito, Y., Mori, Y. & Inoue, R. (2004) Involvement of TRPM7 in cell growth as a spontaneously activated Ca^{2+} entry pathway in human retinoblastoma cells. *J Pharmacol Sci*. 95(4): 403-19

Hara, Y., Wakamori, M., Ishii, M., Maeno, E., Nishida, M., Yoshida, T., Yamada, H., Shimizu, S., Mori, E., Kudoh, J., Shimizu, N., Kurose, H., Okada, Y., Imoto, K. & Mori, Y. (2002) LTRPC2 Ca^{2+}-permeable channel activated by changes in redox status confers susceptibility to cell death. *Mol Cell*. 9: 163-73

Hardie, R.C. & Minke, B. (1993) Novel Ca^{2+} channels underlying transduction of *Drosophila* photoreceptors: implications for phosphoinositide-mediated Ca^{2+} mobilization. *Trends Neurosci*. 16: 371-376

Hardie, R.C. & Minke, B. (2002) The trp gene is essential for a light-activated Ca^{2+} channel in Drosophila photoreceptors. *Neuron*. 8(4): 643-51

Hardie, R.C. (2003) TRP channels in *Drosophila* photoreceptors: the lipid connection. *Cell Calcium*. 33: 385-393

Hartel, M., di Mola, F.F., Selvaggi, F., Mascetta, G., Wente, M.N., Felix, K., Giese, N.A., Hinz, U., Di Sebastiano, P., Büchler, M.W. & Friess, H. (2006) Vanilloids in pancreatic cancer: potential for chemotherapy and pain management. *Gut*. 55(4): 519-28

Harteneck, C., Plant, T.D. & Schultz, G. (2000) From worm to man: three subfamilies of TRP channels. *Trends Neurosci*. 23(4): 159-66

REFERENCES

Hattori, T., Maehashi, H., Miyazawa, T. & Naito, M. (2001) Potentiation by stannous chloride of calcium entry into osteoblastic MC3T3-E1 cells through voltage-dependent L-type calcium channels. *Cell Calcium.* 30(1): 67-72

Hausser, H.J. & Brenner, R.E. (2005) Phenotypic instability of Saos-2 cells in long-term culture. *Biochem Biophys Res Commun.* 333(1): 216-222

Heremans, H., Billiau, A., Cassiman, J., Mulier, J. & de Somer, P. (1978) cited in: Davies, J.H., Evans, B.A.J., Jenney, M.E.M. & Gregory, J.W. (2002) In Vitro Effects of Combination Chemotherapy on Osteoblasts: Implications for Osteopenia in Childhood Malignancy. *Bone.* 31: 319-326

Hille, B. (2001) Ionic channels of excitable membranes, 3rd ed. *Sinauer Associates, Massachusetts, USA*

Hodgkin, A.L. & Horowicz, P. (1959) The influence of potassium and chloride ions on membrane potential of single muscle fibres. *J Physiol.* 148: 127-160

Hoebertz, A., Arnett, T.R. & Burnstock, G. (2003) Regulation of bone resorption and formation in purines and pyrimidines. *TIPS.* 24: 290-297

Hoenderop, J.G., Nilius, B. & Bindels, R.J. (2002) Molecular mechanisms of active Ca^{2+} reabsorption in the distal nephron. *Annu Rev Physiol.* 64: 529-549

Hoenderop, J.G., Nilius, B. & Bindels, R.J. (2003a) Epithelial calcium channels: from identification to function and regulation. *Pflugers Arch.* 446: 304-8

Hoenderop, J.G., van Leeuwen, J.P., van der Eerden, B.C., Kersten, F.F., van der Kemp, A.W., Mérillat, A.M., Waarsing, J.H., Rossier, B.C., Vallon, V., Hummler, E. & Bindels, R.J. (2003b) Renal Ca^{2+} wasting, hyperabsorption, and reduced bone thickness in mice lacking TRPV5. *J Clin Invest.* 112(12): 1906-14

Hoenderop, J.G., Voets, T., Hoefs, S., Weidema, F., Prenen, J., Nilius, B. & Bindels, R.J. (2003c) Homo- and heterotetrameric architecture of the epithelial Ca^{2+} channels TRPV5 and TRPV6. *EMBO J.* 22(4): 776-85

Hofer, A.M. (2005) Another dimension to calcium signaling: a look at extracellular calcium. *J Cell Sci.* 118(Pt 5): 855-62

Hofmann, T., Chubanov, V., Gudermann, T. & Montell, C. (2003) TRPM5 is a voltage-modulated and Ca^{2+}-activated monovalent selective cation channel. *Curr Biol.* 13: 1153-1158

Hofmann, T., Obukhov, A.G., Schaefer, M., Harteneck, C., Gudermann, T. & Schultz, G. (1999) Direct activation of human TRPC6 and TRPC3 channels by diacylglycerol. *Nature.* 397(6716): 259-63

Horoszewicz, J.S., Leong, S.S., Kawinski, E., Karr, J.P., Rosenthal, H., Chu, T.M., Mirand, E.A. & Murphy, G.P. (1983) LNCaP model of human prostatic carcinoma. *Cancer Res.* 43: 1809-1818

Hoth, M. & Penner, R. (1992) Depletion of intracellular calcium stores activates a calcium current in mast cells. *Nature.* 355(6358): 353-6

Hu, H.Z., Gu, Q., Wang, C., Colton, C.K., Tang, J., Kinoshita-Kawada, M., Lee, L.Y., Wood, J.D. & Zhu, M.X. (2004) 2-Aminoethoxydiphenyl borate is a common activator of TRPV1, TRPV2 and TRPV3. *J Biol Chem.* 279: 35741-35748

Huang, C., Hujer, K.M., Wu, Z. & Miller, R.T. (2004) The Ca^{2+}-sensing receptor couples to Galpha$_{12/13}$ to activate phospholipase D in Madin-Darby canine kidney cells. *Am J Physiol Cell Physiol.* 286(1): C22-30

Huang, J.K., Cheng, H.H., Huang, C.J., Kuo, C.C., Chen, W.C., Liu, S.I., Hsu, S.S., Chang, H.T., Lu, Y.C., Tseng, L.L., Chiang, A.J., Chou, C.T. & Jan, C.R. (2006) Effect of capsazepine on cytosolic Ca(2+) levels and proliferation of human prostate cancer cells. *Toxicol In Vitro.* 20(5): 567-74

Hubbard, T. J. P., B. L. Aken, K. Beall, B. Ballester1, M. Caccamo, Y. Chen, L. Clarke, G. Coates, F. Cunningham, T. Cutts, T. Down, S. C. Dyer, S. Fitzgerald, J. Fernandez-Banet, S. Graf, S. Haider, M. Hammond, J. Herrero, R. Holland, K. Howe, K. Howe, N. Johnson, A. Kahari, D. Keefe, F. Kokocinski, E. Kulesha, D. Lawson, I. Longden, C. Melsopp, K. Megy, P. Meidl, B. Overduin, A. Parker, A. Prlic, S. Rice, D. Rios, M. Schuster, I. Sealy, J. Severin, G. Slater, D. Smedley, G. Spudich, S. Trevanion, A. Vilella, J. Vogel, S. White, M. Wood, T. Cox, V. Curwen, R. Durbin, X. M. Fernandez-Suarez, P. Flicek, A. Kasprzyk, G. Proctor, S. Searle, J. Smith, A. Ureta-Vidal & E. Birney. (2007) Ensembl 2007. *Nucleic Acids Res.* Vol. 35, Database issue: D610-D617. [DOI] <10.1093/nar/gkl996> or [WWW] http: //www.ensembl.org/

Hughes, S., Magnay, J., Foreman, M., Publicover, S.J., Dobson, J.P. & El Haj, A.J.(2006) Expression of the mechanosensitive 2PK+ channel TREK-1 in human osteoblasts. *J Cell Physiol.* 206(3): 738-748

Inagaki, N., Tsuura, Y., Namba, N., Masuda, K., Gonoi, T., Horie, M., Seino, Y., Mizuta, M. & Seino, S. (1995) Cloning and functional characterization of a novel ATP-sensitive potassium channel ubiquitously expressed in rat tissues, including pancreatic islets, pituitary, skeletal muscle, and heart. *J Biol Chem.* 270: 5691-5694

Isomoto, S., Kondo, C., Yamada, M., Matsumoto, S., Higashiguchi, O., Horio, Y., Matsuzawa, Y. & Kurachi, Y. (1996) A novel sulfonylurea receptor forms with BIR (Kir6.2) a smooth muscle type ATP-sensitive K1 channel. *J Biol Chem.* 271: 24321-24324

Izbicka, E., Dunstan, C., Esparza, J., Jacobs, C., Sabatini, M. & Mundy, G.R. (1996) Human amniotic tumor that induces new bone formation in vivo produces growth-regulatory activity in vitro for osteoblasts identified as an extended form of basic fibroblast growth factor. *Cancer Res.* 56(3): 633-6

Jan, C.R., Lu, C.H., Chen, Y.C., Cheng, J.S., Tseng, L.L. & Jun-Wen, W. (2000) Ca^{2+} mobilization induced by W-7 in MG63 human osteosarcoma cells. *Pharmacol Res.* 42(4): 323-7

Jancsó, N., Jancsó-Gábor, A. & Szolcsányi, J. (1967) Direct evidence for neurogenic inflammation and its prevention by denervation and by pretreatment with capsaicin. *Brit J Pharmacol.* 31: 138-151

Jee, W.S.S., Wronski, T.J., Morey, E.R., & Kimmel, D.B. (1983) Effects of spaceflight on trabecular bone in rats. *Am J Physiol.* 244: R310-R314

Jiang, J., Li, M.H., Inoue, K., Chu, X.P., Seeds, J. & Xiong, Z.G. (2007) Transient receptor potential melastatin 7-like current in human head and neck carcinoma cells: role in cell proliferation. *Cancer Res.* 67(22): 10929-38

Johnson, J.P. Jr, Mullins, F.M. & Bennett, P.B. (1999) Human ether-à-go-go-related gene K^+ channel gating probed with extracellular Ca^{2+}. Evidence for two distinct voltage sensors. *J Gen Physiol.* 113(4): 565-80

Johnson, J.P. Jr, Balser, J.R. & Bennett, P.B. (2001) A novel extracellular calcium sensing mechanism in voltage-gated potassium ion channels. *J Neurosci.* 21(12): 4143-53

Joiner, W.J., Tang, M.D., Wang, L.Y., Dworetzky, S.I., Boissard, C.G., Gan, L., Gribkoff, V.K., Kaczmarek, L.K. (1998) Formation of intermediate-conductance calcium-activated potassium channels by interaction of Slack and Slo subunits. *Nat Neurosci.* 1(6): 462-9

Jordt, S.E., Tominaga, M. & Julius, D. (2000) Acid potentiation of the capsaicin receptor determined by a key extracellular site. *Proc Natl Acad Sci USA.* 97: 8134-8139

Jung, J., Hwang, S.W., Kwak, J., Lee, S.Y., Kang, C.J., Kim, W.B., Kim, D. & Oh. U. (1999) Capsaicin binds to the intracellular domain of the capsaicin-activated ion channel. *J Neurosci.* 19: 529-538

Jurutka, P.W., Bartik, L., Whitfield, G.K., Mathern, D.R., Barthel, T.K., Gurevich, M., Hsieh, J.C., Kaczmarska, M., Haussler, C.A. & Haussler, M.R. (2007) Vitamin D receptor: key roles in bone mineral pathophysiology, molecular mechanism of action, and novel nutritional ligands. *J Bone Miner Res.* 22(2): V2-10

Justesen, J., Stenderup, K., Ebbesen, E.N., Mosekilde, L., Steiniche, T. & Kassem, M. (2001) Adipocyte tissue volume in bone marrow is increased with aging and in patients with osteoporosis. *Biogerontology.* 2(3): 165-71

Kameda, T., Mano, H., Yamada, Y., Takai, H., Amizuka, N., Kobori, M., Izumi, N., Kawashima, H., Ozawa, H., Ikeda, K., Kameda, A., Hakeda, Y. & Kumegawa, M. (1998) Calcium-sensing receptor in mature osteoclasts, which are bone resorbing cells. *Biochem Biophys Res Commun.* 245: 419-422

Kanis, J. (1989) Osteoporosis - the silent epidemic. *Health Visit.* 62(1): 14-5

Kanis, J.A., Johansson, H., Johnell, O., Oden, A., De Laet, C., Eisman, J.A., Pols, H. & Tenenhouse, A. (2005) Alcohol intake as a risk factor for fracture. *Osteoporos Int.* 16: 737-742

Kanis, J.A., Johansson, H., Oden, A., Johnell, O., De Laet, C., Eisman, J.A., McCloskey, E.V., Mellstrom, D., Melton, L.J., III, Pols, H.A., Reeve, J., Silman, A.J. & Tenenhouse, A. (2004a) A family history of fracture and fracture risk: a meta-analysis. *Bone.* 35: 1029-1037

Kanis, J.A., Johnell, O., Oden, A., Johansson, H., De Laet, C., Eisman, J.A., Fujiwara, S., Kroger, H., McCloskey, E.V., Mellstrom, D., Melton, L.J., Pols, H., Reeve, J., Silman, A. & Tenenhouse, A. (2004b) Smoking and fracture risk: a meta-analysis. *Osteoporos Int.* 16: 155-162

Kanzaki, M., Zhang, Y.Q., Mashima, H., Li, L., Shibata, H. & Kojima, I. (1999) Translocation of a calcium-permeable cation channel induced by insulin-like growth factor-I. *Nat Cell Biol.* 1: 165-70

Karsenty, G. & Wagner, E.F. (2002) Reaching a genetic and molecular understanding of skeletal development. *Dev Cell.* 2(4): 389-406

Kedei, N., Szabo, T., Lile, D.J., Treanor, J.J., Olah, Z., Iadarola, J.M. & Blumberg, M.P. (2001) Analysis of the native quaternary structure of vanilloid receptor 1. *J Biol Chem.* 276: 28613-9

Keen, J.E., Khawaled, R., Farrens, D.L., Neelands, T., Rivard, A., Bond, C.T., Janowsky, A., Fakler, B., Adelman, J.P. & Maylie, J. (1999) Domains responsible for constitutive and Ca^{2+}-dependent interactions between calmodulin and small conductance Ca^{2+}-activated potassium channels. *J Neurosci.* 19: 8830-8838

Kha, H.T., Basseri, B., Shouhed, D., Richardson, J., Tetradis, S., Hahn, T.J. & Parhami, F. (2004) Oxysterols regulate differentiation of mesenchymal stem cells: pro-bone and anti-fat. *J Bone Miner Res.* 19: 830-40

Kifor, O., Diaz, R., Butters, R. & Brown, E.M. (1997) The Ca^{2+}-sensing receptor (CaR) activates phospholipases C, A2, and D in bovine parathyroid and CaR-transfected, human embryonic kidney (HEK293) cells. *J Bone Miner Res.* 12: 715-725

Klimatcheva, E. & Wonderlin, W.F. (1999). An ATP-sensitive K(+) current that regulates progression through early G1 phase of the cell cycle in MCF-7 human breast cancer cells. *J Membr Biol.* 171: 35-46

Koplas, P.A., Rosenberg, R.L. & Oxford, G.S. (1997) The role of calcium in the desensitization of capsaicin responses in rat dorsal root ganglion neurons. *J Neurosci.* 17(10): 3525-37

Kunzelmann, K. (2005) Ion channels and cancer. *J Membr Biol.* 205: 159-173

Kuo, A., Gulbis, J.M., Antcliff, J.F., Rahman, T., Lowe, E.D., Zimmer, J., Cuthbertson, J., Ashcroft, F.M., Ezaki, T. & Doyle, D.A. (2003) Crystal structure of the potassium channel KirBac1.1 in the closed state. *Science*. 300: 1922-1926

Kuzhikandathil, E.V., Wang, H., Szabo, T., Morozova, N., Blumberg, P.M. & Oxford, G.S. (2001) Functional analysis of capsaicin receptor (vanilloid receptor subtype 1) multimerization and agonist responsiveness using a dominant negative mutation. *J Neurosci*. 21: 8697-706

Kwai, K., Tamaki, A., & Hirohata, K. (1985) Steroid induced accumulation of lipid in the osteocytes of the rabbit femoral head. *J Bone Jt Surg*. 67A: 755-763

Labelle, D., Jumarie, C. & Moreau, R. (2007) Capacitative calcium entry and proliferation of human osteoblast-like MG-63 cells. *Cell Prolif*. 40(6): 866-84

Laketić-Ljubojević, I., Suva, L.J., Maathuis, F.J., Sanders, D. & Skerry, T.M. (1999) Functional characterization of N-methyl-D-aspartic acid-gated channels in bone cells. *Bone*. 25(6): 631-7

Lang, F., Föller, M., Lang, K., Lang, P., Ritter, M., Vereninov, A., Szabo, I., Huber, S.M. & Gulbins, E. (2007) Cell volume regulatory ion channels in cell proliferation and cell death. *Methods Enzymol*. 428: 209-25

Lappin, S.C., Randall, A.D., Gunthorpe, M.J. & Morisset, V. (2006) TRPV1 antagonist, SB-366791, inhibits glutamatergic synaptic transmission in rat spinal dorsal horn following peripheral inflammation. *Eur J Pharmacol*. 540(1-3): 73-81

Launay, P., Fleig, A., Perraud, A.L., Scharenberg, A.M., Penner, R. & Kinet, J.P. (2002) TRPM4 is a Ca^{2+}-activated nonselective cation channel mediating cell membrane depolarization. *Cell*. 109: 397-407

Lazzeri, M., Vannucchi, M.G., Spinelli, M., Bizzoco, E., Beneforti, P., Turini, D. & Faussone-Pellegrini, M.S. (2005) Transient receptor potential vanilloid type 1 (TRPV1) expression changes from normal urothelium to transitional cell carcinoma of human bladder. *Eur Urol*. 48(4): 691-8

Lee, N., Chen, J., Sun, L., Wu, S., Gray, K.R., Rich, A., Huang, M., Lin, J.H., Feder, J.N., Janovitz, E.B., Levesque, P.C. & Blanar, M.A. (2003) Expression and characterization of human transient receptor potential melastatin 3 (hTRPM3). *J Biol Chem* 278: 20890-20897

Lehen'kyi, V., Flourakis, M., Skryma, R., & Prevarskaya, N. (2007) TRPV6 channel controls prostate cancer cell proliferation via Ca^{2+}/NFATdependent pathways. *Oncogene*. 26(52): 7380-5

Leonard, R.J., Garcia, M.L., Slaughter, R.S. & Reuben, J.P. (1992) Selective blockers of voltage-gated K^+ channels depolarise human T-lymhocytes: mechanism of the antiproliferative effect. *Proc Nat Acad Sci USA*. 89: 10094-10098

Lévesque, M., Martineau, C., Jumarie, C. & Moreau, R. (2008) Characterization of cadmium uptake and cytotoxicity in human osteoblast-like MG-63 cells. *Toxicol Appl Pharmacol*. Published online ahead of print. doi: 10.1016/j.taap.2008.04.016

Lewis, R.S. & Cahalan, M.D. (1989) Mitogen-induced oscillations of cytosolic Ca^{2+} and transmembrane Ca^{2+} current in human leukemic T cells. *Cell Regul*. 1: 99-112

Lewis, R.S. (2007) The molecular choreography of store-operated calcium channel. *Nature*. 446(7133): 284-7

Li, B., Henney, N.C., Evans, B.A.J. & Wann, K.T. (2007) Large conductance potassium channel in human osteoblast cells. *Proceeding of the British Pharmacological Society* at http://bps.conference-services.net/viewPDF.asp?conferenceID=1175&abstractID=177854

Li, G.-R., Deng, X.-L., Sun, H., Chung, S.S.M., Tse, H.-F. & Lau, C.-P. (2006) Ion channels in mesenchymal stem cells from rat bone marrow. *Stem Cells*. 24: 1519-1528

Li, G.-R., Sun, H., Deng, X. & Lau, C.-P. (2005) Characterisation of ionic currents in human mesenchymal stem cells from bone marrow. *Stem Cells*. 23: 371-382

Li, Z., Lu, J., Xu, P., Xie, X., Chen, L. & Xu, T. (2007) Mapping the interacting domains of STIM1 & Orai1 in Ca^{2+} release activated Ca^{2+} channel activation. *J Biol Chem*. 282: 29448-29456

Lieberherr, M., Grosse, B., Kachkache, M. & Balsan, S. (1993) Cell signaling and estrogens in female rat osteoblasts: a possible involvement of unconventional nonnuclear receptors. *J Bone Miner Res*. 8(11): 1365-76

Liedtke, W., Choe, Y., Marti-Renom, M.A., Bell, A.M., Denis, C.S., Sali, A., Hudspeth, A.J., Friedman, J.M. & Heller, S. (2000) Vanilloid receptor-related osmotically activated channel (VR-OAC), a candidate vertebrate osmoreceptor. *Cell*. 103: 525-35

Ligresti, A., Bisogno, T., Matias, I., De Petrocellis, L., Cascio, M.G., Cosenza, V., D'argenio, G., Scaglione, G., Bifulco, M., Sorrentini, I. & Di Marzo, V. (2003) Possible endocannabinoid control of colorectal cancer growth. *Gastroenterology*. 125: 677-687

Liman, R.E., Corey, P.D. & Dulac, C. (1999) TRP2: a candidate transduction channel for mammalian pheromone sensory signaling. *Proc Natl Acad Sci U S A*. 96: 5791-6

Lips, P. (2006) Vitamin D physiology. *Prog Biophys Mol Biol*. 92(1): 4-8

Lipton, A., Costa, L., Ali, S.M. & Demers, L.M. (2001) Bone markers in the management of metastatic bone disease. *Cancer Treat Rev*. 27(3): 181-185

Liss, B., Bruns, R. & Roeper, J. (1999) Alternative sulfonylurea receptor expression defines metabolic sensitivity of K-ATP channels in dopaminergic midbrain neurones. *EMBO J*. 18: 833-846

Liu, B., Zhang, C. & Qin, F. (2005) Functional recovery from desensitization of vanilloid receptor trpv1 requires resynthesis of phosphatidylinositol 4,5-bisphosphate. *J Neurosci*. 25(19): 4835- 4843

Liu, X., Singh, B.B. & Ambudkar, I.S. (2003) TRPC1 is required for functional store-operated Ca^{2+} channels. Role of acidic amino acid residues in the S5-S6 region. *J Biol Chem*. 278: 11337-11343

Liu, X., Wang, W., Singh, B.B., Lockwich, T.P., Jadlowiec, J., O'Connell, B., Wellner, R., Zhu, M.X. & Ambudkar, I.S. (2000) Trp1, a candidate protein for the store-operated Ca^{2+} influx mechanism in salivary gland cells. *J Biol Chem*. 275: 3403-3411

Long, S.B., Campbell, E.B. & Mackinnin, R. (2005) Crystal structure of a mammalian voltage-dependent shaker family K^+ channel. *Science* 309: 897-903

Lopatin, A.N., Makhina, E.N., & Nichols, C.G. (1994) Potassium channel block by cytoplasmic polyamines as the mechanism of intrinsic rectification. *Nature*. 372: 366-369

Lu, G., Henderson, D., Liu, L., Reinhart, P.H. & Simon, S.A. (2005) TRPV1b, a functional human vanilloid receptor splice variant. *Mol Pharmacol*. 67(4): 1119-27. Erratum in: *Mol Pharmacol*. (2005) 67(5): 1818

Lukacs, V., Thyagarajan, B., Varnai, P., Balla, A., Balla, T. & Rohacs, T. (2007) Dual regulation of TRPV1 by phosphoinositides. *J Neurosci*. 27(26): 7070-80

Maccarrone, M., Lorenzon, T., Bari, M., Melino, G. & Finazzi-Agro, A. (2000) Anandamide induces apoptosis in human cells via vanilloid receptors: evidence for a protective role of cannabinoid receptors. *J Biol Chem*. 275: 31938-31945

Mackie, E.J. (2003) Osteoblasts: novel roles in orchestration of skeletal architecture. *Int J Biochem Cell Biol*. 35: 1301-1305

Maggi, C.A., Patacchini, R., Santicioli, P., Theodorsson, E. & Meli, A. (1988) Several neuropeptides determine the visceromotor response to capsaicin in the guinea-pig isolated ileal longitudinal muscle. *Eur J Pharmacol.* 148(1): 43-9

Malhi, H., Irani, A.N., Rajvanshi, P., Suadicani, S.O., Spray, D.C., McDonald, T.V. and Gupta, S. (2000) K$_{ATP}$ channels regulate mitogenically induced proliferation in primary rat hepatocytes and human liver cell lines. *J Biol Chem.* 275(34): 26050-26057

Mancilla, E.E., Galindo, M., Fertilio, B., Herrera, M., Salas, K., Gatica, H. & Goecke, A. (2007) L-type calcium channels in growth plate chondrocytes participate in endochondral ossification. *J Cell Biochem.* 101(2): 389-98

Mandadi, S., Numazaki, M., Tominaga, M., Bhat, M.B., Armati, P.J. & Roufogalis, B.D. (2004) Activation of protein kinase C reverses capsaicin-induced calcium-dependent desensitization of TRPV1 ion channels. *Cell Calcium.* 35(5): 471-8

Mang, C.F., Erbelding, D. & Kilbinger, H. (2001) Differential effects of anandamide on acetylcholine release in the guinea-pig ileum mediated via vanilloid and non-CB$_1$ cannabinoid receptors. *Br J Pharmacol.* 134(1): 161-7

Marcelli, M., Tilley, W.D., Wilson, C.M., Wilson, J.D., Griffin, J.E. & McPhaul, M.J. (1990) A single nucleotide substitution introduces a premature termination codon into the androgen receptor gene of a patient with receptor-negative androgen resistance. *J Clin Invest.* 85(5): 1522-8

Marotti, G. (2000) The osteocyte as a wiring transmission system. *J Musculoskelet Neuronal Interact.* 1(2): 133-6

Martin, E. & Shapiro, J.R. (2007) Osteogenesis imperfecta: epidemiology and pathophysiology. *Curr Osteoporos Rep.* 5(3): 91-97

Martin, R.B. & Zissimos, S.L. (1991) Relationships between marrow fat and bone turnover in ovariectomized and intact rats. *Bone.* 12: 123-131

Mason, D.J., Suva, L.J., Genever, P.J., Patton, A.J., Stueckle, S., Hillam, R.A. & Skerry, T.M. (1997) Mechanically regulated expression of a neural glutamate transported in bone. A role for excitatory amino acids as osteotropic agents. *Bone.* 20: 199-205

Matthews, G., Neher, E. & Penner, R. (1989) Second messenger-activated calcium influx in rat peritoneal mast cells. *J Physiol.* 418: 105-130

McKallip, R.J., Lombard, C., Fisher, M., Martin, B.R., Ryu, S., Grant, S., Nagarkatti, P.S. & Nagarkatti, M. (2002) Targeting CB$_2$ cannabinoid receptors as a novel therapy to treat malignant lymphoblastic disease. *Blood.* 100: 627-634

McKemy, D.D., Neuhausser, W.M. & Julius, D. (2002) Identification of a cold receptor reveals a general role for TRP channels in thermosensation. *Nature.* 416(6876): 52-8

McKenzie, R., Reynolds, J.C., O'Fallon, A., Dale, J., Deloria, M., Blackwelder, W. & Straus, S.E. (2000) Decreased bone mineral density during low dose glucocorticoid administration in a randomized, placebo controlled trial. *J Rheumatol.* 27: 2222-2226

McQuillan, D.J., Richardson, M.D. & Bateman, J.F. (1995) Matrix deposition by a calcifying human osteogenic sarcoma cell line (SaOS-2). *Bone.* 16: 415-426

Medvedeva, Y.V., Kim, M.S. & Usachev, Y.M. (2008) Mechanisms of prolonged presynaptic Ca^{2+} signaling and glutamate release induced by TRPV1 activation in rat sensory neurons. *J Neurosci.* 28(20): 5295-311

Meggio, F., Donella Deana. A., Ruzzene, M., Brunati, A.M., Cesaro, L., Guerra, B., Meyer, T., Mett, H., Fabbro, D., Furet, P., *et al.* (1995) Different susceptibility of protein kinases to staurosporine inhibition. Kinetic studies and molecular bases for the resistance of protein kinase CK2. *Eur J Biochem.* 234: 317-322

Mentaverri, R., Kamel, S. & Brazier, M. (2003) Involvement of capacitive calcium entry and calcium store refilling in osteoclastic survival and bone resorption process. *Cell Calcium*. 34(2): 169-75

Mercer, J.C., Dehaven, W.I., Smyth, J.T., Wedel, B., Boyles, R.R., Bird, G.S. & Putney, J.W., Jr. (2006) Large store-operated calcium selective currents due to co-expression of Orai1 or Orai2 with the intracellular calcium sensor, Stim1. *J Biol Chem*. 281: 24979-24990

Mergler, S., Strowski, M.Z., Kaiser, S., Plath, T., Giesecke, Y., Neumann, M., Hosokawa, H., Kobayashi, S., Langrehr, J., Neuhaus, P., Plöckinger, U., Wiedenmann, B. & Grötzinger, C. (2007) Transient receptor potential channel TRPM8 agonists stimulate calcium influx and neurotensin secretion in neuroendocrine tumor cells. *Neuroendocrinology*. 85(2): 81-92

Messenger, A.G. & Rundegren, J. (2004) Minoxidil: mechanisms of action on hair growth. *Br J Dermatol*. 150(2): 186-94

Meszaros, J.G., Karin, N.J. & Farach-Carson, M.C. (1996) Voltage-sensitive calcium channels in osteoblasts: mediators of plasma membrane signalling events. *Connect Tissue Res*. 35(1-4): 107-11

Meunier, P., Aaron, J., Edouard, G., & Vignon, G. (1971) Osteoporosis and the replacement of cell populations of the marrow adipose tissue. *Clin Orthop*. 80: 147-154

Meunier, P.J., Roux, C., Seeman, E., Ortolani, S., Badurski, J.E., Spector, T.D., Cannata, J., Balogh, A., Lemmel, E.M., Pors-Nielsen, S., Rizzoli, R., Genant, H.K. & Reginster, J.Y. (2004). The effects of strontium ranelate on the risk of vertebral fracture in women with postmenopausal osteoporosis. *N Engl J Med*. 350(5): 459-68

Meyer, M.B., Watanuki, M., Kim, S., Shevde, N.K. & Pike, J.W. (2006) The human transient receptor potential vanilloid type 6 distal promoter contains multiple vitamin D receptor binding sites that mediate activation by 1,25-dihydroxyvitamin D3 in intestinal cells. *Mol Endocrinol*. 20(6): 1447-61

Miki, H., Maercklein, P.B. & Fitzpatrick, L.A. (1995) Spontaneous oscillations of intracellular calcium in single bovine parathyroid cells may be associated with the inhibition of parathyroid hormone secretion. *Endocrinology*. 136: 2954-2959

Minke, B. & Cook, B. (2002). TRP channel proteins and signal transduction. *Physiol Rev*. 82: 429-72

Minta, A., Kao, J.P. & Tsien, R.Y. (1989) Fluorescent indicators for cytosolic calcium based on rhodamine and fluorescein chromophores. *J Biol Chem*. 264(14): 8171-8

Mohapatra, D.P. & Nau, C. (2003) Desensitization of capsaicin-activated currents in the vanilloid receptor TRPV1 is decreased by the cyclic AMP-dependent protein kinase pathway. *J Biol Chem*. 278: 50080 -50090

Montell, C. (2003) The venerable inveterate invertebrate TRP channels. *Cell Calcium*. 33: 409-417

Montell, C. (2004). Molecular genetics of Drosophila TRP channels. *Novartis Found Symp*. 258: 3-12; discussion 12-7, 98-102, 263-6

Montell, C. (2005a) *Drosophila* TRP channels. *Pflügers Arch*. 451(1): 19-28

Montell, C. (2005b) The TRP superfamily of cation channels. *Sci STKE*. 2005(272): re3

Montell, C. & Rubin, G.M. (1989) Molecular characterization of the Drosophila trp locus: a putative integral membrane protein required for phototransduction. *Neuron*. 2(4): 1313-23

Montell, C., Birnbaumer, L. & Flockerzi, V. (2002a) The TRP channels, a remarkable functional family. *Cell*. 108: 595-598

Montell, C., Birnbaumer, L., Flockerzi, V., Bindels, R.J., Bruford, E.A., Caterina, M.J., Clapham, D., Harteneck, C., Heller, S., Julius, D., Kojima, I., Mori, Y., Penner, R., Prawitt, D., Scharenberg, A.M., Schultz, G., Shimizu, S. & Zhu, M.X. (2002b) A unified nomenclature for the superfamily of TRP cation channels. *Mol Cell.* 9: 229-231

Montell, C., Jones, K., Hafen, E. & Rubin, G. (1985) Rescue of the Drosophila phototransduction mutation trp by germline transformation. *Science.* 230(4729): 1040-3

Moran, M.M., Xu, H. & Clapham, D.E. (2004) TRP ion channels in the nervous system. *Curr Opin Neurobiol.* 14: 362-369

Moreau, R., Aubin, R., Lapointe, J.Y. & Lajeunesse, D. (1997) Pharmacological and biochemical evidence for the regulation of osteocalcin secretion by potassium channels in human osteoblast-like MG63 cells. *J Bone Miner Res.* 12(12): 1984-1992

Moreau, R., Hurst, A.M., Lapointe, J.Y. & Lajeunesse, D. (1996) Activation of maxi-K channels by parathyroid hormone and prostaglandin E_2 in human osteoblast bone cells. *J Membr Biol.* 150: 175-84

Mori, A., Lehmann, S., O'Kelly, J., Kumagai, T., Desmond, J.C., Pervan, M., McBride, W.H., Kizaki, M. & Koeffler, H.P. (2006) Capsaicin, a component of red peppers, inhibits the growth of androgen-independent, p53 mutant prostate cancer cells. *Cancer Res.* 66(6): 3222-9

Motter, A.L. & Ahern, G.P. (2008) TRPV1-null mice are protected from diet-induced obesity. *FEBS Lett.* 582(15): 2257-62

Mourre, C., Ben Ari, Y., Bernardi, H., Forest, M. & Lazdunski, M. (1989) Antidiabetic sulfonylureas: Localization of binding sites in the brain and effects on the hyperpolarization induced by anoxia in hippocampal slices. *Brain Res.* 486: 159-164

Muik, M., Frischauf, I., Derler, I., Fahrner, M., Bergsmann, J., Eder, P., Schindl, R., Hesch, C., Polzinger, B., Fritsch, R., Kahr, H., Madl, J., Gruber, H., Groschner, K. & Romanin, C. (2008) Dynamic coupling of the putative coiled-coil domain of ORAI1 with STIM1 mediates ORAI1 channel activation. *J Biol Chem.* 283(12): 8014-22

Mundy, G.R. (2002) Metastasis to bone: causes, consequences and opportunities. *Nat Rev Cancer.* 2(8): 584-93

Mundy, G.R. (2003) Endothelin-1 and osteoblastic metastasis. *Proc Natl Acad Sci USA.* 10(19): 1954-9

Muraki, K., Iwata, Y., Katanosaka, Y., Ito, T., Ohya, S., Shigekawa, M. & Imaizumi, Y. (2003) TRPV2 is a component of osmotically sensitive cation channels in murine aortic myocytes. *Circ Res.* 93: 829-38

Murphy, C.E. & Rodgers, P.T. (2007) Effects of thiazolidinediones on bone loss and fracture. *Ann Pharmacother.* 41(12): 2014-8

Nadler, M.J., Hermosura, M.C., Inabe, K., Perraud, A.L., Zhu, Q., Stokes, A.J., Kurosaki, T., Kinet, J.P., Penner, R., Scharenberg, A.M., Fleig, A. (2001) LTRPC7 is a Mg-ATP-regulated divalent cation channel required for cell viability. *Nature.* 411: 590-595

National Centre for Biotechnology Information (NCBI). [WWW] <http://www.ncbi.nlm.nih.gov/>

National Osteoporosis Society (2006) Osteoporosis facts and Figures v1.1. Accessed June 2008. [PDF] available from <http://www.nos.org.uk/professionals/support-for-professionals.htm>

Nauli, S. M., Alenghat, F.J., Luo, Y., Williams, E., Vassilev, P., Li, X., Elia, A.E., Lu, W., Brown, E.M., Quinn, S.J., Ingber, D.E. & Zhou, J. (2003) Polycystins 1 and 2 mediate mechanosensation in the primary cilium of kidney cells. *Nature Genet.* 33: 129-137

Neher, E. & Sakmann, B. (1976) Single channel currents recorded from membrane of denervated frog muscle fibres. *Nature.* 260: 799-802

Ng, B. & Barry, P.H. (1995) The measurement of ionic conductivities and mobilities of certain less common organic ions needed for junction potential corrections in electrophysiology. *J Neurosci Methods*. 56(1): 37-41

Nijenhuis, T., Hoenderop, J.G., van der Kemp, A.W. & Bindels, R.J.(2003a) Localization and regulation of the epithelial Ca^{2+} channel TRPV6 in the kidney. *J Am Soc Nephrol*. 14: 2731-2740

Nijenhuis, T., Hoenderop, J.G., Nilius, B. & Bindels, R.J. (2003b) (Patho)physiological implications of the novel epithelial Ca^{2+} channels TRPV5 and TRPV6. *Pflugers Arch*. 446: 401-409

Nilius, B. (2003) From TRPs to SOCs, CCEs, and CRACs: consensus and controversies. *Cell Calcium*. 33(5-6): 293-8

Nilius, B. & Droogmans, G. (1994) A role for K^+ channels in cell proliferation. *News Physiol Sci*. 9: 105-110

Nilius, B. & Voets, T. (2004) Diversity of TRP channel activation. *Novartis Found Symp*. 258: 140-9; discussion 149-59, 263-6

Nilius B, Owsianik G, Voets T, Peters JA. (2007) Transient receptor potential cation channels in disease. *Physiol Rev*. 87(1): 165-217

Nilius, B., Talavera, K., Owsianik, G., Prenen, J., Droogmans, G. & Voets, T. (2005) Gating of TRP channels: a voltage connection? *J Physiol*. 567: 35-44

Nishida, M. & MacKinnon, R. (2002) Structural basis of inward rectification: cytoplasmic pore of the G protein-gated inward rectifier GIRK1 at 1.8 Å resolution. *Cell*. 111: 957-965

Notini, A.J., McManus, J.F., Moore, A., Bouxsein, M., Jimenez, M., Chiu, W.S., Glatt, V., Kream, B.E., Handelsman, D.J., Morris, H.A., Zajac, J.D., Davey, R.A.(2007) Osteoblast deletion of exon 3 of the androgen receptor gene results in trabecular bone loss in adult male mice. *J Bone Miner Res*. 22(3): 347-56

Novakova-Tousova, K., Vyklicky, L., Susankova, K., Benedikt, J., Samad, A., Teisinger, J. & Vlachova, V. (2007) Functional changes in the vanilloid receptor subtype 1 channel during and after acute desensitization. *Neuroscience*. 149(1): 144-54

Numazaki, M., Tominaga, T., Takeuchi, K., Murayama, N., Toyooka, H. & Tominaga, M. (2003) Structural determinant of TRPV1 desensitization interacts with calmodulin. *Proc Natl Acad Sci USA*. 100: 8002- 8006

Nuttall, M.E., Patton, A.J., Olivera, D.L., Nadeau, D.P., & Gowen, M. (1998) Human bone trabecular bone cells are able to express both osteoblastic and adipocytic phenotypes: implications for osteopenic disorders. *J Bone Min Res*. 13: 371-382

Ofek, O., Karsak, M., Leclerc, N., Fogel, M., Frenkel, B., Wright, K., Tam, J., Attar-Namdar, M., Kram, V., Shohami, E., Mechoulam, R., Zimmer, A. & Bab, I. (2006). Peripheral cannabinoid receptor, CB2, regulates bone mass. *Proc Natl Acad Sci USA*. 103: 696-701

Okamoto, F., Kajiya, H., Toh, K., Uchida, S., Yoshikawa, M., Sasaki, S., Kido, M.A., Tanaka, T. & Okabe, K. (2008) Intracellular ClC-3 chloride channels promote bone resorption in vitro through organelle acidification in mouse osteoclasts. *Am J Physiol Cell Physiol*. 294(3): C693-701

Orriss, I.R., Knight, G.E., Ranasinghe, S., Burnstock, G. & Arnett, T.R. (2006) osteoblast responses to nucleotides increase during differentiation. *Bone*. 39: 300-309

Ouadid-Ahidouch, H., Roudbaraki, M., Delcourt, P., Ahidouch, A., Joury, N. & Prevarskaya, N. (2004) Functional and molecular identification of intermediate-conductance Ca^{2+}-activated K^+ channels in breast cancer cells: association with cell cycle progression. *Am J Physiol*. 287: C125-C134

Paget, S. (1889) The distribution of secondary growths in cancer of the breast. *Lancet*. 1: 571-573

Pardo, L.A., Camino, D., Sanchez, A., Alves, F., Brüggemann, A., Beckh, S. & Stühmer, W. (1999) Oncogenic potential of EAG K⁺ channels. *EMBO J.* 18: 5540-5547

Parekh, A.B. & Putney, J.W., Jr. (2005) Store-operated calcium channels. *Physiol Rev.* 85: 757-810

Parfitt, A.M., Shih, M.-S., Rao, D.S., & Kleerekoper, M. (1992) Relationship between bone formation rate and osteoblast surface in aging and osteoporosis: evidence for impaired osteoblast recruitment in pathogenesis. *J Bone Miner Res.* 7(1): 116 (abstract)

Parihar, A.S., Coghlan, M.J., Gopalakrishnan, M. & Shieh, C.C. (2003) Effects of intermediate-conductance Ca²⁺-activated K⁺ channel modulators on human prostate cancer cell proliferation. *Eur J Pharmacol.* 471: 157-164

Patlak, J.B. (1988) Sodium channel subconductance levels measured with a new variance-mean analysis. *J Gen Physiol.* 92(4): 413-30

Pautke, C., Schieker, M., Tischer, T., Kolk, A., Neth, P., Mutschler, W. & Milz, S. (2004) Characterization of osteosarcoma cell lines MG-63, SaOS-2 and U-2 OS in comparison to human osteoblasts. *Anticancer Res.* 24(6): 3743-8

Pedersen, S.F., Owsianik, G. & Nilius, B. (2005) TRP channels: an overview. *Cell Calcium.* 38: 233-252

Peier, A.M., Moqrich, A., Hergarden, A.C., Reeve, A.J., Andersson, D.A., Story, G.M., Earley, T.J., Dragoni, I., McIntyre, P., Bevan, S. & Patapoutian, A. (2002a) A TRP channel that senses cold stimuli and menthol. *Cell.* 108: 705-715

Peier, A.M., Reeve, A.J., Andersson, D.A., Moqrich, A., Earley, T.J., Hergarden, A.C., Story, G.M., Colley, S., Hogenesch, J.B., McIntyre, P., Bevan, S. & Patapoutian, A. (2002b) A heat-sensitive TRP channel expressed in keratinocytes. *Science.* 296: 2046-9

Peinelt, C., Vig, M., Koomoa, D.L., Beck, A., Nadler, M.J., Koblan-Huberson, M., Lis, A., Fleig, A., Penner, R. & Kinet, J.P. (2006) Amplification of CRAC current by STIM1 and CRACM1 (Orai1). *Nat Cell Biol.* 8: 771-773

Peng, J.B., Chen, X.Z., Berger, U.V., Vassilev, P.M., Tsukaguchi, H., Brown, E.M. & Hediger, M.A. (1999) Molecular cloning and characterization of a channel-like transporter mediating intestinal calcium absorption. *J Biol Chem.* 274: 22739-46

Peng, J.B., Chen, X.Z., Berger, U.V., Weremowicz, S., Morton, C.C., Vassilev, P.M. & Brown, E.M. (2000) Human calcium transport protein CaT1. *Biochem Biophys Res Commum.* 278: 326-332

Peng, J.B., Zhuang, L., Berger, U.V., Adam, R.M., Williams, B.J., Brown, E.M., Hediger, M.A. & Freeman, M.R. (2001) CaT1 expression correlates with tumour grade in prostate cancer. *Biochem Biophys Res Commun.* 282: 729-734

Penner, R., Matthews, G. & Neher, E. (1988) Regulation of calcium influx by second messengers in rat mast cells. *Nature.* 334: 499-504

Perraud, A.L., Fleig, A., Dunn, C.A., Bagley, L.A., Launay, P., Schmitz, C., Stokes, A.J., Zhu, Q., Bessman, M.J., Penner, R., Kinet, J.P. & Scharenberg, A.M. (2001) ADP-ribose gating of the calcium-permeable LTRPC2 channel revealed by Nudix motif homology. *Nature.* 411: 595-9

Petty, S.J., O'Brien, T.J. & Wark, J.D. (2007) Anti-epileptic medication and bone health. *Osteoporosis International.* 18(2): 129-42

Piper, A.S., Yeats, J.C., Bevan, S. & Docherty, R.J. (1999) A study of the voltage dependence of capsaicin-activated membrane currents in rat sensory neurones before and after acute desensitization. *J Physiol.* 518: 721-733

Pogatzki-Zahn, E.M., Shimizu, I., Caterina, M. & Raja, S.N. (2005) Heat hyperalgesia after incision requires TRPV1 and is distinct from pure inflammatory pain. *Pain.* 115: 296-307

Poole, K.E. & Reeve, J. (2005) Parathyroid hormone - a bone anabolic and catabolic agent. *Curr Opin Pharmacol.* 5(6): 612-7

Potier, M. & Trebak, M. (2008) New developments in the signaling mechanisms of the store-operated calcium entry pathway. *Pflugers Arch.* (in press) doi: 10.1007/s00424-008-0533-2

Powell, G.J., Southby, J., Danks, J.A., Stillwell, R.G., Hayman, J.A., Henderson, M.A., Bennett, R.C. & Martin, T.J. (1991) Localization of parathyroid hormone-related protein in breast cancer metastases: increased incidence in bone compared with other sites. *Cancer Res.* 51(11): 3059-3061

Prevarskaya, N., Zhang, L. & Barritt, G. (2007) TRP channels in cancer. *Biochim Biophys Acta.* 1772(8): 937-46

Pugsley, L.I. & Selye,H. (1933) The histological changes in the bone responsible for the action of parathyroid hormone on the calcium metabolism of the rat. *J Physiol.* 79: 113-117

Puntambekar, P., Van Buren, J., Raisinghani, M., Premkumar, L.S. & Ramkumar, V. (2004) Direct interaction of adenosine with the TRPV1 channel protein. *J Neurosci.* 24(14): 3663-71

Putney, J.W., Jr (1986) A model for receptor-regulated calcium entry. *Cell Calcium.* 7: 1-12

Putney, J.W., Jr (1990) Capacitative calcium entry revisited. *Cell Calcium.* 11: 611-624

Raisinghani, M., Pabbidi, R.M. & Premkumar, L.S. (2005) Activation of transient receptor potential vanilloid 1 (TRPV1) by resiniferatoxin. *J Physiol.* 567(3): 761-786

Ralston, S.H. (2008) Pathogenesis of Paget's disease of bone. *Bone.* 43(5): 819-825

Rami, K.H., Thompson, M., Wyman, P., Jerman, C.J., Egerton, J., Brough, S., Stevens, J.A., Randall, D.A., Smart, D., Gunthorpe, J.M. & Davis, B.J. (2004) Discovery of small molecule antagonists of TRPV1. *Bioorg Med Chem Lett.* 14: 3631-4

Ramsey, I.S., Delling, M. & Clapham, D.E. (2006) An introduction to TRP channels. *Annu Rev Physiol.* 68: 619-47

Ravesloot, J.H., van Houten, R.J., Ypey, D.L. & Nijweide, P.J. (1990) Identification of Ca^{2+}-activated K^+ channels in cells of embryonic chick osteoblast cultures. *J Bone Miner Res.* 5(12): 1201-10

Rezzonico, R., Cayatte, C., Bourget-Ponzio, I., Romey, G., Belhacene, N., Loubat, A., Rocchi, S., van Obberghen, E., Girault, J.-A., Rossi, B. & Schmid-Antomarchi, H. (2003) Focal adhesion kinase pp125^{KK} interacts with the large conductance calcium-activated hSlo potassium channel in human osteoblasts: potential role in mechanotransduction. *J Bone Miner Res.* 18: 1863-1871

Rezzonico, R., Schmid-Alliana, A., Romey, G., Bourget-Ponzio, I., Breuil, V., Breittmayer, V., Tartare-Deckert, S., Rossi, B. & Schmid-Antomarchi, H. (2002) Prostaglandin E_2 induces interaction between hSlo potassium channel and Syk tyrosine kinase in osteosarcoma cells. *J Bone Miner Res.* 17(5): 869-878

Riccio, A., Medhurst, D.A., Mattei, C., Kelsell, E.R., Calver, R.A., Randall, D.A., Benham, D.C., & Pangalos, N.M. (2002) mRNA distribution analysis of human TRPC family in CNS and peripheral tissues. *Brain Res Mol Brain Res.* 109: 95-104

Richter, C, & Ferrier, J 1991 Continuously Active Sodium Channels in Osteoblastic ROS 17/2.8 Cells. Bone and Mineral 15(1): 57-71

Rodan, S.B., Imai, Y., Thiede, M.A., Wesolowski, G., Thompson, D., Bar-Shavit, Z., Shull, S., Mann, K. & Rodan, G.A. (1987) Characterization of a human osteosarcoma cell line (Saos-2) with osteoblastic properties. *Cancer Research.* 47(18): 4961-4966

Rohács, T., Lopes, C.M., Michailidis, I. & Logothetis, D.E. (2005) PI(4,5)P$_2$ regulates the activation and desensitization of TRPM8 channels through the TRP domain. *Nat Neurosci.* 8(5): 626-34

Roodman, G.D. (1992) Interleukin-6: an osteotropic factor? *J Bone Miner Res.* 7: 475-478

Roos, J., DiGregorio, P.J., Yeromin, A.V., Ohlsen, K., Lioudyno, M., Zhang, S., Safrina, O., Kozak, J.A., Wagner, S.L., Cahalan, M.D., Velicelebi, G. & Stauderman, K.A. (2005) STIM1, an essential and conserved component of store-operated Ca^{2+} channel function. *J Cell Biol.* 169: 435-445

Rosen, C.J. & Bouxsein, M.L. (2006) Mechanisms of Disease: Is osteoporosis the obesity of bone? *Nat Clin Pract Rheumatol.* 2: 35-43

Rosenbaum, T., Gordon-Shaag, A., Munari, M. & Gordon, S.E. (2004) Ca^{2+}/calmodulin modulates TRPV1 activation by capsaicin. *J Gen Physiol.* 123: 53- 62

Roura-Ferrer, M., Solé, L., Martínez-Mármol, R., Villalonga, N. & Felipe, A. (2008) Skeletal muscle Kv7 (KCNQ) channels in myoblast differentiation and proliferation. *Biochem Biophys Res Commun.* 369(4): 1094-7

Rozen, S. & Skaletsky, H.J. (2000) Primer3 on the WWW for general users and for biologist programmers. In: Krawetz S, Misener S (eds) *Bioinformatics Methods and Protocols: Methods in Molecular Biology.* Humana Press, Totowa, NJ, pp 365-386

Rozman, C., Feliu, E., Berga, L., Reverter, J.C., Climent, C., & Ferran, M.-J. (1989) Age related variations of fat tissue fraction in normal human bone marrow depend both on size and number of adipocytes: a stereological study. *Exp Hematol.* 17: 34-7

Runnels, W.L., Yue, L. & Clapham, E.D. (2001) TRP-PLIK, a bifunctional protein with kinase and ion channel activities. *Science.* 291: 1043-7

Ryder, K.D. & Duncan, R.L. (2001) Parathyroid hormone enhances fluid shear-induced $[Ca^{2+}]_i$ signaling in osteoblastic cells through activation of mechanosensitive and voltage-sensitive Ca^{2+} channels. *J Bone Miner Res.* 16(2): 240-8

Ryu, S., Liu, B. & Qin, F. (2003) Low pH potentiates both capsaicin binding and channel gating of VR1 receptors. *J Gen Physiol.* 122: 45-61

Ryu, S., Liu, B., Yao, J., Fu, Q. & Qin, F. (2007) Uncoupling proton activation of vanilloid receptor TRPV1. *J Neurosci.* 27(47): 12797-807

Sakura, H., Ammälä, C., Smith, P.A., Gribble, F.M. & Ashcroft, F.M. (1995) Cloning and functional expression of the cDNA encoding a novel ATP-sensitive potassium channel subunit expressed in pancreatic b-cells, brain, heart and skeletal muscle. *FEBS Lett.* 377: 338-344

Salkoff, L., Butler, A., Ferreira, G., Santi, C. & Wei, A. (2006) High-conductance potassium channels of the SLO family. *Nat Rev Neurosci.* 7(12): 921-31.

Sanchez, M.G., Sanchez, A.M., Collado, B., Malagarie-Cazenave, S., Olea, N., Carmena, M.J., Prieto, J.C. & Diaz-Laviada, I. (2005) Expression of the transient receptor potential vanilloid 1 (TRPV1) in LNCaP and PC-3 prostate cancer cells and in human prostate tissue. *Eur J Pharmacol.* 515(1-3): 20-27

Sarker, K.P. & Maruyama, I. (2003) Anandamide induces cell death independently of cannabinoid receptors or vanilloid receptor 1: possible involvement of lipid rafts. *Cell Mol Life Sci.* 60: 1200-1208

Sartoris, D.J. & Resnick, D. (1989) Dual-energy radiographic absorptiometry for bone densitometry: current status and perspective. *Am J Roentgenol.* 152: 241-246

Savidge, J., Davis, C., Shah, K., Colley, S., Phillips, E., Ranasinghe, S., Winter, J., Kotsonis, P., Rang, H. & McIntyre, P. (2002) Cloning and functional characterization of the guinea pig vanilloid receptor 1. *Neuropharmacology.* 43(3): 450-6

Savidge, J.R., Ranasinghe, S.P. & Rang, H.P. (2001) Comparison of intracellular calcium signals evoked by heat and capsaicin in cultured rat dorsal root ganglion neurons and in a cell line expressing the rat vanilloid receptor, VR1. *Neuroscience.* 102(1): 177-84

Sausbier, M., Hu, H., Arntz, C., Feil, S., Kamm, S., Adelsberger, H., Sausbier, U., Sailer, C.A., Feil, R., Hofmann, F., Korth, M., Shipston, M.J., Knaus, H.G., Wolfer, D.P., Pedroarena, C.M., Storm, J.F. & Ruth, P. (2004) Cerebellar ataxia and Purkinje cell dysfunction caused by Ca^{2+}-activated K^+ channel deficiency. *Proc Natl Acad Sci USA.* 101(25): 9474-8

Sawynok, J. & Liu, X.J. (2003) Adenosine in the spinal cord and periphery: release and regulation of pain. *Prog Neurobiol.* 69: 313-340

Schilling, W.P. & Goel, M. (2004). Mammalian TRPC channel subunit assembly. *Novartis Found Symp.* 258: 18-30; discussion 30-43, 98-102, 263-6

Schlingmann, K.P., Waldegger, S., Konrad, M., Chubanov, V. & Gudermann, T. (2007) TRPM6 and TRPM7 - Gatekeepers of human magnesium metabolism. *Biochim Biophys Acta.* 1772(8): 813-21

Schlingmann, K.P., Weber, S., Peters, M., Niemann Nejsum, L., Vitzthum, H., Klingel, K., Kratz, M., Haddad, E., Ristoff, E., Dinour, D., Syrrou, M., Nielsen, S., Sassen, M., Waldegger, S., Seyberth, H.W. & Konrad, M. (2002) Hypomagnesemia with secondary hypocalcemia is caused by mutations in TRPM6, a new member of the TRPM gene family. *Nat Genet.* 31: 166-170

Schmid-Antomarchi, H., De Weille, J., Fosset, M. & Lazdunski, M. (1987) The receptor for antidiabetic sulfonylureas controls the activity of the ATP-modulated K^+ channel in insulin-secreting cells. *J Biol Chem.* 262: 15840-15844

Schmitz, C., Perraud, A.L., Johnson, C.O., Inabe, K., Smith, M.K., Penner, R., Kurosaki, T., Fleig, A. & Scharenberg, A.M. (2003) Regulation of vertebrate cellular Mg^{2+} homeostasis by TRPM7. *Cell.* 114: 191-200

Schmitz, C., Perraud, L.A., Fleig, A. & Scharenberg, M.A. (2004) Dual-function ion channel/protein kinases: novel components of vertebrate magnesium regulatory mechanisms. *Pediatr Res.* 55: 734-7

Schoeber, J.P., Hoenderop, J.G. & Bindels, R.J. (2007) Concerted action of associated proteins in the regulation of TRPV5 and TRPV6. *Biochem Soc Trans.* 35(1): 115-9

Schumacher, M.A., Moff, I., Sudanagunta, S.P. & Levine, J.D. (2000) Molecular cloning of an N-terminal splice variant of the capsaicin receptor. Loss of N-terminal domain suggests functional divergence among capsaicin receptor subtypes. *J Biol Chem.* 275(4): 2756-62

Schwarz, E.C., Wissenbach, U., Niemeyer, B.A., Strauss, B., Philipp, S.E., Flockerzi, V. & Hoth, M. (2006) TRPV6 potentiates calcium-dependent cell proliferation. *Dep Cell Calcium.* 39(2): 163-73

Shao, L.-R., Halvorsrud, R., Borg-Graham, L. & Storm, J.F. (1999) The role of BK-type Ca^{2+}-dependent K^+ channels in spike broadening during repetitive firing in rat hippocampal pyramidal cells. *J Physiol.* 521: 135-146

Shao, Y., Alocknavitch, M. & Farach-Carson, C. (2005) Expression of voltage sensitive calcium channel (VSCC) L-type Cav1.2 (a1c) and T-type (a1H) subunits during mouse development. *Dev Dyn.* 234: 54-62

Sharif Naeini, R., Witty, M.F., Séguéla, P. & Bourque, C.W. (2006) An N-terminal variant of Trpv1 channel is required for osmosensory transduction. *Nat Neurosci.* 9(1): 93-8

Shuba, Y.M., Prevarskaya, N., Lemonnier, L., Coppenolle, F., Kostyuk, P.G., Mauroy, B. & Skryma, R. (2000) Volume regulated chloride conductance in the LNCaP human prostate cancer cell line. *Am J Physiol Cell Physiol.* 279: C1144-C1154

Shyng, S., Ferrigni, T. & Nichols, C.G. (1997) Regulation of K_{ATP} channel activity by diazoxide and MgADP. Distinct functions of the two nucleotide binding folds of the sulfonylurea receptor. *J Gen Physiol.* 110: 643-654

Siegmund, S.V., Uchinami, H., Osawa, Y., Brenner, D.A. & Schwabe, R.F. (2005) Anandamide induces necrosis in primary hepatic stellate cells. *Hepatology*. 41(5): 1085-95

Smart, D., Gunthorpe, M.J., Jerman, J.C., Nasir, S., Gray, J., Muir, A.I., Chambers, J.K., Randall, A.D. & Davis, J.B. (2000) The endogenous lipid anandamide is a full agonist at the human vanilloid receptor (hVR1). *Br J Pharmacol*. 129(2): 227-30

Smith, P.K., Krohn, R.I., Hermanson, G.T., Mallia, A.K., Gartner, F.H., Provenzano, M.D., Fujimoto, E.K., Goeke, N.M., Olson, B.J. & Klenk, D.C. (1985) Measurement of protein using bicinchoninic acid. *Anal Biochem*. 150(1): 76-85. Erratum in: *Anal Biochem* (1987) 163(1): 279

Smyth, J.T., Dehaven, W.I., Jones, B.F., Mercer, J.C., Trebak, M., Vazquez, G. & Putney, J.W., Jr. (2006) Emerging perspectives in store-operated Ca^{2+} entry: roles of Orai, Stim and TRP. *Biochim Biophys Acta*. 1763: 1147-1160

Soboloff, J., Spassova, M.A., Tang, X.D., Hewavitharana, T., Xu, W. & Gill, D.L. (2006) Orai1 and STIM reconstitute store-operated calcium channel function. *J Biol Chem*. 281: 20661-20665

Soh, H. & Park, C.-S. (2001) Inwardly rectifying current-voltage relationship of small-conductance Ca^{2+}-activated K^+ channels rendered by intracellular divalent cation blockade. *Biochem J*. 80: 2207-2215

Soule, H.D., Vazquez, J., Long, A., Albert, S. & Brennan, M.J. (1973) Human cell line from a pleural effusion derived from breast carcinoma. *J Natl Cancer Inst*. 51: 1409-1413

Steinert, M. & Grissmer, S. (1997) Novel activation stimulus of chloride channels by potassium in human osteoblasts and human leukaemic T-lymphocytes. *J Physiol*. 500(3): 653-660

Stocker, M. (2004) Ca^{2+}-activated K^+ channels: molecular determinants and function of the SK family. *Nat Rev Neurosci*. 5: 758-770

Stone, K.R., Mickey, D.D., Wunderli, H., Mickey, G.H. & Paulson, D.F. (1978) Isolation of a human prostate carcinoma cell line (DU 145). *Int J Cancer*. 21: 274-281

Story, G. M., Peier, A.M., Reeve, A.J., Eid, S.R., Mosbacher, J., Hricik, T.R., Earley, T.J., Hergarden, A.C., Andersson, D.A., Hwang, S.W., McIntyre, P., Jegla, T., Bevan, S. & Patapoutian, A. (2003) ANKTM1, a TRP-like channel expressed in nociceptive neurons, is activated by cold temperatures. *Cell*. 112: 819-829

Stowers, L., Holy, E.T., Meister, M., Dulac, C. & Koentges, G. (2002) Loss of sex discrimination and male-male aggression in mice deficient for TRP2. *Science*. 295: 1493-500

Strotmann, R., Harteneck, C., Nunnenmacher, K., Schultz, G. & Plant, T. D. (2000) OTRPC4, a nonselective cation channel that confers sensitivity to extracellular osmolarity. *Nature Cell Biol*. 2: 695-702

Sweeney, M., Yu, Y., Platoshyn, O., Zhang, S., McDaniel, S.S. & Yuan, J.X. (2002) Inhibition of endogenous TRP1 decreases capacitative Ca^{2+} entry and attenuates pulmonary artery smooth muscle cell proliferation. *Am J Physiol Lung Cell Mol Physiol*. 283: L144-L155

Sweeney, M.I., White, T.D. & Sawynok, J. (1989) Morphine, capsaicin and K^+ release purines from capsaicin-sensitive primary afferent nerve terminals in the spinal cord. *J Pharmacol Exp Ther*. 248(1): 447-54

Szallasi, A., Nilsson, S., Farkas-Szallasi, T., Blumberg, P.M., Hökfelt, T. & Lundberg, J.M. (1995) Vanilloid (capsaicin) receptors in the rat: distribution in the brain, regional differences in the spinal cord, axonal transport to the periphery, and depletion by systemic vanilloid treatment. *Brain Res*. 703(1-2): 175-83

Szolcsányi, J. (2004) Forty years in capsaicin research for sensory pharmacology and physiology. *Neuropeptides*. 38(6): 377-84

Taguchi, Y., Yamamoto, M., Yamate, T., Lin, S.C., Mocharla, H., DeTogni, P., Nakayama, N., Boyce, B.F., Abe, E. & Manolagas, S.C. (1998) Interleukin-6-type cytokines stimulate mesenchymal progenitor differentiation toward the osteoblastic lineage. *Proc Assoc Am Physicians*. 110: 559-574

Takahashi, N., Akatsu, T., Udagawa, N., Sasaki, T., Yamaguchi, A., Moseley, J.M., Martin, T.J. & Suda, T. (1988) Osteoblastic cells are involved in osteoclast formation. *Endocrinology*. 123: 2600-2

Takaki, M., Jin, J.G. & Nakayama, S. (1989) Ruthenium red antagonism of the effect of capsaicin on the motility of the isolated guinea-pig ileum. *Eur J Pharmacol*. 174(1): 57-62. Erratum in: *Eur J Pharmacol* (1990) 178(3): 380

Tam, J., Trembovler, V., Di Marzo, V., Petrosino, S., Leo, G., Alexandrovich, A., Regev, E., Casap, N., Shteyer, A., Ledent, C., Karsak, M., Zimmer, A., Mechoulam, R., Yirmiya, R., Shohami, E. & Bab, I. (2008) The cannabinoid CB1 receptor regulates bone formation by modulating adrenergic signaling. *FASEB J*. 22(1): 285-94

Tamayo, N., Liao, H., Stec, M.M., Wang, X., Chakrabarti, P., Retz, D., Doherty, E.M., Surapaneni, S., Tamir, R., Bannon, A.W., Gavva, N.R. & Norman, M.H. (2008) Design and synthesis of peripherally restricted transient receptor potential vanilloid 1 (TRPV1) antagonists. *J Med Chem*. 51(9): 2744-57; Published online ahead of print. doi: 10.1021/jm7014638

Tang, B.M., Eslick, G.D., Nowson, C., Smith, C. & Bensoussan, A. (2007) Use of calcium or calcium in combination with vitamin D supplementation to prevent fractures and bone loss in people aged 50 years and older: a meta-analysis. *Lancet*. 370(9588): 657-66

Taparia, S., Fleet, J.C., Peng, J.B., Wang, X.D. & R.J. Wood. (2006) 1,25-Dihydroxyvitamin D and 25-hydroxyvitamin D-mediated regulation of TRPV6 (a putative epithelial calcium channel) mRNA expression in Caco-2 cells. *Eur J Nutr*. 45: 196-204

Taylor, A.F. (2002a) Osteoblastic glutamate receptor function regulates bone formation and resorption. *J Musculoskelet Neuronal Interact*. 2(3): 285-90

Taylor, A.F. (2002b) Functional osteoblastic ionotropic glutamate receptors are a prerequisite for bone formation. *J Musculoskelet Neuronal Interact*. 2(5): 415-22

Teng, H.P., Huang, C.J., Yeh, J.H., Hsu, S.S., Lo, Y.K., Cheng, J.S., Cheng, H.H., Chen, J.S., Jiann, B.P., Chang, H.T., Huang, J.K. & Jan, C.R. (2004) Capsazepine elevates intracellular Ca^{2+} in human osteosarcoma cells, questioning its selectivity as a vanilloid receptor antagonist. *Life Sci*. 75(21): 2515-26

Thomas, T., Gori, F., Khosla, S., Jensen, M.D., Burguera, B. & Riggs, B.L. (1999) Leptin acts on human marrow stromal cells to enhance differentiation to osteoblasts and to inhibit differentiation to adipocytes. *Endocrinology*. 140: 1630-1638

Thompson, D.L., Lum, K.D., Nygaard, S.C., Kuestner, R.E., Kelly, K.A., Gimble, J.M. & Moore, E.E. (1998) The derivation and characterization of stromal cell lines from the bone marrow of p53$^{-/-}$ mice: new insights into osteoblast and adipocyte differentiation. *J Bone Miner Res*. 13(2): 195-204

Tian, W., Fu, Y., Wang, D.H. & Cohen, D.M. (2006) Regulation of TRPV1 by a novel renally expressed rat TRPV1 splice variant. *Am J Physiol Renal Physiol*. 290(1): F117-26

Tominaga, M., Wada, M. & Masu, M. (2001) Potentiation of capsaicin receptor activity by metabotropic ATP receptors as a possible mechanism for ATP-evoked pain and hyperalgesia. *Proc Natl Acad Sci USA*. 98(12): 6951-6

Tonnarelli, B., Manferdini, C., Piacentini, A., Codeluppi, K., Zini, N., Ghisu, S., Facchini, A. & Lisignoli, G. (2008) Surface-dependent modulation of proliferation, bone matrix molecules, and inflammatory factors in human osteoblasts. *J Biomed Mater Res A*. Published online ahead of print. doi: 10.1002/jbm.a.32019

REFERENCES

Toro, L., Wallner, M., Meera, P. & Tanaka, Y. (1998) Maxi-K_{Ca}, a unique member of the voltage-gated K channel superfamily. *News Physiol Sci.* 13: 112-117

Tsavaler, L., Shapero, M.H., Morkowski, S. & Laus, R. (2001) Trp-p8, a novel prostate-specific gene, is up-regulated in prostate cancer and other malignancies and shares high homology with transient receptor potential calcium channel proteins. *Cancer Res.* 61: 3760-3769

van Abel, M., Hoenderop, J.G., Dardenn,e O., St-Arnaud, R., van Os, C., van Leeuwen, J.P. & Bindels, R.J. (2002) 1,25(OH)$_2$D$_3$-independent stimulatory effect of estrogen on the expression of ECaC1 in kidney. *J Am Soc Nephrol.* 13: 2102-2109

van Beek, E., Löwik, C., van der Pluijm, G. & Papapoulos, S. (1999) The role of geranylgeranylation in bone resorption and its suppression by bisphosphonates in fetal bone explants in vitro: A clue to the mechanism of action of nitrogen-containing bisphosphonates. *J Bone Miner Res.* 14(5): 722-9

van de Graaf, S.F., Boullart, I., Hoenderop, J.G. & Bindels, R.J. (2004) Regulation of the epithelial Ca^{2+} channels TRPV5 and TRPV6 by 1alpha,25-dihydroxy Vitamin D3 and dietary Ca^{2+}. *J Steroid Biochem Mol Biol.* 89-90(1-5): 303-8

van den Hurk, M.J., Cruijsen, P.M., Schoeber, J.P., Scheenen, W.J., Roubos, E.W. & Jenks, B.G. (2008) Intracellular signal transduction by the extracellular calcium-sensing receptor of Xenopus melanotrope cells. *Gen Comp Endocrinol.* 157(2): 156-64

van der Eerden, B.C., Hoenderop, J.G., de Vries, T.J., Schoenmaker, T., Buurman, C.J., Uitterlinden, A.G., Pols, H.A., Bindels, R.J. & van Leeuwen, J.P. (2005) The epithelial Ca^{2+} channel TRPV5 is essential for proper osteoclastic bone resorption. *Proc Natl Acad Sci USA.* 102(48): 17507-17512

van Staa, T.P., Dennison, E.M., Leufkens, H.G. & Cooper, C. (2001) Epidemiology of fractures in England and Wales. *Bone.* 29: 517-522

Vanderschueren, D., Gaytant, J., Boonen, S., Venken, K. (2008) Androgens and bone. *Curr Opin Endocrinol Diabetes Obes.* 15(3): 250-4

Vanderschueren, D., Vandenput, L., Boonen, S., Lindberg, M.K., Bouillon, R. & Ohlsson, C. (2004) Androgens and bone. *Endocr Rev.* 25(3): 389-425

Vannier, B., Zhu, X., Brown, D., & Birnbaumer, L. (1998) The membrane topology of human transient receptor potential 3 as inferred from glycosylation-scanning mutagenesis and epitope immunocytochemistry. *J Biol Chem.* 273: 8675-8679

Venkatachalam, K., van Rossum, D.B., Patterson, R.L., Ma, H.T. & Gill, D.L. (2002) The cellular and molecular basis of store-operated calcium entry. *Nat Cell Biol.* 4(11): E263-72

Vennekens, R., Hoenderop, J.G.J., Prenen, J., Stuiver, M., Willems, P.H.G.M., Droogmans, G., Nilius, B. & Bindels, R.J.M. (2000) Permeation and gating properties of the novel epithelial Ca^{2+} channel. *J Biol Chem.* 275: 3963-3969

Vig, M., Peinelt, C., Beck, A., Koomoa, D.L., Rabah, D., Koblan- Huberson, M., Kraft, S., Turner, H., Fleig, A., Penner, R. & Kinet, J.P. (2006) CRACM1 is a plasma membrane protein essential for store-operated Ca^{2+} entry. *Science.* 312: 1220-1223

Viguet-Carrin, S., Garnero, P. & Delmas, P.D. (2006) The role of collagen in bone strength. *Osteoporos Int.* 17(3): 319-336

Villareal, D.T., Binder, E.F., Williams, D.B., Schechtman, K.B., Yarasheski, K.E. & Kohrt, W.M. (2001) Bone mineral density response to estrogen replacement in frail elderly women: a randomized controlled trial. *JAMA.* 286(7): 815-20

Voets, T. & Nilius, B. (2007) Modulation of TRPs by PIPs. *J Physiol.* 582(3): 939-44

REFERENCES

Voets, T., Nilius, B., Hoefs, S., van der Kemp, A.W., Droogmans, G., Bindels, R.J. & Hoenderop, J.G. (2004) TRPM6 forms the Mg^{2+} influx channel involved in intestinal and renal Mg^{2+} absorption. *J Biol Chem.* 279: 19-25

Voets, T., Prenen, J., Fleig, A., Vennekens, R., Watanabe, H., Hoenderop, J.G.J., Bindels, R.J.M., Droogmans, G., Penner, R. & Nilius, B. (2001) CaT1 and the calcium release-activated calcium channel manifest distinct pore properties. *J Biol Chem.* 276: 47767-47770

Vos, M.H., Neelands, T.R., McDonald, H.A., Choi, W., Kroeger, P.E., Puttfarcken, P.S., Faltynek, C.R., Moreland, R.B. & Han, P. (2006) TRPV1b overexpression negatively regulates TRPV1 responsiveness to capsaicin, heat and low pH in HEK293 cells. *J Neurochem.* 99(4): 1088-102

Wallace, B.A. & Cumming, R.G. (2000) Systematic review of randomized trials of the effect of exercise on bone mass in pre- and postmenopausal women. *Calcif Tissue Int.* 67: 10-18

Wallner, L., Dai, J., Escara-Wilke, J., Zhang, J., Yao, Z., Lu, Y., Trikha, M., Nemeth, J.A., Zaki, M.H. & Keller, E.T. (2006) Inhibition of interleukin-6 with cnto328, an anti-interleukin-6 monoclonal antibody, inhibits conversion of androgen-dependent prostate cancer to an androgen-independent phenotype in orchiectomized mice. *Cancer Res.* 66(6): 3087-3095

Wang, C., Hu, H.-Z., Colton, C.K., Wood, J.D. & Zhu, M.X. (2004) An alternative splicing product of the murine trpv1 gene dominant degatively modulates the ativity of TRPV1 channels. *J Biol Chem.* 279: 37423-37430

Wang, H.P., Pu, X.Y. & Wang, X.H. (2007) Distribution profiles of transient receptor potential melastatin-related and vanilloid-related channels in prostatic tissue in rat. *Asian J Androl.* 9(5): 634-40

Wang, X., Pluznick, J.L., Wei, P., Padanilam, B.J. & Sansom, S.C. (2004) TRPC4 forms store-operated Ca^{2+} channels in mouse mesangial cells. *Am J Physiol Cell Physiol.* 287: C357-C364

Wang, X.T., Nagaba, Y., Cross, H.S., Wrba, F., Zhang, L. & Guggino, S.E. (2000) The mRNA of L-type calcium channel elevated in colon cancer: protein distribution in normal and cancerous colon. *Am J Pathol.* 157: 1549-1562

Wang, Y. (2008) The functional regulation of trpv1 and its role in pain sensitization. *Neurochem Res.* (Published online ahead of print). doi: 10.1007/s11064-008-9750-5

Wang, Y.-W., Ding, J.P., Xia, X.-M. & Lingle, C.J. (2002) Consequences of the stoichiometry of Slo1 and auxiliary subunits on functional properties of large-conductance Ca^{2+}-activated K^+ Channels. *J Neurosci.* 22(5): 1550-1561

Wang, Z. (2004) Roles of K^+ channels in regulating tumour cell proliferation and apoptosis. *Pflugers Arch.* 448: 274-286

Wann, K.T. & Richards, C.D. (1994) Properties of single calcium-activated potassium channels of large conductance in rat hippocampal neurons in culture. *Eur J Neurosci.* 6(4): 607-17

Weber, K., Erben, R. G., Rump, A., & Adamski, J. (2001) Gene structure and regulation of the murine epithelial calcium channels ECaC1 and 2. *Biochem Biophys Res Commun.* 289: 1287-1294

Wei, W.L., Sun, H.S., Olah, M.E., Sun, X., Czerwinska, E., Czerwinski, W., Mori, Y., Orser, B.A., Xiong, Z.G., Jackson, M.F., Tymianski, M. & MacDonald, J.F. (2007) TRPM7 channels in hippocampal neurons detect levels of extracellular divalent cations. *Proc Natl Acad Sci USA.* 104(41): 16323-8

Weiner, S. & Traub, W. (1992) Bone structure: from angstroms to microns. *FASEB J.* 6: 879-885

Welch, J.M., Simon, S.A. & Reinhart, P.H. (2000) The activation mechanism of rat vanilloid receptor 1 by capsaicin involves the pore domain and differs from the activation by either acid or heat. *Proc Natl Acad Sci USA*. 97: 13889-13894

Wes, P.D., Chevesich, J., Jeromin, A., Rosenberg, C., Stetten, G. & Montell, C. (1995) TRPC1, a human homolog of a Drosophila store-operated channel. *Proc Natl Acad Sci U S A*. 92: 9652-6

Weskamp, M., Seidl, W., & Grissmer, S. (2000) Characterisation of the increase in $[Ca^{2+}]_i$ during hypotonic shock and the involvement of Ca^{2+}-activated K^+ channels in the regulatory volume decrease in human osteoblast-like cells. *J Membr Biol*. 178(1): 11-20

WHO Scientific Group on the Prevention and Management of Osteoporosis (2000: Geneva, Switzerland) (2003). Prevention and management of osteoporosis

WHO Study Group (1994) Assessment of fracture risk and its application to screening for post menopausal osteoporosis. WHO Technical Report Series. 843: 1-129

Wisnoskey, B.J., Sinkins, W.G. & Schilling, W.P. (2003) Activation of vanilloid receptor type I in the endoplasmic reticulum fails to activate store-operated Ca^{2+} entry. *Biochem J*. 372(2): 517-28

Wissenbach, U., Niemeyer, B. Himmerkus, N., Fixemer, T., Bonkhoff, H. & Flockerzi, V. (2004a) TRPV6 and prostate cancer: cancer growth beyond the prostate correlates with increased TRPV6 Ca^{2+} channel expression. *Biochem Biophys Res Commun*. 322: 1359-1363

Wissenbach, U., Niemeyer, A.B., & Flockerzi, V. (2004b) TRP channels as potential drug targets. *Biol Cell*. 96: 47-54

Wondergem, R., Cregan, M., Strickler, L., Miller, R. & Suttles, J. (1998) Membrane potassium channels and human bladder tumor cells: II. Growth properties. *J Membr Biol*. 161(3): 257-62

Wonderlin, W.F. & Strobl, J.S. (1996) Potassium channels, proliferation and G1 progression. *J Membr Biol*. 154(2): 91-107

Wong, P.K., Christie, J.J. & Wark, J.D. (2007). The effects of smoking on bone health. *Clin Sci*. 113(5): 233-41

Woodfork, K.A., Wonderlin, W.F., Peterson, V.A. & Strobl, J.S. (1995) Inhibition of ATP-sensitive potassium channels causes reversible cell-cycle arrest of human breast cancer cells in tissue culture. *J Cell Physiol*. 162(2): 163-71

Worley, P.F., Zeng, W., Huang, G.N., Yuan, J.P., Kim, J.Y., Lee, M.G. & Muallem, S. (2007) TRPC channels as STIM1-regulated store-operated channels. *Cell Calcium*. 42(2): 205-11

Wu, M.M., Buchanan, J., Luik, R.M. & Lewis, R.S. (2006) Ca^{2+} store depletion causes STIM1 to accumulate in ER regions closely associated with the plasma membrane. *J Cell Biol*. 174: 803-813

Wykes, R.C., Lee, M., Duffy, S.M., Yang, W., Seward, E.P. & Bradding, P. (2007) Functional transient receptor potential melastatin 7 channels are critical for human mast cell survival. *J Immunol*. 179(6): 4045-52

Xia, X.-M., Fakler, B., Rivard, A., Wayman, G., Johnson-Pais, T., Keen, J.E., Ishii, T., Hirschberg, B., Bond, C.T., Lutsenko, S., Maylie, J. & Adelman, J.P. (1998) Mechanism of calcium gating in small-conductance calcium-activated potassium channels. *Nature*. 395: 503-507

Xue, Q., Yu, Y., Trilk, S.L., Jong, B.E. & Schumacher, M.A. (2001) The genomic organization of the gene encoding the vanilloid receptor: evidence for multiple splice variants. *Genomics*. 76(1-3): 14-20

Yamamura, H., Ugawa, S., Ueda, T., Nagao, M. & Shimada, S. (2004) Capsazepine is a novel activator of the delta subunit of the human epithelial Na$^+$ channel. *J Biol Chem.* 279(43): 44483-9

Yang, J., Jan, Y.N. & Jan, L.Y. (1995) Control of rectification and permeation by residues in two distinct domains in an inward rectifier K+ channel. *Neuron.* 14: 1047-1054

Yasuda, H., Shima, N., Nakagawa, N., Yamaguchi, K., Kinosaki, M., Mochizuki, S., Tomoyasu, A., Yano, K., Goto, M., Murakami, A., Tsuda, E., Morinaga, T., Higashio, K., Udagawa, N., Takahashi, N. & Suda, T. (1998) Osteoclast differentiation factor is a ligand for osteoprotegerin/osteoclastogenesis-inhibitory factor and is identical to TRANCE/RANKL. *Proc Natl Acad Sci U S A.* 95(7): 3597-602

Yellen, G. (1984a) Relief of Na$^+$ block of Ca^{2+}-activated K$^+$ channels by external cations. *J Gen Physiol.* 84(2): 187-99

Yellen, G. (1984b) Ionic permeation and blockade in Ca^{2+}-activated K$^+$ channels of bovine chromaffin cells. *J Gen Physiol.* 1984b 84(2): 157-86

Yellowley, C.E., Hancox, J.C., Skerry, T.M. & Levi, A.J. (1998) Whole-cell membrane currents from human osteoblast-like cells. *Calcif Tissue Int.* 62: 122-132

Yeromin, A.V., Zhang, S.L., Jiang, W., Yu, Y., Safrina, O. & Cahalan, M.D. (2006) Molecular identification of the CRAC channel by altered ion selectivity in a mutant of Orai. *Nature.* 443: 226-229

Yin, J.J., Mohammad, K.S., Käkönen, S.M., Harris, S., Wu-Wong, J.R., Wessale, J.L., Padley, R.J., Garrett, I.R., Chirgwin, J.M. & Guise, T.A. (2003) A causal role for endothelin-1 in the pathogenesis of osteoblastic bone metastases. *Proc Natl Acad Sci USA.* 100(19): 10588-9

Yoshitake, F., Itoh, S., Narita, H., Ishihara, K. & Ebisu, S. (2008) Interleukin-6 directly inhibits osteoclast differentiation by suppressing receptor activator of NF-kappaB signaling pathways. *J Biol Chem.* 283(17): 11535-40

Ypey, D.L., Ravesloot, J.H., Buisman, H.P. & Nijweide, P.J. (1988) Voltage-activated ionic channels and conductances in embryonic chick osteoblast cultures. *J Membr Biol.* 101: 141-150

Yuan, J.P., Zeng, W., Huang, G.N., Worley, P.F. & Muallem, S. (2007) STIM1 heteromultimerizes TRPC channels to determine their function as store operated channels. *Nat Cell Biol.* 9: 636-645

Zerangue, N. Schwappach, B., Jan, Y.N. & Jan, L.Y. (1999) A new ER trafficking signal regulates the subunit stoichiometry of plasma membrane K(ATP) channels. *Neuron.* 22: 537-548

Zhang, J. & Webb, D.M. (2003) Evolutionary deterioration of the vomeronasal pheromone transduction pathway in catarrhine primates. *Proc Natl Acad Sci U S A.* 100: 8337-41

Zhang, L. & Barritt, G.J. (2004) Evidence that TRPM8 is an androgen-dependent Ca^{2+} channel required for the survival of prostate cancer cells. *Cancer Res.* 64: 8365-8373

Zhang, L. & Barritt, G.J. (2006) TRPM8 in prostate cancer cells: a potential diagnostic and prognostic marker with a secretory function? *Endocr-Relat Cancer.* 13: 27-38

Zhang, L.L., Yan Liu, D., Ma, L.Q., Luo, Z.D., Cao, T.B., Zhong, J., Yan, Z.C., Wang, L.J., Zhao, Z.G., Zhu, S.J., Schrader, M., Thilo, F., Zhu, Z.M. & Tepel, M. (2007) Activation of transient receptor potential vanilloid type-1 channel prevents adipogenesis and obesity. *Circ Res.* 100(7): 1063-70

Zhang, R.W., Supowit, S.C., Xu, X., Li, H., Christensen, M.D., Lozano, R. & Simmons, D.J. (1995). Expression of selected osteogenic markers in the fibroblast-like cells of rat marrow stroma. *Calcif Tissue Int.* 56: 283-291

Zhang, S.L., Yeromin, A.V., Zhang, X.H., Yu, Y., Safrina, O., Penna, A., Roos, J., Stauderman, K.A. & Cahalan, M.D. (2006) Genome-wide RNAi screen of Ca^{2+} influx identifies genes that regulate Ca^{2+} release-activated Ca^{2+} channel activity. *Proc Natl Acad Sci USA*. 103: 9357-9362

Zhang, Y., Hoon, M.A., Chandrashekar, J., Mueller, K.L., Cook, B., Wu, D., Zuker, C.S. & Ryba, N.J. (2003) Coding of sweet, bitter, and umami tastes: different receptor cells sharing similar signaling pathways. *Cell*. 112: 293-301

Zhao, S., Zhang, Y.K., Harris, S., Ahuja, S.S. & Bonewald, L.F. (2002) MLO-Y4 osteocyte-like cells support osteoclast formation and activation. *J Bone Miner Res*. 17: 2068-79

Zhou, H., Choong, P., McCarthy, R., Chou, S.T., Martin, T.J. & Ng, K.W. (1994) In situ hybridization to show sequential expression of osteoblast gene markers during bone formation in vivo. *J Bone Miner Res*. 9: 1489-1499

Zmuda, J.M., Sheu, Y.T. & Moffett, S.P. (2006) The search for human osteoporosis genes. *J Musculoskelet Neuronal Interact*. 6(1): 3-15